

Appendix A.2.13.8 DSC (Basket) Structural Evaluation

CONTENTS

A.2.13.8.1	Introduction.....	A.2.13.8-1
A.2.13.8.2	Approach.....	A.2.13.8-1
A.2.13.8.2.1	Normal Condition of Transport (NCT) Analysis	A.2.13.8-1
A.2.13.8.2.2	Hypothetical Accident Condition (HAC) Analysis.....	A.2.13.8-2
A.2.13.8.3	Loading	A.2.13.8-2
A.2.13.8.4	Design Criteria	A.2.13.8-3
A.2.13.8.5	NUH61BT/NUH61BTH Baskets.....	A.2.13.8-4
A.2.13.8.5.1	Basket Side Drop.....	A.2.13.8-4
A.2.13.8.5.2	Basket End Drop	A.2.13.8-9
A.2.13.8.6	NUH69BTH Basket	A.2.13.8-9
A.2.13.8.6.1	Basket Side Drop.....	A.2.13.8-9
A.2.13.8.6.2	Basket End Drop	A.2.13.8-11
A.2.13.8.7	NUH24PTH	A.2.13.8-12
A.2.13.8.7.1	Basket Side Drop.....	A.2.13.8-12
A.2.13.8.7.2	Basket End Drop	A.2.13.8-15
A.2.13.8.7.3	Fusion Welds.....	A.2.13.8-15
A.2.13.8.8	NUH32PT Basket	A.2.13.8-16
A.2.13.8.8.1	Basket Side Drop.....	A.2.13.8-16
A.2.13.8.8.2	Basket End Drop	A.2.13.8-18
A.2.13.8.9	NUH32PTH and 32PTH Type 1/NUH32PTH Type 1 and Type 2 Baskets	A.2.13.8-19
A.2.13.8.9.1	Basket Side Drop.....	A.2.13.8-19
A.2.13.8.9.2	Basket End Drop	A.2.13.8-23
A.2.13.8.9.3	Fusion Welds.....	A.2.13.8-24
A.2.13.8.10	NUH37PTH Basket	A.2.13.8-25
A.2.13.8.10.1	Basket Side Drop.....	A.2.13.8-25
A.2.13.8.10.2	Basket End Drop	A.2.13.8-27
A.2.13.8.11	NUH24PT4 Basket	A.2.13.8-28
A.2.13.8.11.1	Spacer Disk	A.2.13.8-28
A.2.13.8.11.2	Guide Sleeve Assemblies	A.2.13.8-30
A.2.13.8.11.3	Support Rod Assemblies	A.2.13.8-31
A.2.13.8.12	Basket Deformations for Effect of Criticality Analyses	A.2.13.8-32
A.2.13.8.13	References.....	A.2.13.8-33

LIST OF TABLES

Table A.2.13.8-1	Summary of Impact G-loads for Basket Analyses.....	A.2.13.8-34
Table A.2.13.8-2	Basket NCT Load Combinations.....	A.2.13.8-35
Table A.2.13.8-3	Basket HAC Load Combinations	A.2.13.8-35
Table A.2.13.8-4	Basket Stress Limits	A.2.13.8-36
Table A.2.13.8-5	NUH61BT/61BTH Type 1 Normal Condition - Maximum Stress Summary	A.2.13.8-37
Table A.2.13.8-6	NUH61BTH Type 2 Normal Condition - Maximum Stress Summary	A.2.13.8-38
Table A.2.13.8-7	NUH61BT/61BTH Type 1 Normal Condition - Limit Analysis Summary.....	A.2.13.8-39
Table A.2.13.8-8	NUH61BTH Type 2 Normal Condition - Limit Analysis Summary.....	A.2.13.8-39
Table A.2.13.8-9	NUH61BT HAC - Maximum Stress Summary	A.2.13.8-40

Table A.2.13.8-10 NUH61BTH Type 1 HAC – Maximum Stress Summary	A.2.13.8-41
Table A.2.13.8-11 NUH61BTH Type 2 HAC – Maximum Stress Summary	A.2.13.8-42
Table A.2.13.8-12 NUH69BTH Normal Condition - Maximum Stress Summary.....	A.2.13.8-43
Table A.2.13.8-13 NUH69BTH Normal Condition - Limit Analysis Summary	A.2.13.8-45
Table A.2.13.8-14 NUH69BTH HAC - Maximum Stress Summary	A.2.13.8-46
Table A.2.13.8-15 NUH69BTH HAC – Buckling Analysis Results Summary	A.2.13.8-47
Table A.2.13.8-16 NUH24PTH Normal Condition - Maximum Stress Summary	A.2.13.8-48
Table A.2.13.8-17 NUH24PTH Normal Condition - Limit Analysis Summary	A.2.13.8-50
Table A.2.13.8-18 NUH24PTH HAC - Maximum Stress Summary.....	A.2.13.8-51
Table A.2.13.8-19 NUH32PT Normal Condition - Limit Analysis Summary	A.2.13.8-52
Table A.2.13.8-20 NUH32PT HAC - Maximum Stress Summary.....	A.2.13.8-53
Table A.2.13.8-21 NUH32PTH1 Type 1 Normal Condition - Maximum Stress Summary	A.2.13.8-54
Table A.2.13.8-22 NUH32PTH/NUH32PTH1 Type 2 Normal Condition - Maximum Stress Summary	A.2.13.8-55
Table A.2.13.8-23 NUH32PTH/NUH32PTH1 Normal Condition - Limit Analysis Summary ..	A.2.13.8-56
Table A.2.13.8-24 NUH32PTH1 Type 1 HAC - Maximum Stress Summary.....	A.2.13.8-57
Table A.2.13.8-25 NUH32PTH1 Type 2 HAC - Maximum Stress Summary.....	A.2.13.8-58
Table A.2.13.8-26 NUH32PTH HAC - Maximum Stress Summary.....	A.2.13.8-59
Table A.2.13.8-27 NUH32PTH1 HAC – Buckling Analysis Results Summary	A.2.13.8-60
Table A.2.13.8-28 NUH32PTH HAC – Buckling Analysis Results Summary	A.2.13.8-60
Table A.2.13.8-29 NUH37PTH Normal Condition - Maximum Stress Summary	A.2.13.8-61
Table A.2.13.8-30 NUH37PTH Normal Condition - Limit Analysis Summary	A.2.13.8-62
Table A.2.13.8-31 NUH37PTH HAC - Maximum Stress Summary.....	A.2.13.8-63
Table A.2.13.8-32 NUH37PTH HAC – Buckling Analysis Results Summary	A.2.13.8-64
Table A.2.13.8-33 NUH24PT4 Normal Condition – Spacer Disk Maximum Stress Summary ..	A.2.13.8-65
Table A.2.13.8-34 NUH24PT4 Normal Condition – Spacer Disk Limit Analysis Summary	A.2.13.8-66
Table A.2.13.8-35 NUH24PT4 HAC - Maximum Stress Summary.....	A.2.13.8-66
Table A.2.13.8-36 Summary of Guide Sleeve Stresses from Side Drops.....	A.2.13.8-67
Table A.2.13.8-37 Summary of Guide Sleeve Stresses from End Drops	A.2.13.8-67
Table A.2.13.8-38 Summary of Support Rod Assembly Stresses from Side Drops.....	A.2.13.8-68
Table A.2.13.8-39 Summary of Spacer Sleeve Analysis from End Drops	A.2.13.8-68

LIST OF FIGURES

Figure A.2.13.8-1 NUH61BT/61BTH Type 1 Finite Element Model – Full Basket Section.....	A.2.13.8-69
Figure A.2.13.8-2 NUH61BTH Type 2 Finite Element Model – Full Basket Section.....	A.2.13.8-70
Figure A.2.13.8-3 NUH69BTH Finite Element Model	A.2.13.8-71
Figure A.2.13.8-4 NUH24PTH Finite Element Model.....	A.2.13.8-72
Figure A.2.13.8-5 NUH32PT Solid Aluminum Rails Finite Element Model.....	A.2.13.8-73
Figure A.2.13.8-6 NUH32PT 3 Piece Aluminum Rails Finite Element Model.....	A.2.13.8-74
Figure A.2.13.8-7 NUH32PTH/NUH32PTH1 Type 2 Finite Element Model	A.2.13.8-75
Figure A.2.13.8-8 NUH37PTH Finite Element Model.....	A.2.13.8-76
Figure A.2.13.8-9 NUH24PT4 Spacer Disk Finite Element Model for Side Drop	A.2.13.8-77
Figure A.2.13.8-10 NUH24PT4 Spacer Disk Finite Element Model for End Drop.....	A.2.13.8-78
Figure A.2.13.8-11 Permanent Deformation of the 37PTH Basket following 45° HAC Side Drop.....	A.2.13.8-79

Appendix A.2.13.8 DSC (Basket) Structural Evaluation

NOTE: References in this Appendix are shown as [1], [2], etc. and refer to the reference list in Section A.2.13.8.13.

A.2.13.8.1 Introduction

The purpose of this appendix is to determine the structural integrity of the basket assemblies that are part of the payload of the MP197HB transport package. The structural evaluations are performed for loads due to Normal Conditions of Transport and Hypothetical Accident Conditions. There are seven basket configurations evaluated in this section. Due to differences in maximum allowed heat load some basket configurations consist of more than one basket type. For example the 61BTH Type 2 basket has a higher heat load capacity than the 61BTH Type 1 basket and, therefore, the welded steel transition rails in the type 1 basket are replaced with solid aluminum transition rails in the type 2 basket. Separate analyses are performed for each basket type in each basket configuration.

The structural evaluations for the following basket configurations are presented in this Appendix:

1. NUH 61BT/NUH61BTH (Type 1 and Type 2)
2. NUH69BTH
3. NUH24PTH
4. NUH32PT
5. NUH32PTH and NUH32PTH Type 1/NUH32PTH1 (Type 1 and Type 2)
6. NUH37PTH
7. NUH24PT4

Appendices A.1.4.1 to A.1.4.9 provide a detailed description of each of these basket configurations. Drawings are provided in Section A.1.4.10.

A.2.13.8.2 Approach

A.2.13.8.2.1 Normal Condition of Transport (NCT) Analysis

The fuel baskets are evaluated for normal free drop impact and thermal loads. The basket stress analysis is performed using the finite element method for the side drop and thermal load cases and analytical calculations for the end drop load cases.

The structural evaluations of the baskets for side drops are performed in a tiered manner. First non-linear elastic analyses are performed and the resulting stresses are compared against the Service Level A allowable stress limits. In these analyses, the material properties are linear elastic and the nonlinearities are due solely to the modeling of gap/contacts between the various basket/canister shell/cask components. If, for a given basket, the stresses for all the basket components are below the applicable ASME allowable stress limits, the basket is considered qualified for the side drop condition.

However, if the stress limits on primary membrane, P_m , or primary membrane plus bending, $P_m + P_b$, are exceeded, then, the provisions of NG-3222 are invoked whereby the limit analyses provisions of NG-3228.2 [1] are used to show that the specified loading does not exceed two-thirds of the lower bound limit load. In the implementation of the limit analysis the yield point is equal to $1.5 S_m$ and the lower bound limit load is calculated from an ideally plastic analysis (Note 9, Fig. NG-3221-1). If the stress limits on primary plus secondary stress intensity, $P_m + P_b + Q$, are exceeded, the simplified elastic-plastic analysis provisions of NG-3228.3 [1] are used to demonstrate that the cumulative fatigue usage does not exceed a value of 1.0. If requirement (a) of the simplified elastic-plastic analysis procedure (the range of primary plus secondary membrane plus bending excluding thermal bending stresses is equal or below $3 S_m$) cannot be met, then the $P_m + P_b + Q$ stress is qualified by showing that after a few cycles of load application the deformation stabilizes and subsequent structural response is elastic per the definition of shakedown in NG-3213.17 and the provisions of Note 10 to Fig NG-3221-1[1].

Compressive stresses in the basket are calculated for end drops assuming that the fuel assemblies and fuel compartments are forced against the bottom of the cask and, thus not contribute to basket stresses. Basket stresses are due to its own weight, the resulting stresses are compared against the allowable stress limits.

A.2.13.8.2.2 Hypothetical Accident Condition (HAC) Analysis

The fuel baskets are evaluated for accident free drop impact loads. The basket stress analyses are performed using quasi-static elastic plastic finite element analyses for the side drop load cases and analytical calculations are used for the end drop load cases. Non-linear elastic plastic finite element analyses are performed to calculate the critical loads for buckling.

A.2.13.8.3 Loading

Baseline g-loads for NCT and HAC drop analyses are calculated in Appendix A.2.13.12. For the quasi-static static analyses the baseline g-loads are multiplied by a dynamic amplification factor calculated for each basket type in Appendix A.2.13.9. These calculated maximum g-loads are further increased for purposes of the analysis. The maximum g-loads and the g-loads used for the analysis of each basket type are summarized in Table A.2.13.8-1. The NCT and HAC load combinations are summarized in Table A.2.13.8-2 and Table A.2.13.8-3.

No explicit analyses are performed for HAC slap down drops. Slap down drops are considered to be bounded by the end drop and the side drop evaluations because of the following:

- Temperature
 - The basket temperatures used in the end drop and side analyses correspond to the highest location in the basket (at the axial center of the DSC) for the hot ambient condition.
 - For the slap down drops the region of maximum g loads are at basket ends where the temperatures are significantly lower and thus, have higher allowable stress and higher buckling load.

- Fuel weight
 - The fuel weight used in the side drop analyses correspond to the maximum fuel weight in the active fuel region.
 - For the slap down drops the region of maximum g loads are at basket ends where the fuel assembly weight is lower than in the active fuel region and thus, lower stresses are expected.

The baseline g loads for the end and side drop analyses are calculated in Section A.2.13.12.10 of the Appendix A.2.13.12. These baseline g loads are conservatively using the wood temperature effect at -40°F (10CFR Part 71 only require -20°F). For the basket end and side drop analyses, first, the g loads are multiplied by appropriate dynamic load factors and then these g loads are increased by additional factors and used for basket structural evaluation. The calculated maximum g loads and g loads used for the analysis of each basket type are summarized in Table A.2.13.8-1.

Thermal stresses for -20 °F and 100 °F ambient conditions are calculated for all baskets. Furthermore thermal stresses for the -40 °F ambient conditions are also calculated for the 69BTH and 37PTH baskets.

A.2.13.8.4 Design Criteria

The basis for the basket stress allowables is the ASME Code, Section III, Subsection NG [1]. The primary membrane stress intensity and membrane plus bending stress intensities are limited to code allowable stress intensity, S_m , and $1.5 S_m$, respectively, at any location in the basket for Normal Conditions of Transport (Service Level A) load combinations. If the limits on primary membrane stress intensity and primary membrane plus primary bending stress intensity are not satisfied at a specific location the primary membrane stress intensity and primary membrane plus primary bending stress are qualified by means of limit analysis (NG-3228.2) to demonstrate that the specified loadings do not exceed two-thirds of the lower bound collapse load.

The ASME Code provides a basic $3S_m$ limit on primary plus secondary stress intensity for Level A conditions. That limit is specified to prevent ratcheting of a structure under cyclic loading and to provide controlled linear strain cycling in the structure so that a valid fatigue analysis can be performed. If the primary plus secondary stress intensity exceeded $3S_m$, the criteria of ASME Code NG-3228.3 (Simplified Elastic-Plastic Analysis) are used in lieu of elastic analysis methods. The primary plus secondary stresses are also qualified by demonstrating that shakedown to elastic action occurs, as defined in NG-3228.1.

The baskets are evaluated under Hypothetical Accident Condition (Level D Service) loadings in accordance with the Level D Service limits for components in Appendix F of Section III of the Code [2]. The HAC free drops are evaluated as short duration Level D conditions. For elastic analysis, the primary membrane stress is limited to the smaller of $2.4S_m$ or $0.7S_u$ and membrane plus bending stress intensities are limited to the lesser of $3.6 S_m$ or S_u . The maximum primary shear stress is limited to $0.42 S_u$. The results from the non-linear elastic-plastic analysis for the accident conditions, the general primary membrane stress intensity, P_m , shall not exceed the greater of $0.7S_u$ or $S_y + 1/3 (S_u - S_y)$ and the maximum stress intensity at any location (P_1 or $P_1 + P_b$) shall not exceed $0.9 S_u$.

Finite element non-linear buckling analyses are used in calculating the critical loads for buckling of the basket. Since the structure experiences large deformations before buckling, the large displacement option of ANSYS is used, whereby the deflections during each load step are used to continuously redefine the geometry of the structure, thus producing an updated stiffness matrix at each time step. The analysis is carried out with increasing loading until convergence can no longer be achieved. The load achieved at the last converged step is the buckling load.

The allowable stress criteria for both normal and accident conditions are summarized in Table A.2.13.8-4.

A.2.13.8.5 NUH61BT/NUH61BTH Baskets

A.2.13.8.5.1 Basket Side Drop

A detailed description of the NUH61BT and NUH61BTH baskets is presented in Appendix A.1.4.7 and Appendix A.1.4.8, respectively. From a stress analysis perspective there are two types of 61BTH baskets. The 61BTH Type 1 has welded steel transition rails around the compartment tube assembly. The Type 2 has a combination of welded steel and aluminum transition rails. The 61BT and 61BTH Type 1 baskets are identical in geometry, however the 61BTH Type 1 has a higher heat load capacity than the 61BT basket. Thus, the analyses performed for 61BTH Type 1 basket are bounding.

A. Finite Element Model

An ANSYS [10] three-dimensional finite element model of the basket is constructed using shell (SHELL43) and solid (SOLID45) elements. The overall finite element model of the 61BT/61BTH Type 1 and 61BTH Type 2 fuel basket are shown in Figure A.2.13.8-1 and Figure A.2.13.8-2, respectively. The fuel compartment tubes, stainless steel transition rails, aluminum transition rails (only for Type 2 basket), and canister are included in the model. For conservatism, the strength of wraps, aluminum and poison plates in the basket are neglected by excluding these from the finite element model. However, their weights are accounted for by increasing the material density for the fuel compartment tubes.

Because of the large number of plates in the basket and the large dimensions of the basket, certain modeling approximations were necessary. In view of continuous support of the fuel compartment tubes by the peripheral rails along the entire basket length during a side drop, a 3.0 inch long slice of the basket and rail is modeled. At the two cut faces of the model, symmetry boundary conditions are applied ($U_Y = ROT_X = ROT_Z = 0$).

The nodes between the steel tubes are coupled together in the out-of-plane direction so that they will bend in unison under surface pressure or other lateral loading to simulate through the thickness support provided by wraps, aluminum and poison plates.

Gap elements (CONTACT 52) are used to simulate the interface between the basket rails and the inner side of the canister, as well as between the outer side of the canister and the inside of the cask. Each gap element contains two nodes; one on each surface of the structure. The gap nodes specified at the inner side of the cask are restrained in the x, y and z directions. The gap size at

each gap element is determined by the difference between the basket rails radius and the inside radius of the cask inner shell; and by the difference between the outer side of the canister radius and the inside radius of the cask.

B. Material Properties

SA-240, Gr. 304 stainless steel material properties are used for the stainless steel boxes and stainless steel transition rails; 6061-O aluminum alloy (annealed) material properties are used for the aluminum transition rails. Material properties are taken from ASME Section II, Part D [9] for steel components and for 6061-O (annealed) aluminum alloy the material properties are taken from Reference [12].

Bilinear stress-strain material relationships are used for the NCT elastic-perfectly plastic limit load analyses, where the yield strength, $S_y = 1.5 S_m$ and $E_p/E = 0.0$ for the stainless steel components. For the aluminum components, the actual yield strength, S_y , and $E_p/E = 1\%$ is used.

Bilinear stress-strain relationships are used for the HAC elastic-plastic analyses, where the Code-defined yield strength, S_y , of the material is used for the stainless steel and aluminum components. The plastic modulus of elasticity is taken as 5% of the elastic modulus for the stainless steel components and 1% for the aluminum components.

C. Loading Conditions

The basket structure is analyzed for 0° , 30° , 45° and 180° azimuth side drops. Due to the basket structure symmetry, these orientations of side drops are considered to envelop all other possible drop orientations.

A fuel assembly weight of 705 lb. is used in the analysis. A uniform fuel weight distribution is assumed over the entire length of the basket. The weight of the steel wraps, aluminum, and poison plates are accounted for by increasing the material density of the fuel compartment tubes. The stiffness's of the un-modeled components are conservatively neglected in the analysis.

The material properties used in the stress analysis correspond to those at 500°F . However, the resulting stresses are compared with the allowable based on a bounding temperature of 750°F (average basket temperature is less than 750°F). This combination is conservative because using lower E , S_y and E_t (for temperatures above 500°F) in the analysis would result in higher than actual stress and compared to lower than actual allowable stress. A bounding temperature distribution that envelops the heat loads for the 100°F ambient conditions for both the Type 1 and Type 2 is used for the limit and buckling analyses. The use of a higher temperature for material properties gives lower E and S_y values and therefore, gives a conservative, lower buckling capacity.

The load resulting from the fuel assembly weight is applied as pressure on the fuel compartment plates of the basket. For the 0° and 180° orientation, the pressure acts only on the horizontal plates. For the 30° and 45° orientation, the pressure was divided into components that act on both

horizontal and vertical plates of the basket. The pressures for all orientations are calculated below for 1g accelerations.

- At 0° and 180° degrees; Pressure, $p = \text{Fuel assembly wt.} / (\text{Panel span} \times \text{Panel length})$
 $= 705 \text{ lb} / (6.22" \times 164") = 0.6911 \text{ psi}$
- At 30°; p_v on horizontal plates $= p \cos 30^\circ = 0.6911 \times 0.866 = 0.5985 \text{ psi}$
 p_h on vertical plates $= p \sin 30^\circ = 0.6911 \times 0.5 = 0.3456 \text{ psi}$
- At 45°; p_v on horizontal plates $= p \sin 45^\circ = 0.6911 \times 0.7071 = 0.4887 \text{ psi}$
 p_h on vertical plates $= p \cos 45^\circ = 0.6911 \times 0.7071 = 0.4887 \text{ psi}$

For all loadings, the above pressure values are multiplied by the g-load used.

D. Results

The maximum stress intensities resulting from the equivalent static analysis for the 30 g NCT maximum acceleration are summarized in Table A.2.13.8-5 (for the 61BT/61BTH Type 1 basket) and Table A.2.13.8-6 (for the 61BTH Type 2 basket) for critical components of the basket assemblies. Membrane (P_m), membrane-plus-bending ($P_m + P_b$), and range of primary plus secondary ($P_m + P_b + Q$) stresses are reported for components modeled with ANSYS SHELL43 shell elements. The larger of the top and bottom stresses across the thickness of the shell elements are taken as the maximum primary membrane plus bending stresses. All primary membrane stresses meet the Service Level A allowable stress limits. For some components the $P_m + P_b$ and the $P_m + P_b + Q$ stress intensities exceed the code allowable stress limits. These exceedances are localized and have characteristics of secondary stresses. Therefore, in accordance with the provisions of NG-3222 for Service Level A loads, the limit and simplified elastic-plastic analyses provisions of NG-3228.2 and NG-3228.3 are invoked.

Limit analyses per NG-3228.2 are performed to address the $P_m + P_b$ stress exceedances shown in Table A.2.13.8-5 and Table A.2.13.8-6. The results of the limit analysis are summarized in Table A.2.13.8-7 and Table A.2.13.8-8. The simplified elastic-plastic analysis procedure, per NG-3228.3, is used to address the $P_m + P_b + Q$ stress exceedances. This evaluation is described below.

The equivalent-static analyses performed for the Part 72 storage accident conditions for the 61BT and 61BTH baskets and documented in [3] and [6] used a bounding acceleration of 75g. This 75g acceleration bounds with significant margin the calculated 55g-load for the HAC drops, as shown in Table A.2.13.8-1. Therefore, the 75g analyses as described in Section K.3.7.5.3 [3] and Section T.3.7.4.3 [6] for the 61BT and 61BTH baskets, respectively are applicable. The maximum stress intensities are summarized in Table A.2.13.8-9 to Table A.2.13.8-11.

Since the analyses showed that a converged solution was attained at 75g, a conservative factor of safety against buckling for the 61BT and 61BTH baskets is 1.36 (75/55).

E. Simplified Elastic-Plastic Analysis

As shown in Table A.2.13.8-5 and Table A.2.13.8-6, the stress intensities obtained from the range of primary + secondary exceeds the $3S_m$ stress limit for some basket components. These

exceedances are addressed per ASME Code Section NG-3228.3 which stipulates that the $3S_m$ limit on the range of primary plus secondary stress intensity (NG-3222.2) may be exceeded provided the requirements of (a) through (f) below are met. The analysis demonstrating that the requirements of NG-3228.3 (a) through (f) are met is as follows:

From the stress intensity results shown in Table A.2.13.8-5 for the 61BT/61BTH Type 1 and A.2.13.8-6 for the 61BTH Type 2 baskets, the maximum $P_m + P_b + Q$ stress intensity is 63.52 ksi and corresponds to the 30 degrees orientation drop case. The evaluation below is performed for this bounding drop orientation.

Per ASME NG-3228.3,

- (a) *The range of primary plus secondary membrane plus bending stress intensity, excluding thermal bending stresses, shall be $\leq 3S_m$.*

The resulting maximum stress intensity is

$$P_m + P_b = 43.32 \text{ ksi}$$

$$Q_{\text{memb}} = 4.54 \text{ ksi}$$

The resulting maximum stress intensity is

$$P_m + P_b + Q_{\text{memb}} = 43.32 + 4.54 = 47.86$$

This is below the 49.20 ksi value of $3S_m$ for the basket material at 600°F.

Conservatively addressing this stress as the range of stress addressed in NG-3228.3(a), the requirements of NG-3228.3(a) are satisfied.

- (b) *The value of S_a used for entering the design fatigue curve is multiplied by the factor K_e , where:*

$$\begin{aligned} K_e &= 1.0 \text{ for } S_n \leq 3S_m \\ &= 1.0 + [(1-n)/n(m-1)](S_n/3S_m - 1), \text{ for } 3S_m < S_n < 3mS_m \\ &= 1.0 + [(1-0.3)/(0.3*(1.7-1))]*(63.52/49.20 - 1) \\ &= 1.96 \\ &= 1/n, \text{ for } S_n \geq 3mS_m \\ n &= 0.3 \quad \text{Table NG-3228.3(b)-1} \\ m &= 1.7 \quad \text{Table NG-3228.3(b)-1} \\ S_n &= \text{range of primary plus secondary stress intensity} \\ &= 63.52 \text{ ksi} \end{aligned}$$

The values of material parameters m and n for the various classes of permitted material are given in Table NG-3228.3(b)-1. The range of primary plus secondary stress intensity is set to the maximum stress intensity identified above of 63.52 ksi. Conservatively using ten cycles, the value of 710 ksi is taken for S_a from Figure I-9.2.1 of the ASME 2004 Section III, Division I-Appendices [2].

$$S_a = 710 \text{ ksi} \quad (\text{when number of cycles} = 10)$$

This value of S_a is used in the following section.

- (c) *The rest of the fatigue evaluation stays the same as required in NG-3222.4, except that the procedure of NG-3227.6 need not be used.*

The maximum stress identified above, multiplied by K_e is $63.52 \text{ ksi} * 1.96 = 124.49 \text{ ksi}$
This value is much less than S_a of 710 ksi. OK

The maximum temperature difference between adjacent points for both the startup and shutdown and normal service is determined as follows.

As stated above, the value for S_a is conservatively taken as 710 ksi. The instantaneous coefficient of thermal expansion, α and Young's modulus, E , are $9.8 \times 10^{-6} \text{ in/in/}^\circ\text{F}$ and $25.3 \times 10^6 \text{ psi}$, respectively. The values of α and E are evaluated at the approximate mean temperature of the basket, which is taken to be 600°F . The maximum allowable temperature difference between adjacent points is:

$$S_a / (2 \alpha E) = 1,431^\circ \text{ F}$$

The maximum temperature difference between adjacent points is well below this; therefore, the requirements of NG-3228.3(c) are met.

- (d) *The structure meets the thermal ratcheting requirements of NG-3222.5.*

Thermal ratcheting can only occur with cyclic loading. The thermally induced stresses in this analysis are due to a single occurrence; therefore no thermal ratcheting is possible.

- (e) *The temperature does not exceed those listed in Table NG-3228.3(b)-1 for various classes of materials.*

The maximum temperature is within the allowable range of 700° F for all points except at the center of the disc. The stress at the center of the disc is small and is less than the primary + secondary stress limit of $3S_m$. Therefore, paragraph NG-3228.3 of the ASME Code does not apply at that location.

- (f) *The material shall have specified minimum yield strength to specified minimum tensile strength ratio of less than 0.80.*

The yield to tensile strength ratio for basket material is listed below. Therefore, the requirements of NG-3228.3(f) are satisfied. For a temperature of 600°F $S_y / S_u = 18.4/63.4 = 0.29 < 0.80$ @ $200^\circ\text{F} = 25.0/71 = 0.35 < 0.80$ OK

Thus the range of primary + secondary stress intensity for 61BT/61BTH TYPE 1 and Type 2 basket satisfies the fatigue evaluation criteria per ASME section NG-3228.3.

A.2.13.8.5.2 Basket End Drop

During an end drop, the fuel assemblies and fuel compartments are forced against the bottom of the canister/cask. Thus, for any vertical or near vertical loading, the fuel assemblies react directly against the bottom or top end of the canister/cask and not through the basket structure as in the case for lateral loading. It is the weight of the basket assembly that causes axial compressive stress during an end drop. Axial compressive stresses are conservatively computed as if all the weight of the basket assembly will be taken by the compartment tubes and outer boxes. A conservative bounding weight for the 61BT and 61BTH Type 1 basket of 23.5 kips and a conservative bounding weight for the 61BTH Type 2 basket of 28.0 kips are used in the end drop stress calculations.

Furthermore, the evaluation is performed for the maximum acceleration of 75g corresponding to the Service Level D HAC load and the resulting stress is evaluated against the NCT Service Level A stress allowable.

Compressive Stress at Fuel Compartment Tubes and Outer Wrappers

Enveloping weight of 61BT and 61BTH baskets is used in the following evaluation:

Total weight = 28.0 kips

Fuel compartment tubes and outer wrappers section area = 266.02 in²

Stress due to 1g = $-28.0 / 266.02 = -0.105$ ksi

At 75g = $-0.105 \text{ ksi} \times 75 = -7.86 \text{ ksi} < S_m @ 700^\circ\text{F} = 16.0 \text{ ksi}$

A.2.13.8.6 NUH69BTH Basket

The details and description for the NUH69BTH basket are presented in Appendix A.1.4.9.

A.2.13.8.6.1 Basket Side Drop

A. Finite Element Model

An ANSYS [10] three-dimensional finite element model of the basket is constructed using shell (SHELL43) and solid (SOLID45) elements. The overall finite element model of the 69BTH fuel basket is shown in Figure A.2.13.8-3. The fuel compartment tubes, stainless steel wraps, aluminum transition rails, and canister are included in the model. For conservatism, the strength of the aluminum and poison plates in the basket are neglected by excluding these from the finite element model. However, the weight of these basket components is accounted for by increasing the material density for the fuel compartment tubes.

Because of the large number of plates in the basket and the large dimensions of the basket, certain modeling approximations were necessary. In view of continuous support of fuel compartment tubes by the peripheral rails along the entire basket length during a side drop, a 1.0 inch long slice of the basket and rail is modeled. At the two cut faces of the model, symmetry boundary conditions are applied ($U_Z = ROT_X = ROT_Y = 0$).

Gap elements (CONTAC 52) are used to simulate the interface between the fuel tubes, between the stainless steel wraps, and between the fuel tubes and stainless steel wraps. The gaps between these interfaces were modified to take the thickness of the aluminum and poison plates into account.

Gap elements (CONTACT 52) are used to simulate the interface between the basket rails and the inner side of the canister as well as between the outer side of the canister and the inside of the cask. Each gap element contains two nodes; one on each surface of the structure. The gap nodes specified at the inner side of the cask are restrained in the x, y and z directions. The gap size at each gap element is determined by the difference between the basket rails radius and the inside radius of the cask inner shell; and by the difference between the outer side of the canister radius and the inside radius of the cask.

B. Material Properties

SA-240, Gr. 304 stainless steel material properties are used for the stainless steel fuel compartment tubes and stainless steel wraps; 6061-O aluminum alloy (annealed) material properties are used for the aluminum transition rails. Material properties are taken from ASME Section II, Part D [9] for steel components and for 6061-O (annealed) aluminum alloy the material properties are taken from Reference [12].

Bilinear stress-strain material relationships are used for the NCT elastic-perfectly plastic limit load analyses where the yield strength, $S_y = 1.5 S_m$ and $E_p/E = 0.0$ for the stainless steel components. For the aluminum components, the actual yield strength, S_y , and $E_p/E = 1\%$ is used.

Bilinear stress-strain relationships are used for the HAC elastic-plastic analyses, where the Code-defined yield strength, S_y , of the material is used for the stainless steel and aluminum components. The plastic modulus of elasticity is taken as 5% of the elastic modulus for the stainless steel components and 1% for the aluminum components.

C. Loading Conditions

The basket structure is analyzed for 0° , 30° , 45° and 180° azimuth side drops. Due to the basket structure symmetry, these orientations of side drops are considered to envelop all other possible drop orientations.

A fuel assembly weight of 705 lb. is used in the analysis. A uniform fuel weight distribution is conservatively assumed over the active fuel length. The weight of the aluminum and poison plates are accounted for by increasing the density of the fuel compartment tubes. The stiffness's of the un-modeled components are conservatively neglected in the analysis.

The material properties used in the analysis are at 700°F for the stainless steel tubes and wraps and 500°F for the aluminum rails and canister.

The load resulting from the fuel assembly weight is applied as pressure on the fuel compartment plates of the basket. For the 0° and 180° orientation, the pressure acts only on the horizontal plates. For the 30° and 45° orientation, the pressure was divided into components that act on both horizontal and vertical plates of the basket. The pressures for all orientations are calculated below for 1g accelerations.

- At 0° and 180° degrees; Pressure, $p = \text{Fuel assembly wt.} / (\text{Panel span} \times \text{Panel length}^*)$
 $= 705 \text{ lb} / (6.165" \times 150") = 0.762 \text{ psi}$
- At 30°;
 p_v on horizontal plates $= p \cos 30^\circ = 0.762 \times 0.866 = 0.660 \text{ psi}$
 p_h on vertical plates $= p \sin 30^\circ = 0.762 \times 0.5 = 0.381 \text{ psi}$
- At 45°;
 p_v on horizontal plates $= p \sin 45^\circ = 0.762 \times 0.7071 = 0.539 \text{ psi}$
 p_h on vertical plates $= p \cos 45^\circ = 0.762 \times 0.7071 = 0.539 \text{ psi}$

Note * - Conservatively active fuel length is used instead of panel length

For all loadings, the above pressure values are multiplied the g-load used.

D. Results

The maximum stress intensities resulting from the equivalent static analysis for the 30 g NCT maximum acceleration are summarized in Table A.2.13.8-12 for the critical components of the basket assembly. The larger of the top and bottom stresses across the thickness of the elements are taken as the maximum primary membrane plus bending stresses. All primary membrane stress intensities and primary plus secondary stress intensities meet the Service Level A allowable stress limits. For some components the $P_m + P_b$ stress intensities exceed the code allowable stress limits. These exceedances are localized and have characteristics of secondary stresses. Therefore, in accordance with the provisions of NG-3222 for Service Level A loads, the limit analysis provisions of NG-3228.2 are invoked. The results of the NG-3228.2 limit analysis evaluations are summarized Table A.2.13.8-13.

Per Table A.2.13.8-1, the calculated maximum acceleration for the 69BTH basket for the HAC free drop is 55.6g. Conservatively, the HAC analysis is performed using a maximum acceleration of 75g. Maximum stress intensities for 75 g maximum HAC drop accelerations are reported in Table A.2.13.8-14 for critical components of the assembly. The larger of the top and bottom stresses across the thickness of the elements are taken as the maximum primary membrane plus bending stresses.

The analysis is carried out with increasing loading until convergence can no longer be achieved. The load achieved at the last converged step is the buckling load. The buckling loads are summarized in Table A.2.13.8-15.

A.2.13.8.6.2 Basket End Drop

During an end drop, the fuel assemblies and fuel compartments are forced against the bottom of the canister/cask. Thus, for any vertical or near vertical loading, the fuel assemblies react directly against the bottom or top end of the canister/cask and not through the basket structure as in the case for lateral loading. It is the weight of the basket assembly that causes axial compressive

stress during an end drop. Axial compressive stresses are conservatively computed as if all the weight of the basket assembly will be taken by the compartment tubes and outer boxes only.

Furthermore, the end drop evaluation is performed for the maximum acceleration of 75g corresponding to the Service Level D HAC load and the resulting stress is evaluated against the NCT Service Level A stress allowable to bound both NCT and HAC loads.

Compressive Stress at Fuel Compartment Tubes and Outer Wrappers

Total Basket Assembly Weight: = 30.694 kips

Fuel compartment tubes and outer wrappers sectional area = 350.25 in²

Stress due to 1g = 30.694/350.25 = 0.0876 ksi

At 75g = - 0.088 ksi \times 75 = - 6.57 ksi < S_m @ 700 °F = 16.0 ksi

A.2.13.8.7 NUH24PTH

The details and description for the NUH24PTH basket is presented in Appendix A.1.4.3.

A.2.13.8.7.1 Basket Side Drop

A. Finite Element Model

An ANSYS [10] three-dimensional finite element model of the basket is constructed for NCT loads analysis using shell (SHELL43) and solid (SOLID45) elements. The overall finite element model of the 24PTH basket is shown in Figure A.2.13.8-4. The fuel compartment tubes, stainless steel transition rails, aluminum transition rails, and canister are included in the model. For conservatism, aluminum and poison plates in the basket are neglected by excluding these from the finite element model. However, the weight of these basket components is accounted for by increasing the material density for the fuel compartment tubes.

Because of the large number of plates in the basket and the large dimensions of the basket, certain modeling approximations were necessary. In view of continuous support of fuel compartment tubes by the peripheral rails along the entire basket length during a side drop, a 24 inch long slice of the basket and rail is modeled. At the two cut faces of the model, symmetry boundary conditions are applied (UZ = ROTX = ROTY = 0).

The gap elements (CONTACT 52) are used to simulate the interface between the fuel compartments, basket rails and the inner side of the canister as well as between the outer side of the canister and the inside of the cask/sleeve or sleeve rails (for 180-degree drop). Each gap element contains two nodes; one on each surface of the structure. The gap nodes specified at the inner side of the cask/sleeve and sleeve rails are restrained in the x, y and z directions. The gap size at each gap element is determined by the difference between the basket rails radius and the inside radius of the DSC shell; and by the difference between the outer side of the DSC shell radius and the inside radius of the cask/sleeve or sleeve rails.

A similar model is developed for HAC loads analyses using LS-DYNA [11]. LS-DYNA is used for the analysis of the 24PTH basket because of its robust contact algorithms which are able to

model contact between the different components of the basket assembly. A detailed description of the model is documented in Section P.3.6.1.3.1 of Reference [3], a summary is provided below.

The model uses fully integrated shell elements (with five integration points through the thickness) to represent the fuel compartment tubes, the steel insert plates (straps) that are welded to the tubes, and the R45 transition rails. Fully integrated solid elements are used for the aluminum R90 transition rails. The model is a 24-inch long section of the basket assembly. This span corresponds to the 24" periodicity of the basket assembly steel insert plates (straps) and strap-to fuel compartment tube welds, and to twice (12") the periodicity of the stiffener plates in the R45 transition rails. The steel insert (straps) plates, steel insert plates-to-tube welds, and a full thickness R45 transition rail stiffener plate are modeled at $Z=0.0''$. The model is extended half way to the next strap plate/weld location to $Z=+12''$ and $Z=-12''$. Half-thickness R45 stiffeners are included at the ends of the model ($Z=+12''$). The model includes a segment of the DSC shell, which is also modeled with fully integrated shell elements. The steel insert plates-to-tube welds are modeled with beam elements. Symmetry boundary conditions are applied at the $+Z$ faces of the model. At the $-Z$ face the model is unrestrained to permit axial thermal expansion.

The TC shell and TC rails, which are extremely rigid relative to the other parts of the structure, are included as rigid bodies and are fixed. Therefore, the TC shell is modeled with only one through-thickness element. Contact is specified between all adjacent surfaces throughout the model. Contact elements are included between the following interfacing components:

- Fuel compartment tubes to adjacent tubes
- Fuel compartment tubes to basket straps
- Fuel compartment tubes to transition rails,
- Transition rails to DSC shell ID, and
- DSC shell OD to TC ID and TC rails.

The heat conducting aluminum and neutron absorbing poison plates are not explicitly modeled (their weight is accounted for by adjusting the density of the materials used for the fuel compartment tubes and R45 transition rails). The thicknesses of the shell elements for the fuel compartment tubes and the R45 transition rails are adjusted to properly account for the contact that exists between these adjacent surfaces. Generally, contact is modeled using the LS-DYNA surface-to-surface contact algorithm, except for the contact between the edges of the R45 transition rail plates that interface with the DSC shell (including the stiffener plates), which is modeled using the nodes-to-surface contact algorithm.

B. Material Properties

SA-240, Gr. 304 stainless steel material properties are used for the stainless steel boxes and stainless steel transition rails; 6061-O aluminum alloy (annealed) material properties are used for the aluminum transition rails. Material properties are taken from ASME Section II, Part D [9] for steel components and for 6061-O (annealed) aluminum alloy the material properties are taken from Reference [12].

Bilinear stress-strain material relationships are used for the NCT elastic-perfectly plastic limit load analyses where the yield strength, $S_y = 1.5 S_m$ and $E_p/E = 0.0$ for the stainless steel components. For the aluminum components, the actual yield strength, S_y , and $E_p/E = 1\%$ is used.

Bilinear stress-strain relationships are used for the HAC elastic-plastic analyses, where the Code-defined yield strength, S_y , of the material is used for the stainless steel and aluminum components. The plastic modulus of elasticity is taken as 5% of the elastic modulus for the stainless steel components and 1% for the aluminum components..

C. Loading Conditions

The basket structure is analyzed for 0° , 30° , 45° and 180° azimuth side drops. Due to the basket structure symmetry, these orientations of side drops are considered to envelop all other possible drop orientations.

A fuel assembly weight of 11 lb/in is used in the analysis. A uniform fuel weight distribution is assumed over the entire length of the basket. The weight of the aluminum and poison plates are accounted for by increasing the material density of the fuel compartment tubes. The stiffness's of the un-modeled components are conservatively neglected in the analysis.

Material properties used in the stress analysis are at 700°F for the stainless steel components and 525°F for the aluminum rails.

The load resulting from the fuel assembly weight is applied as pressure on the fuel compartment plates of the basket. For the 0° and 180° orientation, the pressure acts only on the horizontal plates. For the 30° and 45° orientation, the pressure was divided into components that act on both horizontal and vertical plates of the basket. The pressures for all orientations are calculated below for 1g accelerations.

- At 0 and 180 degrees; Pressure, $p = \text{Fuel assembly wt. per unit length} / \text{Model Panel span}$
 $= 11.0 \text{ lb} / (8.9 + .25) = 1.202 \text{ psi}$
 - At 30° ; p_v on horizontal plates $= p \cos 30^\circ = 1.202 \times 0.866 = 1.041 \text{ psi}$
 p_h on vertical plates $= p \sin 30^\circ = 1.202 \times 0.5 = 0.601 \text{ psi}$
 - At 45° ; p_v on horizontal plates $= p \sin 45^\circ = 1.202 \times 0.7071 = 0.850 \text{ psi}$
 p_h on vertical plates $= p \cos 45^\circ = 1.202 \times 0.7071 = 0.850 \text{ psi}$

For all loadings, the above pressure values are multiplied the g-load used.

D. Results

The maximum stress intensities resulting from the 25 g NCT maximum acceleration are summarized in Table A.2.13.8-16 for the critical components of the basket assembly. Membrane (P_m), membrane-plus-bending ($P_m + P_b$), and range of primary + secondary ($P_m + P_b + Q$) stresses are reported for components modeled with ANSYS SHELL43 shell elements. The larger of the top and bottom stresses across the thickness of the shell elements are taken as the maximum primary membrane plus bending stresses. For some basket components the P_m and $P_m + P_b$

stress intensities exceed the code allowable stress limits. These exceedances are localized and have characteristics of secondary stresses. Therefore, in accordance with the provisions of NG-3222 for Service Level A loads, the limit analysis provisions of NG-3228.2 are used.

The results of the limit analysis are summarized in Table A.2.13.8-17.

Per Table A.2.13.8-1, the calculated maximum acceleration for the 24PTH basket for the HAC free drop is 55.6g. Conservatively, the HAC analysis is performed using a maximum acceleration of 75g.

The equivalent-static analyses performed for the Part 72 storage accident conditions for the 24PTH basket and documented in [3] used a bounding acceleration of 75g. This 75g acceleration bounds with significant margin the calculated 55.6g-load for the HAC drops, as shown in Table A.2.13.8-1. Therefore, the 75g analyses as described in Section P.3.7.4.3 [3] for the 24PTH baskets is applicable. The maximum stress intensities are summarized in Table A.2.13.8-18.

Since the analyses showed that a converged solution was attained at 75g, a conservative factor of safety against buckling for the 24PTH basket is 1.33 (75/56.6).

A.2.13.8.7.2 Basket End Drop

During an end drop, the fuel assemblies and fuel compartments are forced against the bottom of the canister/cask. Thus, for any vertical or near vertical loading, the fuel assemblies react directly against the bottom or top end of the canister/cask and not through the basket structure as in the case for lateral loading. It is the weight of the basket assembly that causes axial compressive stress during an end drop. Axial compressive stresses are conservatively computed as if all the weight of the basket assembly will be taken by the compartment tubes. Furthermore, the end drop evaluation is performed for the maximum acceleration of 75g corresponding to the Service Level D HAC load and the resulting stress is evaluated against the NCT Service Level A stress allowable.

Compressive Stress at Fuel Compartment Tubes

Basket Assembly Weight per tube (including aluminum and poison plates weights) = 800 lbs

Sectional Area per tube = 9.15 in²

Stress due to 1g = 800/9.15 = 0.087 ksi

At 75g = - 0.087 ksi × 75 = - 6.56 ksi < S_m @ 700 °F = 16.0 ksi

A.2.13.8.7.3 Fusion Welds

The most severe loading for the fusion welds are the HAC side drops. Loads on the welds connecting the steel insert plates (straps) and the fuel compartment tubes are evaluated using the beam element forces obtained from the HAC side drop analysis (Section P.3.7.4.3 of Reference [3]). On each face of the fuel tubes, two welds (beams) are modeled between the tube and the adjacent basket straps(s). The Resultant loads on the face of each fuel compartment tube are determined as follows:

$$F_{Resultant} = \sqrt{(F_{Ax}^1 + F_{Ax}^2)^2 + (F_{V1}^1 + F_{V1}^2)^2 + (F_{V2}^1 + F_{V2}^2)^2}$$

Where :

F_{Ax}^i = Axial force at weld element 'i'. Compressive forces are set to zero (0 lb) since compression loads will be transmitted by bearing through the parts and will not stress the welds.

F_{V1}^i = Shear force (Direction 1) at weld element 'i'.

F_{V2}^i = Shear force (Direction 2) at weld element 'i'.

The maximum steel insert plates (straps) to fuel compartment tube weld load is 18.8 kips (bounding of all drop orientations and all tube/insert plate locations).

A.2.13.8.8 NUH32PT Basket

The details and description for the NUH32PT basket are presented in Appendix A.1.4.2.

A.2.13.8.8.1 Basket Side Drop

A. Finite Element Model

An ANSYS [10] three-dimensional finite element model of the fuel basket is constructed using plane (PLANE42) elements. The overall finite element model of the 32PT basket with solid aluminum transition rails and 3-piece aluminum transition rails are shown in Figure A.2.13.8-5 and Figure A.2.13.8-6, respectively. The basket plates that make up the fuel compartment grid, the transition rail cover plates, the aluminum transition rails, and a section of the canister are included in the model. For conservatism, aluminum and poison plates in the basket are neglected by excluding these from the finite element model. However, the weight of these components is accounted for by increasing the material density of the plate material that makes up the fuel compartment grid.

The ANSYS finite element model uses PLANE42 elements to represent a unit length of the 32PT basket. Loads from fuel with appropriate drop g load multiplier and temperature are considered. Three elements through thickness of all parts except cask shell are used. The MP197HB Cask shell which is extremely rigid relative to the other parts is included. The 3 in wide and 0.12 inch thick Cask rails at $\pm 18.5^\circ$ and $\pm 38^\circ$ (two pairs) from the bottom of the Cask are also modeled using PLANE42 element.

Contact (CONTA171) and target (TARGE169) surface to surface contact elements are used between fuel support grid and transition rails, between transition rails and inner surface of the canister shell and between outer surface of canister shell and inner surface of the Cask.

The boundary condition of the model consists of restraining all nodes at the outer diameter of the Cask in both X and Y directions.

B. Material Properties

SA240, Type XM-19 stainless steel material properties are used for the fuel compartments and transition rail cover plates; 6061-O aluminum alloy (annealed) material properties are used for the aluminum transition rails. Material properties are taken from ASME Section II, Part D [9] for steel components and for 6061-O (annealed) aluminum alloy the material properties are taken from Reference [12].

Bilinear stress-strain material relationships are used for the NCT elastic-perfectly plastic limit load analyses where the yield strength, $S_y = 1.5 S_m$ and $E_p/E = 0.0$ for the stainless steel components. For the aluminum components, the actual yield strength, S_y , and $E_p/E = 1\%$ is used.

Bilinear stress-strain relationships are used for the HAC elastic-plastic analyses, where the Code-defined yield strength, S_y , of the material is used for the stainless steel and aluminum components. The plastic modulus of elasticity is taken as 5% of the elastic modulus for the stainless steel components and 1% for the aluminum components.

C. Loading Conditions

The basket structure is analyzed for 0° , 30° , 45° and 180° azimuth side drops. Due to the basket structure symmetry, these orientations of side drops are considered to envelop all other possible drop orientations.

A fuel assembly weight of 11 lb/in is used in the analysis. A uniform fuel weight distribution is assumed over the entire length of the basket. The weight of the aluminum and poison plates are accounted for by increasing the density of the plate material making up the fuel compartment grid.

Temperature dependent material properties are used and the temperatures from 100°F ambient case are applied to all nodes in the model.

The load resulting from the fuel assembly weight is applied as pressure on the fuel compartment plates of the basket. For the 0° and 180° orientation, the pressure acts only on the horizontal plates. For the 30° and 45° orientation, the pressure was divided into components that act on both horizontal and vertical plates of the basket. The pressures for all orientations are calculated below for 1g accelerations.

- At 0 and 180 degrees; Pressure, $p = \text{Fuel assembly wt. per unit length} / \text{Model Panel span}$

$$= 1.25 \text{ psi}$$
- At 30° ; p_v on horizontal plates $= p \cos 30^\circ = 1.25 \times 0.866 = 1.083 \text{ psi}$
 p_h on vertical plates $= p \sin 30^\circ = 1.25 \times 0.5 = 0.625 \text{ psi}$
- At 45° ; p_v on horizontal plates $= p \sin 45^\circ = 1.25 \times 0.7071 = 0.884 \text{ psi}$
 p_h on vertical plates $= p \cos 45^\circ = 1.25 \times 0.7071 = 0.884 \text{ psi}$

For all loadings, the above pressure values are multiplied the g-load used.

D. Results

Qualification of the 32PT basket for the NCT side drop load is demonstrated using the limit analysis provisions of NG-3228.2. Results are summarized in Table A.2.13.8-19 for the 32PT basket with solid aluminum transition rails and 3-piece aluminum transition rails.

In addition to performing a limit load analysis for NCT side drop, the basket components are qualified for Primary + Secondary stress intensities by performing linear elastic stress analyses for 25g side drop load combined with the bounding temperature distribution corresponding to the 100 °F ambient condition. For this analysis, the basket and canister shell material properties are assumed to be linear elastic. The aluminum transition rail material is assumed to be elastic-plastic with 1% strain hardening modulus. This assumption will result in conservative stresses in the basket components. The maximum stress intensities for the different components are as follows:

Fuel Support Grid	Max $P_m + P_b + Q = 53.15 \text{ ksi} < 84.6 \text{ ksi} (3S_m)$
Transition Rail Cover	Max $P_m + P_b + Q = 24.57 \text{ ksi} < 87.6 \text{ ksi} (3S_m)$
DSC Shell	Max $P_m + P_b + Q = 35.56 \text{ ksi} < 49.2 \text{ ksi} (3S_m)$

The equivalent-static analyses performed for the storage accident conditions for the 32PT basket and documented in [3] used a bounding acceleration of 75g. This 75g acceleration bounds with significant margin the calculated 55.6g-load for the HAC drops, as shown in Table A.2.13.8-1. Therefore, the 75g analyses as described in Section M.3.7.5.3 [3] for the 32PT baskets is applicable. The 75g side drop analyses are described in Section M.3.7.5.3 of [3]. The maximum stress intensities are summarized in Table A.2.13.8-20.

Since the side drop analyses in [3] showed that a converged solution at 75g, was attained a conservative factor of safety for buckling for the 32PT basket is 1.33 (75/56.6).

Welds in the fuel support structure are sized to maintain full moment capacity of the plates across all welded connections.

A.2.13.8.2 Basket End Drop

When subjected to end drop loads, the basket fuel support grid supports only its self weight. The fuel, neutron absorbing and aluminum heat transfer material will slide and will bear on the stop plates at the basket end. Also, the transition rails are full length and will be self supporting under end drop load.

The cross sectional area of each cell of the basket = $4 \times 8.825'' \times 0.25'' = 8.825 \text{ in}^2$

Length of the basket = 175 in

Therefore, weight of each cell = $8.825 \text{ in}^2 \times 175 \text{ in} \times 0.2853 \text{ lb/in}^3 = 440.61 \text{ lb}$

Axial stress for 1g drop load = $\sigma_a = 440.61/8.825 = 49.93 \text{ psi}$

Therefore, axial stress for NCT end drop load = $49.93 \times 25/1000 = 1.25 \text{ ksi}$

Axial stress for HAC end drop load = $49.93 \times 75/1000 = 3.75 \text{ ksi}$

The allowable axial compressive stress is 23.7 ksi for NCT load and 31.8 ksi for HAC load. The allowable bearing stress for NCT load is $S_y = 35.3$ ksi assuming a bounding 800 degree F. Calculation of bearing stresses for HAC drop load, is not required. Therefore, the computed compressive stress and bearing stress (for NCT load) in the fuel support grid are less than the allowable.

A.2.13.8.9 NUH32PTH and 32PTH Type 1/NUH32PTH1 Type 1 and Type 2 Baskets

A detailed description of the NUH32PTH and NUH32PTH1 baskets are presented in Appendix A.1.4.4 and Appendix A.1.4.5, respectively. There are two 32PTH basket types: the 32PTH and the 32PTH Type 1 basket. There are two 32PTH1 basket types: the 32PTH1 Type 1 and the 32PTH1 Type 2. These four baskets have similar fuel compartment geometry and materials, and except for the 32PTH1 Type 1 basket, the transition rails are made of welded stainless steel plates. The 32PTH1 baskets allow heavier fuel assemblies than the 32PTH baskets. Moreover, the 32PTH1 Type 1 basket with aluminum transition rails has a higher heat load capacity. Therefore, separate analyses are performed for this basket. Also, the fusion welds between fuel compartment tubes thru the insert plates (straps) for the 32PTH1 baskets are tested at a higher load than the fusion welds for the 32PTH baskets. Thus, analyses for 32PTH1 Type 2 basket bound 32PTH baskets except for the fusion welds.

A.2.13.8.9.1 Basket Side Drop

A. Finite Element Model

An ANSYS [10] three-dimensional finite element model of the basket is constructed using shell (SHELL43/SHELL181) and solid (SOLID45) elements. The overall finite element model of the 32PTH/32PTH1 (Type 2) and 32PTH1 Type 1 baskets is shown in Figure A.2.13.8-7. The fuel compartment tubes, the stainless steel transition rails (for the 32PTH, 32PTH Type 1, and 32PTH1 Type 2), the aluminum transition rails (for the 32PTH1 Type 1), and a segment of the canister are included in the model. For conservatism, aluminum and poison plates in the basket are neglected by excluding these from the finite element model. However, the weight of these components is accounted for by increasing the density for the fuel compartment tubes material.

Because of the large number of plates in the basket and large dimensions of the basket, certain modeling approximations were necessary. In view of continuous support of fuel compartment tubes by the peripheral rails along the entire basket length during a side drop, a 15 inch long slice of the basket and rail is modeled. At the two cut faces of the model, symmetry boundary conditions are applied ($U_Z = ROT_X = ROT_Y = 0$).

The nodes between the steel tubes are coupled together in the out-of-plane direction so that they will bend in unison under surface pressure or other lateral loading to simulate through the thickness support provided by wraps, aluminum and poison plates.

The gap elements (CONTACT 52) are used to simulate the interface between the basket rails and the inner side of the canister as well as between the outer side of the canister and the inside of the cask. Each gap element contains two nodes; one on each surface of the structure. The gap nodes specified at the inner side of the cask are restrained in the x, y and z directions. The gap size at

each gap element is determined by the difference between the basket rails radius and the inside radius of the cask inner shell; and by the difference between the outer side of the canister radius and the inside radius of the cask.

B. Material Properties

SA-240, Gr. 304 stainless steel material properties are used for the stainless steel boxes and stainless steel transition rails; 6061-O aluminum alloy (annealed) material properties are used for the aluminum transition rails. Material properties are taken from ASME Section II, Part D [9] for steel components and for 6061-O (annealed) aluminum alloy the material properties are taken from Reference [12].

Bilinear stress-strain material relationships are used for the NCT elastic-perfectly plastic limit load analyses where the yield strength, $S_y = 1.5 S_m$ and $E_p/E = 0.0$ for the stainless steel components. For the aluminum components, the actual yield strength, S_y , and $E_p/E = 1\%$ is used.

Bilinear stress-strain relationships are used for the HAC elastic-plastic analyses, where the Code-defined yield strength, S_y , of the material is used for the stainless steel and aluminum components. The plastic modulus of elasticity is taken as 5% of the elastic modulus for the stainless steel components and 1% for the aluminum components.

C. Loading Conditions

The basket structure is analyzed for 0° , 30° , 45° and 180° azimuth side drops. Due to the basket structure symmetry, these orientations of side drops are assumed to envelop all other possible drop orientations.

A fuel assembly weight of 11.86 lb/in is used in the analysis. A uniform fuel weight distribution is assumed over the entire length of the basket. The weight of the aluminum and poison plates are accounted for by increasing the density of the fuel compartment tube material. The stiffness's of the un-modeled components are conservatively neglected in the analysis.

The load resulting from the fuel assembly weight is applied as pressure on the fuel compartment plates of the basket. For the 0° and 180° orientation, the pressure acts only on the horizontal plates. For the 30° and 45° orientation, the pressure was divided into components that act on both horizontal and vertical plates of the basket.

$$P = g\text{-load} \times \text{fuel weight per inch} / \text{compartment width}$$

The above pressures are in the drop direction. The horizontal and vertical components of these pressures are applied appropriately to the horizontal and vertical inner surfaces of the fuel compartments. For all loadings, the above pressure values are multiplied the g-load used.

D. Results

The maximum stress intensities resulting from the equivalent static analysis for the 23.3 g NCT maximum acceleration are summarized in Table A.2.13.8-21 for the 32PTH1 Type 1 basket and Table A.2.13.8-22 for the 32PTH and 32PTH1 Type 2 baskets for critical components of the basket assemblies. Membrane (P_m), membrane-plus-bending ($P_m + P_b$), and range of primary plus secondary ($P_m + P_b + Q$) stresses are reported for components modeled with ANSYS SHELL43/SHELL181 plastic shell elements. The larger of the top and bottom stresses across the thickness of the shell elements are taken as the maximum primary membrane plus bending stresses. The stresses at sharp corners are neglected due to the unrealistic point contact loads they create. The actual 32PTH/32PTH1 baskets have rounded corners that could not generate these large point contact stresses. For some basket components the P_m , and/or $P_m + P_b$, and/or the $P_m + P_b + Q$ stress intensities exceed the code allowable stress limits based on elastic analysis. These exceedances are localized and have characteristics of secondary stresses. Therefore, in accordance with the provisions of NG-3222 for Service Level A loads, the limit analysis provisions of NG-3228.2 and the simplified elastic analysis provisions of NG-3228.3 are invoked and carried out.

Limit analyses per NG-3228.2 are performed to address the P_m and $P_m + P_b$ stress exceedances shown in Table A.2.13.8-21 and Table A.2.13.8-22. The results of the limit analysis are summarized in Table A.2.13.8-23. The results of the limit analysis show that a minimum factor of safety of 2.1 with respect to the lower bound collapse load, confirming the fact that the stress exceedances are localized and do not affect the overall structure. The simplified elastic-plastic analysis procedure, per NG-3228.3, is used to address the $P_m + P_b + Q$ stress exceedances. This evaluation is described in Section A.2.13.8.9.1.E below.

Maximum stress intensities resulting from the equivalent static analysis for the 55 g HAC maximum acceleration in the 32PTH1 Type 1 and Type 2 baskets are reported in Table A.2.13.8-24 and Table A.2.13.8-25, respectively, for critical components of the basket assembly.

To determine the buckling loads for the 32PTH1 baskets, the elastic-plastic analyses were carried out with increasing load until convergence was no longer achieved. The last load step with a converged solution is the buckling load of the model. The buckling loads are summarized in Table A.2.13.8-27.

The equivalent static analyses performed for the storage accident conditions for the 32PTH baskets and documented in [5] used a bounding acceleration of 75g. This 75g acceleration bounds with significant margin the calculated g-loads for the HAC drops, as shown in Table A.2.13.8-1. Therefore, the 75g analyses as described in Section 3.9.1.2.3.B.5 of Reference 5 are applicable. The maximum stress intensities are summarized in Table A.2.13.8-26.

The minimum buckling load of 83.9g for the 32PTH basket was calculated in Section 3.9.1.2.4 of Reference 5 and summarized in Table A.2.13.8-28. Therefore, the minimum factor of safety for buckling is 1.50 (83.9/56) for the 32PTH baskets.

E. Simplified Elastic-Plastic Analysis

As shown in Table A.2.13.8-21 and A.2.13.8-22, the stress intensities from the range of primary plus secondary stresses exceed the $3S_m$ stress limit for some basket components. These exceedances are addressed per ASME Code Section NG-3228.3, which stipulates that the $3 S_m$ limit on the range of primary plus secondary stress intensity (NG-3222.2) may be exceeded provided the requirements (a) through (f) are met. The bounding load case is the Alternate Type 2 Rail, 180° drop, Transition Rails, where $P_m + P_b + Q$ exceeds $3 S_m$ by 18%. This bounding case is evaluated against requirements (a) through (f) of NG-3228.3 here.

- (a) *The range of primary plus secondary membrane plus bending stress intensity, excluding thermal bending stresses, shall be $< 3 S_m$.*

The maximum primary plus secondary membrane plus bending stress intensity, excluding peak stresses is 45.97 ksi and the maximum thermal membrane stress $Q_{\text{membrane}} = 5.2$ ksi,

$$P_m + P_b + Q_{\text{membrane}} = 45.97 + 5.20 = 51.17 \text{ ksi}$$

which is less than $3 S_m = 51.83$ at 529 °F (max temperature in rails is 529 °F)

- (b) *The value of S_a used for entering the design fatigue curve is multiplied by the factor K_e where:*

$$\begin{aligned} K_e &= 1.0 \text{ for } S_n < 3 S_m \\ &= 1.0 + [(1 - n)/n/(m - 1)](S_n / 3S_m - 1), \text{ for } 3S_m < S_n < 3mS_m \\ &= 1.0 + [(1 - 0.3)/(0.3 \times (1.7 - 1))] \times (60.47 / 51.83 - 1) \\ &= 1.56 \\ &= 1/n, \text{ for } S_n > 3mS_m \end{aligned}$$

$$n = 0.3 \text{ (Table NG-3228.3(b)-1)}$$

$$m = 1.7 \text{ (Table NG-3228.3(b)-1)}$$

$$S_n = \text{Range of primary plus secondary stress intensity} = 60.47 \text{ ksi}$$

The values of material parameters m and n for the various classes of permitted materials are given in Table NG-3228.3(b)-1.

The range of primary plus secondary stress intensity is set to the maximum stress intensity is 60.47 ksi. Conservatively using ten cycles (for the stress range considered here; the 1 foot normal condition free drop should never occur), the value of 700 ksi is taken for S_a from Figure I-9.2.1 of the ASME code [2].

$$S_a = 700 \text{ ksi. (when number of cycles} = 10)$$

This value of S_a is used in the next section.

- (c) *The rest of the fatigue evaluation stays the same as required in NG-3222.4, except that the procedure of NG-3227.6 need not be used.*

The maximum stress identified above, multiplied by K_e

$$60.47 \text{ ksi} \times 1.56 = 94.3 \text{ ksi}$$

This value is much less than $S_a = 700 \text{ ksi}$. OK

The maximum temperature difference between adjacent points for both the startup and shutdown and normal service is determined as follows.

As stated above the value for S_a is conservatively taken to be 700 ksi. The instantaneous coefficient of thermal expansion, α , and Young's Modulus, E , are $9.8 \times 10^{-6} \text{ in./in./}^\circ\text{F}$ and 25.3×10^6 respectively. The values of α and E are evaluated at 600° F , which is an approximate mean temperature of the basket and conservatively bounds the transition rails. Therefore, the maximum allowable temperature difference between adjacent points is:

$$S_a / (2\alpha E) = 1412^\circ \text{ F}$$

The maximum temperature difference between adjacent points is well below this. Therefore, the requirements of NG-3228.3(c) are met.

- (d) *The structure meets the ratcheting requirements of NG-3222.5.*

Thermal ratcheting can only occur with cyclic loading. The thermal induced stresses in the basket are due to a single occurrence. Therefore, no thermal ratcheting is possible.

- (e) *The temperature does not exceed those listed in Table NG-3228.3(b)-1 for various classes of material.*

The maximum temperature for all basket components are less than the allowable range of 700° F . Therefore, paragraph NG-3228.3(e) of the ASME code does not apply.

- (f) *The material shall have a specified minimum yield strength to specified minimum tensile strength ratio of less than 0.80.*

The yield to tensile strength ratio for the fuel compartments is listed below. Therefore the requirements of NG-3228.3(f) are satisfied.

$$\text{at } 550^\circ \text{ F } S_y/S_u = 18.9/63.4 = 0.30 < 0.80$$

$$\text{at } 700^\circ \text{ F } S_y/S_u = 17.6/63.4 = 0.28 < 0.80$$

A.2.13.8.9.2 Basket End Drop

The stress in the 32PTH1 basket fuel compartments and transition rails are evaluated for conservatively high loads of 25 g for normal condition and 75 g for accident condition end drops by hand calculation. Only the alternate type 2 rails are evaluated for stress, since the alternate type 1 rails are solid aluminum, which must only carry their own inertial load. The inertial load of the fuel compartments, stainless steel straps and aluminum / poison plates is transferred to the

DSC end plates by the fuel compartments. The inertial load of the transition rails are carried by the rails themselves, because the holes for the rail attachment studs are slotted to provide clearance to allow for thermal expansion. The inertial load of the fuel assemblies are transferred directly to the DSC end plates and are not carried by the basket structure.

The stresses in the fuel compartments and transition rails for the 25 g normal condition end drop are computed by dividing the 25 g inertial load by the relevant cross section area, in the following table.

Basket Component	25 g Inertial Load (lb.)	Cross Section Area (in ²)	Calculated Component Stress (ksi)	Allowable Membrane Stress (ksi)
Fuel Compartments	25 g × 18,375 = 459,375	179.74	2.56	16.00
R45 Rails	25 g × 814.5 = 20,363	11.84	1.72	16.95
R90 Rails	25 g × 1,171 = 29,275	17.47	1.68	16.95

The stresses in the fuel compartments and transition rails for the conservatively high 75 g accident condition end drop are computed by dividing the 75 g inertial load by the relevant cross section area, in the following table.

Basket Component	75 g Inertial Load (lb.)	Cross Section Area (in ²)	Calculated Component Stress (ksi)	Allowable Membrane Stress (psi)
Fuel Compartments	75 g × 18,375 = 1,378,125	179.74	7.67	44.38
R45 Rails	75 g × 814.5 = 61,088	11.84	5.16	44.38
R90 Rails	75 g × 1,171 = 87,825	17.47	5.03	44.38

A.2.13.8.9.3 Fusion Welds

The most severe loading for the fusion welds are due to the HAC side drops. Loads on the welds connecting the steel insert plates (straps) and the fuel compartment tubes are evaluated using the beam element forces obtained from the HAC side drop analysis performed. Basket fusion weld forces are calculated for each of the four drop orientations for the 32PTH1 Type 1 and Type 2. The combined fusion weld loads are computed by SRSS using the following formula.

$$F_{TOTAL} = \sqrt{F_X^2 + F_Y^2 + F_Z^2}$$

Where, F_X , F_Y and F_Z are the beam element loads in the global X , Y and Z directions computed by ANSYS. The maximum weld load in a single weld is 13.0 kips (bounding of all drop orientations and all tube/insert plate locations) for the 32PTH1 baskets.

The maximum weld load in a single weld is 7.2 kips (bounding of all drop orientations and all tube/insert plate locations) for the 32PTH baskets, which is calculated in Section 3.9.1.2.3.B.5 of Reference [5].

A.2.13.8.10 NUH37PTH Basket

The details and description for the NUH37PTH basket are presented in Appendix A.1.4.6.

A.2.13.8.10.1 Basket Side Drop

A. Finite Element Model

An ANSYS [10] three-dimensional finite element model of the fuel basket is constructed using shell (SHELL43) and solid (SOLID45) elements. The overall finite element model of the 37PTH fuel basket is shown in Figure A.2.13.8-8. The stainless steel plates that make up the fuel compartment grid, the aluminum transition rails, and a segment of the canister shell are included in the model. For conservatism, the strength of the aluminum and poison plates in the basket are neglected by excluding these from the finite element model. However, their weights are accounted for by increasing the density of the grid plate material.

Because of the large number of plates in the basket and large dimension of the basket, certain modeling approximations were necessary. In view of continuous support of fuel compartment tubes by the peripheral rails along the entire basket length during a side drop, only 1.0 inch long slice of the basket and rail is modeled. At the two cut faces of the model, symmetry boundary conditions are applied ($U_Z = ROT_X = ROT_Y = 0$).

Gap elements (CONTAC 52) are used to simulate the interface between the stainless steel plates and aluminum transitional rails.

Gap elements (CONTACT 52) are used to simulate the interface between the basket rails and the inner side of the canister as well as between the outer side of the canister and the inside of the cask. Each gap element contains two nodes; one on each surface of the structure. The gap nodes specified at the inner side of the cask are restrained in the x, y and z directions. The gap size at each gap element is determined by the difference between the basket rails radius and the inside radius of the cask inner shell; and by the difference between the outer side of the canister radius and the inside radius of the cask.

B. Material Properties

SA-240, Gr. 304 stainless steel material properties are used for the stainless steel plates; 6061-O aluminum alloy (annealed) material properties are used for the aluminum transition rails. Material properties are taken from ASME Section II, Part D [9] for steel components and for 6061-O (annealed) aluminum alloy the material properties are taken from Reference [12].

Bilinear stress-strain material relationships are used for the NCT elastic-perfectly plastic limit load analyses where the yield strength, $S_y = 1.5 S_m$ and $E_P/E = 0.0$ for the stainless steel components. For the aluminum components, the actual yield strength, S_y , and $E_P/E = 1\%$ is used.

Bilinear stress-strain relationships, with plastic modulus of 1%, are used for the HAC elastic-plastic analyses for stainless steel and aluminum components. Strain rates are taken into account for SA-240, Gr. 304 where the Code-defined yield strength, S_y , is multiplied by the factors for 22 in/in/sec strain rate in Table 2 of Reference [13].

C. Loading Conditions

The basket structure is analyzed for 0°, 30°, 45°, 90° and 180° azimuth side drops. Due to the basket structure symmetry, these orientations of side drops are assumed to envelop all other possible drop orientations.

The weight of the aluminum and poison plates are accounted for by increasing the density of the fuel boxes. The stiffness's of the un-modeled components are conservatively neglected in the analysis.

A bounding fuel assembly weight per inch, 10.56 lbs /in, in the active fuel region is calculated for all fuel assemblies for the 37PTH by assuming all of the empty fuel rod spaces are filled with steel rods, $\rho = 0.29 \text{ lb/in}^3$.

The material properties used in the NCT analyses are at 600 °F for the stainless steel plates and 500 °F for the aluminum rails and canister. For HAC analyses temperature dependent material properties are used and the temperatures from 100 °F ambient case are applied to all nodes in the model.

The load resulting from the fuel assembly weight is applied as pressure on the fuel compartment plates of the basket. For the 0° and 180° orientation, the pressure acts only on the horizontal plates. For the 30° and 45° orientation, the pressure was divided into components that act on both horizontal and vertical plates of the basket.

$$P = g\text{-load} \times \text{fuel weight per inch} / \text{compartment width}$$

The above pressures are in the drop direction. The horizontal and vertical components of these pressures are applied appropriately to the horizontal and vertical inner surfaces of the fuel compartments. For all loadings, the above pressure values are multiplied the g-load used.

D. Results

The maximum stress intensities resulting from the equivalent static analysis for the 25 g NCT maximum acceleration are summarized in Table A.2.13.8-29 for the critical components of the basket assembly. The larger of the top and bottom stresses across the thickness of the shell elements are taken as the maximum membrane plus bending stresses. The primary membrane stresses and the primary plus secondary stresses for all the reported basket components meet the Service Level A allowable stress limits. For some components the $P_m + P_b$ stress intensities exceed the code allowable stress limits. These exceedances are localized and have characteristics

of secondary stresses. Therefore, in accordance with the provisions of NG-3222 for Service Level A loads, the limit analysis provisions of NG-3228.2 are used.

Limit analyses per NG-3228.2 are performed to address the $P_m + P_b$ stress exceedances shown in Table A.2.13.8-29. The results of the limit analysis are summarized in Table A.2.13.8-30.

Maximum stress intensities at 55 g for HAC are reported in Table A.2.13.8-31 for critical components of the assembly. Maximum bending-plus-membrane stresses are assumed to be the larger of top and bottom layer stresses.

To determine the buckling loads for the 37PTH basket, the elastic-plastic analyses were carried out with increasing load until convergence was no longer achieved. The last load step with a converged solution is the buckling load of the model. The buckling loads are summarized in Table A.2.13.8-32.

Welds in the fuel support structure are sized to maintain full moment capacity of the plates across all welded connections.

A.2.13.8.10.2 Basket End Drop

During an end drop, the fuel assemblies and fuel compartments are forced against the bottom of the canister/cask. Thus, for any vertical or near vertical loading, the fuel assemblies react directly against the bottom or top end of the canister/cask and not through the basket structure as in lateral loading. It is the weight of the basket assembly that causes axial compressive stress during an end drop. Axial compressive stresses are conservatively computed as all the weight of the poison and aluminum plates will be taken by the stainless steel plates only.

Compressive Stress at Fuel Compartment Tubes

Total Basket Assembly Weight: = 11.9 kips

Sectional Area = 295.1 in²

Stress due to 1g = 11.9 / 295.1 = 0.04026 ksi

At 75g = 0.04026 ksi × 75 = 3.0 < S_m @ 600 °F = 16.6 ksi

Normal Conditions are bounded

Compressive Stress at Aluminum Rails

Total Basket Rail Weight: = 11.4 kips

Sectional Area = 688.7 in²

Stress due to 1g = 11.4 / 688.7 = 0.0165 ksi

At 25g = 0.0165 ksi × 25 = 0.4 ksi < S_y @ 500 °F = 5.5 ksi

Aluminum rails at accident loads are not evaluated since the rail bodies are captured between the fuel compartment tubes and DSC shell thus large displacement of the rails are prevented.

A.2.13.8.11 NUH24PT4 Basket

The details and description for the NUH24PT4 basket are presented in Appendix A.1.4.1.

A.2.13.8.11.1 Spacer Disk

A. Side Drop

An ANSYS [10] three-dimensional finite element model of the spacer disk is constructed using solid (SOLID45) elements and shell (SHELL43) elements. The overall finite element model of the 24PT4 spacer disk is shown in Figure A.2.13.8-9. The spacer disk and a segment of the canister are included in the model.

The ANSYS finite element model uses SOLID45 elements to represent a half of the spacer disk. Loads from fuel with appropriate drop g load multiplier and temperature are considered.

Contact (CONTAC52) elements are used between the spacer disk and inner surface of the canister shell and between outer surface of canister shell and inner surface of the Cask.

The boundary condition of the model consists of restraining all nodes at the outer diameter of the Cask in both X and Y directions and since half of the spacer disk is modeled symmetry boundary conditions are applied at the symmetry boundary ($U_Z = 0$).

SA-533 Grade B steel material properties are used for the spacer disk and SA-240, Gr. 304 stainless steel material properties are used for the canister. Material properties are taken from ASME Section II, Part D [9].

Bilinear stress-strain material relationships are used for the NCT elastic-perfectly plastic limit load analyses where the yield strength, $S_y = 1.5 S_m$ and $E_p/E = 0.0$ for the stainless steel components.

Bilinear stress-strain relationships are used for the HAC elastic-plastic analyses, where the Code-defined yield strength, S_y , of the material is used. The plastic modulus of elasticity is taken as 5% of the elastic modulus.

Bilinear stress-strain curves are used for shakedown analyses where $S_y = S_y$ and $E_p/E = 0.0$ for all components.

The basket structure is analyzed for 0° , 30° , 45° and 180° azimuth side drops. Due to the basket structure symmetry, these orientations of side drops are assumed to envelop all other possible drop orientations.

A fuel assembly weights of 11.28 lb/in and 11.74 lb/in are used for the interior type "Y" and exterior type "X" holes, respectively, in the analysis, these weights include the weight of the guide sleeve assemblies. A uniform fuel weight distribution is assumed over the entire length of the basket. The weight of the support rod assemblies are included as MASS21 elements. The stiffness's of the un-modeled components are conservatively neglected in the analysis.

The load resulting from the fuel assembly and guidesleeve assembly weight is applied as pressure on the fuel compartment plates of the basket. For the 0° and 180° orientation, the pressure acts only on the horizontal plates. For the 30° and 45° orientation, the pressure is divided into components that act on both horizontal and vertical plates of the basket.

$$P = g\text{-load} \times (\text{fuel} + \text{guidesleeve weight per inch}) \times \text{distance between spacer disks} / \text{spacer grid ligament area}$$

The above pressures are in the drop direction. The horizontal and vertical components of these pressures are applied appropriately to the horizontal and vertical inner surfaces of the fuel compartments. For all loadings, the above pressure values are multiplied the g-load used.

The maximum stress intensities resulting from the equivalent static analysis for the 20 g NCT are reported in Table A.2.13.8-33 for the spacer disk. Stresses are linearized using ANSYS PPATH and PRSECT commands at critical locations. The maximum $P_m + P_b$ stress intensities shown are a combination of $P_m + P_b$ and secondary stresses. To further qualify the $P_m + P_b$ stresses, limit analyses per NG-3228.2 were performed. The results are summarized in Table A.2.13.8-34.

Since the secondary stresses for the spacer disk are above the $3S_m$ limit, shakedown analyses (NG-3213.17) are performed to qualify the spacer disk for secondary stresses. The yield strength of carbon steel (SA-533 Grade B) is increased by a factor of 1.2682 based on strain rate of 1 in/in, which is obtained from Reference [7]. Fuel weight is applied as a vertical downward pressure on the spacer disc ligament for 0° and 180° drop on two pairs of rail case. For 30° and 45° drop orientations these pressures are applied as gradient (slope) pressure which is linearly varying (0 at start to max along drop corners) in a triangular fashion. The drop loads are applied and removed for 10 cycles and it is shown that the deformation is stable for the end of the 9th and 10th cycle and that there is no plastic strain in the 10th cycle. Therefore, the spacer disk is qualified for secondary stresses.

Quasi-static analyses at 75g were used to qualify the 24PT4 baskets for the Part 72 storage license [8]. 75g bounds the g-loads for the HAC drops thus these analyses bound the analyses for HAC drops. The 75g analyses are described in Section A.3.6.1.2 [8]. The maximum stress intensities are summarized in Table A.2.13.8-35.

Since the analyses converged till 75g, the minimum factor of safety for buckling is 1.34 (75/56).

B. End Drop

The weight of the fuel and guidesleeve assemblies is supported by the DSC inner cover plate. Therefore, the vertical deadweight analysis of the basket assembly does not need to consider the effect of the fuel weight. The spacer disc by itself is evaluated for out-of-plane loads.

The out-of-plane model is a 90° (quarter-symmetry) model developed using ANSYS Shell43 elements. A typical model is shown in Figure A.3.6-6. The out-of-plane model is used for the vertical dead weight and end drop analyses. The fuel does not load the spacer discs out of plane;

therefore, no fuel loads are applied to the spacer disc. Analyses were performed modeling the connection between the spacer disc and the support rod as both pinned and fixed to determine bounding spacer disc stresses.

Stress intensities at the mid-thickness of the element are classified as general membrane stress, P_m . Stress intensities at the element surfaces (top and bottom) are classified as primary membrane plus bending, $P_m + P_b$. These values are used directly in the compliance evaluations of primary stress.

The maximum membrane and membrane plus bending stresses for normal condition end drops (25g) are 8.75 ksi and 35.25 ksi, respectively, which are below the allowable stresses of 26.7 ksi and 40.1 ksi.

The maximum membrane and membrane plus bending stresses for HAC end drops (75g) are 20.2 ksi and 61.6 ksi, respectively, which are below the allowable stresses of 56 ksi and 72 ksi.

A.2.13.8.11.2 Guide Sleeve Assemblies

The guide sleeve assemblies consist of guide sleeve tubes, over sleeves, and shim plates, fabricated from SA-240, Type 304 stainless steel. In addition, neutron absorber plates are sandwiched between the guide sleeves and over sleeves. Depending on its location in the basket, each guide sleeve assembly contains two or four neutron absorber plates such that there are two absorber plates between any two adjacent SFAs. The neutron absorber plates are not welded or bolted to the stainless steel guide sleeve, but are held in place by the geometry of the over sleeves and the shim plates. The over sleeves and shim plates are welded to the guide sleeves.

The structural component of the guide sleeve assembly is the guide sleeve tube. The neutron absorber plates provide criticality control only and are not used for structural support. No credit is taken for the structural capacity of the neutron absorber plates.

Stress analyses of the guide sleeve assemblies are performed using a combination of closed-form calculations and finite element analyses using an ANSYS model of the guide sleeve. Elastic analyses are used for normal conditions, whereas elastic-plastic analyses are used for the postulated side drop accident load case.

An enveloping temperature of 700°F is used for the analyses of the guide sleeve assemblies.

Lateral loads on the guide sleeve assemblies are evaluated using an ANSYS model of the guide sleeve, 27g is used for NCT side drop and 75g is used for HAC side drop. In the ANSYS analyses, the load from the fuel is applied as a uniform pressure on the guide sleeve panels, without taking credit for the structural capacity of the fuel assemblies, the over sleeves, or the neutron absorber panels. The maximum stresses on the guide sleeves are summarized in Table A.2.13.8-36.

The guide sleeves are free-standing in the DSC basket. They are not attached to any part of the basket or shell. Thus, for axial loading the sleeves are supported by bearing on the canister, and are loaded by self weight and appropriate accelerations only. Stability of the guide sleeves is assessed by evaluation of both overall guide sleeve stability and single panel stability in addition

to the stress criteria of ASME Code Subsection NG. Overall stability is evaluated by considering the guide sleeve as a column under axial loads, laterally supported at the spacer discs, and applying the column stability criteria of NF-3322.1 [14] and F-1334.3 [2]. Panel stability is evaluated using equations from Roark [15] for plates under in-plane loading. The maximum stresses on the guide sleeves are summarized in Table A.2.13.8-37.

A.2.13.8.11.3 Support Rod Assemblies

The 24PT4-DSC support rod assemblies, including the support rods, spacer sleeves and support rod to spacer sleeve mechanical connections, are analyzed using the criteria of Subsection NF and Appendix F for linear component supports. The criteria of NF-3322.1(e)(1) and F-1334.5 for combined axial compression and bending are applied to the spacer sleeves. The (tension only) rods are evaluated using the criteria of NF-3322.1(a) and F-1334.1.

An enveloping temperature of 600°F is used for the analyses of the support rod assemblies.

The support rod assembly analyses are simplified by the following:

- (a) the support rod assemblies are unaffected by pressure loads, and
- (b) thermal expansion of the support rod assemblies is not constrained by the 24PT4-DSC

Lateral loads on the support rod assemblies are evaluated using hand calculations, 30g is used for NCT side drop and 100g is used for HAC side drop.

For loads transverse to the axis of the DSC, the rod assemblies are loaded by self (and inertial) weight. Maximum axial and bending stresses are calculated in the support rods and spacer sleeves based on span length and support conditions. The maximum stresses on the support rod assemblies are summarized in Table A.2.13.8-38.

Analysis for axial loading is based on a combination of ANSYS analysis and hand calculations. A simple ANSYS beam model is used to determine the loads and load distribution in the support rod system. Hand calculations are used to calculate the stresses and to demonstrate the acceptability of the system.

Under most loading conditions the support rods carry only tensile loads. Under end drop conditions, compressive loads on the spacer sleeves are such that “preload” in the rod is relieved and the rod may be subjected to compressive loads from its own self weight/inertia (i.e., the rod must support its own self load in compression). Under all conditions, stability of the rod is ensured since it is laterally supported along its entire length (by the spacer sleeves).

The spacer sleeves carry all the compressive and bending loads. The distributions of the compressive and bending loads are calculated by ANSYS analyses. The stress checks for the spacer sleeves are performed using the interaction equations of NF-3322.1(e)(1). The maximum interaction values are summarized in Table A.2.13.8-39.

A.2.13.8.12 Basket Deformations for Effect of Criticality Analyses

To evaluate the effect of basket deformation on the criticality analysis in Chapter A.6, it is necessary to know the plastic deformations of the basket. For this purpose, the relative deflections in the critical fuel compartments during side drops are calculated. The maximum deflections of all the inner and peripheral fuel compartments except for the 37PTH baskets are below the following deflections.

Basket	24PTH	24PT4	32PTH1	32PTH	32PT	37PTH	61 BTH	61 B	69BTH
Inner compartment Deflections (in.)	0.10	0.10	0.05	0.05	0.08	0.02	0.10	0.10	0.05
Outer compartment Deflections (in.)	0.10	0.10	0.08	0.09	0.15	0.10	0.10	0.10	0.10

The criticality analyses (Section A.6.5.7.4) assumes that the worst location for all of the fuel assemblies in the 37PTH basket are when they are all positioned closest to each other relative to the center of the basket, thus any deformation which will cause the fuel assemblies to move further apart is covered by the criticality analysis. Therefore, for the 37PTH basket the relative deformation of the basket is calculated for the fuel compartments which will cause the fuel to move closer together. The average relative permanent deformations of the fuel compartments which will cause the fuel assemblies to move closer together are equal to or less than 0.01 in. Figure A.2.13.8-11 shows the permanent deformation of the 37PTH basket after the bounding HAC 45° side drop.

A.2.13.8.13 References

1. American Society of Mechanical Engineers, ASME Boiler and Pressure Vessel Code, Section III, Subsection NG, see Chapter A.2, Section A.2.1.2.1 for applicable editions.
2. American Society of Mechanical Engineers, ASME Boiler and Pressure Vessel Code, Section III, Appendices, see Chapter A.2, Section A.2.1.2.1 for applicable editions.
3. Updated Final Safety Analysis Report for the Standardized NUHOMS[®] Horizontal Modular Storage System for Irradiated Nuclear Fuel, NUH-003, Rev. 10.
4. Manual of Steel Construction, American Institute of Steel Construction, 9th Edition, 1990.
5. Final Safety Analysis Report for NUHOMS[®] HD Horizontal Modular Storage System for Irradiated Nuclear Fuel, Rev. 1.
6. The Draft Certificate of Compliance (CoC) and Preliminary Safety Evaluation Report for Amendment 10 to Part 72 CoC 1004 were issued on February 12, 2009.
7. BMI-1954 "A Survey of Strain-Rate Effects for Some Common Structural Materials used in Radioactive Material Packaging and Transportation Systems," Topical Report, August, 1976.
8. Updated Final Safety Analysis Report for the Standardized Advanced NUHOMS[®] Horizontal Modular Storage System for Irradiated Nuclear Fuel, ANUH-01.0150, Rev. 3.
9. American Society of Mechanical Engineers, ASME Boiler and Pressure Vessel Code, Section II, Part D, see Chapter A.2, Section A.2.1.2.1 for applicable editions.
10. ANSYS Engineering Analysis System, User's Manual for ANSYS Rev 8.1 and 10.
11. LS-DYNA Version 960 Keyword User's Manual, Non Linear Dynamic Analysis.
12. Kaufman, J.G., ed., "Properties of Aluminum Alloys: Tensile, Creep, and Fatigue Data and High and Low Temperatures," The Aluminum Association (Washington, D.C.) and ASM International (Metals Park, Ohio), 1999.
13. Blandford, Robert K. and Spencer D. Snow, "Impact Testing of Stainless Steel Material at Cold Temperatures," 2008 ASME Pressure Vessels and Piping Division Conference, Chicago, Illinois (PVP2008-61215).
14. American Society of Mechanical Engineers, ASME Boiler and Pressure Vessel Code, Section III, Subsection NF, see Chapter A.2, Section A.2.1.2.1 for applicable editions.
15. W.C. Young, Roark's Formulas for Stress and Strain, Sixth Edition, McGraw Hill, New York, N.Y., (1989).

Table A.2.13.8-1
Summary of Impact G-loads for Basket Analyses

Type	Drop Orientation	MP197HB G Loads		Analyzed G Loads	
		Normal Condition	Accident Condition	Normal Condition	Accident Condition
NUH24PT4 ⁽¹⁾	End Drop	sd - 18 x 1.36 = 24.5 gs - 18 x 1.00 = 18.0 sr - 18 x 1.33 = 23.9	sd - 55 x 1.31 = 72.1 gs - 55 x 1.00 = 55.0 sr - 55 x 1.17 = 64.4	sd - 25 g gs - 30 g sr - 30 g	sd - 75 g gs - 75 g sr - 65 g
	Side Drop	sd - 19 x 1.05 = 20.0 gs - 19 x 1.00 = 19.0 sr - 19 x 1.04 = 19.8	sd - 55 x 1.00 = 55.0 gs - 55 x 1.00 = 55.0 sr - 55 x 1.01 = 55.6	sd - 21 g gs - 27 g sr - 30 g	sd - 75 g gs - 75 g sr - 100 g
NUH24PTH	End Drop	18 x 1.00 = 18.0	55 x 1.25 = 68.8	25 g	75 g
	Side Drop	19 x 1.13 = 21.5	55 x 1.01 = 55.6	25 g	75 g
NUH32PT	End Drop	18 x 1.00 = 18.0	55 x 1.25 = 68.8	25 g	75 g
	Side Drop	19 x 1.26 = 23.9	55 x 1.01 = 55.6	25 g	75 g
NUH32PTH	End Drop	18 x 1.00 = 18.0	55 x 1.25 = 68.8	23.3 g	75 g
	Side Drop	19 x 1.13 = 21.5	55 x 1.01 = 55.6	23.3 g	75 g
NUH32PTH1	End Drop	18 x 1.00 = 18.0	55 x 1.25 = 68.8	23.3 g	75 g
	Side Drop	19 x 1.13 = 21.5	55 x 1.01 = 55.6	23.3 g	55 g
NUH37PTH	End Drop	18 x 1.00 = 18.0	55 x 1.25 = 68.8	25 g	75 g
	Side Drop	19 x 1.25 = 23.8	55 x 1.00 = 55.0	25 g	55 g
NUH61BT	End Drop	18 x 1.00 = 18.0	55 x 1.25 = 68.8	25 g	75 g
	Side Drop	19 x 1.05 = 20.0	55 x 1.00 = 55.0	30 g	75 g
NUH61BTH	End Drop	18 x 1.00 = 18.0	55 x 1.25 = 68.8	25 g	75 g
	Side Drop	19 x 1.05 = 20.0	55 x 1.00 = 55.0	30 g	75 g
NUH69BTH	End Drop	18 x 1.00 = 18.0	55 x 1.25 = 68.8	30 g	75 g
	Side Drop	19 x 1.06 = 20.1	55 x 1.01 = 55.6	30 g	75 g

Note 1. sd - spacer disk; gs - guide sleeve assembly; sr - support rod assembly

Table A.2.13.8-2
Basket NCT Load Combinations

Load Case	Individual Loads ⁽¹⁾			
	1 Ft Side Drop	1 Ft End Drop	Thermal Hot	Thermal Cold
1	X		X	
2	X			X
3		X	X	
4		X		X
5			X	
6				X

1. All stresses due to different individual load (except thermal hot and cold) are calculated using material properties (E) from thermal hot condition. However, thermal stresses due to thermal gradient from load steps of thermal hot and cold will be calculated using actual temperature distribution from thermal runs and combined with the different individual loads.

Table A.2.13.8-3
Basket HAC Load Combinations

Load Case	Individual Loads ⁽¹⁾		
	30 Ft Side Drop	30 Ft Bottom End Drop	Thermal Hot/Cold
7	X		X
8		X	X
9			X

1. All stresses due to different individual load (except thermal hot and cold) are calculated using material properties (E) from thermal hot condition. For Level D accident loads, no thermal stresses due to thermal gradient from load steps of thermal hot and cold are required to be calculated and combined with the individual loads.

Table A.2.13.8-4
Basket Stress Limits

Stress Category	Allowable Stresses	
	Normal Conditions ⁽¹⁾	Accident Conditions ⁽²⁾⁽³⁾
Primary Membrane General P_m Local P_L	S_m $1.5 S_m$	Lesser of $2.4 S_m$ or $0.7 S_u$ $3.6 S_m$ or S_u
Primary Membrane + Bending $(P_m \text{ or } P_L) + P_b$	$1.5 S_m$	Lesser of $3.6 S_m$ or S_u
Range of Primary + Secondary $(P_m \text{ or } P_L) + P_b + Q$	$3.0 S_m$	Not applicable
Bearing Stress	S_y	Not applicable
Max. Primary Shear Stress	$0.8 S_m$	$0.42 S_u$
Buckling	N/A	See Section A.2.13.8.4

Notes:

1. Classification and stress limits are as defined in ASME Code, Section III, Subsection NG. Limit analysis specified in Section NG-3228.2 also can be used for structural evaluation of the basket. Simplified elastic-plastic analysis specified in Section NG-3228.3 also can be used for structural evaluation of the basket. Shakedown analysis specified in NG-3228.1 also can be used for structural evaluation of the basket.
2. Classification and stress limits are as defined in ASME Code, Section III, Appendix F.
3. When evaluating the results from the nonlinear elastic-plastic analysis for the accident conditions, the general primary membrane stress intensity, P_m , shall not exceed greater of $0.7 S_u$ or $S_y + 1/3 (S_u - S_y)$ and the maximum primary stress intensity at any location (P_L or $P_L + P_b$) shall not exceed $0.9 S_u$. These limits are in accordance with Appendix F of Section III of the Code.

Table A.2.13.8-5
NUH61BT/61BTH Type 1 Normal Condition - Maximum Stress Summary

Drop Orientation	Component	Stress Category	Maximum Stress (ksi)	Allowable Stress (ksi)
0 degrees	Fuel Compartments	P_m	7.98	16.40
		$P_m + P_b$	13.81	24.60
		$P_m + P_b + Q$	34.01	49.20
	Canister	P_m	1.26	17.50
		$P_m + P_b$	8.08	26.25
		$P_m + P_b + Q$	-	52.50
	Rails	P_m	15.32	17.50
		$P_m + P_b$	26.13	26.25
		$P_m + P_b + Q$	27.53	52.50
30 degrees ⁽¹⁾⁽²⁾	Fuel Compartments	P_m	7.99	16.40
		$P_m + P_b$	43.32	24.60
		$P_m + P_b + Q$	63.52	49.20
	Canister	P_m	1.04	17.50
		$P_m + P_b$	13.71	26.25
		$P_m + P_b + Q$	-	52.50
	Rails	P_m	12.80	17.50
		$P_m + P_b$	31.63	26.25
		$P_m + P_b + Q$	33.03	52.50
45 degrees ⁽¹⁾	Fuel Compartments	P_m	6.72	16.40
		$P_m + P_b$	40.12	24.60
		$P_m + P_b + Q$	60.31	49.20
	Canister	P_m	1.16	17.50
		$P_m + P_b$	12.19	26.25
		$P_m + P_b + Q$	-	52.50
	Rails	P_m	10.26	17.50
		$P_m + P_b$	41.85	26.25
		$P_m + P_b + Q$	43.25	52.50
180 degrees ⁽¹⁾	Fuel Compartments	P_m	7.88	16.40
		$P_m + P_b$	28.67	24.60
		$P_m + P_b + Q$	48.87	49.20
	Canister	P_m	3.22	17.50
		$P_m + P_b$	47.99	26.25
		$P_m + P_b + Q$	-	52.50
	Rails	P_m	19.16	17.50
		$P_m + P_b$	45.40	26.25
		$P_m + P_b + Q$	46.80	52.50

Notes:

(1) The exceedances for stresses are localized and have characteristics of secondary stresses. Limit analyses (NG-3228.2) are performed for these cases.

(2) Simplified Elastic-Plastic Analyses performed for these cases

Table A.2.13.8-6
NUH61BTH Type 2 Normal Condition - Maximum Stress Summary

Drop Orientation	Component	Stress Category	Maximum Stress (ksi)	Allowable Stress (ksi)
0 degrees	Fuel Compartments	P_m	8.57	16.40
		$P_m + P_b$	14.57	24.60
		$P_m + P_b + Q$	34.77	49.20
	Canister	P_m	1.81	17.50
		$P_m + P_b$	6.32	26.25
		$P_m + P_b + Q$	-	52.50
	Rails	P_m	13.78	17.50
		$P_m + P_b$	24.42	26.25
		$P_m + P_b + Q$	25.82	52.50
30 degrees ⁽¹⁾	Fuel Compartments	P_m	9.96	16.40
		$P_m + P_b$	31.79	24.60
		$P_m + P_b + Q$	51.99	49.20
	Canister	P_m	1.98	17.50
		$P_m + P_b$	12.44	26.25
		$P_m + P_b + Q$	-	52.50
	Rails	P_m	10.33	17.50
		$P_m + P_b$	33.03	26.25
		$P_m + P_b + Q$	34.43	52.50
45 degrees ⁽¹⁾	Fuel Compartments	P_m	9.83	16.40
		$P_m + P_b$	31.93	24.60
		$P_m + P_b + Q$	52.12	49.20
	Canister	P_m	1.46	17.50
		$P_m + P_b$	13.98	26.25
		$P_m + P_b + Q$	-	52.50
	Rails	P_m	9.61	17.50
		$P_m + P_b$	30.51	26.25
		$P_m + P_b + Q$	31.91	52.50
180 degrees ⁽¹⁾	Fuel Compartments	P_m	9.07	16.40
		$P_m + P_b$	16.29	24.60
		$P_m + P_b + Q$	36.68	49.20
	Canister	P_m	3.04	17.50
		$P_m + P_b$	31.60	26.25
		$P_m + P_b + Q$	-	52.50
	Rails	P_m	14.12	17.50
		$P_m + P_b$	31.10	26.25
		$P_m + P_b + Q$	32.48	52.50

Notes:

(1) The exceedances for stresses are localized and have characteristics of secondary stresses. Limit analyses (NG-3228.2) are performed for these cases.

Table A.2.13.8-7
NUH61BT/61BTH Type 1 Normal Condition - Limit Analysis Summary

Drop Orientation	Last Converged Load (G)	Actual Max Load (G)
30 degrees	$88.27*(2/3) = 58.84$	30
45 degrees	$80.21*(2/3) = 53.47$	30
180 degrees	$56.89*(2/3) = 37.92$	30

Table A.2.13.8-8
NUH61BTH Type 2 Normal Condition - Limit Analysis Summary

Drop Orientation	Last Converged Load (G)	Actual Max Load (G)
30 degrees	$83.07*(2/3) = 55.38$	30
45 degrees	$82.79*(2/3) = 55.19$	30
180 degrees	$98.02*(2/3) = 65.34$	30

Table A.2.13.8-9
NUH61BT HAC - Maximum Stress Summary

Drop Orientation	Component	Stress Category	Max. Stress (ksi)	Allowable Stress (ksi) ⁽¹⁾
45° Side Drop	Basket	Pm	14.54	44.38
		Pm + Pb	27.12	57.06
	Rails	Pm	16.52	44.38
		Pm + Pb	25.27	57.06
	Canister	Pm	2.01	44.38
		Pm + Pb	19.60	57.06
60° Side Drop	Basket	Pm	14.43	44.38
		Pm + Pb	27.30	57.06
	Rails	Pm	20.85	44.38
		Pm + Pb	28.72	57.06
	Canister	Pm	2.44	44.38
		Pm + Pb	19.57	57.06
90° Side Drop ⁽²⁾	Basket	Pm	18.02	44.38
		Pm + Pb	22.78	57.06
	Rails	Pm	29.03	44.38
		Pm + Pb	32.79	57.06
	Canister	Pm	3.17	44.38
		Pm + Pb	16.83	57.06
180° Side Drop Impact on two Transfer cask Support rails ⁽³⁾	Basket	Shear	17.43	26.63
		Pm	16.22	44.38
	Rails	Pm + Pb	23.55	57.06
		Pm	28.09	44.38
	Canister	Pm + Pb	34.71	57.06
		Pm	4.72	44.38
		Pm + Pb	26.13	57.06

Notes:

⁽¹⁾ Allowables are taken at a temperature of 650°F

⁽²⁾ The 90° drop is equivalent to 0° drop

⁽³⁾ MP197HB Transport Cask has four support rails which provide more support, thus analysis with two support rails is bounding

Table A.2.13.8-10
 NUH61BTH Type 1 HAC – Maximum Stress Summary

Drop Orientation	Component ⁽¹⁾	Stress Category	Max. Stress (ksi)	Allowable Stress (ksi) ⁽²⁾
45° Side Drop	Basket	P_m	14.54	44.38
		$P_m + P_b$	27.12	57.06
	Rails	P_m	16.52	44.38
		$P_m + P_b$	25.27	57.06
	Canister	P_m	2.01	44.38
		$P_m + P_b$	19.60	57.06
60° Side Drop	Basket	P_m	14.43	44.38
		$P_m + P_b$	27.30	57.06
	Rails	P_m	20.85	44.38
		$P_m + P_b$	28.72	57.06
	Canister ⁽³⁾	P_m	2.44	44.38
		$P_m + P_b$	19.57	57.06
90° Side Drop ⁽⁴⁾	Basket	P_m	18.02	44.38
		$P_m + P_b$	22.78	57.06
	Rails	P_m	29.03	44.38
		$P_m + P_b$	32.79	57.06
	Canister ⁽³⁾	P_m	3.17	44.38
		$P_m + P_b$	16.83	57.06
180° Side Drop Impact on two Transfer cask Support rails ⁽⁵⁾	Basket	P_m	16.22	44.38
		$P_m + P_b$	23.55	57.06
	Rails	P_m	28.09	44.38
		$P_m + P_b$	34.71	57.06
	Canister ⁽³⁾	P_m	4.72	44.38
		$P_m + P_b$	26.13	57.06

Notes:

1. Reported rails are stainless steel rails only.
2. Based on elastic/plastic analyses and allowable at 750°F.
 $P_m \leq \max (0.7 S_U, S_Y + 1/3 (S_U - S_Y))$
 $P_m + P_b \leq 0.9 S_U$
3. Canister stresses excluded pressure.
4. The 90° drop is equivalent to 0° drop
5. MP197HB Transport Cask has four support rails which provide more support, thus analysis with two support rails is bounding

Table A.2.13.8-11
NUH61BTH Type 2 HAC – Maximum Stress Summary

Drop Orientation	Component ⁽¹⁾	Stress Category	Max. Stress (ksi) ⁽²⁾	Allowable Stress (ksi) ⁽³⁾
45° Side Drop	Basket	P_m	17.47	44.38
		$P_m + P_b$	28.35	57.06
	Rails	P_m	19.43	44.38
		$P_m + P_b$	38.65	57.06
	Canister	P_m	2.34	44.38
		$P_m + P_b$	20.08	57.06
60° Side Drop	Basket	P_m	15.43	44.38
		$P_m + P_b$	27.87	57.06
	Rails	P_m	21.88	44.38
		$P_m + P_b$	44.77	57.06
	Canister ⁽⁴⁾	P_m	2.79	44.38
		$P_m + P_b$	21.42	57.06
90° Side Drop ⁽⁵⁾	Basket	P_m	20.42	44.38
		$P_m + P_b$	25.75	57.06
	Rails	P_m	19.61	44.38
		$P_m + P_b$	42.16	57.06
	Canister ⁽⁴⁾	P_m	1.66	44.38
		$P_m + P_b$	14.12	57.06
180° Side Drop Impact on two Transfer cask Support rails ⁽⁶⁾	Basket	P_m	18.96	44.38
		$P_m + P_b$	27.85	57.06
	Rails	P_m	20.34	44.38
		$P_m + P_b$	45.34	57.06
	Canister ⁽⁴⁾	P_m	3.75	44.38
		$P_m + P_b$	25.13	57.06

Notes:

1. Reported rails are stainless steel rails only. The function of the solid aluminum R90 basket support rails is to support the fuel compartment tube structure such that stresses and displacements in the compartment tube structure are acceptable. Since the solid aluminum rails are entrapped between the fuel compartment tube structure and DSC shell, no additional checks of the aluminum are required for accident loading.
2. ANSYS results are conservatively increased by 8% to account for any missing weight.
3. Based on elastic/plastic analyses and allowable at 750°F.
 $P_m \leq \max(0.7 S_U, S_Y + 1/3 (S_U - S_Y))$
 $P_m + P_b \leq 0.9 S_U$
4. Canister stresses excluded pressure.
5. The 90° drop is equivalent to 0° drop
6. MP197HB Transport Cask has four support rails which provide more support, thus analysis with two support rails is bounding

Table A.2.13.8-12
NUH69BTH Normal Condition - Maximum Stress Summary

Drop Orientation	Component	Stress Category	Maximum Stress (ksi)	Allowable Stress (ksi)
0 degrees ⁽¹⁾	Fuel Compartments	P_m	7.15	15.8
		$P_m + P_b$	15.44	24.0
		$P_m + P_b + Q$	25.16	47.4
	Fuel Compartment Wrap Plates	P_m	8.52	15.8
		$P_m + P_b$	31.11	24.0
		$P_m + P_b + Q$	40.83	47.4
	Canister	P_m	0.65	17.5
		$P_m + P_b$	8.55	26.3
		$P_m + P_b + Q$	29.05	52.5
	Aluminum Rails	Bearing Stress	3.37	5.50
30 degrees ⁽¹⁾	Fuel Compartments	P_m	9.67	15.8
		$P_m + P_b$	26.31	24.0
		$P_m + P_b + Q$	36.03	47.4
	Fuel Compartment Wrap Plates	P_m	9.22	15.8
		$P_m + P_b$	34.41	24.0
		$P_m + P_b + Q$	44.13	47.4
	Canister	P_m	9.89	17.5
		$P_m + P_b$	24.92	26.3
		$P_m + P_b + Q$	45.42	52.5
	Aluminum Rails	Bearing Stress	3.33	5.50
45 degrees ⁽¹⁾	Fuel Compartments	P_m	6.39	15.8
		$P_m + P_b$	31.12	24.0
		$P_m + P_b + Q$	40.84	47.4
	Fuel Compartment Wrap Plates	P_m	16.21	15.8
		$P_m + P_b$	28.62	24.0
		$P_m + P_b + Q$	38.34	47.4
	Canister	P_m	2.43	17.5
		$P_m + P_b$	16.03	26.3
		$P_m + P_b + Q$	36.53	52.5
	Aluminum Rails	Bearing Stress	1.92	5.50

Table A.2.13.8-12
 NUH69BTH Normal Condition - Maximum Stress Summary
 (concluded)

Drop Orientation	Component	Stress Category	Maximum Stress (ksi)	Allowable Stress (ksi)
180 degrees ⁽¹⁾	Fuel Compartments	P_m	7.09	16.0
		$P_m + P_b$	21.27	24.0
		$P_m + P_b + Q$	30.99	47.4
	Fuel Compartment Wrap Plates	P_m	7.64	16.0
		$P_m + P_b$	37.09	24.0
		$P_m + P_b + Q$	46.81	47.4
	Canister	P_m	3.18	17.5
		$P_m + P_b$	30.41	26.3
		$P_m + P_b + Q$	50.91	52.5
	Aluminum Rails	Bearing Stress	2.63	5.50

Notes:

(1) The exceedances for stresses are localized and have characteristics of secondary stresses. Limit analyses (NG-3228.2) are performed for these cases.

Table A.2.13.8-13
NUH69BTH Normal Condition - Limit Analysis Summary

Side Drop Orientation	Last Converged Load Step (g)	Actual Max Load (g)
0 deg	$117.0 \times (2/3) = 78.0$	30
30 deg	$81.0 \times (2/3) = 54.0$	30
45 deg	$103.1 \times (2/3) = 68.7$	30
180 deg	$84.8 \times (2/3) = 56.5$	30

Table A.2.13.8-14
NUH69BTH HAC - Maximum Stress Summary

Drop Orientation	Component	Stress Category	Maximum Stress (ksi)	Allowable Stress (ksi) ⁽²⁾
0 degrees	Fuel Compartment	P_m	18.89	37.92
		$P_m + P_b$	21.38	56.88
	Fuel Compartment Wrap Plates	P_m	18.75	37.92
		$P_m + P_b$	26.63	56.88
	Aluminum Rails ⁽¹⁾	-	-	Note ⁽¹⁾
	Canister	P_m	1.52	42.00
		$P_m + P_b$	12.23	63.00
30 degrees	Fuel Compartment	P_m	19.30	37.92
		$P_m + P_b$	25.12	56.88
	Fuel Compartment Wrap Plates	P_m	20.53	37.92
		$P_m + P_b$	33.98	56.88
	Aluminum Rails ⁽¹⁾	-	-	Note ⁽¹⁾
	Canister	P_m	24.25	42.00
		$P_m + P_b$	27.43	63.00
45 degrees	Fuel Compartment	P_m	20.13	37.92
		$P_m + P_b$	22.77	56.88
	Fuel Compartment Wrap Plates	P_m	19.54	37.92
		$P_m + P_b$	36.46	56.88
	Aluminum Rails ⁽¹⁾	-	-	Note ⁽¹⁾
	Canister	P_m	18.69	42
		$P_m + P_b$	24.39	63
180 degrees Side Drop, Impact on Support Rails	Fuel Compartment	P_m	17.27	37.92
		$P_m + P_b$	30.09	56.88
	Fuel Compartment Wrap Plates	P_m	25.19	37.92
		$P_m + P_b$	41.73	56.88
	Aluminum Rails ⁽¹⁾	-	-	Note ⁽¹⁾
	Canister	P_m	8.19	42.00
		$P_m + P_b$	25.09	63.00

Notes:

(1) Not considered for the hypothetical accident conditions

(2) Allowable stress for fuel compartments and wraps are based on 700 °F and for canister it is based on 500 °F

Table A.2.13.8-15
NUH69BTH HAC – Buckling Analysis Results Summary

Analysis	Last Converged Load⁽¹⁾ (g)	Actual Max Load (g)	Factor of Safety
0 deg.	100.0	75	1.33
30 deg.	90	75	1.20
45 deg.	90	75	1.20
180 deg.	85	75	1.13

Notes:

(1) All the g-loads are taken to be the time of last converged solution

Table A.2.13.8-16
NUH24PTH Normal Condition - Maximum Stress Summary

Drop Orientation	Component	Stress Category	Maximum Stress (ksi)	Allowable Stress (ksi)
0 degrees ⁽¹⁾	Fuel Compartments	P_m	35.33	15.60
		$P_m + P_b$	21.68 ⁽²⁾	23.40
		$P_m + P_b + Q$	29.53 ⁽²⁾	46.80
	Canister	P_m	3.00	15.60
		$P_m + P_b$	8.92	23.40
		$P_m + P_b + Q$	28.4	46.80
	Basket Straps	P_m	4.88	15.60
		$P_m + P_b$	22.76	23.40
		$P_m + P_b + Q$	28.12	46.80
	R45 Transition Rails	P_m	26.49	15.60
		$P_m + P_b$	27.37	23.40
		$P_m + P_b + Q$	36.09	46.80
	R90 Transition Rails	Bearing	3.91	5.2
30 degrees ⁽¹⁾	Fuel Compartments	P_m	27.22	15.60
		$P_m + P_b$	32.49 ⁽²⁾	23.40
		$P_m + P_b + Q$	40.34 ⁽²⁾	46.80
	Canister	P_m	3.33	15.60
		$P_m + P_b$	10.70	23.40
		$P_m + P_b + Q$	30.2	46.80
	Basket Straps	P_m	13.59	15.60
		$P_m + P_b$	38.82	23.40
		$P_m + P_b + Q$	44.18	46.80
	R45 Transition Rails	P_m	34.52	15.60
		$P_m + P_b$	34.52	23.40
		$P_m + P_b + Q$	43.24	46.80
	R90 Transition Rails	Bearing	3.57	5.2
45 degrees ⁽¹⁾	Fuel Compartments	P_m	25.94	15.60
		$P_m + P_b$	36.53 ⁽²⁾	23.40
		$P_m + P_b + Q$	44.38 ⁽²⁾	46.80
	Canister	P_m	3.24	15.60
		$P_m + P_b$	6.77	23.40
		$P_m + P_b + Q$	26.3	46.80
	Basket Straps	P_m	13.78	15.60
		$P_m + P_b$	37.38	23.40
		$P_m + P_b + Q$	42.74	46.80
	R45 Transition Rails	P_m	34.79	15.60
		$P_m + P_b$	34.79	23.40
		$P_m + P_b + Q$	43.51	46.80
	R90 Transition Rails	Bearing	2.80	5.2

Table A.2.13.8-16
 NUH24PTH Normal Condition - Maximum Stress Summary (concluded)

Drop Orientation	Component	Stress Category	Maximum Stress (ksi)	Allowable Stress (ksi)
180 degrees ⁽¹⁾	Fuel Compartments	P_m	31.41	15.60
		$P_m + P_b$	23.18 ⁽²⁾	23.40
		$P_m + P_b + Q$	31.03 ⁽²⁾	46.80
	Canister	P_m	5.18	15.60
		$P_m + P_b$	24.03	23.40
		$P_m + P_b + Q$	43.5	46.80
	Basket Straps	P_m	4.91	15.60
		$P_m + P_b$	26.17	23.40
		$P_m + P_b + Q$	31.53	46.80
	R45 Transition Rails	P_m	20.61	15.60
		$P_m + P_b$	23.41	23.40
		$P_m + P_b + Q$	32.13	46.80
	R90 Transition Rails	Bearing	3.77	5.2

Note:

(1) The exceedances for stresses are localized and have characteristics of secondary stresses. Limit analyses (NG-3228.2) are performed for these cases.

(2) Maximum stress excludes the local peak concentrated stresses.

Table A.2.13.8-17
NUH24PTH Normal Condition - Limit Analysis Summary

Drop Orientation	Last Converged Load (G)	Actual Max Load (G)
0 degrees	$87.72^{*(2/3)} = 58.48$	25
30 degrees	$62.66^{*(2/3)} = 41.77$	25
45 degrees	$66.43^{*(2/3)} = 44.29$	25
180 degrees	$67.26^{*(2/3)} = 44.84$	25

Table A.2.13.8-18
NUH24PTH HAC - Maximum Stress Summary

Component	Stress Category	Maximum Drop SI	Allowable SI ⁽¹⁾	Stress Ratio
Fuel Compartment Tubes	Pm	37.9	44.0	0.86
	Pm + Pb	48.2	56.5	0.85
	Pm + Pb + Q	N/A	N/A	N/A
R45 Transition Rail Main Plates	Pm	39.1	44.0	0.89
	Pm + Pb	53.9	56.5	0.95
	Pm + Pb + Q	N/A	N/A	N/A
R45 Transition Rail Stiffeners	Pm	31.1	44.0	0.71
	Pm + Pb	39.5	56.5	0.70
	Pm + Pb + Q	N/A	N/A	N/A
Steel Insert Plates (Straps)	Pm	20.9	44.0	0.47
	Pm + Pb	31.8	56.5	0.56
	Pm + Pb + Q	N/A	N/A	N/A

Note:

(1) Level D allowables for SA-240 Type 304 at 800°

Table A.2.13.8-19
NUH32PT Normal Condition - Limit Analysis Summary

Drop Orientation	Last Converged Load (G) – Solid Aluminum Rails	Last Converged Load (G) – Solid Aluminum Rails	Actual Max Load (G)
0 degrees	$75^{(1)} * (2/3) = 50$	$75^{(1)} * (2/3) = 50$	25
30 degrees	$75^{(1)} * (2/3) = 50$	-	25
45 degrees	$75^{(1)} * (2/3) = 50$	$75^{(1)} * (2/3) = 50$	25
180 degrees	$75^{(1)} * (2/3) = 50$	$97.43 * (2/3) = 65.27$	25

Note:

(1) Maximum applied load was 75g, actual $L_L > 75g$

Table A.2.13.8-20
NUH32PT HAC - Maximum Stress Summary

Component	Stress Category	Stress Intensity		Stress Ratio	Notes
		Calculated	Allowable		
Basket with 1-Piece R90 Transition Rails					
Fuel Support Grid	P _m	26.2 ksi	59.4 ksi	.44	XM-19, 800°F ⁽²⁾
	P _m + P _b	73.9 ksi	76.3 ksi	.97	
Transition Rail Cover Plates	P _m	7.63 ksi	59.4 ksi	0.13	XM-19, 800°F ⁽²⁾
	P _m + P _b	64.4 ksi	76.3 ksi	.84	
Basket with 3-Piece R90 Transition Rails					
Fuel Support Grid	P _m	27.0	60.4	0.45	XM-19, 705°F ⁽³⁾
	P _m + P _b	76.2	77.7	0.98	

Notes:

1. Although all the listed values include thermal effects, evaluation of secondary stress not required for Level D events.
2. Allowable stress based on an enveloping temperature of 800°F.
3. Allowable stress based on maximum basket temperature.

Table A.2.13.8-21
NUH32PTH1 Type 1 Normal Condition - Maximum Stress Summary

Drop Orientation	Component	Stress Category	Maximum Stress Intensity (ksi)	Allowable Stress Intensity (ksi)
0 degrees ⁽²⁾	DSC Shell	P_m	0.88	17.5
		$P_m + P_b$	9.63	26.25
	Transition Rails	<i>Bearing Stress</i>	2.50	4.85
	Fuel Compartments	P_m	10.54 ⁽¹⁾	15.80
		$P_m + P_b$	14.33	23.70
		$P_m + P_b + Q$	25.93	47.40
	Basket Straps	P_m	15.58	15.80
		$P_m + P_b$	16.61	23.70
		$P_m + P_b + Q$	28.21	47.40
30 degrees ⁽²⁾	DSC Shell	P_m	1.17	17.5
		$P_m + P_b$	15.58	26.25
	Transition Rails	<i>Bearing Stress</i>	2.57	4.85
	Fuel Compartments	P_m	16.39 ⁽¹⁾	15.80
		$P_m + P_b$	25.33 ⁽¹⁾	23.70
		$P_m + P_b + Q$	36.93	47.40
	Basket Straps	P_m	8.78 ⁽¹⁾	15.80
		$P_m + P_b$	28.68	23.70
		$P_m + P_b + Q$	40.28	47.40
45 degrees ⁽²⁾	DSC Shell	P_m	1.11	17.5
		$P_m + P_b$	14.19	26.25
	Transition Rails	<i>Bearing Stress</i>	2.69	4.85
	Fuel Compartments	P_m	14.16 ⁽¹⁾	15.80
		$P_m + P_b$	25.45 ⁽¹⁾	23.70
		$P_m + P_b + Q$	37.05	47.40
	Basket Straps	P_m	7.82 ⁽¹⁾	15.80
		$P_m + P_b$	28.68	23.70
		$P_m + P_b + Q$	40.28	47.40
180 degrees ⁽²⁾	DSC Shell	P_m	2.11	17.5
		$P_m + P_b$	8.25	26.25
	Transition Rails	<i>Bearing Stress</i>	2.76	4.85
	Fuel Compartments	P_m	10.21 ⁽¹⁾	15.80
		$P_m + P_b$	14.03 ⁽¹⁾	23.70
		$P_m + P_b + Q$	25.63	47.40
	Basket Straps	P_m	8.01 ⁽¹⁾	15.80
		$P_m + P_b$	16.81	23.70
		$P_m + P_b + Q$	28.41	47.40

Notes:

(1) Maximum stress intensity excluding point contact loaded elements

(2) The exceedances for stresses are localized and have characteristics of secondary stresses. Limit analyses (NG-3228.2) are performed for these cases.

Table A.2.13.8-22
 NUH32PTH/NUH32PTH1 Type 2 Normal Condition - Maximum Stress Summary

Drop Orientation	Component	Stress Category	Maximum Stress Intensity (ksi)	Allowable Stress Intensity (ksi)
0 degrees ⁽²⁾	DSC Shell	P_m	1.15	17.5
		$P_m + P_b$	6.13	26.25
	Transition Rails	P_m	11.14	17.05
		$P_m + P_b$	33.80 ⁽¹⁾	25.58
		$P_m + P_b + Q$	48.30	51.15
	Fuel Compartments	P_m	9.32	15.80
		$P_m + P_b$	20.23 ⁽¹⁾	23.70
		$P_m + P_b + Q$	29.43	47.40
	Basket Straps	P_m	13.56	15.80
		$P_m + P_b$	20.30	23.70
		$P_m + P_b + Q$	29.50	47.40
30 degrees ⁽²⁾⁽³⁾	DSC Shell	P_m	2.35	17.5
		$P_m + P_b$	12.72	26.25
	Transition Rails	P_m	10.93	17.05
		$P_m + P_b$	22.96 ⁽¹⁾	25.58
		$P_m + P_b + Q$	37.46	51.15
	Fuel Compartments	P_m	20.10	15.80
		$P_m + P_b$	29.02 ⁽¹⁾	23.70
		$P_m + P_b + Q$	38.22	47.40
	Basket Straps	P_m	11.50 ⁽¹⁾	15.80
		$P_m + P_b$	41.11 ⁽¹⁾	23.70
		$P_m + P_b + Q$	50.31	47.40
45 degrees ⁽²⁾⁽³⁾	DSC Shell	P_m	1.32	17.5
		$P_m + P_b$	9.95	26.25
	Transition Rails	P_m	8.89	17.05
		$P_m + P_b$	25.20	25.58
		$P_m + P_b + Q$	39.7	51.15
	Fuel Compartments	P_m	15.92	15.80
		$P_m + P_b$	26.58 ⁽¹⁾	23.70
		$P_m + P_b + Q$	35.78	47.40
	Basket Straps	P_m	7.61 ⁽¹⁾	15.80
		$P_m + P_b$	39.01 ⁽¹⁾	23.70
		$P_m + P_b + Q$	48.21	47.40
180 degrees ⁽²⁾⁽³⁾	DSC Shell	P_m	6.72	17.5
		$P_m + P_b$	48.21	26.25
	Transition Rails	P_m	14.93	17.05
		$P_m + P_b$	45.97 ⁽¹⁾	25.58
		$P_m + P_b + Q$	60.47	51.15
	Fuel Compartments	P_m	9.99	15.80
		$P_m + P_b$	11.47 ⁽¹⁾	23.70
		$P_m + P_b + Q$	20.67	47.40
	Basket Straps	P_m	13.82	15.80
		$P_m + P_b$	22.15 ⁽¹⁾	23.70
		$P_m + P_b + Q$	31.35	47.40

Notes:

- (1) Maximum stress intensity excluding point contact loaded elements
- (2) The exceedances for stresses are localized and have characteristics of secondary stresses. Limit analyses (NG-3228.2) are performed for these cases:
- (3) $P_m + P_b + Q$ may exceed the $3 S_m$ stress limit provided requirements (a) through (f) of NG-3228.3 [7] are met.

Table A.2.13.8-23
NUH32PTH/NUH32PTH1 Normal Condition - Limit Analysis Summary

Basket Type	Orientation	Last Converged Load Step (g)	Actual Max Load (g)
32PTH1 Type 1	0	$100 \times (2/3) = 66.7$	23.3
	30	$58.7 \times (2/3) = 39.1$	23.3
	45	$100 \times (2/3) = 66.7$	23.3
	180	$89.6 \times (2/3) = 59.7$	23.3
32PTH/32PTH1 Type 2	0	$50.0 \times (2/3) = 33.3$	23.3
	30	$68.5 \times (2/3) = 45.7$	23.3
	45	$83.3 \times (2/3) = 55.5$	23.3
	180	$85.6 \times (2/3) = 57.1$	23.3

Table A.2.13.8-24
NUH32PTH1 Type 1 HAC - Maximum Stress Summary

Drop Orientation	Component	Stress Category	Maximum Stress Intensity (ksi)	Allowable Stress Intensity (ksi)
0 degree	DSC Shell	P_m	1.89	44.38
		$P_m + P_b$	9.13	57.06
	Interior Fuel Compartments	P_m	14.93	44.38
		$P_m + P_b$	21.40	57.06
	Periphery Fuel Compartments	P_m	23.54	44.38
		$P_m + P_b$	35.69	57.06
30 degree	DSC Shell	P_m	13.88	44.38
		$P_m + P_b$	23.91	57.06
	DSC Shell	P_m	2.42	44.38
		$P_m + P_b$	21.19	57.06
	Interior Fuel Compartments	P_m	17.03	44.38
		$P_m + P_b$	23.57	57.06
45 degree	Periphery Fuel Compartments	P_m	22.12	44.38
		$P_m + P_b$	32.12	57.06
	Basket Straps	P_m	16.17	44.38
		$P_m + P_b$	24.09	57.06
	DSC Shell	P_m	2.63	44.38
		$P_m + P_b$	22.48	57.06
180 degree	Interior Fuel Compartments	P_m	16.13	44.38
		$P_m + P_b$	23.51	57.06
	Periphery Fuel Compartments	P_m	20.51	44.38
		$P_m + P_b$	31.72	57.06
	Basket Straps	P_m	15.78	44.38
		$P_m + P_b$	24.16	57.06
180 degree	DSC Shell	P_m	4.40	44.38
		$P_m + P_b$	22.16	57.06
	Interior Fuel Compartments	P_m	13.66	44.38
		$P_m + P_b$	21.38	57.06
	Periphery Fuel Compartments	P_m	20.76	44.38
		$P_m + P_b$	37.70	57.06
180 degree	Basket Straps	P_m	13.76	44.38
		$P_m + P_b$	23.67	57.06

Table A.2.13.8-25
 NUH32PTH1 Type 2 HAC - Maximum Stress Summary

Drop Orientation	Component	Stress Category	Maximum Stress Intensity (ksi)	Allowable Stress Intensity (ksi)
0 degree	DSC Shell	P_m	1.32	44.38
		$P_m + P_b$	5.46	57.06
	Transition Rails	P_m	22.00	44.38
		$P_m + P_b$	31.53	57.06
	Interior Fuel Compartments	P_m	17.00	44.38
		$P_m + P_b$	20.77	57.06
	Periphery Fuel Compartments	P_m	27.24	44.38
		$P_m + P_b$	29.14	57.06
30 degree	DSC Shell	P_m	17.29	44.38
		$P_m + P_b$	21.97	57.06
	Transition Rails	P_m	3.24	44.38
		$P_m + P_b$	17.48	57.06
	Interior Fuel Compartments	P_m	18.15	44.38
		$P_m + P_b$	31.84	57.06
	Periphery Fuel Compartments	P_m	17.14	44.38
		$P_m + P_b$	23.31	57.06
45 degree	DSC Shell	P_m	20.57	44.38
		$P_m + P_b$	23.92	57.06
	Transition Rails	P_m	18.97	44.38
		$P_m + P_b$	24.95	57.06
	Interior Fuel Compartments	P_m	2.18	44.38
		$P_m + P_b$	16.40	57.06
	Periphery Fuel Compartments	P_m	25.21	44.38
		$P_m + P_b$	31.19	57.06
180 degree	DSC Shell	P_m	15.73	44.38
		$P_m + P_b$	23.70	57.06
	Transition Rails	P_m	19.71	44.38
		$P_m + P_b$	24.07	57.06
	Interior Fuel Compartments	P_m	20.12	44.38
		$P_m + P_b$	24.87	57.06
	Periphery Fuel Compartments	P_m	8.19	44.38
		$P_m + P_b$	34.05	57.06

Table A.2.13.8-26
NUH32PTH HAC - Maximum Stress Summary

Drop Orientation	Component	Stress Category	Max. Stress (ksi)	Allowable Stress (ksi)
0° Side Drop	Fuel Compartment and Plates	P_m	24.5	44.38
		$P_m + P_b$	25.6	57.06
	Rails	P_m	22.0	44.38
		$P_m + P_b$	22.3	57.06
	Canister	P_m	4.61	44.38
		$P_m + P_b$	10.9	57.06
30° Side Drop	Fuel Compartment and Plates	P_m	28.3	44.38
		$P_m + P_b$	29.7	57.06
	Rails	P_m	20.6	44.38
		$P_m + P_b$	22.1	57.06
	Canister	P_m	4.81	44.38
		$P_m + P_b$	11.3	57.06
45° Side Drop	Fuel Compartment and Plates	P_m	26.4	44.38
		$P_m + P_b$	27.6	57.06
	Rails Canister	P_m	19.8	44.38
		$P_m + P_b$	22.7	57.06
		P_m	4.53	44.38
		$P_m + P_b$	12.1	57.06
180° Side Drop	Fuel Compartment and Plates	P_m	25.5	44.38
		$P_m + P_b$	31.8	57.06
	Rails	P_m	13.6	44.38
		$P_m + P_b$	37.1	57.06
	Canister	P_m	13.2	44.38
		$P_m + P_b$	36.8	57.06

Table A.2.13.8-27
NUH32PTH1 HAC – Buckling Analysis Results Summary

Load Case	Collapse Load
Alt. Type 1 Rail, 0° drop	77.23 g
Alt. Type 1 Rail, 30° drop	65.10 g
Alt. Type 1 Rail, 45° drop	66.84 g
Alt. Type 1 Rail, 180° drop	78.32 g
Alt. Type 2 Rail, 0° drop	76.64 g
Alt. Type 2 Rail, 30° drop	64.39 g
Alt. Type 2 Rail, 45° drop	68.27 g
Alt. Type 2 Rail, 180° drop	80.57 g

Table A.2.13.8-28
NUH32PTH HAC – Buckling Analysis Results Summary

Drop Orientation	Buckling g-load
0 degrees	102.5
30 degrees	83.9
45 degrees	85.6

Table A.2.13.8-29
NUH37PTH Normal Condition - Maximum Stress Summary

Drop Orientation	Component	Stress Category	Maximum Stress (ksi)	Allowable Stress (ksi)
0 degrees	Fuel Compartments	P_m	10.97	16.4
		$P_m + P_b$	23.92	24.6
		$P_m + P_b + Q$	31.43	49.2
	Canister	P_m	0.60	17.5
		$P_m + P_b$	13.61	26.25
	Rails	Max. Bearing stress ⁽³⁾	5.38	5.5
30 degrees ⁽¹⁾	Fuel Compartments	P_m	8.11	16.4
		$P_m + P_b$	43.87	24.6
		$P_m + P_b + Q$	45.26	49.2
	Canister	P_m	2.72	17.5
		$P_m + P_b$	24.86	26.25
	Rails	Max. Bearing stress ⁽³⁾	3.89	5.5
45 degrees ⁽¹⁾	Fuel Compartments	P_m	7.40	16.4
		$P_m + P_b$	41.10	24.6
		$P_m + P_b + Q$	48.61	49.2
	Canister	P_m	2.75	17.5
		$P_m + P_b$	19.87	26.25
	Rails	Max. Bearing stress ⁽³⁾	3.45	5.5
90 degrees	Fuel Compartments	P_m	11.0	16.4
		$P_m + P_b$	23.96	24.6
		$P_m + P_b + Q$	31.47	49.2
	Canister	P_m	0.59	17.5
		$P_m + P_b$	13.59	26.25
	Rails	Max. Bearing stress ⁽³⁾	5.37	5.5
180 degrees ⁽¹⁾	Fuel Compartments	P_m	8.07	16.4
		$P_m + P_b$ ⁽²⁾	31.37	24.6
		$P_m + P_b + Q$	38.88	49.2
	Canister	P_m	4.04	17.5
		$P_m + P_b$	31.03	26.25
	Rails	Max. Bearing stress ⁽³⁾	4.6	5.5

Notes:

⁽¹⁾ The exceedances for stresses are localized and have characteristics of secondary stresses. Limit analyses (NG-3228.2) are performed for these cases.

⁽²⁾ The stress values exclude the corner stress concentration elements occurring at the bottom ends of compartments.

⁽³⁾ Maximum bending stress from the aluminum rails are reported.

Table A.2.13.8-30
NUH37PTH Normal Condition - Limit Analysis Summary

Drop Orientation	Last Converged Load (g)	Actual Max Load (g)
30 degrees	$65 \times (2/3) = 43.3$	25
45 degrees	$60 \times (2/3) = 40.0$	25
180 degrees	$50 \times (2/3) = 33.3$	25

Table A.2.13.8-31
NUH37PTH HAC - Maximum Stress Summary

Drop Orientation	Component	Stress Category	Maximum Stress (ksi)	Allowable Stress (ksi)
0 degrees	Fuel Compartments	P_m	16.81	44.38
		$P_m + P_b$	28.38	57.06
	Canister	P_m	0.94	44.38
		$P_m + P_b$	25.76	57.06
30 degrees	Fuel Compartments	P_m	17.12	44.38
		$P_m + P_b$	29.96	57.06
	Canister	P_m	5.21	44.38
		$P_m + P_b$	26.03	57.06
45 degrees	Fuel Compartments	P_m	15.90	44.38
		$P_m + P_b$	29.77	57.06
	Canister	P_m	1.72	44.38
		$P_m + P_b$	29.06	57.06
90 degrees	Fuel Compartments	P_m	16.80	44.38
		$P_m + P_b$	28.44	57.06
	Canister	P_m	0.94	44.38
		$P_m + P_b$	25.58	57.06
180 degrees	Fuel Compartments	P_m	15.14	44.38
		$P_m + P_b$	34.51	57.06
	Canister	P_m	4.91	44.38
		$P_m + P_b$	31.48	57.06

Table A.2.13.8-32
NUH37PTH HAC – Buckling Analysis Results Summary

Drop Orientation	Buckling g-load	Design g-load	Ratio
0 degrees	75	55	1.36
30 degrees	67	55	1.22
45 degrees	67	55	1.22
90 degrees	75	55	1.36
180 degrees	70	55	1.27

Table A.2.13.8-33
NUH24PT4 Normal Condition – Spacer Disk Maximum Stress Summary

Drop Orientation	Stress Category	Linearized Stress (ksi)	Allowable Stress (ksi)
0 degrees	P_m	12.5	26.7
	$P_m + P_b$	56.3*	40.1
30 degrees	P_m	11.8	26.7
	$P_m + P_b$	90.7*	40.1
45 degrees	P_m	6.8	26.7
	$P_m + P_b$	93.1*	40.1
180 degrees	P_m	18.44	26.7
	$P_m + P_b$	62.20*	40.1

Note: * The exceedances for stresses are localized and have characteristics of secondary stresses. Limit analyses (NG-3228.2) are performed for these cases.

Table A.2.13.8-34
NUH24PT4 Normal Condition – Spacer Disk Limit Analysis Summary

Drop Orientation	Last Converged Load (g) ⁽¹⁾	Actual Max Load (g)
0 degrees	$100 \times (2/3) = 66.7$	21
30 degrees	$100 \times (2/3) = 66.7$	21
45 degrees	$100 \times (2/3) = 66.7$	21
180 degrees	$100 \times (2/3) = 66.7$	21

Note:

(1) Maximum applied load was 100g, actual $L_L > 100g$

Table A.2.13.8-35
NUH24PT4 HAC - Maximum Stress Summary

Loading	Stress Classification	Stress Intensity (ksi)	Allowable Stress (ksi)	Maximum Stress Ratio
0° Side Drop	Pm	53.4	56.0	0.95
	Pm+Pb	67.4	72.0	0.94
18.5° Side Drop	Pm	52.9	56.0	0.94
	Pm+Pb	69.4	72.0	0.96
45° Side Drop	Pm	46.6	56.0	0.83
	Pm+Pb	69.0	72.0	0.96

Table A.2.13.8-36
Summary of Guide Sleeve Stresses from Side Drops

Side Loads	g-load	Stress Category	Calculated SI	Allowable SI	Stress Ratio
1 ft Side Drop	27.0g	P_m	2.35 ksi	16.0 ksi	0.15
		P_m+P_b	23.3 ksi	24.0 ksi	0.97
30 ft Side Drop	75g	P_m	8.51 ksi	44.5 ksi	0.19
		P_m+P_b	25.6 ksi	57.2 ksi	0.45

Table A.2.13.8-37
Summary of Guide Sleeve Stresses from End Drops

Side Loads	g-load	Guide Sleeve Stress, f_a	Allowable Stress, F_a	Stress Ratio
1 ft End Drop	30g	3.3 ksi	6.48 ksi	0.51
30 ft End Drop	75g	8.25 ksi	11.0 ksi	0.75

Table A.2.13.8-38
Summary of Support Rod Assembly Stresses from Side Drops

Side Loads	Component	g-load	Max Interaction ⁽¹⁾	Allowable	Stress Ratio
1 ft Side Drop	Support Rod	30g	0.36	1	0.36
	Support Sleeve	30g	0.08	1	0.08
30 ft Side Drop	Support Rod	100g	0.89	1	0.89
	Support Sleeve	100g	0.05	1	0.05

Note: (1) The reported interaction ratios are the maximum values from Equations 20 through 22 of NF 3322.1(e)(1).

Table A.2.13.8-39
Summary of Spacer Sleeve Analysis from End Drops

Side Loads	g-load	Max Interaction	Allowable	Ratio
1 ft End Drop	30g	0.89	1	0.89
30 ft End Drop	65g	0.97	1	0.97

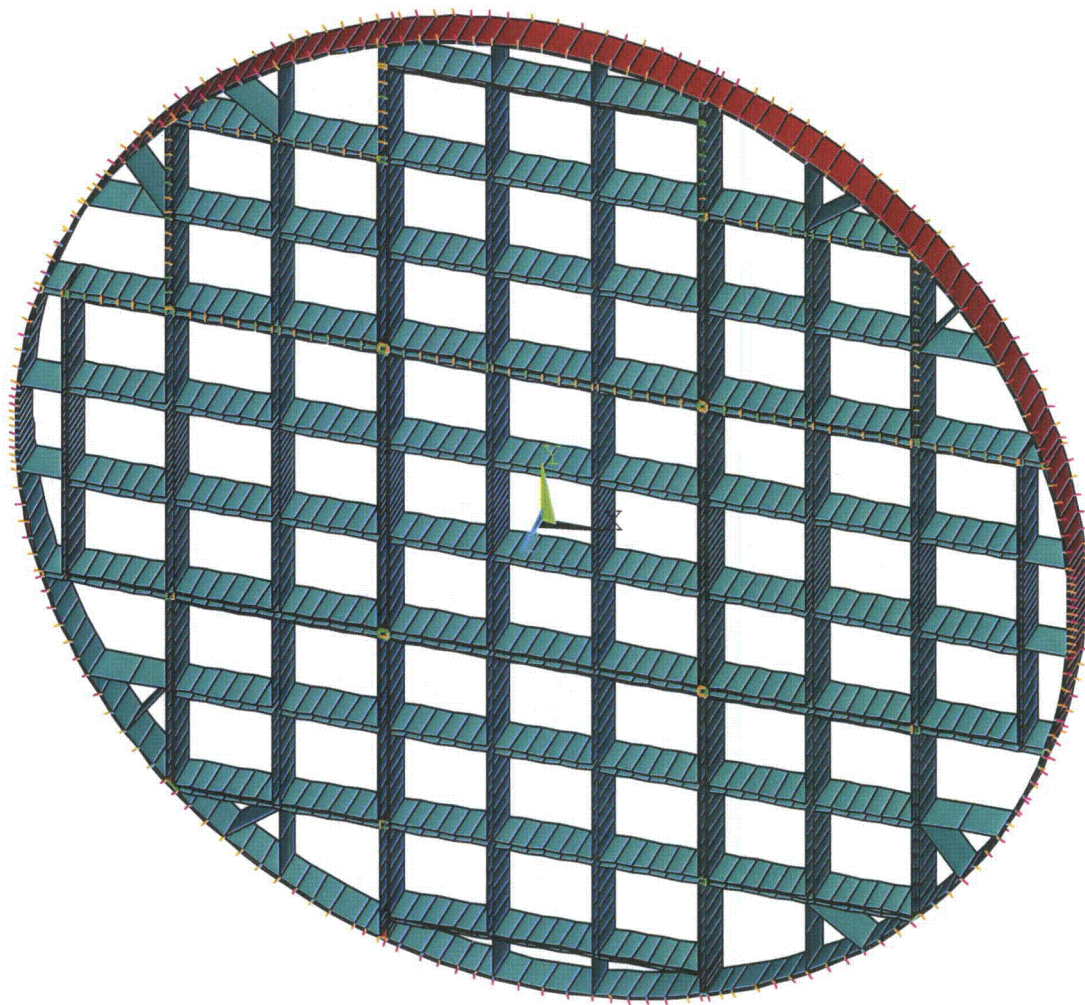


Figure A.2.13.8-1
NUH61BT/61BTH Type 1 Finite Element Model – Full Basket Section

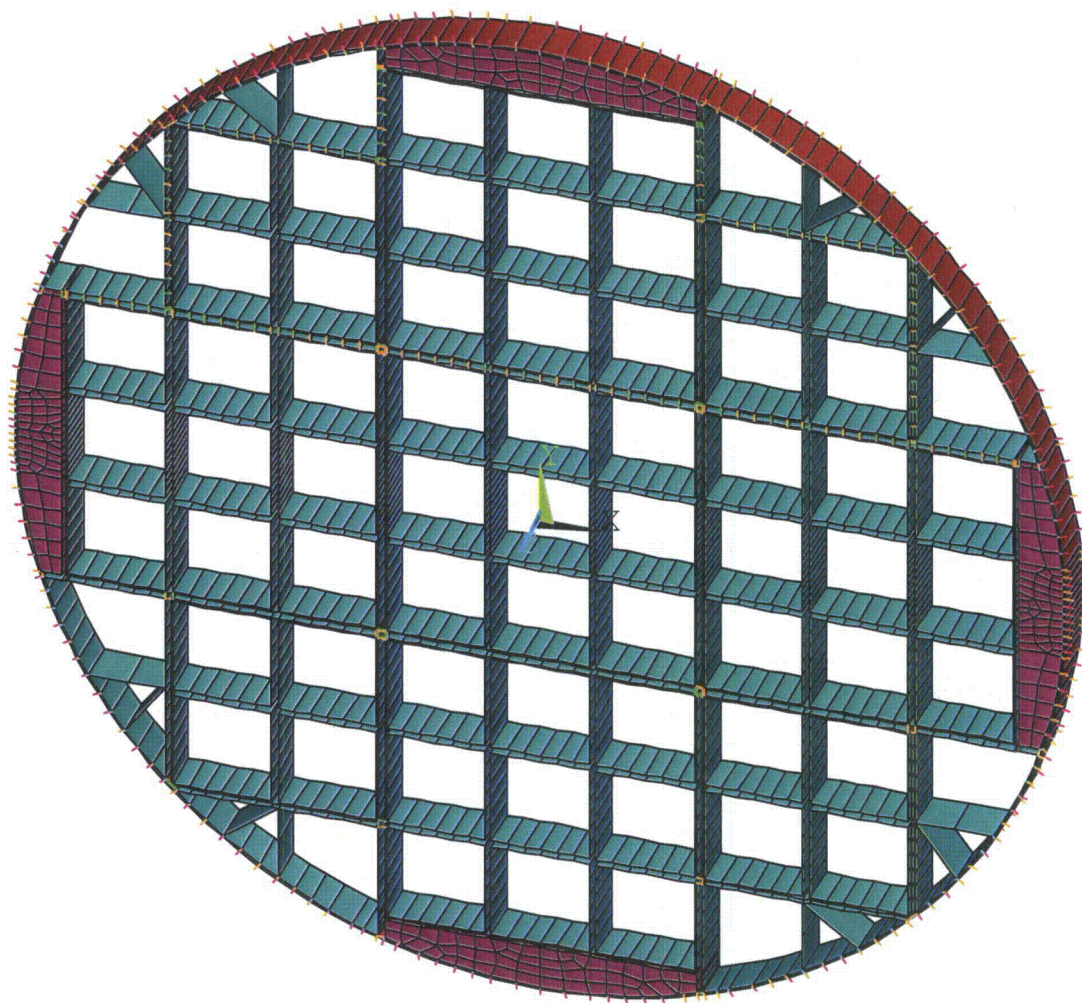


Figure A.2.13.8-2
NUH61BTH Type 2 Finite Element Model – Full Basket Section

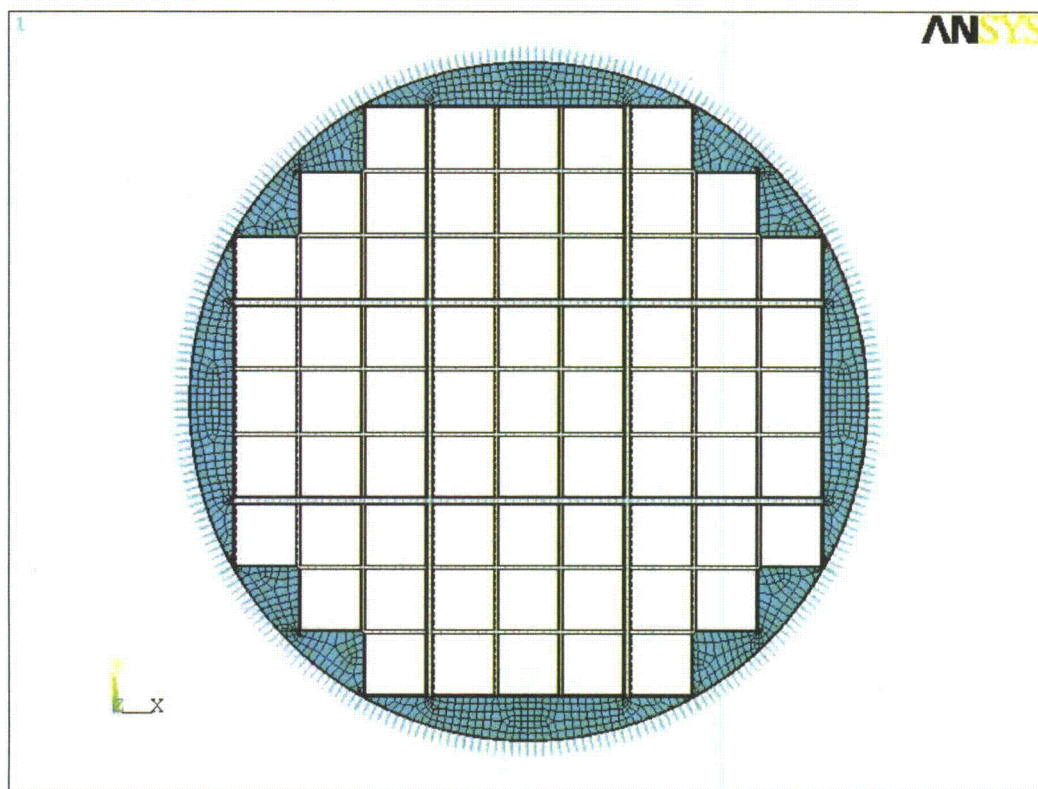


Figure A.2.13.8-3
NUH69BTH Finite Element Model

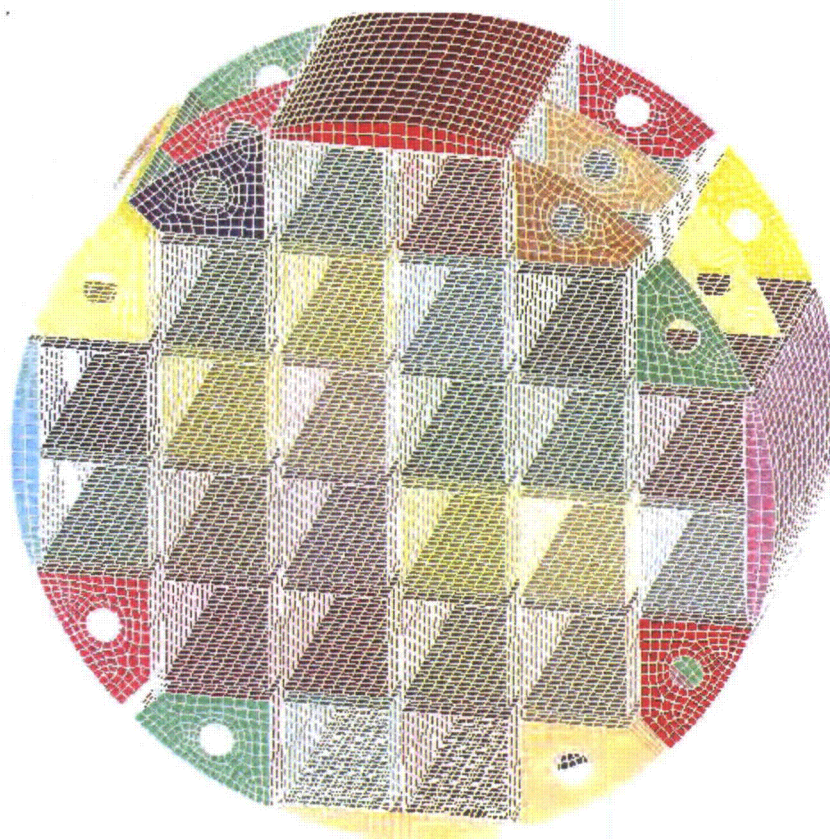


Figure A.2.13.8-4
NUH24PTH Finite Element Model

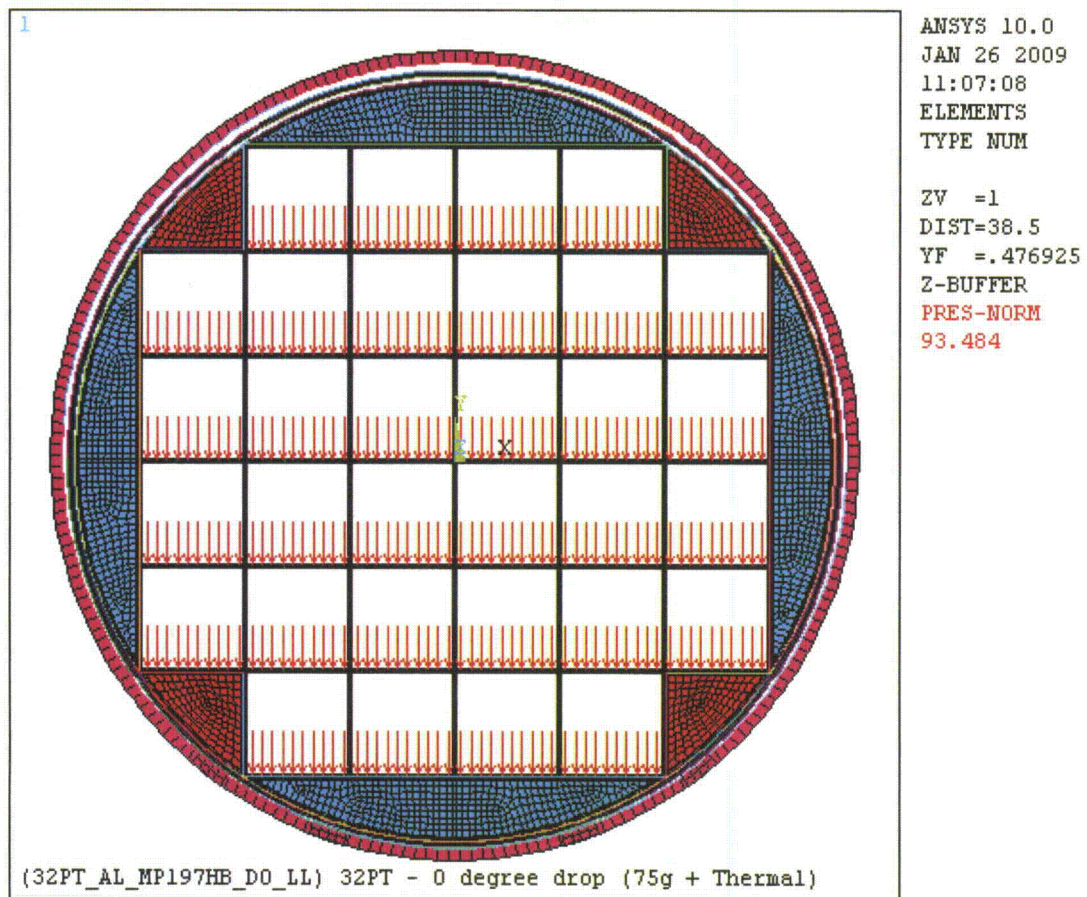


Figure A.2.13.8-5
NUH32PT Solid Aluminum Rails Finite Element Model

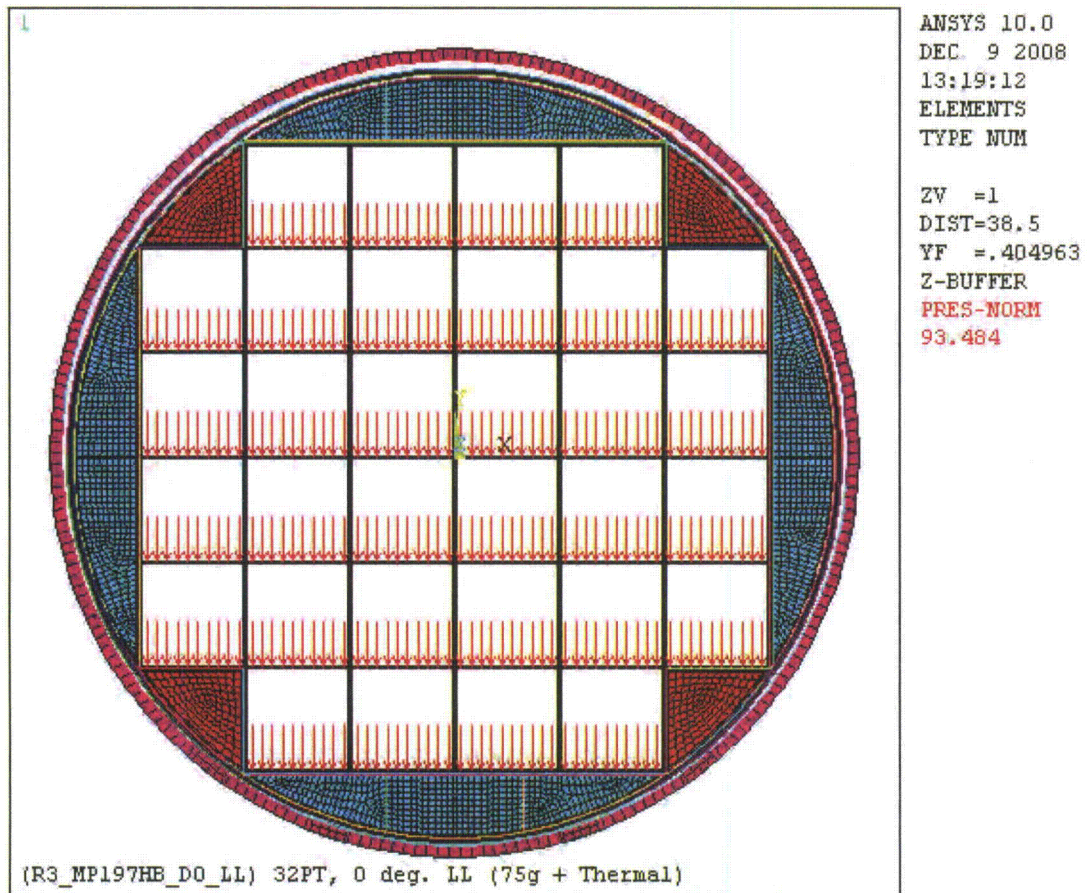


Figure A.2.13.8-6
NUH32PT 3 Piece Aluminum Rails Finite Element Model

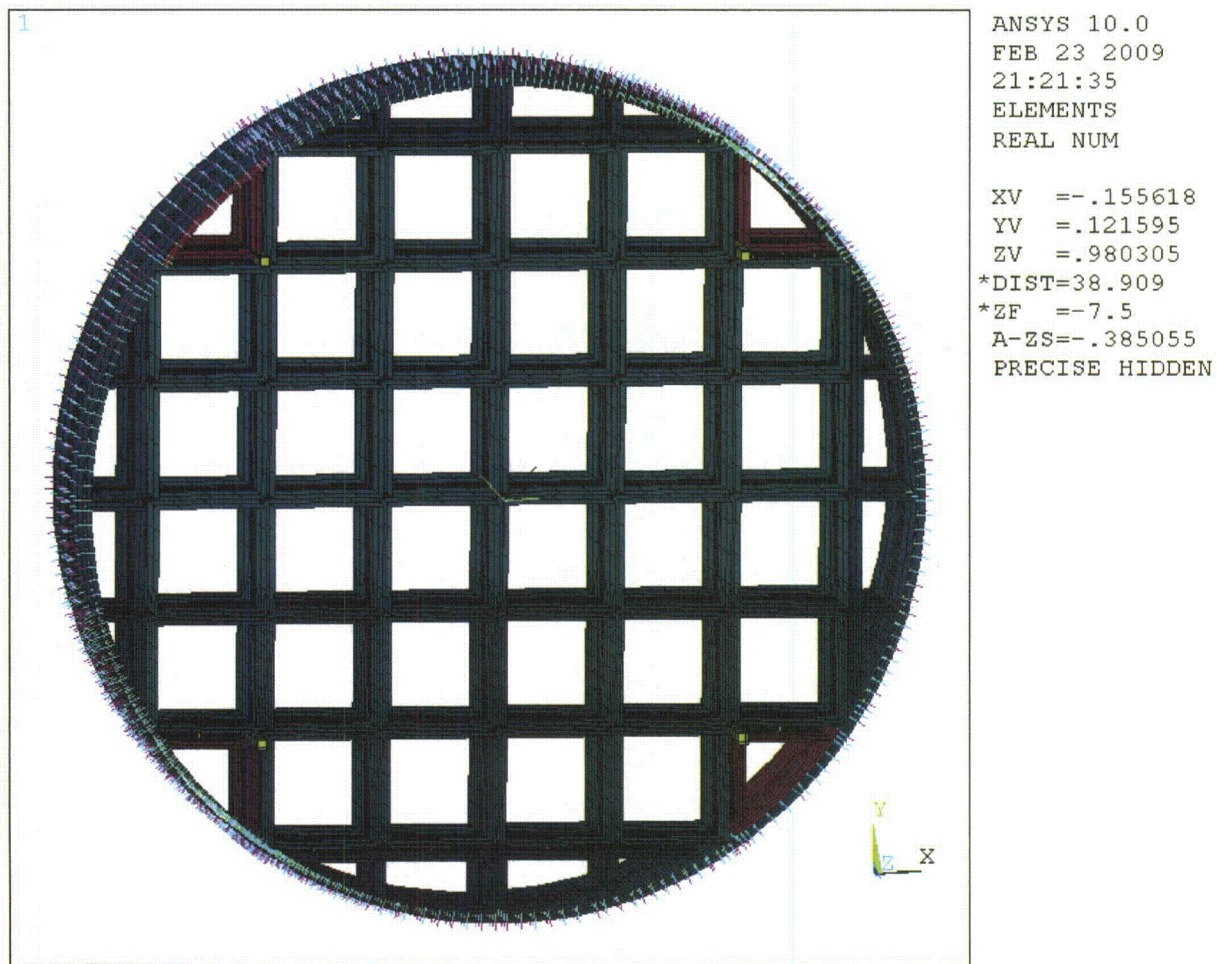


Figure A.2.13.8-7
NUH32PTH/NUH32PTH1 Type 2 Finite Element Model
(NUH32PTH1 Type 1 Basket Finite Element Model is the same except the transition rails are solid aluminum)

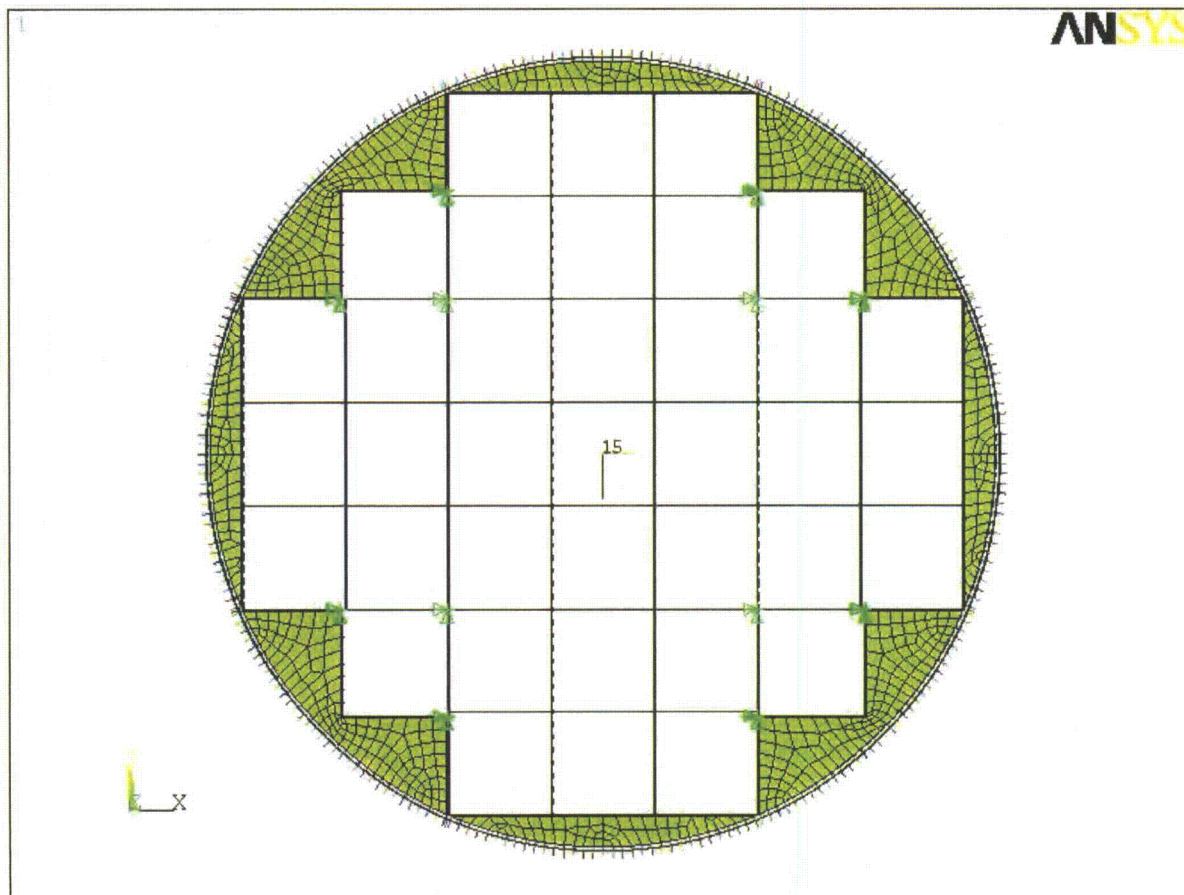


Figure A.2.13.8-8
NUH37PTH Finite Element Model

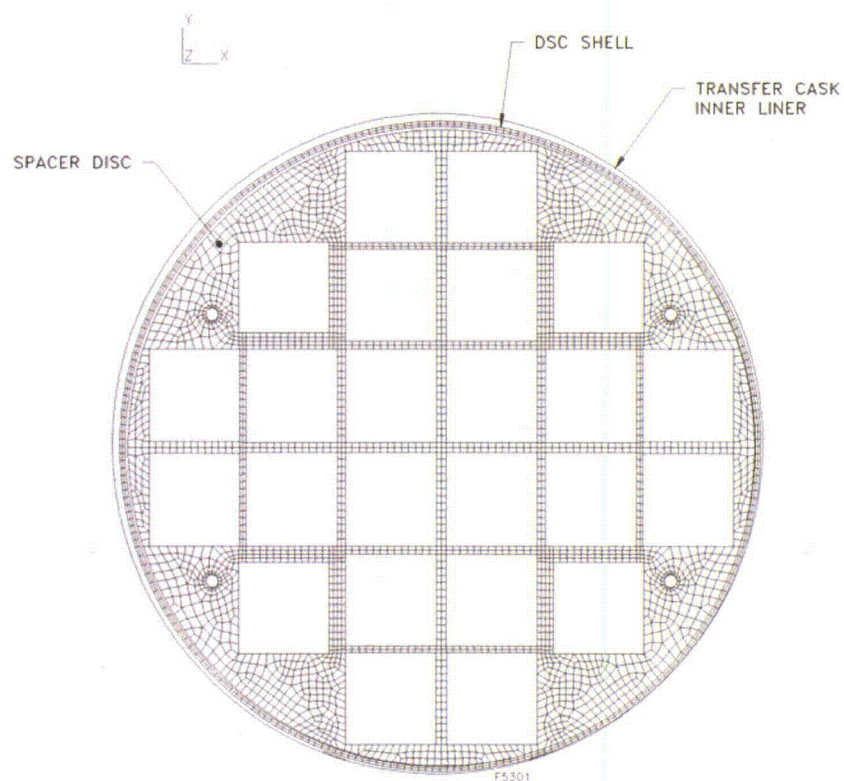


Figure A.2.13.8-9
NUH24PT4 Spacer Disk Finite Element Model for Side Drop

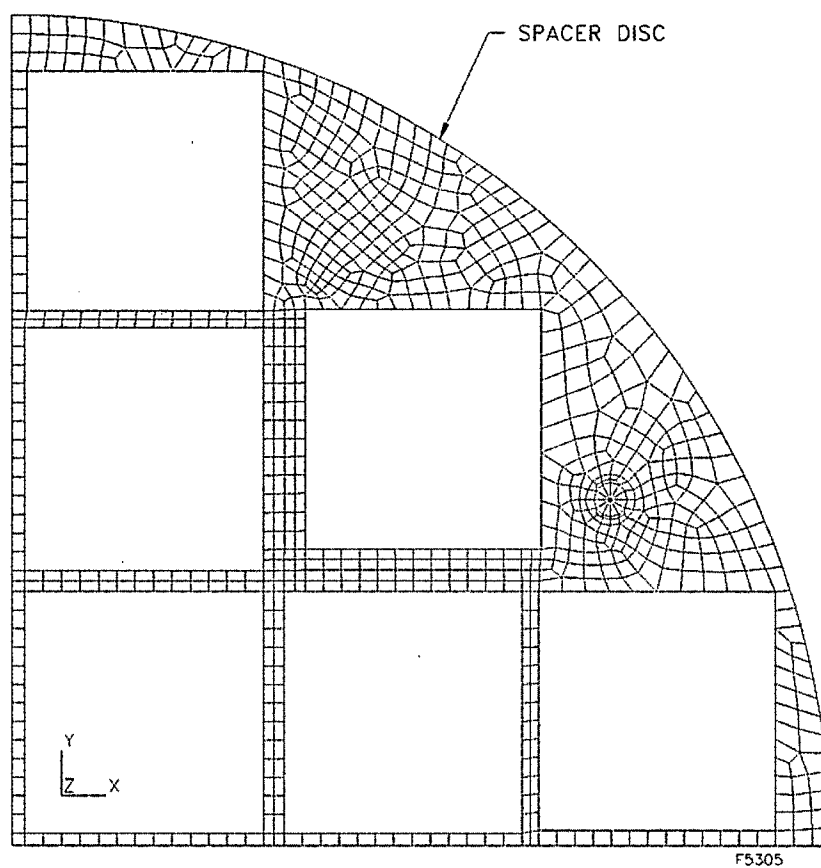


Figure A.2.13.8-10
NUH24PT4 Spacer Disk Finite Element Model for End Drop

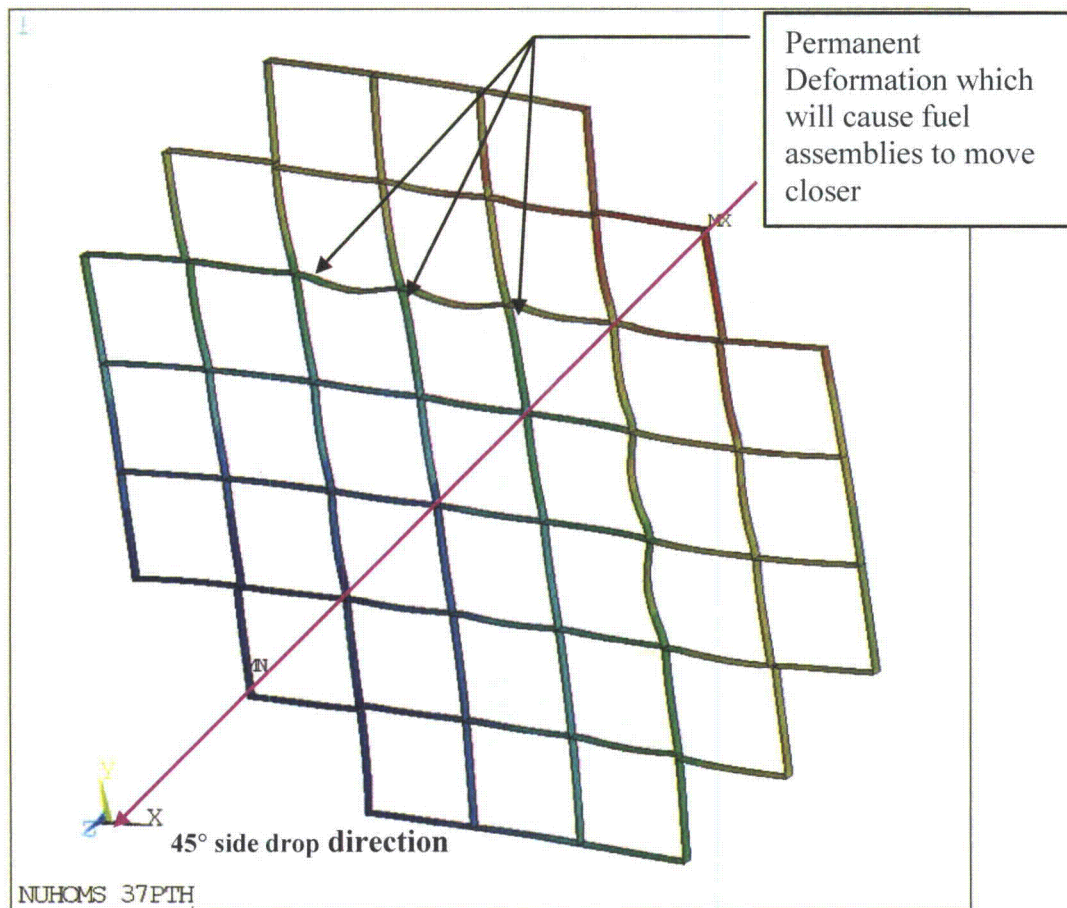


Figure A.2.13.8-11
Permanent Deformation of the 37PTH Basket following 45° HAC Side Drop
(Deformations are exaggerated for effect)

Appendix A.2.13.9
MP197HB Dynamic Load Factor Determination

TABLE OF CONTENTS

A.2.13.9.1 Introduction.....	A.2.13.9-1
A.2.13.9.2 Natural Frequencies during End Drop	A.2.13.9-2
A.2.13.9.3 Natural Frequencies during Side Drop.....	A.2.13.9-5
A.2.13.9.4 Dynamic Load Factor Calculations.....	A.2.13.9-7
A.2.13.9.5 References.....	A.2.13.9-8

LIST OF TABLES

Table A.2.13.9-1 Lowest Natural Frequencies of the Canister Shell during End Drop.....	A.2.13.9-9
Table A.2.13.9-2 Lowest Natural Frequencies of the Basket during End Drop	A.2.13.9-10
Table A.2.13.9-3 Lowest Natural Frequencies of the Canister Shell during Side Drop	A.2.13.9-11
Table A.2.13.9-4 Lowest Natural Frequencies of the Basket during Side Drop.....	A.2.13.9-12
Table A.2.13.9-5 Lowest Natural Frequencies of Bounding BWR and PWR Fuel Claddings During Side Drop.....	A.2.13.9-13
Table A.2.13.9-6 Dynamic Load Factor Results Summary	A.2.13.9-14
Table A.2.13.9-7 BWR and PWR Fuel Rods Dynamic Load Factor Results Summary	A.2.13.9-14

LIST OF FIGURES

Figure A.2.13.9-1 Lowest Natural Frequency of the 24PT4 Spacer Disk in the End Drop Direction	A.2.13.9-15
Figure A.2.13.9-2 NUHOMS 32PT Basket Model and Boundary Conditions.....	A.2.13.9-16
Figure A.2.13.9-3 NUHOMS 32PT Basket First Mode Shape—45 Degree Orientation	A.2.13.9-17
Figure A.2.13.9-4 Bounding BWR 10x10 Fuel Cladding First Mode Shape	A.2.13.9-18
Figure A.2.13.9-5 Finite Element Model for DLF Calculation	A.2.13.9-19
Figure A.2.13.9-6 MP197HB Transport Cask DLF Curves	A.2.13.9-20

Appendix A.2.13.9 MP197HB Dynamic Load Factor Determination

NOTE: References in this Appendix are shown as [1], [2], etc. and refer to the reference list in Section A.2.13.9.5.

A.2.13.9.1 Introduction

The purpose of the analysis presented in this appendix is to determine the dynamic load factor (DLF) for the MP197HB transport package internals. The DLF accounts for the difference of rigid body acceleration between the MP197HB transport cask and canisters, baskets, and fuel during the cask drop events.

The DLF is calculated using a spring-mass finite element model [1]. Acceleration time-history from the cask side and end drops from Appendix A.2.13.12 is applied on the spring-mass model and DLF is calculated based on the ratio between the maximum dynamic displacement ($u_{\max \text{ dynamic}}$) and the maximum static displacement ($u_{\max \text{ static}}$).

Three components of the MP197HB transport package internals with the longest and most significant natural periods are the canister, basket, and fuel assemblies. The DLFs for each component are calculated separately.

DLF is evaluated in this analysis for two load cases, i.e., longitudinal loading and transverse loading. During an end drop, the fundamental natural periods of the components are taken to be that of simply supported cylindrical shells without axial constraint, under longitudinal vibration. The masses of the basket components and fuel assemblies are conservatively lumped together, so that an average density is used. During a side drop, the fundamental natural period of the canister shell is taken to be that of a cylinder in an ovaling mode and a simply supported cylindrical shell without axial constraint. For the basket and fuel assemblies, a modal analysis is conducted using ANSYS [1].

Notations

The notations used in this analysis are taken from Blevins [2], and are listed as follows:

- E , Modulus of Elasticity, (psi).
- f_1, f_{11} , Fundamental natural frequency, (Hz.).
- I , Moment of inertia of the beam, (in.^4).
- L , Length of beam or cylindrical shell, (in.).
- m , Mass per unit length of the beam, (lbm.in.^{-1}).
- μ , Mass density, (lbm.in.^{-3}).
- ν , Poisson's ratio.
- R , Outer radius of the cylindrical shell, (in.).

A.2.13.9.2 Natural Frequencies during End Drop

Canister Shell

The canister frequency is calculated using the following equation from Reference [2].

Natural frequency is calculated by,

$$f_1 = \frac{1}{2\pi} \left(\frac{g}{\Delta} \right)^{1/2}$$

where,

$$g = 386.4$$

$$\Delta = \text{Max. Deflection ratio} = (W \cdot L) / (A \cdot E),$$

where,

W = weight of canister – weight of bottom shield plug,

L = length of cavity,

E = Young's modulus,

A = Cross sectional area

The natural frequencies for the entire set of canister shells are calculated and summarized in Table A.2.13.9-1; a sample calculation for the bounding canister shell, i.e., the 32PT canister, is presented below:

The maximum temperature in the canister shell for normal transport condition is less than 500 °F (Chapter A.3). However, the canister material property is conservatively taken at 500 °F. The canister shell is constructed from SA-240 Type 304, which has a modulus of elasticity of 25.8×10^6 psi at 500 °F. The cavity length of the canister between top and bottom assemblies is 175.6 in.

$$W = 24,393 - 5,366 = 19,027 \text{ lbs}$$

$$A = (\pi/4) \cdot (67.19^2 - 66.19^2) = 104.77 \text{ in}^2$$

$$\Delta = WL/AE = (19,027 \cdot 175.6) / (104.77 \cdot 25.8 \times 10^6) = 0.001236$$

$$f_1 = \frac{1}{2\pi} \left(\frac{g}{\Delta} \right)^{1/2} = \frac{1}{2\pi} \left(\frac{386.4}{0.001236} \right)^{1/2} = 88.9 \text{ Hz}$$

Basket

The fundamental natural frequency of a simply supported basket structure under axial vibration simplifies to that of a uniform beam axially free at both ends, for all baskets except for the 24PT4 basket. The fundamental natural frequency of a uniform beam free at both ends under longitudinal load vibration is as follows [2]:

$$f_1 = \frac{\lambda_1}{2\pi L} \left(\frac{E}{\mu} \right)^{1/2}$$

where,

$$\lambda_1 = \pi$$

E = Young's modulus

L = Minimum length of the basket in inches

μ = Average mass density (lbm. in.⁻³)

It should be noted that for a vertical vibration due to an end drop, the weight of the fuel is not lumped with the basket. However, the weight of the fuel is considered during side drop vibrations.

The natural frequency for the entire set of baskets is calculated and summarized in Table A.2.13.9-2; sample calculation for the bounding basket, the 32PT basket, is presented below:

The maximum temperature in the basket for normal transport condition is 720 °F (Chapter A.3). However, the average temperature of the basket is much less than 700 °F which is conservatively used. The basket is constructed from SA-240 Type XM19, which has a modulus of elasticity of 24.8×10^6 psi at 700 °F. The length of the basket is 164 inch.

Based on a stainless steel density of 0.2853 lb/in³ and an aluminum density of 0.098 lb/in³ the average mass density, μ , is calculated in the following way

Component	Weight	Volume
	(lb.)	in ³
Grid Plate Segments	8,486	29743.3
R45 Transition Rails	2,738	9595.3
R90 Transport Rails (Top & Bot)	3,643	12768.4
R90 Transition Rails (2 Sides)	3,643	12768.4
Neutron Absorbing & Aluminum Sheets	4,405	44,954
Total	22,914	109829.4

$$\mu = 22,914 / 109,829.4 / 386.4 = 0.00054 \text{ lbm/in}^3$$

Therefore,

$$f_1 = \frac{\lambda_1}{2\pi L} \left(\frac{E}{\mu} \right)^{1/2} = \frac{\pi}{2\pi(175)} \left(\frac{24.8 \times 10^6}{0.00054} \right)^{1/2} = 612.3 \text{ Hz}$$

The 24PT4 basket consists of spacer disks, guide sleeves, and support rods. The fundamental natural frequency of the spacer disk is calculated via ANSYS finite element model; the fundamental natural frequency of the guide sleeve is calculated assuming the guide sleeves act as a fixed beam with the weight of the four neutron absorber sheets uniformly distributed along the beam; and the fundamental frequency of the support rod is calculated assuming that the support rod sleeve acts as a series of springs to which equal masses are attached. The natural frequencies are 60.8 Hz, 229.1 Hz, and 87.3 Hz for the spacer disc, guide sleeve, and support rod assemblies, respectively. The lowest mode for the spacer disc is shown in Figure A.2.13.9-1.

Fuel

Since fuel end drops are evaluated using dynamic analyses, DLF for the fuel claddings is not needed and thus the natural frequency for the fuel is not calculated.

A.2.13.9.3 Natural Frequencies during Side Drop

Canister Shell

The fundamental natural frequency of the canister is assumed to be caused by a cylindrical shell ovaling mode. The fundamental natural frequency of the canister shell ovaling (Radial-Axial) mode is determined assuming the cylindrical shell is simply supported without axial constraints. The natural frequency of the cylindrical shell ovaling mode is given by the following ([2], p. 305, Table 12-2, Frame 5).

$$f_{ij} = \frac{\lambda_{ij}}{2\pi R} \left(\frac{E}{\mu(1-\nu^2)} \right)^{1/2}$$

where,

E = Young's modulus

R = Average shell radius

ν = Poisson's ratio

μ = Mass density, (lbm.in.⁻³).

For the fundamental mode, $i = 2$ and $j = 1$.

$$\lambda_{ij} = \frac{\left\{ (1-\nu^2)(j\pi R/L)^4 + (h^2/12R^2) \left[i^2 + (j\pi R/L)^2 \right]^4 \right\}^{1/2}}{(j\pi R/L)^2 + i^2}$$

where,

ν = Poisson's ratio

R = Average shell radius

L = Cavity length

h = thickness

The natural frequency for the entire set of canister shells is calculated and summarized in Table A.2.13.9-3; a sample calculation for the bounding canister shell, i.e., the 24PT4 canister, is presented below:

The maximum temperature in the canister shell for normal transport condition is less than 500 °F (Chapter A.3). However, the canister material property is conservatively taken at 500 °F. The canister shell is constructed from SA-240 Type 304, which has a modulus of elasticity of 25.8×10^6 psi at 500 °F. The cavity length of the canister between top and bottom assemblies is 180.2 and the average radius is 33.28. Poisson's Ratio of 0.3 and weight density of 0.2853 is used.

$$\lambda_{ij} = \frac{\left\{ (1-0.3^2) (\pi \times 33.28/180.2)^4 + (0.625^2/12 \times 33.28^2) \left[2^2 + (\pi 33.28/180.2)^2 \right]^4 \right\}^{1/2}}{(\pi 33.28/180.2)^2 + 2^2} = 0.076352$$

$$f_{21} = \frac{0.076352}{2\pi \times 33.28} \left(\frac{25.8 \times 10^6}{0.0008(1 - 0.3^2)} \right) = 71.1 \text{ Hz}$$

Basket

The fundamental natural frequencies of all baskets, except for the guide sleeve and support rod assemblies for the 24PT4 basket, during side drops are calculated via ANSYS finite element analysis. The finite element models from Appendix A.2.13.8 are used for the modal analyses. The canister shell and gap elements are removed, and the boundary conditions are directly applied to the rails. It is assumed that the basket is supported by the rail periphery. This assumption causes the basket natural frequencies to be strongly dependent on the inertial mass of the fuel compartment.

All weight densities were converted to mass densities, and the density of the steel plates supporting the fuel assemblies were increased to account for the weight of the fuel depending on the drop angle. Modal analyses for 0 and 45 degree drop orientations were performed to bound all drop orientations.

The fundamental natural frequency of the support rod assemblies in the 24PT4 basket are calculated using the free-free multiple span beam with pinned intermediate supports (spacer disk) equation. The most significant loading on the guide sleeve assemblies in the 24PT4 basket during side drops is due to fuel assemblies. Since nearly all of the load on the guide sleeve bottom panel is due to the fuel assembly, the loading on the guide sleeve bottom panel will be controlled by the response of the fuel assembly. Therefore, the fundamental bending frequency of a single fuel rod, conservatively ignoring friction between fuel rods within a fuel assembly, is used to determine the DLFs for the guide sleeve panel bending mode. The fundamental frequency of the fuel assembly fuel tubes in bending is calculated for a single span of 6.76 inches, assuming fixed boundary conditions at both ends. Structural credit is taken only for the fuel cladding. The calculated fundamental frequency is 527 Hz.

The natural frequencies for the entire set of baskets are summarized in Table A.2.13.9-4 and the finite element model with boundary conditions and the lowest natural frequency for the bounding basket, i.e., 32PT, are shown in Figure A.2.13.9-2 and Figure A.2.13.9-3, respectively.

Fuel

ANSYS modal analyses are performed to determine the lateral natural frequencies for the fuel rods. For the PWR fuel rods no changes are made to the ANSYS model described in Appendix A.2.13.11 and modal analyses are performed to determine the lowest natural frequencies. For the BWR fuel rods, the lowest natural frequency of the bottom-most fuel rod (after contact at the top of the basket) is determined by performing modal analyses in ANSYS.

The natural frequencies for the fuel claddings are summarized in Table A.2.13.9-5 and the lowest frequency for the bounding fuel cladding is shown in Figure A.2.13.9-4.

A.2.13.9.4 Dynamic Load Factor Calculations

ANSYS transient dynamic analysis was performed using a finite element model consisting of a damped spring oscillator, COMBIN14, and structural mass, MASS21, elements to calculate DLFs for 1' and 30' end and side drops. The finite element model is shown in Figure A.2.13.9-5. The acceleration time history of the 1 ft and 30 ft end and side drops are applied to the mass element and DLF is calculated by:

$$DLF = u_{\max \text{ dynamic}} / u_{\max \text{ static}}$$

where,

$u_{\max \text{ static}}$ – calculated by max g load x mass / stiffness

$u_{\max \text{ dynamic}}$ – calculated by ANSYS

Unit mass is assumed for all analyses, and the stiffness and damping (7% damping is used) are calculated based on the desired frequency of the spring using the following equations:

$$k = m(2\pi f)^2$$

where,

m – mass

f – desired frequency

$$c = 2\zeta \sqrt{(km)}$$

where,

ζ – damping ratio

k – stiffness

m – mass

DLFs are calculated for each drop condition for a frequency range from 5 to 200 Hz and are shown in Figure A.2.13.9-6. The DLFs for all baskets, canisters, and fuel claddings are summarized in Table A.2.13.9-6 and Table A.2.13.9-7.

The LSDYNA analyses in Appendix A.2.13.12 have been updated in Rev. 7, however since the effect on acceleration time histories is minimal, the results for the DLF are unaffected.

A.2.13.9.5 References

1. ANSYS Computer Code and User's Manual, Release, 8.1 and 10A1.
2. Blevins, Robert D., "Formulas for Natural Frequency and Mode Shape," Krieger Publishing Company, Florida, 1995.

Table A.2.13.9-1
Lowest Natural Frequencies of the Canister Shell during End Drop

Canisters	61BT/ 61BTH	69BTH	24PTH	24PT4	32PT	32PTH/ 32PTH1	37PTH
Cavity Length of Canister (in)	179.5	178.4	175.1	180.2	175.6	181.75	171.63
Weight of Entire Canister (lbs)	22329	24594	22013	15626	24393	24048	24388
Weight of Bottom Shield Plug (lb)	3957	7805	3927	4211	5366	7203	7758
Outer Diameter of Canister (in)	67.25	69.75	67.19	67.19	67.19	69.75	69.75
Inner Diameter of Canister (in)	66.25	68.75	66.19	65.94	66.19	68.75	68.75
Cross Sectional Area (in ²)	104.86425	108.791	104.769	130.717	104.769	108.791	108.79
Young's Modulus @ 500 Deg F	2.58E+07	2.58E+07	2.58E+07	2.58E+07	2.58E+07	2.58E+07	2.58E+07
Maximum Static Vertical Deflection Δ (in)	0.001219	0.00106	0.00117	0.000610	0.00123	0.00109	0.0010
Natural Frequency of Canister (End Drop), f_1 Hz	89.52	95.67	91.31	126.55	88.90	94.63	98.01

Table A.2.13.9-2
Lowest Natural Frequencies of the Basket during End Drop

Basket	61BT/ 61BTH	69BTH	24PTH	24PT4 ⁽¹⁾	32PT	32PTH/ 32PTH1	37PTH
Length of Basket	164	164	174.6	-	175	178.75	169
Weight of Steel + Aluminum	27,789	30,649	31,213	-	22,914	30,999	23,288
Volume of Steel + Aluminum	160,372	195,238	197,629	-	109,829	225,467	166,267
Average Weight Density (wt/volume)	0.17327	0.1569	0.157937	-	0.208633	0.137843	0.140064
Average Mass Density (Wt Density/386.4)	0.000448	0.00040	0.00041	-	0.00054	0.000357	0.00036
Young's Modulus (700 F)	2.48E+07	2.48E+07	2.48E+07	-	2.48E+07	2.48E+07	2.48E+07
Frequency of Basket (End Drop), f _i , Hz	716.97	753.26	705.39	sd-60.8 gs-229.9 sr-87.3	612.33	738.48	773.86

Note 1: sd-spacer disk; gs-guide sleeve; sr-support rod

Table A.2.13.9-3
Lowest Natural Frequencies of the Canister Shell during Side Drop

Canister	61BT/ 61BTH	69BTH	24PTH	24PT4	32PT	32PTH/ 32PTH1	37PTH
v - Poisson's ratio	0.3	0.3	0.3	0.3	0.3	0.3	0.3
i For fundamental mode i =2	2	2	2	2	2	2	2
j For fundamental mode j =1	1	1	1	1	1	1	1
μ - Mass Density	0.0007	0.0008	0.0007	0.0008	0.0007	0.0008	0.0008
E @ 500F	2.58E+07	2.58E+07	2.58E+07	2.58E+07	2.58E+07	2.58E+07	2.58E+07
h - thickness	0.5	0.5	0.5	0.625	0.5	0.5	0.5
R - Average Shell Radius	33.345	34.625	33.345	33.2825	33.345	34.625	34.625
L - Cavity Length	179.5	178.4	175.6	180.2	175.6	181.75	171.63
λ_{ij}	0.0764	0.082461	0.079377	0.076352	0.079377	0.079732	0.088413
Ovalling Frequency	71.29	73.78	74.35	71.07	74.35	71.34	79.11

Table A.2.13.9-4
Lowest Natural Frequencies of the Basket during Side Drop

Basket	61BT/ 61BTH	69BTH	24PTH	24PT4 ⁽¹⁾	32PT	32PTH/ 32PTH1	37PTH
Basket Side Drop Frequency	131.39	172.80	106.56	sd-131.30 gs-527 sr-169.40	65.90	106.56	93.50

Note 1: sd-spacer disk; gs-guide sleeve; sr-support rod.

Table A.2.13.9-5

Lowest Natural Frequencies of Bounding BWR and PWR Fuel Claddings
During Side Drop

BWR Fuel Assembly	7x7	8x8	9x9	10x10
Lowest Natural Frequency (Hz)	42.12	35.38	31.67	30.62
PWR Fuel Assembly	14x14	15x15	16x16	17x17
Lowest Mode Natural Frequency (Hz)	33.2	33.7	73.99	34.7

Table A.2.13.9-6
Dynamic Load Factor Results Summary

	61BT/ 61BTH	69BTH	24PTH	24PT4⁽¹⁾	32PT	32PTH/ 32PTH1	37PTH
1 ft Basket End Drop	1.00	1.00	1.00	sd-1.36 gs-1.00 sr-1.33	1.00	1.00	1.00
1 ft Canister End Drop	1.32	1.31	1.32	1.18	1.33	1.31	1.30
30 ft Basket End Drop	1.25	1.25	1.25	sd-1.31 gs-1.00 sr-1.17	1.25	1.25	1.25
30 ft Canister End Drop	1.17	1.16	1.16	1.17	1.17	1.16	1.15
1 ft Basket Side Drop	1.06	1.06	1.13	sd-1.05 gs-1.00 sr-1.04	1.27	1.17	1.25
1 ft Canister Side Drop	1.27	1.29	1.30	1.26	1.30	1.26	1.31
30 ft Basket Side Drop	1.00	1.014	1.014	sd-1.00 gs-1.00 sr-1.01	1.04	1.01	1.00
30 ft Canister Side Drop	1.01	1.00	1.00	1.01	1.00	1.01	1.02

Note: (General) For component frequencies >200 Hz, the frequency of 200 Hz is conservatively used to calculate the DLF.

(1) sd-spacer disk; gs-guide sleeve; sr-support rod

Table A.2.13.9-7
BWR and PWR Fuel Rods Dynamic Load Factor Results Summary

	BWR	PWR
1 ft fuel side drop	1.51	1.47
30 ft fuel side drop	1.39	1.36

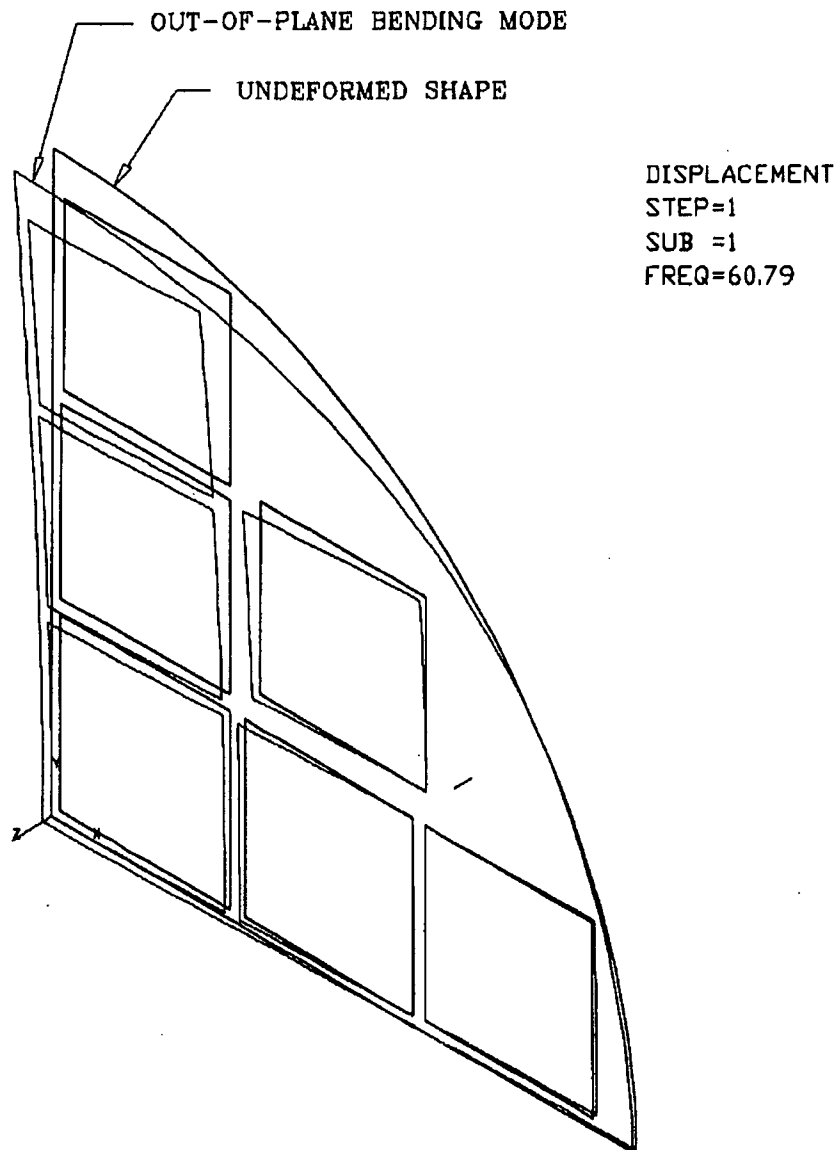


Figure A.2.13.9-1
Lowest Natural Frequency of the 24PT4 Spacer Disk in the End Drop Direction

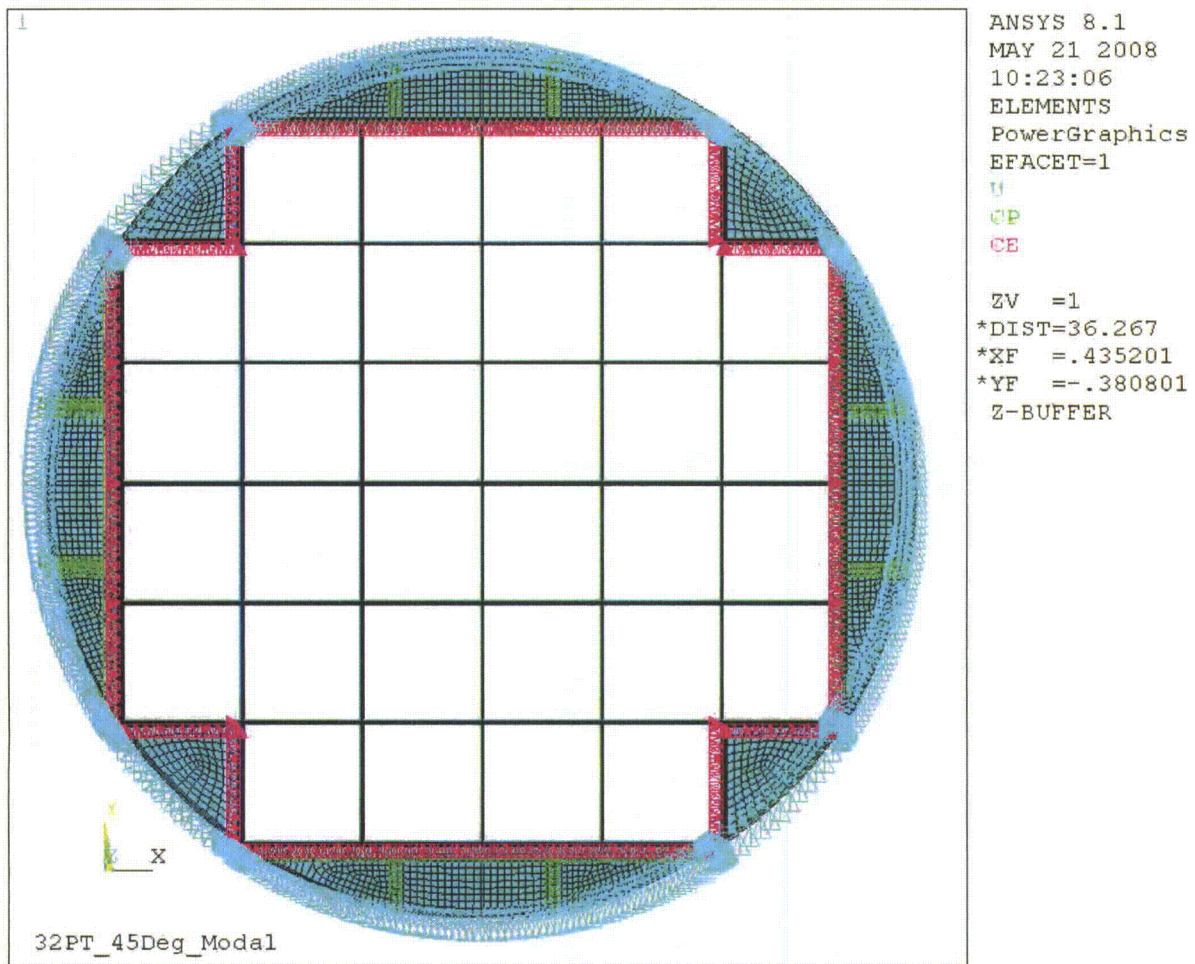


Figure A.2.13.9-2
NUHOMS 32PT Basket Model and Boundary Conditions

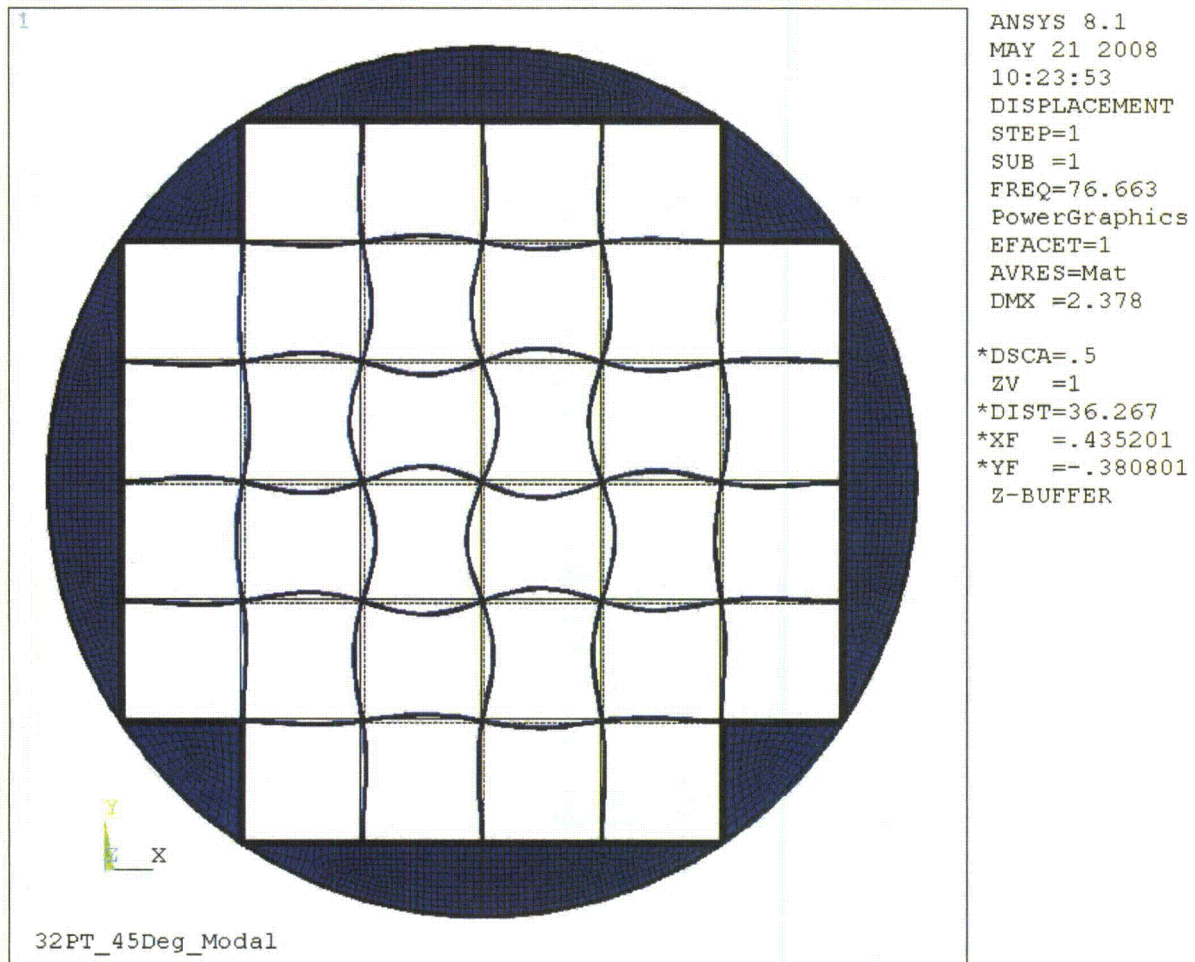


Figure A.2.13.9-3
NUHOMS 32PT Basket First Mode Shape—45 Degree Orientation

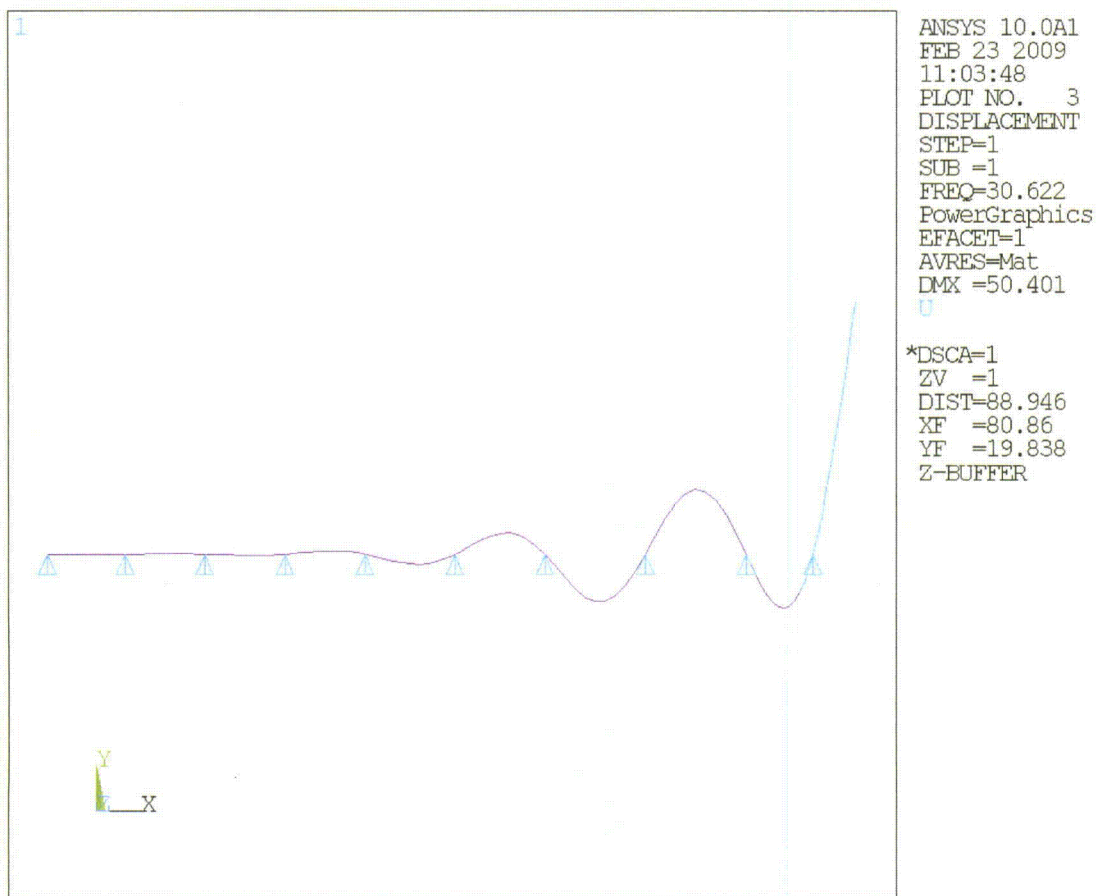


Figure A.2.13.9-4
Bounding BWR 10x10 Fuel Cladding First Mode Shape

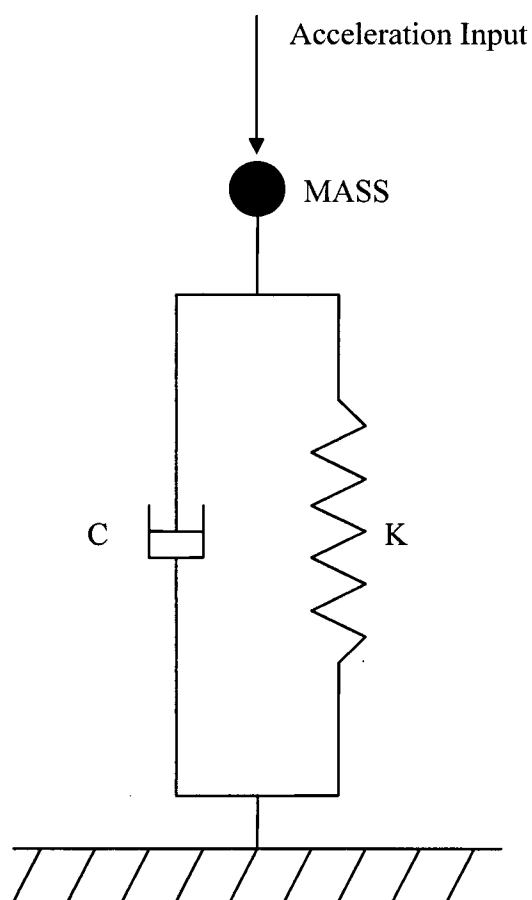


Figure A.2.13.9-5
Finite Element Model for DLF Calculation

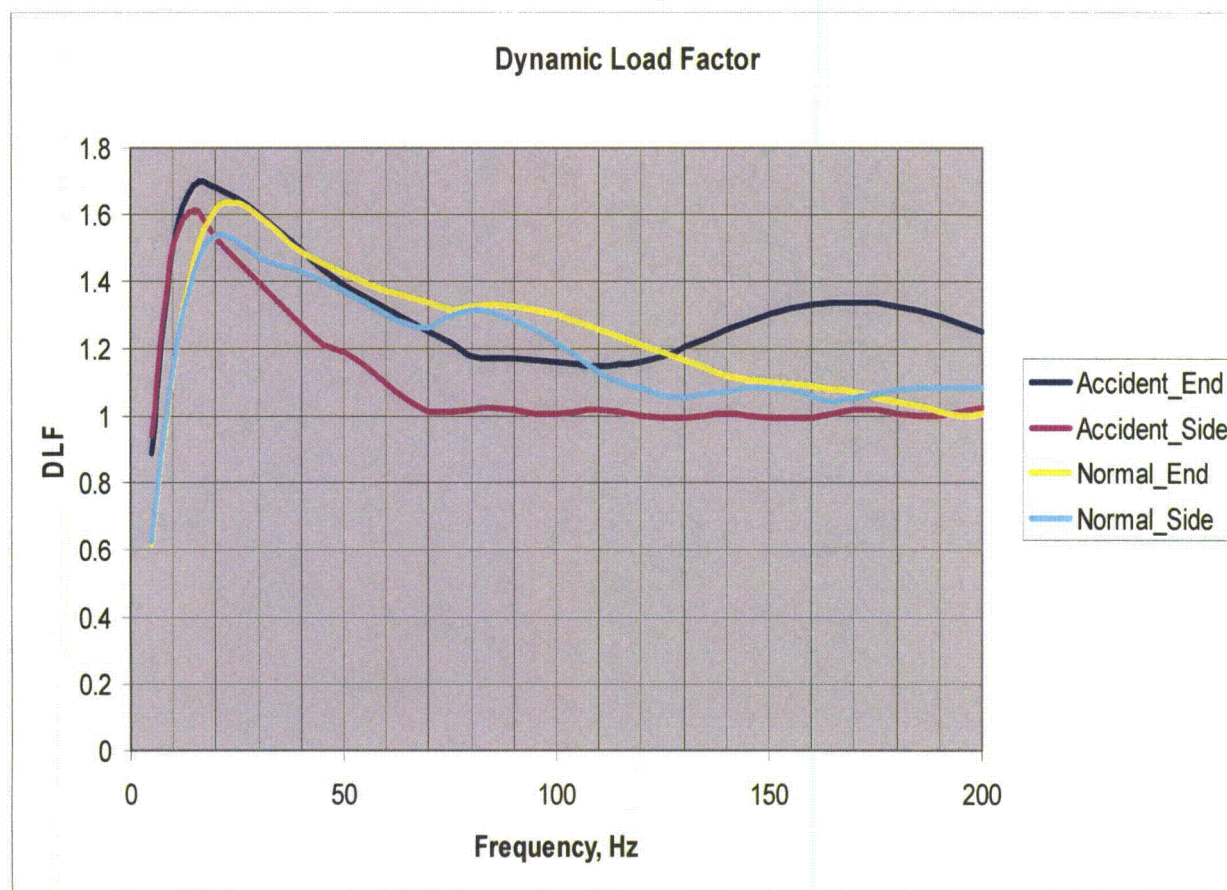


Figure A.2.13.9-6
MP197HB Transport Cask DLF Curves

Appendix A.2.13.10
MP197HB Transport Package Thermal Expansion Evaluation

TABLE OF CONTENTS

A.2.13.10.1	Purpose.....	A.2.13.10-1
A.2.13.10.2	Radial Thermal Expansion.....	A.2.13.10-3
A.2.13.10.3	Axial Thermal Expansion	A.2.13.10-5
A.2.13.10.4	Results and Conclusions	A.2.13.10-9
A.2.13.10.5	Reference	A.2.13.10-10

Appendix A.2.13.10 MP197HB Transport Package Thermal Expansion Evaluation

NOTE: References in this Appendix are shown as [1], [2], etc. and refer to the reference list in Section A.2.13.10.5.

A.2.13.10.1 Purpose

In this appendix, the thermal expansion of the components of the MP197HB transport cask (TC) is evaluated. The thermal load considered is the 100°F ambient normal condition of transport (NCT) temperature distribution computed in Chapter A.3. The requirements of the thermal gaps based on the 100°F ambient temperature distribution calculation bounds the -20°F and -40°F ambient temperature distribution calculations.

The thermal analysis of the DSCs for NCT is described in Chapter A.3. This analysis is performed to determine the transport cask components temperatures for the condition with maximum solar heating, maximum decay heat from the canister contents, and 100°F ambient temperature. The results of the thermal analysis are used to evaluate the effects of axial and radial thermal expansion in the transport cask components.

Volumetric average temperatures of the DSC shell, transport cask inner shell and sleeve are obtained using ANSYS [1] from 100°F ambient NCT thermal analysis results from Chapter A.3. The results are listed in the following table. The average volumetric temperatures for DSC shell, MP197HB sleeve and inner shell from the hottest cross section of the DSC are used in computing the radial hot gaps. Axial hot gaps are computed using the average volumetric temperature computed over the full length of the DSC shell and TC inner shell.

Summary of 100°F Ambient NCT Thermal Analysis

Component	Average Calculated Temperatures for Radial Gap (°F)			Average Calculated Temperatures for Axial Gap (°F)	
	DSC shell	Cask shell	Sleeve	DSC shell	Cask shell
69BTH	467	391	N/A	420	351
37PTH	383	319	N/A	357	294
32PTH	402	331	N/A	378	312
32PTH Type 1	402	331	N/A	378	312
32PTH1 Type 1	402	331	N/A	378	312
32PTH1 Type 2	383	316	N/A	361	299
61BTH Type 1	376	310	313	343	284
61BTH Type 2	396	326	329	360	303
61BT	338	280	283	310	262
32PT	398	321	325	373	304
24PTH	418	338	342	391	319
24PT4	385	312	315	370	305

To verify that adequate clearance exists between the canister and cask cavity for free thermal expansion, the thermal expansions between various components are calculated.

The following table lists the coefficients of thermal expansion used in this section. The most conservative thermal expansion coefficients of SA-240 Type 304 material among various code years are used in this section.

Thermal Expansion Coefficients α_{AVG} (10^{-6} in./in./°F)

T (°F)	SA-203 Gr. E	SA-240 Type 304	SA-240 Type 316	Aluminum (Al 6061)
250	6.8	9.1	8.9	13.1
300	6.9	9.2	9.0	13.3
350	7.0	9.4	9.1	13.4
400	7.1	9.5	9.2	13.6
450	7.2	9.6	9.3	13.8
500	7.3	9.7	9.4	13.9

As seen in the table above, the thermal expansion coefficients of SA-240 Type 304 steel bound those of SA-240 Type 316 steel. These bounding values are used for SA-240 Type 316 steel.

The following table presents the dimensions used in this calculation:

Dimensions used in Calculating Thermal Expansion (in.)

DSC	Heat Load [kW]	OD _{DSC}	L _{DSC}	ID _{CaskShell}	L _{CaskCavity}	L _{Spacer}	Spacer Material
69BTH	32	69.75	196.04	70.5	199.25	2.2	Aluminum
37PTH-M	22 ⁽²⁾ (3)		189.25			9	Stainless Steel
37PTH-S	22 ⁽²⁾		182.00			16.25	Stainless Steel
32PTH	26		185.75			12.5	Stainless Steel
32PTH, Type 1	26 ⁽⁴⁾		193.00			5.25	Stainless Steel
32PTH1, Type 1 (32PTH1-S)	26		185.75			12.5	Stainless Steel
32PTH1, Type 1 (32PTH1-L)	26 ⁽³⁾		198.50			N/A	N/A
32PTH1, Type 2 (32PTH1-S)	24		185.75			12.5	Steel
32PTH1, Type 2 (32PTH1-L)	24 ⁽³⁾		198.50			N/A	N/A
				ID _{Sleeve}			
61BTH, Type 1 ⁽¹⁾	22	67.25	196.04	68	199.25	2.2	Aluminum
61BTH, Type 2 ⁽¹⁾	24					2.2	Aluminum
61BT	18					2.2	Aluminum
32PT S-125	24	67.19	186.55			11.7	Stainless Steel
32PT L-125	24 ⁽³⁾		192.55			5.7	Stainless Steel
24PTH ⁽¹⁾	26		186.67			11.7	Stainless Steel
24PT4	24		196.30			2.2	Aluminum

(see notes on next page)

- (1): DSCs 61BTHF and 24PTHF have the same dimensions and use the same MP197HB features as DSCs 61BTH and 24PTH, respectively. The thermal expansion of 61BTHF and 24PTHF DSCs is bounded by values for 61BTH and 24PTH DSCs and is not analyzed separately.
- (2): Thermal expansion for 37PTH DSC was calculated at a bounding heat load of 23 kW whereas the maximum allowed heat load is 22 kW.
- (3): Thermal expansion for these configurations was calculated based on the average temperatures from shorter DSC configurations.
- (4): Thermal expansion for this DSC was calculated based on the average temperatures from 32PTH1 Type 1 (32PTH1-S) configuration.

A.2.13.10.2 Radial Thermal Expansion

The maximum outside diameter of a canister when exposed to the hot environment is:

$$OD_{DSC,Hot} = OD_{DSC,Cold} [1 + \alpha_{DSC} (T_{avg,DSC} - T_{ref})]$$

where:

- $OD_{DSC,Hot}$ = Hot outer diameter of DSC, *in*
- $OD_{DSC,Cold}$ = Cold outer diameter of DSC at room temperature, *in*
- α_{DSC} = Thermal expansion coefficient of DSC shell, 10^{-6} in./in./°F
- $T_{avg,DSC}$ = Volumetric average temperature of DSC shell, °F
- T_{ref} = Reference Temperature = 70°F

The maximum outside diameter of each canister is calculated in the table below.

Maximum Outside Diameter of Hot DSC (in.)

DSC	$OD_{DSC,Cold}$	$T_{avg,DSC}$	α_{DSC}	$OD_{DSC,Hot}$
69BTH	69.75	467	9.63E-06	70.017
37PTH		383	9.47E-06	69.957
32PTH		402	9.50E-06	69.970
32PTH Type 1			9.50E-06	
32PTH1 Type 1			9.50E-06	
32PTH1 Type 2		383	9.47E-06	69.957
61BTH Type 1	67.25	376	9.45E-06	67.444
61BTH Type 2		396	9.49E-06	67.458
61BT		338	9.35E-06	67.419
32PT	67.19	398	9.50E-06	67.399
24PTH		418	9.54E-06	67.413
24PT4		385	9.47E-06	67.390

The minimum hot inside diameter of the cask cavity and sleeve is:

$$ID_{CaskShell,Hot} = ID_{CaskShell,Cold} [1 + \alpha_{CaskShell} (T_{avg,CaskShell} - T_{ref})]$$

$$ID_{Sleeve,Hot} = ID_{Sleeve,Cold} [1 + \alpha_{Sleeve} (T_{avg,Sleeve} - T_{ref})]$$

where:

- $ID_{CaskShell,Hot}$ = Hot inner diameter of TC inner shell, *in*
- $ID_{CaskShell,Cold}$ = Cold inner diameter of TC inner shell at room temperature, *in*

- $\alpha_{CaskShell}$ = Thermal expansion coefficient of inner shell, 10^{-6} in./in./ $^{\circ}$ F
- $T_{avg,CaskShell}$ = Volumetric average temperature of TC inner shell, $^{\circ}$ F
- $ID_{Sleeve,Hot}$ = Hot inner diameter of sleeve, in
- $ID_{Sleeve,Cold}$ = Cold inner diameter of sleeve at room temperature, in
- α_{Sleeve} = Thermal expansion coefficient of sleeve, 10^{-6} in./in./ $^{\circ}$ F
- $T_{avg,Sleeve}$ = Volumetric average temperature of sleeve, $^{\circ}$ F
- T_{ref} = Reference Temperature = 70° F

The minimum inside diameter of the cask cavity is calculated in the table below.

Minimum Inner Diameter of Hot Cavity (in.)

DSC	$ID_{CaskShell,Cold}$	$T_{avg,CaskShell}$	$\alpha_{CaskShell}$	$ID_{CaskShell,Hot}$
69BTH	70.5	391	7.08E-06	70.660
37PTH		319	6.94E-06	70.662
32PTH		331	6.96E-06	70.628
32PTH Type 1				
32PTH1 Type 1		316	6.93E-06	70.620
32PTH1 Type 2				
	$ID_{Sleeve,Cold}$	$T_{avg,Sleeve}$	α_{Sleeve}	$ID_{Sleeve,Hot}$
61BTH Type 1	68.00	313	1.33E-05	68.220
61BTH Type 2		329	1.34E-05	68.235
61BT		283	1.32E-05	68.191
32PT		325	1.33E-05	68.231
24PTH		342	1.34E-05	68.247
24PT4		315	1.33E-05	68.222

The resulting hot diametrical gaps between the DSC and the cask cavity or the sleeve are calculated as follows and are presented in the table below.

$$\Delta_{HOT_GAP,Dia} = ID_{S,Hot} - OD_{DSC,Hot}$$

where, $ID_{S,Hot} = ID_{Sleeve,Hot}$ for transport cask with sleeve
 $= ID_{CaskShell,Hot}$ for transport cask without sleeve.

Diametrical Hot Gap (in.)

DSC	Sleeve	Hot Diametrical Gap, $\Delta_{HOT_GAP,Dia}$
69BTH	No	0.64
37PTH		0.66
32PTH		0.66
32PTH Type 1		0.66
32PTH1 Type 1		0.66
32PTH1 Type 2		0.66
61BTH Type 1	Yes	0.78
61BTH Type 2		0.78
61BT		0.77
32PT		0.83
24PTH		0.83
24PT4		0.83

Adequate clearance has been provided between the outside diameter of the canister and the inside diameter of the cask cavity to permit free thermal expansion.

A.2.13.10.3 Axial Thermal Expansion

The length of a canister and spacer when exposed to the hot environment is:

$$L_{DSC,Hot} = L_{DSC,Cold} [1 + \alpha_{DSC} (T_{avg,DSC} - T_{ref})]$$

$$L_{Spacer,Hot} = L_{Spacer} [1 + \alpha_{Spacer} (T_{avg,DSC} - T_{ref})]$$

where:

- $L_{DSC,Hot}$ = Maximum hot length of the DSC, *in*
- $L_{DSC,Cold}$ = Maximum cold length of the DSC at room temperature, *in*
- $L_{Spacer,Cold}$ = Length of the spacer at room temperature, *in*
- $L_{Spacer,Hot}$ = Hot Length of the spacer, *in*
- α_{Spacer} = Thermal expansion coefficient of spacer, 10^{-6} in./in./°F
- α_{DSC} = Thermal expansion coefficient of DSC shell, 10^{-6} in./in./°F
- $T_{avg,DSC}$ = Volumetric average temperature of DSC shell, °F
- T_{ref} = Reference Temperature = 70°F

The maximum length of each canister and spacer when applicable is calculated as follows and is presented in the table below.

$$L_{DSC+Spacer,Hot} = L_{DSC,Hot} + L_{Spacer,Hot}$$

Maximum Length of Hot DSC and Spacer

DSC	$T_{avg,DSC}$	α_{DSC}	$L_{DSC,Hot}$	α_{Spacer}	$L_{Spacer,Hot}$	$L_{DSC+Spacer,Hot}$
	$^{\circ}F$	$^{\circ}F^{-1}$	in	$^{\circ}F^{-1}$	in	in
69BTH	420	9.54E-06	196.695	1.37E-05	2.211	198.905
37PTH-S	357	9.41E-06	182.491	9.41E-06	16.294	198.785
37PTH-M ⁽¹⁾	357	9.41E-06	189.761	9.41E-06	9.024	198.785
32PTH	378	9.46E-06	186.291	9.46E-06	12.536	198.828
32PTH, Type 1 ⁽²⁾	378	9.46E-06	193.562	9.46E-06	5.265	198.828
32PTH1, Type 1 (32PTH1-L) ⁽¹⁾	378	9.46E-06	199.078	N/A	N/A	199.078
32PTH1, Type 1 (32PTH1-S)	378	9.46E-06	186.291	9.46E-06	12.536	198.828
32PTH1, Type 2 (32PTH1-L) ⁽¹⁾	361	9.42E-06	199.044	N/A	N/A	199.044
32PTH1, Type 2 (32PTH1-S)	361	9.42E-06	186.259	9.42E-06	12.534	198.794
61BTH, Type 1	343	9.37E-06	196.541	1.34E-05	2.208	198.749
61BTH, Type 2	360	9.42E-06	196.576	1.34E-05	2.209	198.784
61BT	310	9.24E-06	196.474	1.33E-05	2.207	198.681
32PT S-125	373	9.45E-06	187.084	9.45E-06	11.733	198.817
32PT L-125 ⁽¹⁾	373	9.45E-06	193.101	9.45E-06	5.716	198.817
24PTH	391	9.48E-06	187.238	9.48E-06	11.736	198.973
24PT4	370	9.44E-06	196.856	1.35E-05	2.209	199.065

(1) Thermal expansion for these configurations was calculated based on the average temperatures from shorter DSC configurations.

(2) Thermal expansion for this DSC was calculated based on the average temperatures from 32PTH1 Type 1 (32PTH1-S) configuration.

The length of the cask cavity, $L_{CaskCavity,Cold}$ at room temperature is 199.25 in. The length of the cask cavity when exposed to the hot environment is:

$$L_{CaskCavity,Hot} = L_{CaskCavity,Cold} [1 + \alpha_{CaskShell} (T_{avg,CaskShell} - T_{ref})]$$

where:

- $L_{CaskCavity,Hot}$ = Hot TC cavity length, in
- $L_{CaskCavity,Cold}$ = Cold TC cavity length at room temperature, in
- $\alpha_{CaskShell}$ = Thermal expansion coefficient of inner shell, 10^{-6} in./in./ $^{\circ}F$
- $T_{avg,CaskShell}$ = Volumetric average temperature of TC inner shell, $^{\circ}F$
- T_{ref} = Reference Temperature = 70 $^{\circ}F$

The minimum length of the hot cask cavity is calculated in the table below.

Minimum Length of Hot Cask Cavity

DSC	$\alpha_{\text{CaskShell}}$	$L_{\text{CaskCavity,Hot}}$
	$^{\circ}\text{F}^{-1}$	in
69BTH	7.00E-06	199.642
37PTH-S	6.89E-06	199.558
37PTH-M ⁽¹⁾	6.89E-06	199.558
32PTH	6.92E-06	199.585
32PTH, Type 1 ⁽²⁾	6.92E-06	199.585
32PTH1, Type 1 (32PTH1-L) ⁽¹⁾	6.92E-06	199.585
32PTH1, Type 1 (32PTH1-S)	6.92E-06	199.585
32PTH1, Type 2 (32PTH1-L) ⁽¹⁾	6.90E-06	199.565
32PTH1, Type 2 (32PTH1-S)	6.90E-06	199.565
61BTH, Type 1	6.87E-06	199.543
61BTH, Type 2	6.91E-06	199.570
61BT	6.82E-06	199.511
32PT S-125	6.91E-06	199.573
32PT L-125 ⁽¹⁾	6.91E-06	199.572
24PTH	6.94E-06	199.594
24PT4	6.91E-06	199.573

- (1) Thermal expansion for these configurations was calculated based on the average temperatures from shorter DSC configurations.
- (2) Thermal expansion for this DSC was calculated based on the average temperatures from 32PTH1 Type 1 (32PTH1-S) configuration.

The resulting hot axial gap between the DSC (and spacer when used) and the cask cavity is calculated as follows and is listed in the table below.

$$\Delta_{Hot_Gap,Axial} = L_{CaskCavity,HOT} - (L_{DSC,Hot} + L_{Spacer,Hot})$$

Axial Hot Gap

DSC	Spacer	Hot Axial Gap, $\Delta_{Hot_Gap,Axial}$ in
69BTH	Yes	0.74
37PTH-S	Yes	0.77
37PTH-M ⁽¹⁾	Yes	0.77
32PTH	Yes	0.76
32PTH, Type 1 ⁽²⁾	Yes	0.76
32PTH1, Type 1 (32PTH1-L) ⁽¹⁾	No	0.51
32PTH1, Type 1 (32PTH1-S)	Yes	0.76
32PTH1, Type 2 (32PTH1-L) ⁽¹⁾	No	0.52
32PTH1, Type 2 (32PTH1-S)	Yes	0.77
61BTH, Type 1	Yes	0.79
61BTH, Type 2	Yes	0.79
61BT	Yes	0.83
32PT S-125	Yes	0.76
32PT L-125 ⁽¹⁾	Yes	0.75
24PTH	Yes	0.62
24PT4	Yes	0.51

- (1) Thermal expansion for these configurations was calculated based on the average temperatures from shorter DSC configurations.
- (2) Thermal expansion for this DSC was calculated based on the average temperatures from 32PTH1 Type 1 (32PTH1-S) configuration.

Adequate clearance has been provided between the canister and the cask cavity length to permit free thermal expansion.

A.2.13.10.4 Results and Conclusions

Based on the results of the above analyses, there is adequate clearance between the various components of the canister and cask to allow free thermal expansion. Consequently, no significant stress will develop in the NUHOMS® MP197HB transport cask due to thermal expansion. The following table summarizes the thermal expansion calculation results from the above analyses.

Thermal Expansion of MP197HB Components

DSC	Sleeve	Spacer	Hot Diametrical Gap	Hot Axial Gap
			in	in
69BTH	No	Yes	0.64	0.74
37PTH-S			0.66	0.77
37PTH-M				0.77
32PTH			0.66	0.76
32PTH, Type 1			0.66	0.76
32PTH1, Type 1 (32PTH1-L)		No	0.66	0.51
32PTH1, Type 1 (32PTH1-S)		Yes		0.76
32PTH1, Type 2 (32PTH1-L)		No	0.66	0.52
32PTH1, Type 2 (32PTH1-S)		Yes		0.77
61BTH, Type 1	Yes	Yes	0.78	0.79
61BTH, Type 2			0.78	0.79
61BT			0.77	0.83
32PT S-125			0.83	0.76
32PT L-125				0.75
24PTH			0.83	0.62
24PT4			0.83	0.51

A.2.13.10.5 Reference

1. ANSYS Computer Code and User's Manual, Release 10.0.

*Proprietary information on pages A.2.13.11-i, A.2.13.11-ii, and A.2.13.11-1
through A.2.13.11-15 withheld pursuant to 10 CFR 2.390*

This page intentionally left blank.

This page intentionally left blank.

This page intentionally left blank.

This page intentionally left blank.

This page intentionally left blank.

*Proprietary information on pages A.2.13.11-21 through A.2.13.11-52
withheld pursuant to 10 CFR 2.390*

Figure A.2.13.11-15
DELETED

Figure A.2.13.11-16
DELETED

Figure A.2.13.11-17
DELETED

Figure A.2.13.11-18
DELETED

Figure A.2.13.11-19
DELETED

Figure A.2.13.11-20
DELETED

Figure A.2.13.11-21
DELETED

Figure A.2.13.11-22
DELETED

Figure A.2.13.11-23
DELETED

Figure A.2.13.11-24
DELETED

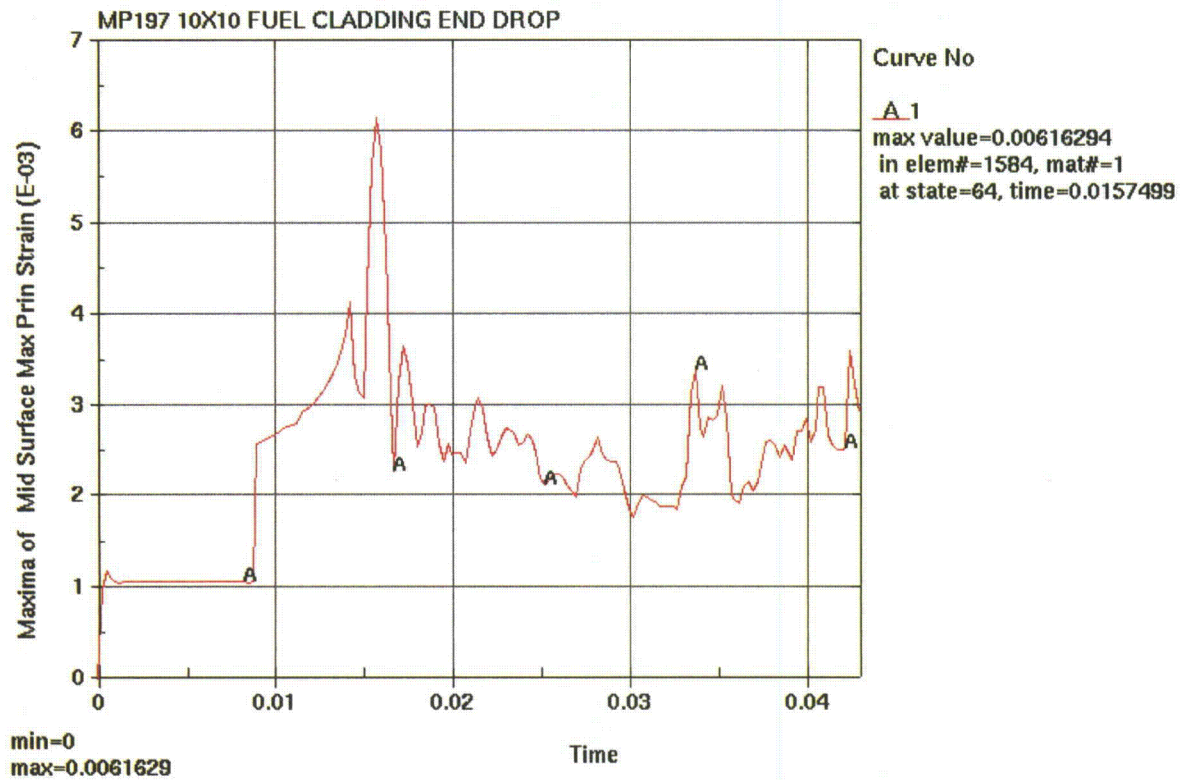


Figure A.2.13.11-25
Maximum Principal Strain Time-History of 10x10 HB Fuel Rod

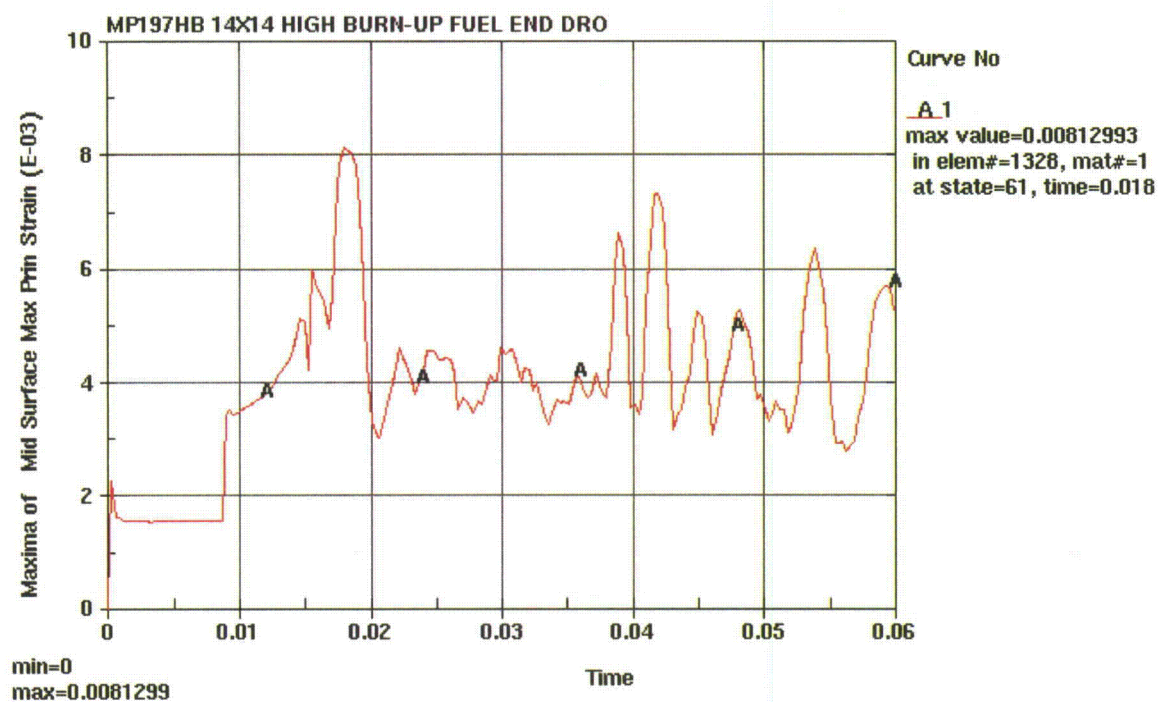


Figure A.2.13.11-26
Maximum Principal Strain Time-History of 14x14 HB Fuel Rod

MP197 10X10 FUEL CLADDING END DROP
Time = 0.01575
Contours of Mid Surface Max Prin Strain
min=0, at elem# 20137
max=0.00616294, at elem# 1584

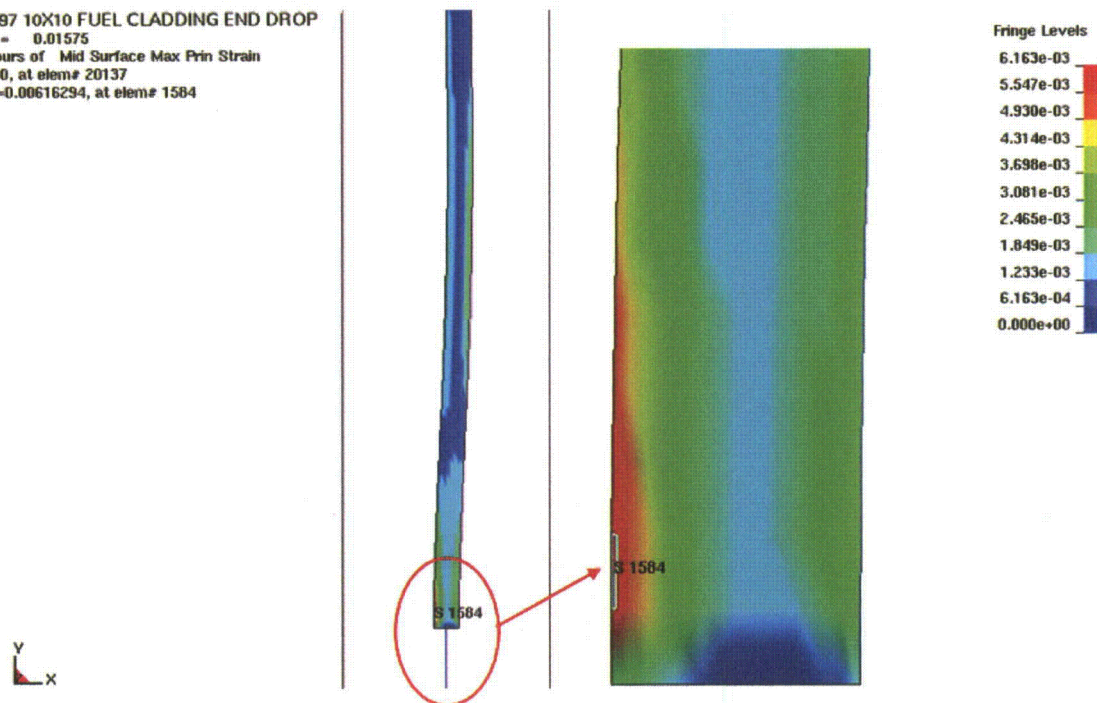


Figure A.2.13.11-27
Maximum Principal Strain Contour Plot of 10x10 HB Fuel Rod

MP197HB 14X14 HIGH BURN-UP FUEL END DRO
Time = 0.018
Contours of Mid Surface Max Prin Strain
min=0, at elem# 16889
max=0.00812993, at elem# 1328

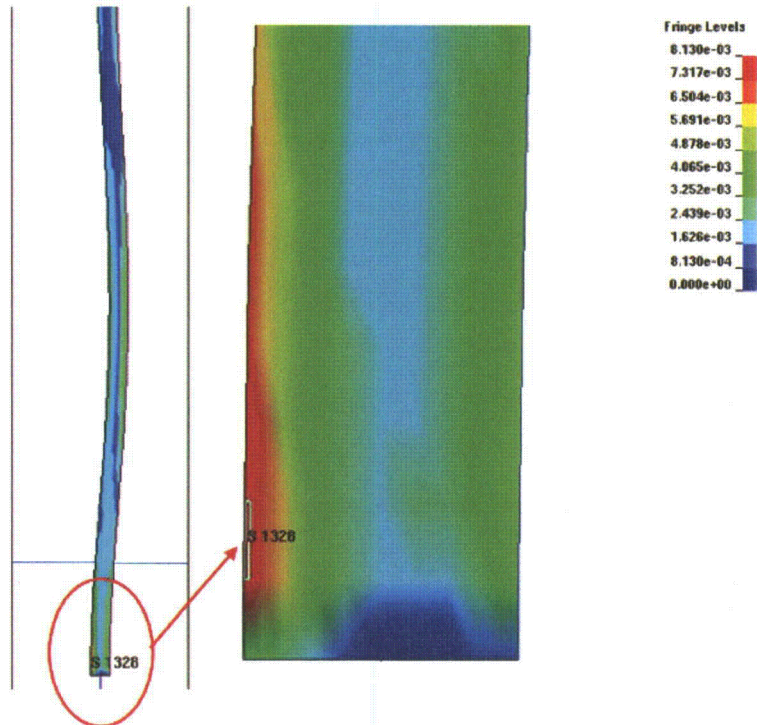


Figure A.2.13.11-28
Maximum Principal Strain Contour Plot of 14x14 HB Fuel Rod

Figure A.2.13.11-29
DELETED

Figure A.2.13.11-30
DELETED

*Proprietary information on pages A.2.13.11-69 through A.2.13.11-77
withheld pursuant to 10 CFR 2.390*

Appendix A.2.13.12 MP197HB Transport Package Impact Limiter Analysis Using LS-DYNA

TABLE OF CONTENTS

A.2.13.12.1	Introduction.....	A.2.13.12-1
A.2.13.12.2	NUHOMS®-MP197 Transport Package 1/3 Scale Impact Limiter	
	Drop Testing	A.2.13.12-1
A.2.13.12.3	MP197 1/3 Scale LS-DYNA Benchmark Analysis	A.2.13.12-2
A.2.13.12.4	1/3 Scale Impact Limiter Benchmark Analysis Results.....	A.2.13.12-6
A.2.13.12.5	MP197HB Full Scale Transport Package LS-DYNA Impact Analysis.....	A.2.13.12-8
A.2.13.12.6	Analysis Results.....	A.2.13.12-13
A.2.13.12.7	Additional Analysis Results for Slap Down Drop Analyses	A.2.13.12-13
A.2.13.12.8	End Drop Analysis Based on -40 °F Wood Properties	A.2.13.12-14
A.2.13.12.9	Sensitivity Studies of MP197HB Impact Limiter Analysis	A.2.13.12-14
A.2.13.12.10	Baseline g Loads for Structural Evaluations.....	A.2.13.12-18
A.2.13.12.11	Impact Limiter Bolt Evaluation	A.2.13.12-19
A.2.13.12.12	References.....	A.2.13.12-27

LIST OF TABLES

Table A.2.13.12-1	Effective plastic strain vs. scale factor for concrete material	A.2.13.12-28
Table A.2.13.12-2	Tabulated pressures vs. volumetric strain for concrete material.....	A.2.13.12-28
Table A.2.13.12-3	Wood Segment Room Temperature Material Properties.....	A.2.13.12-29
Table A.2.13.12-4	Wood Segment Material Properties - 20 °F.....	A.2.13.12-29
Table A.2.13.12-5	Pressure vs. Volumetric Strain for 100% Average Room Temperature Wood	
	Properties	A.2.13.12-30
Table A.2.13.12-6	Pressure vs. Volumetric Strain for Wood Properties -20 °F	A.2.13.12-31
Table A.2.13.12-7	Peak Nodal Accelerations, Wood Crush Depths, and Impact Duration	
	Comparisons	A.2.13.12-32
Table A.2.13.12-8	Summary of the Full Scale Impact Limiter Analysis Results.....	A.2.13.12-33
Table A.2.13.12-9	Calculation of Total Moment.....	A.2.13.12-34
Table A.2.13.12-10	Summary of Stresses (ksi)	A.2.13.12-35

LIST OF FIGURES

Figure A.2.13.12-1	1/3 Scale Impact Limiter Finite Element Model Overview	A.2.13.12-36
Figure A.2.13.12-2	1/3 Scale Impact Limiter Finite Element Model for Side Drop	A.2.13.12-37
Figure A.2.13.12-3	1/3 Scale Impact Limiter Finite Element Model for End Drop	A.2.13.12-38
Figure A.2.13.12-4	1/3 Scale Impact Limiter Finite Element Model for 20° Slap Down Drop	A.2.13.12-39
Figure A.2.13.12-5	Plot of Maximum Deformation for 1/3 Scale Side Drop.....	A.2.13.12-40
Figure A.2.13.12-6	Plot of Maximum Deformation for 1/3 Scale End Drop (-20°F).....	A.2.13.12-41
Figure A.2.13.12-7	Plot of Maximum Deformation for 1/3 Scale 20° Slap Down Drop	A.2.13.12-42
Figure A.2.13.12-8	Plot of Maximum Deformation for 1/3 Scale 20° Slap Down Drop	A.2.13.12-43
Figure A.2.13.12-9	1/3 Scale Side Drop Acceleration Time History	A.2.13.12-44
Figure A.2.13.12-10	1/3 Scale Side Drop Acceleration Time History, Accelerometer 1	A.2.13.12-45
Figure A.2.13.12-11	1/3 Scale Side Drop Acceleration Time History, Accelerometer 10.....	A.2.13.12-46
Figure A.2.13.12-12	1/3 Scale End Drop (-20°F) Acceleration Time History	A.2.13.12-47
Figure A.2.13.12-13	1/3 Scale End Drop (-20°F) Acceleration Time History,	
	Accelerometer 11	A.2.13.12-48

Figure A.2.13.12-14 1/3 Scale End Drop (-20°F) Acceleration Time History, Accelerometer 7	A.2.13.12-49
Figure A.2.13.12-15 1/3 Scale 20° Slap Down Drop Acceleration Time History	A.2.13.12-50
Figure A.2.13.12-16 1/3 Scale 20° Slap Down Drop Acceleration Time History	A.2.13.12-51
Figure A.2.13.12-17 1/3 Scale 20° Slap Down Drop Acceleration Time History, Accelerometer 10	A.2.13.12-52
Figure A.2.13.12-18 1/3 Scale 20° Slap Down Drop Acceleration Time History, Accelerometer 1	A.2.13.12-53
Figure A.2.13.12-19 Full Scale MP-197HB Impact Limiter Finite Element Model Overview	A.2.13.12-54
Figure A.2.13.12-20 Full Scale MP-197HB Impact Limiter Finite Element Model for End Drop Orientation	A.2.13.12-55
Figure A.2.13.12-21 Full Scale MP-197HB Impact Limiter Finite Element Model for Side Drop Orientation	A.2.13.12-56
Figure A.2.13.12-22 Full Scale MP-197HB Impact Limiter Finite Element Model for CG Over Corner Orientation	A.2.13.12-57
Figure A.2.13.12-23 Full Scale MP-197HB Impact Limiter Finite Element Model for 20° Slap Down Orientation	A.2.13.12-58
Figure A.2.13.12-24 Full Scale MP-197HB Impact Limiter Finite Element Model for 10° Slap Down Orientation	A.2.13.12-59
Figure A.2.13.12-25 Region of Nodes Averaged for Time History (All cases other than Slap Down)	A.2.13.12-60
Figure A.2.13.12-26 Region of Nodes Averaged for Time History (Slap Down Cases)	A.2.13.12-61
Figure A.2.13.12-27 Full Scale 30' End Drop Acceleration Time History (Room Temperature)	A.2.13.12-62
Figure A.2.13.12-28 Full Scale 30' End Drop Acceleration Time History (-20 °F and -40 °F)	A.2.13.12-63
Figure A.2.13.12-29 Full Scale 30' Side Drop Acceleration Time History	A.2.13.12-64
Figure A.2.13.12-30 Full Scale 30' CG Over Corner Drop Acceleration Time History	A.2.13.12-65
Figure A.2.13.12-31 Full Scale 30' 20° Slap Down Drop Acceleration Time History (First Impact)	A.2.13.12-66
Figure A.2.13.12-32 Full Scale 30' 20° Slap Down Drop Acceleration Time History (Second Impact)	A.2.13.12-67
Figure A.2.13.12-33 Full Scale 30' 10° Slap Down Drop Acceleration Time History (First Impact)	A.2.13.12-68
Figure A.2.13.12-34 Full Scale 30' 10° Slap Down Drop Acceleration Time History (Second Impact)	A.2.13.12-69
Figure A.2.13.12-35 Full Scale 1 Foot Normal Condition End Drop Acceleration Time History	A.2.13.12-70
Figure A.2.13.12-36 Full Scale 1 Foot Normal Condition Side Drop Acceleration Time History	A.2.13.12-71
Figure A.2.13.12-37 Plot of Maximum Deformation for 30' End Drop- Full Scale	A.2.13.12-72
Figure A.2.13.12-38 Plot of Maximum Deformation for 30' End Drop (-20°F) – Full Scale ...	A.2.13.12-73
Figure A.2.13.12-39 Plot of Maximum Deformation for 30' Side Drop – Full Scale	A.2.13.12-74
Figure A.2.13.12-40 Plot of Maximum Deformation for 30' CG Over Corner Drop – Full Scale	A.2.13.12-75
Figure A.2.13.12-41 Plot of Maximum Deformation for 30' 20° Slap Down Drop – Full Scale (First Impact)	A.2.13.12-76
Figure A.2.13.12-42 Plot of Maximum Deformation for 30' 20° Slap Down Drop – Full Scale (Second Impact)	A.2.13.12-77

Figure A.2.13.12-43 Plot of Maximum Deformation for 30' 10° Slap Down Drop – Full Scale (First Impact).....	A.2.13.12-78
Figure A.2.13.12-44 Plot of Maximum Deformation for 30' 10° Slap Down Drop – Full Scale (Second Impact).....	A.2.13.12-79
Figure A.2.13.12-45 Plot of Maximum Deformation for 1 Foot Normal Condition End Drop – Full Scale	A.2.13.12-80
Figure A.2.13.12-46 Plot of Maximum Deformation for 1 Foot Normal Condition Side Drop – Full Scale	A.2.13.12-81
Figure A.2.13.12-47 Locations of Nodes Used to Compute Rotational Acceleration – Full Scale	A.2.13.12-82
Figure A.2.13.12-48 Vertical Acceleration Along Cask During First And Second Impact to Compute Rotational Acceleration for 20° Slap Down Drop.....	A.2.13.12-83
Figure A.2.13.12-49 Vertical Acceleration Along Cask During First And Second Impact to Compute Rotational Acceleration for 10° Slap Down.....	A.2.13.12-84
Figure A.2.13.12-50 Bolt Forces Around Top and Bottom Impact Limiters for 20° Slap Down Drop.....	A.2.13.12-85
Figure A.2.13.12-51 Bolt Forces Around Top and Bottom Impact Limiters for 10° Slap Down Drop.....	A.2.13.12-86
Figure A.2.13.12-52 Cask Rigid Body Resultant Acceleration for 20° Slap Down Drop – Full Scale.....	A.2.13.12-87
Figure A.2.13.12-53 Cask Rigid Body Resultant Acceleration for 10° Slap Down Drop – Full Scale.....	A.2.13.12-88
Figure A.2.13.12-54 Overview of New Cask Model with Three Density Sections – Full Scale.....	A.2.13.12-89
Figure A.2.13.12-55 Free Body Diagram of Top Impact Limiter during Shallow Angle Slap Down Drop	A.2.13.12-90
Figure A.2.13.12-56 Location of Nodes Selected to Average Accelerations	A.2.13.12-91
Figure A.2.13.12-57 LS-DYNA Energy Plots (in-lbf) 30' End Drop–1/3 Scale Benchmark Model	A.2.13.12-92
Figure A.2.13.12-58 LS-DYNA Energy Plots (in-lbf) 30' Side Drop–1/3 Scale Benchmark Model.....	A.2.13.12-93
Figure A.2.13.12-59 LS-DYNA Energy Plots (in-lbf) 30' Slap Down–1/3 Scale Benchmark Model.....	A.2.13.12-94
Figure A.2.13.12-60 LS-DYNA Energy (in-lbf) Plots 30' End Drop (Room Temperature)–Full Scale Model.....	A.2.13.12-95
Figure A.2.13.12-61 LS-DYNA Energy (in-lbf) Plots 30' End Drop (-20 °F) –Full Scale Model.....	A.2.13.12-96
Figure A.2.13.12-62 LS-DYNA Energy (in-lbf) Plots 30' End Drop (-40 °F)–Full Scale Model.....	A.2.13.12-97
Figure A.2.13.12-63 LS-DYNA Energy (in-lbf) Plots 30' CG Over Corner–Full Scale Model.....	A.2.13.12-98
Figure A.2.13.12-64 LS-DYNA Energy (in-lbf) Plots 30' Side Drop–Full Scale Model	A.2.13.12-99
Figure A.2.13.12-65 LS-DYNA Energy (in-lbf) Plots 30' Side Drop Slap Down 20°–Full Scale Model	A.2.13.12-100
Figure A.2.13.12-66 LS-DYNA Energy (in-lbf) Plots 30' Side Drop Slap Down 10° –Full Scale Model.....	A.2.13.12-101

Appendix A.2.13.12

MP197HB Transport Package Impact Limiter Analysis Using LS-DYNA

NOTE: References in this Appendix are shown as [1], [2], etc. and refer to the reference list in Section A.2.13.12.12.

A.2.13.12.1 Introduction

The results of the 1/3 scale drop tests of the impact limiters previously performed for the NUHOMS[®]-MP197 Transport Package, main SAR, are used to benchmark the analysis model and methodology for the NUHOMS[®]-MP197HB impact limiters. For this purpose, a 1/3 scale model of the NUHOMS[®]-MP197 in the tested configuration is developed and analyzed using the LS-DYNA [2] computer program, and the analysis results are compared to the 1/3 scale NUHOMS[®]-MP197 drop test results as described in Appendix 2.10.9 of NUHOMS[®]-MP197 Transport Package, main SAR. The benchmarked model, methodology, and material properties are then used to develop the full scale MP197HB LS-DYNA transport package model as described in Section A.2.13.12.5.

A.2.13.12.2 NUHOMS[®]-MP197 Transport Package 1/3 Scale Impact Limiter Drop Testing

A series of drop tests have been previously performed on a one-third scale mockup of the MP197 Transport Package equipped with impact limiters. The test program details and test results are described in Appendix 2.10.9 of the NUHOMS[®]-MP197 Transport Package, main SAR. The tests were performed to evaluate impact limiter performance for the 30 foot free drop hypothetical accident conditions. The cask was dropped in three different orientations, including a 90° End Drop, 0° Side Drop and a 20° Slap Down. The 90° End Drop orientation was performed with the impact limiters chilled to -20°F in order to analyze the effects of low temperature on impact limiter performance.

For purposes of carrying out the testing program, four 1/3 scale impact limiters were constructed and tested. These are identified as impact limiter numbers 1, 2, 3, and 4 in the table below. The various drop test orientations were performed in the sequence shown in the following table.

Test Number	Drop Orientation	Drop Height	Impact Limiter Number	Location of Impact Limiter in Cask
1	0° Side Drop	30 Feet	1	Top
			2	Bottom
2	20° Slap Down	30 Feet	3	Top (2 nd Impact)
			2	Bottom (1 st Impact)
3	90° End Drop	30 Feet	3	Top
			4	Bottom (Impact End, -20°F)

A.2.13.12.3 MP197 1/3 Scale LS-DYNA Benchmark Analysis

This section describes the series of analysis used to benchmark the impact limiter analysis methodology against the results of the 1/3 scale impact limiter drop testing program documented in NUHOMS®-MP197 Transport Package, main SAR. For this purpose a finite element model of the 1/3 scale MP197 cask mockup equipped with impact limiters is developed using the LS-DYNA computer program [2]. The LS-DYNA finite element model is analyzed for the same three hypothetical accident conditions as those in the test program, as summarized in Section A.2.13.12.2: 30' End Drop (-20°F), 30' Side Drop (Room Temperature), and 30' 20° Slap Down (Room Temperature). The finite element analysis results are compared to the actual drop test results documented in Appendix 2.10.9 of the NUHOMS®-MP197 Transport Package, main SAR, to benchmark the adequacy of the finite element model.

A. Description of Finite Element Model

The finite element analysis model is a representation of the surrogate 1/3 scale MP197 cask used for the actual drop tests with an impact limiter installed on each end of the cask. The impact limiter model incorporates the individual balsa or redwood sections that make up the impact limiter and the stainless steel cover shell. The impact limiter incorporates a thermal shield consisting of an aluminum plate interfacing with the cask and aluminum spacer blocks that create a thermal gap with the cask lid at each end. The finite element model includes the aluminum spacer blocks. The aluminum plate itself is not modeled as it would have negligible contribution to the structural performance of the cask. Additional features such as the impact limiter attachment bolts and alignment tubes are also included in the LS-DYNA model. The impact surface, which consists of a steel plate over a thick concrete pad is also included in the model.

The impact limiter wood sections, the concrete pad, *the steel plate, and the cask model* are modeled *with default* LS-DYNA *constant stress* solid elements. The impact limiter shell is modeled with fully integrated shell elements.

The impact limiter attachment bolts and associated inner and outer bolt tubes are modeled as a combination of spring elements and beam elements. The outer alignment tubes and inner welded bolt tubes are modeled as beam elements with the proper dimensions. The inner bolt tube is welded to the stainless steel impact limiter shell. The section of bolt extending from the bolt boss to the impact limiter shell is modeled as a beam section. The beam is fixed to the bolt boss on one end. The other end is fixed to the impact limiter shell in a way that approximates the bolt penetrating the shell. For the end drop condition, this end of the beam is coupled to the shell in the X and Y directions. For the side drop and slap-down conditions, this end of the beam is coupled to the shell in the Y and Z directions. The remaining section of bolt is modeled as a non-linear spring. The spring has a tensile stiffness and a negligibly small compression stiffness. This is done in order to model the bolt slipping through the tube during compression. The small compression spring rate prevents instabilities within LS-DYNA. Bolts located on the axis of symmetry are modeled with modified dimensions that have half the moment of inertia and half the cross sectional area.

Only one-half of the cask, impact limiters, steel plate and concrete are modeled, as the entire arrangement is reasonably symmetric about the x-y plane. The distribution of the thermal shield spacer blocks is not symmetric to the plane of symmetry. However, the slight asymmetry is negligible since the effect of the blocks is still captured.

The three analyzed drop accident conditions are as follows:

1. 30' End Drop (-20°F)
2. 30' Side Drop (Room Temperature)
3. 30' 20° Slap Down (Room Temperature)

Drop models have consistent *material properties for the room temperature and chilled (-20 °F) cases. The wood properties for the chilled end drop are modified to simulate a -20°F environment. The slap down scenario has the cask initially rotated 20° from the horizontal side drop position and includes an impact limiter at both ends.*

The finite element model and different drop orientations can be seen in Figure A.2.13.12-1 through Figure A.2.13.12-4.

B. Cask Model and Steel Plate Material

The cask model and steel impact plate are modeled as A36 steel with the following properties:

$$E = 27.7 \times 10^6 \text{ psi}$$

$$\nu = 0.3$$

$$S_y = 30.0 \text{ ksi}$$

$$\text{Tangent Modulus, } E_T = 2\% E = 5.540 \times 10^5 \text{ psi}$$

Material properties at 400 °F are used; material properties at room temperature and at -20 °F would have negligible effect on the results.

C. Impact Limiter Shell Material

The impact limiter shell is modeled as SA-240 Type 304 stainless steel with the following properties *applicable to the -20 °F and room temperature cases.*

$$E = 28.3 \times 10^6 \text{ psi}$$

$$\nu = 0.3$$

$$S_y = 30.0 \text{ ksi}$$

$$\text{Tangent Modulus, } E = 1.0 \times 10^5 \text{ psi}$$

$$\text{Mass density, } \rho_{eff} = 9.405 \times 10^{-4} \text{ lb sec}^2/\text{in}^4$$

The density of the impact limiter shell is adjusted to account for the weight of those components not included in the model, such as the lifting lugs. The measured weight of the actual 1/3 scale cask mockup with both impact limiters installed is 9,750 lbs.

D. Concrete Material

The concrete is modeled using material law 16 in LS-DYNA, which was developed specifically for granular type materials. Material constants are implemented into Material Model 16, Mode II.B in LS-DYNA. The material modeled represents 4,200 psi compressive strength concrete. A summary of the input used in the analysis is as follows:

Yield stress versus pressure relationships used:

$$\sigma_{\max} = a_0 + \frac{P}{a_1 + a_2 P}$$

$$\sigma_{\text{failed}} = a_{0f} + \frac{P}{a_{1f} + a_2 P}$$

$$\rho = 2.09675 \times 10^{-4} \text{ lb. sec.}^2 / \text{in.}^4$$

$$\nu = 0.22$$

$$a_0 = 1606$$

$$a_1 = 0.418$$

$$a_2 = 8.35 \times 10^{-5}$$

$$b_1 = 0$$

$$a_{0f} = 0.0 \text{ psi.}$$

$$a_{1f} = 0.385$$

The above yield stress versus pressure curves are used to describe either a hardening or softening behavior of the concrete material, as follows:

$$\sigma_{\text{yield}} = \sigma_{\text{failed}} + \eta(\sigma_{\max} - \sigma_{\text{failed}})$$

The scale factor η as a function of plastic strain is tabulated in Table A.2.13.12-1.

The maximum principal stress tensile failure cutoff is set at 870 psi. Strain rate effects are neglected in the analysis.

The pressure-volume behavior of the concrete is modeled with the pressure versus volumetric strain relationship shown in Table A.2.13.12-2 using the equation of state feature (EOS_Tabulated_Compaction) in LS-DYNA.

An unloading bulk modulus of 700,000 psi is assumed to be constant at any volumetric strain.

One percent reinforcement is assumed in the concrete pad to account for the pad reinforcement. The material properties used for the reinforcing bar are as follows.

$$E = 30 \times 10^6 \text{ psi.}$$

$$\nu = 0.3$$

$S_y = 30,000$ psi.

Tangent Modulus, $E_T = 30 \times 10^4$ psi.

E. Impact Limiter Wood Segment Material

The impact limiter wood is modeled using the *Mat_Modified_Honeycomb* material model in LS-DYNA (material type 126), which models crushable materials with anisotropic behavior.

References [4] and [5] document the use of *Mat_Honeycomb* material model in LS-DYNA to model wood in a similar application. Since the crush strength of wood is not isotropic, separate material properties are used in directions parallel and perpendicular to the wood grain. Strain rate effects are neglected in the analysis. Table A.2.13.12-3 summarizes the wood segment material properties. Table A.2.13.12-4 summarizes the wood segment material properties increased by 20% for the -20° F temperature condition.

The pressure versus volumetric strain relationship defines the crush strength of the wood segments. Table A.2.13.12-5 shows the pressure versus strain curves for redwood and balsa parallel and perpendicular to the wood grain for the average room temperature wood properties. Table A.2.13.12-6 shows the same for the 20% increased wood properties for the -20° F ambient condition. The pressure strain curve is assumed to be initially linear with a slope of the modulus of elasticity E , and then flat up to a locking strain of 0.8 for balsa and 0.6 for redwood.

F. Bolt and Alignment Tube Material

There are 12 bolts that attach each impact limiter to the cask. The following elastic, linearly plastic material properties are used for the bolts in the finite element model *for the -20 °F and room temperature cases*.

SA-540 Grade B24 Class 1

$E = 27.8 \times 10^6$ psi

$\nu = 0.3$

$S_y = 150.0$ ksi

Tangent Modulus, $E_T = 2\% E = 5.54 \times 10^5$ psi

The bolts that attach the impact limiters to the cask are modeled as circular cross section beams. For the Side Drop and Slap Down conditions, the bolt tube sections at the symmetry plane are modeled as hollow circular cross section beams with modified dimensions to represent half the area and moment of inertia.

The springs representing the sections of bolts within the impact limiter were given spring rates representing that of the bolt. The length of bolt used for the spring rate calculation is 10". For the Side Drop and Slap Down conditions, the springs at the plane of symmetry were given half the spring rate. The springs at the plane of symmetry for the End Drop condition were left unchanged as the bolts would be in compression and therefore would have negligible affect on the analysis.

Bolt alignment tubes are modeled as tube beams. The alignment tubes modeled at the plane of symmetry are also full-size as their strength difference is minimal in this analysis. The following elastic, linearly plastic material properties are used for the bolt tubes *for the -20 °F and room temperature cases*.

SA-249 Type 304

$$E = 28.3 \times 10^6 \text{ psi}$$

$$\nu = 0.3$$

$$S_y = 30.0 \text{ ksi}$$

$$\text{Tangent Modulus, } E = 10^5 \text{ psi}$$

G. Boundary Conditions and Initial Conditions

One-half of the cask and impact limiters are modeled with symmetry boundary conditions used to simulate the full structure. The lowest point of the impact limiter shell is initially placed within 0.25" of the steel impact plate to minimize run time. An initial velocity corresponding to the drop height is applied to the model. The initial velocity computed for a 30' drop is 527.45 in/sec.

The automatic *general* contact definition in LS-DYNA (*Contact_Automatic_General*) is applied to model the contact between any two parts of the model. A conservatively low coefficient of friction of 0.25 is applied between all the contact surfaces. The use of a low value for the coefficient of friction is conservative because less energy is absorbed due to friction resulting in greater impact acceleration forces.

An interior contact (*Contact_Interior*) contact definition is applied to the elements modeling the wood sections to prevent *elements from inverting and becoming negative volumes*. *Hourglass controls are applied to control the underintegrated solid elements used in the model*.

Non-reflecting boundaries are applied to the bottom and sides of the modeled concrete not aligned with the plane of symmetry (bottom, left side, right side, and back) to prevent artificial stress waves from reflecting.

A.2.13.12.4 1/3 Scale Impact Limiter Benchmark Analysis Results

Table A.2.13.12-7 summarizes the results of the LS-DYNA analysis in terms of peak filtered accelerations, maximum crush depths, and impact durations for the three drop cases analyzed and compare them with similar parameters obtained from the test results. The maximum accelerations from the tests and the LS-DYNA analyses model are divided by three to represent the accelerations of a full scale MP197 cask. Impact durations and crush depths are unchanged (compare 1/3 scale analysis results to 1/3 scale test results). Figures A.2.13.12-5 through A.2.13.12-8 show the deformed shapes of the impact limiters for each drop case analyzed. *Figures A.2.13.12-57 to A.2.13.12-59 show the energy plots (total, kinetic, internal, hourglass) for the 1/3 scale benchmark analyzed cases.*

The acceleration time histories from the LS-DYNA analyses and from the 1/3 scale testing are shown in the figures summarized in the table below:

Drop Test Case	Figures from LS-DYNA Analysis	Figures from 1/3 Scale Testing	
		Figure A.2.13.12-10	Figure A.2.13.12-11
Side Drop	Figure A.2.13.12-9	Figure A.2.13.12-10	Figure A.2.13.12-11
End Drop	Figure A.2.13.12-12	Figure A.2.13.12-13	Figure A.2.13.12-14
20° Slap Down	Figure A.2.13.12-15 (1 st Impact)	Figure A.2.13.12-17 (1 st Impact)	
	Figure A.2.13.12-16 (2 nd Impact)	Figure A.2.13.12-18 (2 nd Impact)	

As described in Appendix 2.10.9 of NUHOMS®-MP197 Transport Package, main SAR, twelve (12) accelerometers were used to measure the response deceleration time histories for each test. The accelerometers were placed along the test body at 0°, 90°, 180°, and 270° orientations at approximately the center of gravity location and adjacent to each impact limiter. *The location of the 12 accelerometers is shown in Figure 2.10.9-7 of Appendix 2.10.9. The locations correspond to the locations at which the LS-DYNA analysis results are compared, as shown in Figure A.2.13.12-56.*

The test response acceleration time histories shown in Figures A.2.13.12-10, -11, -13, -14, -17, and -18 are representative of the test case indicated. The peak g load calculated from the LS-DYNA analysis *obtained at the locations shown in Figure A.2.13.12-56* is compared with the measured averaged g loads from all the accelerometers.

The analysis results shown in Table A.2.13.12-7 agree well with the measured results of the impact limiter drop tests. The impact time durations match closely with those of the measured results. Wood crush depths are also similar. Therefore, it can be concluded that the LS-DYNA model and analysis methodology implemented as described in this section accurately predicts the response of the impact limiters during the accidental drop.

A.2.13.12.5 MP197HB Full Scale Transport Package LS-DYNA Impact Analysis

The benchmarked model and analysis methodology used for the 1/3 scale LS DYNA analysis of the MP197 described in Section A.2.13.12.3 are used to develop a full scale LS-DYNA model of the MP-197HB Transport Cask equipped with impact limiters. The model is used to determine the rigid body acceleration time history and impact limiter crush depths for the following hypothetical drop conditions:

1. 30' End Drop (room temperature)
2. 30' End Drop (-20°F)
3. 30' End Drop (-40°F)
4. 30' Side Drop
5. 30' CG Over Corner Drop
6. 30' Slap Down 20°
7. 30' Slap Down 10°
8. 1' Normal Condition End Drop
9. 1' Normal Condition Side Drop

Impact limiter attachment bolt forces are also determined for the 30 foot 20° Slap Down Drop and 30 foot 10° Slap Down Drop scenarios.

A. Finite Element Model Description

A finite element model of the surrogate MP197HB transport cask with impact limiters installed at each end of the cask is developed in order to determine the cask's rigid body acceleration and impact limiter crush depths due to normal conditions of transport and hypothetical accident conditions drop scenarios.

Because of the complexity of the analysis, the modeled surrogate cask is a simplified version of the actual MP197HB transport cask. The simplified cask model maintains the same geometry as the actual cask in those areas that interface with the impact limiters. However, density and other dimensions are modified so that the modeled cask has the same dynamic characteristics (mass, center of gravity, and mass moments of inertia properties) as the actual MP197HB cask.

The material properties used in the analysis of the MP197HB cask are the same as those used for the 1/3 scale MP197 benchmarking analysis described in Section A.2.13.12.3. The density of the modeled cask and the stainless steel impact limiter shell are modified in order to duplicate the dynamic characteristics of the actual MP197HB cask.

The finite element analysis model includes a surrogate representation of the actual MP197HB cask with an impact limiter installed on each end of the cask. The impact limiter section of the model incorporates the individual balsa or redwood sections that make up the impact limiter and the stainless steel cover shell. The aluminum spacer blocks of the thermal shield are included in the model. The model includes a concrete block with a steel plate on top to represent the impact

surface. Only $\frac{1}{2}$ of the cask, impact limiters, steel plate and concrete are modeled as the entire arrangement is reasonably symmetric about the x-y plane.

The impact limiter wood sections, the concrete pad, steel plate, *and cask model* are modeled in LS-DYNA using *constant stress* elements. The impact limiter shell is modeled with fully integrated shell elements.

Additional features, such as the impact limiter attachment bolts and associated outer alignment and inner welded tubes are modeled as a combination of spring elements and beam elements. The alignment tubes and welded tubes are modeled as beam elements welded to the stainless steel impact limiter shell.

The drop scenarios analyzed include the hypothetical accident condition drop with a drop height of 30 feet and the 1-foot normal condition of transport drop. Consistent wood properties are used for all analysis cases except for the 30 feet end drop for which modified wood properties to simulate -20°F and -40°F environments are used. The Slap Down cases are 20° and 10° from the horizontal side drop position. The CG over corner drop is 65° from the horizontal side drop position.

Figures A.2.13.12-19 through A.2.13.12-24 show the MP197HB finite element models for the different drop orientations analyzed.

B. Material Properties

The material properties used in this analysis are the same as those used for the 1/3 Scale MP197 Drop Analysis Benchmark. The material properties required to perform the analysis include modulus of elasticity, E , shear modulus, G , Poison's Ratio, ν , and material density, ρ , for the cask model, impact limiter shell, wood segments, steel plate and concrete. *The mechanical properties used are the same as those used in the 1/3 scale benchmark analysis in Section A.2.13.12.2.*

C. Cask Model and Steel Plate Material

The following elastic, linearly plastic material properties for mild steel (A-36) are used for the steel plate and cask model.

$$E = 27.7 \times 10^6 \text{ psi}$$

$$\nu = 0.3$$

$$S_y = 30.0 \text{ ksi}$$

$$\text{Tangent Modulus, } E_T = 2\% E = 5.540 \times 10^5 \text{ psi}$$

Material properties at 400 °F are used ; material properties at room temperature and at -20 °F would have negligible effect on the results.

D. Cask Model

The cask model has the same mass, center of gravity, and moment of inertia as the actual cask. The critical moment of inertia is about Y-axis which is perpendicular to the plane of symmetry of the model. The moments of inertia about the other two axes do not influence this analysis due to the boundary conditions.

The dimensions and density of the modeled cask are adjusted to have the same mass, center of gravity, and moment of inertia as the actual cask. The geometry of the modeled cask is similar to the actual cask except that the center section has a smaller diameter. The reduced diameter area is offset from the geometric center to affect the center of gravity.

E. Impact Limiter Shell

The following elastic, linearly plastic material properties are used for the impact limiter shell.

Stainless Steel (SA-240 Type 304) at room temperature and -20 °F

$$E = 28.3 \times 10^6 \text{ psi}$$

$$\nu = 0.3$$

$$S_y = 30.0 \text{ ksi}$$

$$\text{Tangent Modulus} = 10^5 \text{ psi}$$

The density of the impact limiter shell is adjusted to calibrate the weight of the impact limiter model. This is to take into account for the mass of those impact limiter parts not included in the model.

F. Concrete

The concrete material model and properties are identical to those used for the 1/3 scale MP197 model in Section A.2.13.12.3.

G. Impact Limiter Wood Segments

The impact limiter wood is modeled using the Mat_Modified_Honeycomb material model (Material type 126) in LS-DYNA [2], which models crushable materials with anisotropic behavior such as wood. Since the crush strength of wood is not isotropic, separate material properties are used in directions parallel and perpendicular to the wood grain. Wood crush strengths and density are taken from the MP197HB 1/3 Scale Benchmark Analysis.

H. Bolt and Alignment Tubes

There are 12 bolts that attach each impact limiter to the cask model. The following elastic, linearly plastic material properties are used for the bolts.

SA-540 Grade B23 Class 1 at room temperature and -20 °F

$$E = 27.8 \times 10^6 \text{ psi}$$

$$\nu = 0.3$$

$$S_y = 150.0 \text{ ksi}$$

$$\text{Tangent Modulus, } E_T = 2\% E = 5.56 \times 10^5 \text{ psi}$$

Bolts at the symmetry plane are modeled as hollow circular cross section beams with modified dimensions to represent approximately half the area and moment of inertia.

Each bolt has a bolt alignment tube and a welded bolt tube. The following elastic, linearly plastic material properties are used for the bolt tubes:

SA-312 Type 304 *at room temperature and -20 °F*

$$E = 28.3 \times 10^6 \text{ psi}$$

$$\nu = 0.3$$

$$S_y = 30.0 \text{ ksi}$$

$$\text{Tangent Modulus, } E = 10^5 \text{ psi}$$

Bolt alignment tubes are modeled as tube beams. Bolt alignment tubes at the plane of symmetry represent approximately half the area and moment of inertia.

Welded bolt alignment tubes are modeled as tube beams. Welded bolt alignment tubes at the plane of symmetry represent approximately half the area and moment of inertia.

I. Boundary and Initial Conditions

Because of symmetric one-half of the cask and impact limiters are modeled with symmetry boundary conditions used to simulate the full structure. The initial velocity is computed by equating potential and kinetic energies. For a 30 foot drop, the initial velocity is 527.5 in/sec. For a 1 foot drop, the initial velocity is 96.3 in/sec.

An automatic surface to surface (contact_automatic_single_surface) contact definition is applied between all parts where contact is feasible. *An interior* (contact_interior) contact definition is also applied to the wood parts to prevent elements from inverting and becoming negative volumes. *Hourglass controls are applied to all materials.* A conservatively low coefficient of friction (static and kinetic) of 0.25 is applied between all contact surfaces.

Non-reflecting boundaries are applied to the bottom and sides of the modeled concrete not aligned with the plane of symmetry (bottom, left side, right side, and back) to prevent artificial stress waves from *reflecting*. Both dilatation and shear waves are damped.

J. Data Reduction

The following table lists the duration of the analysis for each drop condition. The time step was automatically chosen by the LS-DYNA program based on the minimum model element size.

Drop Condition	Run Duration (sec)
30° End Drop (Room temperature)	0.06
30° End Drop (-20°F)	0.06
30° End Drop (-40°F)	0.06
30° Side Drop	0.06
30° Slap Down 20°	0.2
30° Slap Down 10°	0.2
30° CG Over Corner Drop	0.1
1' Normal Condition End Drop	0.04
1' Normal Condition Side Drop	0.06

The resulting nodal acceleration time histories are computed by LS-DYNA. The nodal accelerations obtained at the center of the cask model are averaged for all drop conditions except for the slap down analysis cases where the accelerations are averaged for both the top and bottom of the cask due to the dual impacts. Figures A.2.13.12-25 and A.2.13.12-26 show the regions of nodes averaged.

For the Slap Down 20° scenario, the cask is 17.9° counterclockwise from horizontal during the peak acceleration of the first impact and 3.5° clockwise from horizontal during the peak acceleration of the second impact.

For the Slap Down 10° scenario, the cask is 8.48° counterclockwise from horizontal during the peak acceleration of the first impact and 2.35° clockwise from horizontal during the peak acceleration of the second impact.

The time step in the LS-DYNA analysis is 50 μsec. Therefore, by the Nyquist theorem, the frequency content of the nodal acceleration data ranges from zero Hz, up to the following maximum frequency, f_{\max} .

$$f_{\max} = \frac{1}{2 \cdot 50 \times 10^{-6} \text{ sec}} = 10 \text{ kHz}$$

The natural frequencies of the MP197HB cask model, which can be excited by an impact event, are significantly lower than 10kHz. These natural modes of the transport cask involve small displacements (and therefore low stresses) at frequencies higher than that of the rigid body motion of the transport cask. These high frequency accelerations mask the true rigid body motion of the transport cask, because both the low frequency rigid body acceleration and the high frequency natural vibration accelerations superimpose. The net acceleration is contained in the raw data computed by LS-DYNA. Therefore, filtering is necessary to remove these high frequency accelerations.

The averaged raw data for each cross section is filtered using a low pass Butterworth filter with different cutoff frequencies depending on the orientation of the model in order to recover the actual rigid body acceleration of the cask model. A 180 Hz cutoff frequency is used for the End Drop, *side drop*, and the CG Over Corner drop *conditions*. A 120 Hz cutoff frequency is used for the Slap Down runs. The cutoff frequencies are conservative because they will filter out some but not all of the high vibration modes of the cask model in their respective locations and drop orientations. Therefore, the response predicted by the filtered results includes more dynamics than simply the rigid body motion of the transport cask.

A.2.13.12.6 Analysis Results

Table A.2.13.12-8 summarizes the results of the LS-DYNA analysis in terms of peak filtered accelerations, impact durations, maximum crush depths, and provides the corresponding time history plot for the drop scenarios analyzed. Impact limiter crush depth is based on the deformation of the cask into the impact limiter in the vertical direction.

Impact durations are visually determined from the acceleration time history plots (Figures A.2.13.12-27 through A.2.13.12-36).

Figure A.2.13.12-37 through Figure A.2.13.12-46 show the maximum impact limiter deformation plots. *Energy plots (total, kinetic, internal, hourglass) are presented in Figures A.2.13.12-60 to A.2.13.12-66.*

A.2.13.12.7 Additional Analysis Results for Slap Down Drop Analyses

The peak rotational acceleration is calculated for the Slap Down conditions based on the cask interface forces and rotational centers. Figure A.2.13.12-47 shows the locations of nodes groups selected to determine acceleration during peak acceleration of the first and second impacts. Figures A.2.13.12-48 and A.2.13.12-49 show the plot results for the 20° and 10° slap down drop cases respectively.

The rotational centers are at 172.86" from the bottom for the first impact and 55.69" from the bottom for the second impact of the Slap Down 20°. The rotational centers are at 159.61" from the bottom for the first impact and 46.33" from the bottom for the second impact of the Slap Down 10°.

Axial and shear bolt forces at various positions around the impact limiter are plotted for the Slap Down 20° and Slap Down 10° cases in Figures A.2.13.12-50 and A.2.13.12-51 respectively.

Rigid body accelerations for the entire cask model are shown in Figures A.2.13.12-52 and A.2.13.12-53 for the Slap Down 20° and Slap Down 10° runs respectively. The following table shows the cask rigid body accelerations and rotational acceleration at the CG of the cask body.

Cask Rigid Body Accelerations and Rotational Acceleration at CG of the Cask Body
(10° and 20° Slap Down)

Drop Orientation		Peak rigid body deceleration at CG of the cask
30 feet slap down (10°)	1 st impact	Translation (20.2g)
		Rotational ($\alpha = 106.8 \text{ rad/sec}^2$)
	2 nd impact	Translation (25.7g)
		Rotational ($\alpha = 144.9 \text{ rad/sec}^2$)
30 feet slap down (20°)	1 st impact	Translation (15.8g)
		Rotational ($\alpha = 62.9 \text{ rad/sec}^2$)
	2 nd impact	Translation (24.1g)
		Rotational ($\alpha = 138.7 \text{ rad/sec}^2$)

A.2.13.12.8 End Drop Analysis Based on -40 °F Wood Properties

An additional analysis was performed using the wood properties at -40°F temperature. For the -40°F chilled case, the wood modulus of elasticity and shear modulus are increased by 30% [3] from the room temperature. The results of this analysis are shown on Table A.2.13.12-8.

A.2.13.12.9 Sensitivity Studies of MP197HB Impact Limiter Analysis

Sensitivity studies are performed to determine how the analysis results are affected by various model characteristics. The sensitivity studies performed are summarized as follows:

A. Effect of Wood Element Mesh Density and Effect of Bolts on Calculated Impact Load

Two sensitivity studies are performed to evaluate the sensitivity of the analysis results to changes in mesh discretization of the wood elements in the impact limiter model and changes in the modeling of the attachment bolts. The first study run is an end drop at room temperature with double wood elements in the lower impact limiter. The second study run is a side drop with all bolts and bolt alignment tubes removed in order to evaluate the affect of the bolts and their influence on the peak accelerations. The following table summarizes the results of these sensitivity analyses. The comparison indicates that the wood mesh density used is sufficiently accurate. The study run without bolts indicates that the bolt model functions properly and does not significantly stiffen the impact limiter.

Summary of Wood Element Mesh Density and Effect of Bolt Sensitivity Studies

Run	Changes to Model	Original Results Max Accel./ Max Crush	Study Run Results Max Accel./ Max Crush	% Change
1	Wood Elements Doubled	46.2g	45.9g	-0.65%
		10.2"	10.2"	0%
2	Bolts Removed	45.5g	42.4g	-6.8%
		11.5"	12"	+4.3%

B. Unyielding Impact Surface Sensitivity

This sensitivity study is performed to determine if the modeled concrete and steel plate modeled as the impact surface can be considered an unyielding surface. This run uses the same model analyzed for the 30' End Drop Room Temperature case except the concrete is removed and all the nodes of the steel plate are fixed in space. The following table summarizes the results of the sensitivity run. The comparison indicates that the concrete and steel plate modeled as the impact surface can be considered an unyielding surface.

Summary of Impact Surface Sensitivity Study

Run	Changes to Model	Original Results Max Accel./ Max Crush	Study Run Results Max Accel./ Max Crush	% Change
1	End Drop w/ Concrete Removed and All Nodes of Steel Impact Plate Fixed	46.2g	46.2g	0%
		10.2"	10.2"	0%

C. Bolt Forces with Radial Perpendicular Wood Properties

This study is performed to determine the bolt forces with the perpendicular wood properties oriented radial to the cask centerline as opposed to the perpendicular wood properties defined globally. This analysis is based on the 10° Slap Down because it has the critical bolt forces. In this analysis, the circumferential wood sections divided in 30° increments will have perpendicular wood properties rotated so that the strong axis will be radial to the cask centerline, as per drawings shown in Appendix A.1.4.10. The perpendicular wood in the undivided center section will remain globally defined as it will have minimal effects for this drop orientation. Wood orientation can be seen in Figure C-1 as the properties are defined for the more critical 2nd impact. Bolt forces can be seen in Figure C-2. With the wood properties being oriented differently, sections of the perpendicular wood are softer in the impact direction. As a result, the cask acceleration is lower, the impact limiter experiences more deformation, and the bolt forces are lower due to the reduced acceleration.

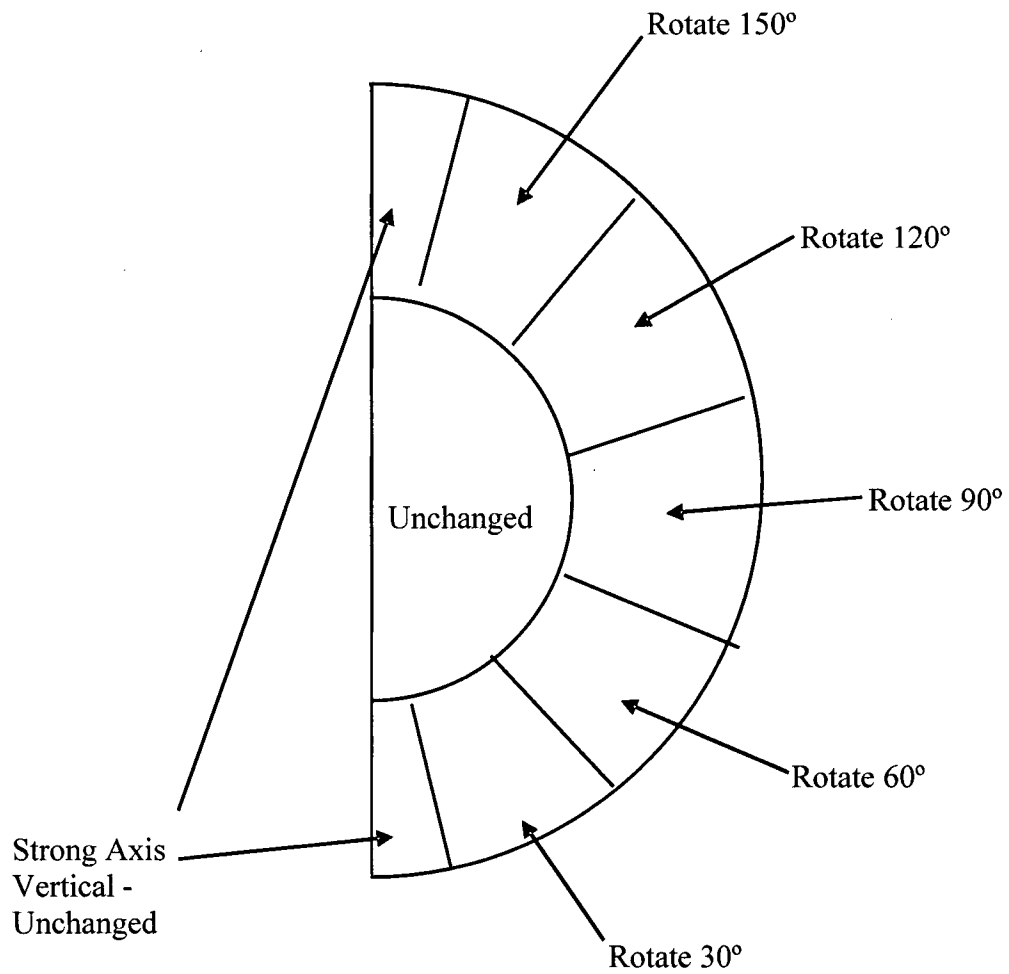


Figure C-1: Radial Perpendicular Wood Orientation

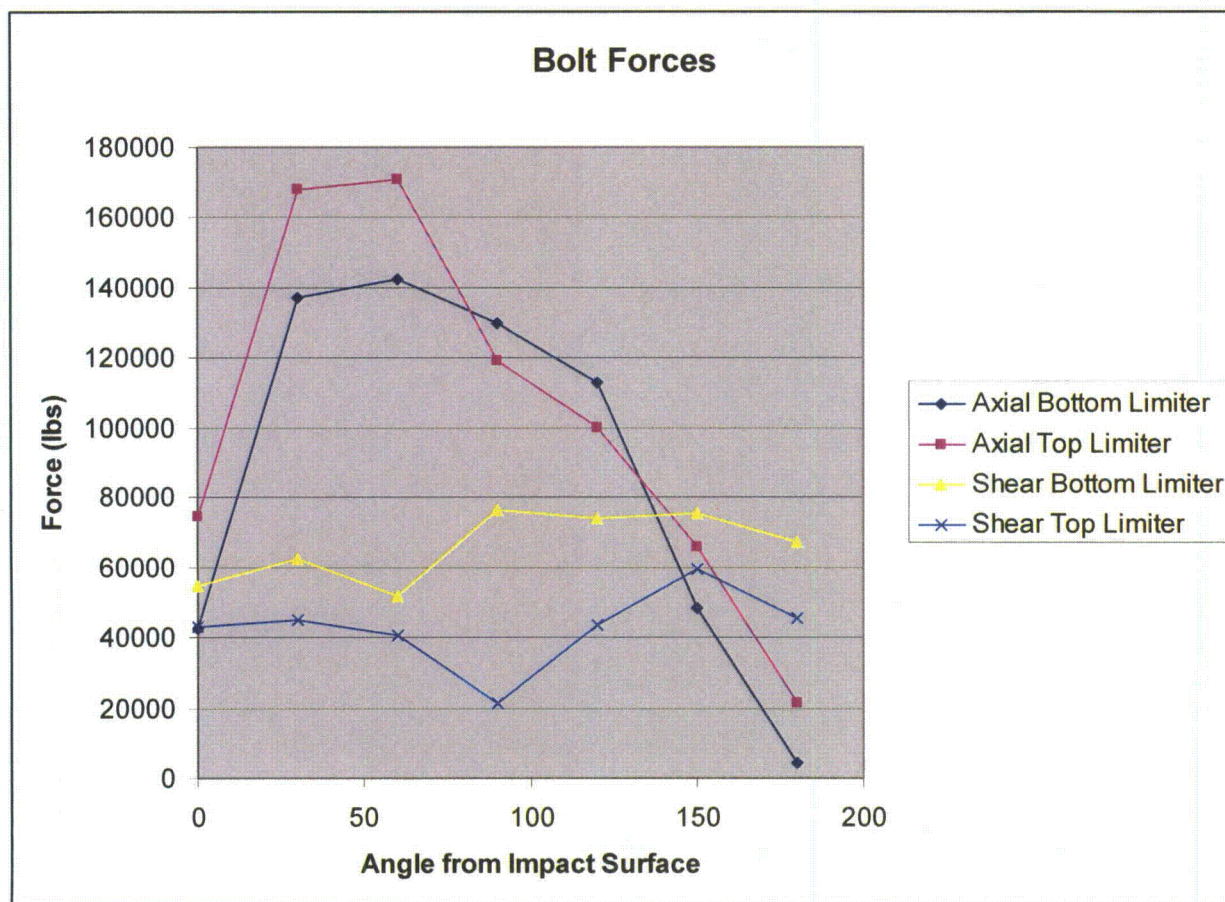


Figure C-2: Bolt Forces of Slap Down 10° with Radial Perpendicular Wood

D. Cask Model Geometry and Friction Sensitivity

This sensitivity study is performed to determine how much the analysis results are affected by changes in the cask model geometry and the friction coefficient between the steel impact surface plate and impact limiter shell. The previous analyses used a cask model of uniform density with a thinned down center section in order to modify the mass, center of gravity, and moment of inertia. A new cask model was developed without the thinned down section. The new model is made of three different sections where the density was modified in order to calibrate the mass, center of gravity, and moment of inertia. The three density sections of the cask can be seen in Figure A.2.13.12-54. The model was run in the Slap Down 10° orientation. Two additional runs were made with friction coefficient between the impact limiter and steel impact plate changed to 0.125 and 0.375. Results of these runs can be seen in the following table.

Summary of Model Geometry and Friction Coefficient Sensitivity Studies

	First Impact Peak Acceleration	Second Impact Peak Acceleration
0.125 μ	42.5 g	48.6 g
0.25 μ	40.5 g	50.2 g
0.375 μ	40.0 g	49.2 g
Original Slap Down 10°	40.4 g	53.2 g

Based on the results shown in this table, the friction coefficient does not significantly affect the results. The results from the original are bounding.

A.2.13.12.10 Baseline g Loads for Structural Evaluations

Based on the LS-DYNA calculated impact accelerations shown in Table A.2.13.12-8, the effect of wood properties at -20 °F temperature is to increase the g-loads approximately by 11% ($49.7/44.9=1.11$). The effect of wood properties at -40 °F temperature is to increase the g-loads approximately by 16% ($52.0/44.9=1.16$). Therefore, the g-loads resulting from the room temperature case for all drop orientations are increased by 11% and 16% to account for the effect of wood properties at -20 °F and -40 °F, respectively. The table below shows the analysis-based peak rigid body accelerations and the g-loads increased by the above factors. The table below also shows the baseline g-loads used for the structural evaluations.

Drop Orientation		Peak rigid body deceleration	-20°F Case Factor	-40°F Case Factor	Factored g-loads (-20°F Case)	Factored g-loads (-40°F Case)	g-loads Used In Structural Evaluations
30' End Drop		44.9 g	1.11	1.16	49.8	52.1	55.0
30' Side Drop		47.3 g	1.11	1.16	52.5	54.9	55.0
30' CG Over Corner Drop		33.4 g (Vertical Direction)	1.11	1.16	37.1	38.7	40.0
30' Slap (20°)	1 st Impact	Translation (15.8g)	1.11	1.16	17.5	18.3	22.0
		Rotational ($\alpha = 62.9$ rad/sec ²)	1.11	1.16	$\alpha = 69.8$ rad/sec ²	$\alpha = 73.0$ rad/sec ²	$\alpha = 93$ rad/sec ²
	2 nd Impact	Translation (24.1g)	1.11	1.16	26.8	28.0	28.0
		Rotational ($\alpha = 138.7$ rad/sec ²)	1.11	1.16	$\alpha = 154.0$ rad/sec ²	$\alpha = 160.9$ rad/sec ²	$\alpha = 164$ rad/sec ²
30' Slap (10°)	1 st Impact	Translation (20.2g)	1.11	1.16	22.4	23.4	25.0
		Rotational ($\alpha = 106.8$ rad/sec ²)	1.11	1.16	$\alpha = 118.5$ rad/sec ²	$\alpha = 123.9$ rad/sec ²	$\alpha = 132$ rad/sec ²
	2 nd Impact	Translation (25.7g)	1.11	1.16	28.5	29.8	32.0
		Rotational ($\alpha = 144.9$ rad/sec ²)	1.11	1.16	$\alpha = 160.8$ rad/sec ²	$\alpha = 168.1$ rad/sec ²	$\alpha = 166$ rad/sec ²
1' End Drop		15.4 g	1.11	1.16	17.1	17.9	18.0
1' Side Drop		11.0 g	1.11	1.16	12.2	12.8	19.0

A.2.13.12.11 Impact Limiter Bolt Evaluation

The purpose of this section is to determine the stresses in the NUHOMS® – MP197HB impact limiter attachment bolts and blocks.

The worst loading occurs in the top impact limiters attachment blocks during the second impact of a shallow angle slap–down drop.

Twelve impact limiter attachment bolts take the moment applied during a shallow angle slap–down drop.

The impact limiter bolts are evaluated using two approaches. The first evaluation is made using the maximum tensile force from the LS-DYNA analysis taken from Figure A.2.13.12-51 for a bolt during a shallow angle slap–down drop, which is about 200,000 lb. The maximum tensile force F in a bolt considered in this case will be conservatively taken equal to 210,000 lb.

In order to benchmark the above method, a second evaluation is made where the tensile force in the bolts is calculated by considering the equilibrium of moments each bolt is subjected to, conservatively assuming that:

1. The lateral force exerted on the impact limiter by the cask comes from the full weight of the cask (306,500 lbs) and is centered in the middle of the impact limiter cavity (at a distance 15.375 in from the bottom of the impact limiter);
2. The g load for the second impact of a shallow angle slap–down drop is conservatively taken equal to 35 g (see Section A.2.13.12.10, baseline g load is 32 g);
3. The friction coefficient μ between the cask and the impact limiter and between the impact limiter and the impact surface is 0.42 [6], based on hard steel against hard steel friction properties.

Since the bottom impact limiter crushes during the first impact, the top impact limiter impacts with a slight angle during the second impact, and its bottom edge crushes first. Therefore, the reaction force on the impact limiter is located close to the bottom edge of the impact limiter. However, to maximize bolt forces, we conservatively assume that the reaction force is exerted on the other side of the lateral force exerted by the cask, at a distance from that lateral force equal to 10% of the depth of the impact limiter cavity.

Material mechanical properties for the impact limiter and attachment bolts are taken at 200°F, and at 300°F for the attachment bolts blocks and for the cask shell. However, material properties used for checking thread engagement length are taken at room temperature.

Nut factor for empirical relation between the applied torque and achieved preload is 0.135 for neolube lubricant.

A.2.13.12.11.1 Stress Calculations

A. Evaluation Based on the Calculated Tensile Force**A.1 Bolt Stress**

The 1 ½ – 6UNC attachment bolts are made of SA–540 Gr. B23, Cl. 1 (see Appendix A.1.4.10), which has an ultimate strength $S_u = 165.0$ ksi at 200°F [7].

The diameter D of the shank is 1.293 in. Its maximum diameter is 1.50 in (see Appendix A.1.4.10).

The critical tensile area of the attachment bolt is in the bolt shank since the threads are 1 ½ – 6UNC. The minimum tensile area of the bolt is:

$$A = 0.25 \times \pi \times D^2 = 0.25 \times \pi \times 1.293^2 = 1.313 \text{ in}^2.$$

The tensile stress in the bolts is equal to:

$$\sigma = \frac{F}{A} = \frac{210,000}{1.313} = 159.9 \text{ ksi}$$

The allowable tensile stress in the impact limiter attachment bolts for hypothetical accident conditions of transport is taken equal to their ultimate strength, 165 ksi.

A.2 Attachment Bolt Block Analysis

The material used for the impact limiter bolts attachment blocks is SA–182 Type F316N ($S_u = 80.0$ ksi). The material used for the cask body top flange is SA–350–LF3 ($S_u = 70.0$ ksi).

Each block (dimensions 6.81 × 8.00) is welded to the cask body with an all-around $e = 0.5$ in groove weld.

The allowable primary plus bending stress for the impact limiter bolts attachment blocks is $S_u = 80.0$ ksi.

The allowable shear stress in the welds between the top flange of the cask and the attachment blocks is taken equal to $0.42 \times S_u = 29.4$ ksi, using the lowest ultimate strength value of the two.

The weld area of a single attachment bolt block is:

$$A_{\text{weld}} = L_1 \times L_2 - (L_1 - 2 \times e) \times (L_2 - 2 \times e)$$

Where L_1 and L_2 are the dimensions of the block ($L_1 = 6.81$ in and $L_2 = 8.00$ in), and e is the size of the weld (see above).

$$A_{\text{weld}} = 6.81 \times 8.00 - (6.81 - 2 \times 0.5) \times (8.00 - 2 \times 0.5) = 13.81 \text{ in}^2$$

The weld moment of inertia is:

$$I_{weld} = \frac{L_1 \times L_2^3 - (L_1 - 2 \times e) \times (L_2 - 2 \times e)^3}{12} = \frac{6.81 \times 8.00^3 - 5.81 \times 7.00^3}{12} = 124.5 \text{ in}^4$$

The maximum moment applied to the block weld is:

$$M_{weld} = F \times \frac{D_1 - D_2}{2}$$

Where D_1 is the bolt circle diameter, 88.25 in and D_2 the outer diameter of the cask, 84.50 in.

$$M_{weld} = 210,000 \times \frac{88.25 - 84.50}{2} = 393,750 \text{ in.lb}$$

The bending stress in the block weld is:

$$\sigma_b = \frac{M_{weld} \times \frac{L_2}{2}}{I_{weld}} = \frac{393,750 \times \frac{8}{2}}{124.5} = 12.7 \text{ ksi}$$

The shear stress in the block weld is:

$$\tau = \frac{F}{A_{weld}} = \frac{210,000}{13.81} = 15.2 \text{ ksi}$$

The stress intensity in the block weld is:

$$S.I. = \sqrt{\sigma_b^2 + 4\tau^2} = \sqrt{12.7^2 + 4 \times 15.2^2} = 32.9 \text{ ksi}$$

B. Evaluation Based on Moments Equilibrium

B.1 Bolt Force

The lateral force exerted by the cask on the top impact limiter is equal to:

$$R = W \times g = 306,500 \times 35 = 10,727,500 \text{ lb}$$

Where W is the weight of the cask and g is the g-load assumed for the second impact.

Figure A.2.13.12-55 shows the free body diagram of top impact limiter during slap down drop.

The location of the reaction force on the impact limiter when the second impact occurs is:

$$x_3 = x_1 + \frac{d}{10} = \frac{d}{2} + \frac{d}{10} = \frac{6 \times d}{10} = 18.45 \text{ in}$$

Where d is the depth of the cavity in the impact limiter.

The crush depth of the top impact limiter is approximately 11.30 in. (see Table A.2.13.12-8). Therefore:

$$x_2 = \frac{O.D._{IL} - D_2}{2} - [Crush Depth] = \frac{126.00 - 84.50}{2} - 11.30 = 9.45 \text{ in}$$

Where $O.D._{IL}$ is the outer diameter of the impact limiter.

The moment applied to the impact limiter is (the associated force acts to pull the impact limiter away from the cask when the moment is clockwise):

$$M = (x_3 - x_1) \times R = (18.45 - 15.375) \times 10,727,500 = 3.30 \times 10^7 \text{ in.lb (clockwise).}$$

There is also an additional frictional force that acts to pull the impact limiter away from the cask. The magnitude of this force is equal to:

$$F_f = \mu \times R = 0.42 \times 10,727,500 = 4.51 \times 10^6 \text{ lb}$$

The resulting moment due to friction is:

$$M_f = F_f \times x_2 = 4.51 \times 10^6 \times 9.45 = 4.26 \times 10^7 \text{ in.lb (clockwise)}$$

The total prying moment is:

$$M_{tot} = M_f + M = 4.26 \times 10^7 + 3.30 \times 10^7 = 7.56 \times 10^7 \text{ in.lb (clockwise)}$$

Assume that only the impact limiter bolts hold the impact limiters in place, and that the impact limiter tends to pivot around the edge of the cask. The force distribution among the bolts will be linearly proportional to their distance from the pivot point. The angular location α is measured from 0° , which corresponds to the upper vertical orientation.

The vertical distance is equal to:

$$V.D. = \frac{I.L._{DBC} \times \cos(\alpha) + O.D._{Cask}}{2}$$

Where $I.L._{DBC}$ is the bolt circle diameter for the impact limiters (88.25 in).

Negative vertical distances correspond to bolts that are below the crush line of the impact limiter. These bolts are conservatively considered to be ineffective and do not carry any of the prying load.

The bolts farthest away from the target surface (bolts 1 and 12) are assumed to carry the maximum tensile force F_{\max} . All other bolts are assumed to carry a tensile force linearly proportional to their distance from the target surface. Therefore, each bolt carries the prying moment listed in Table A.2.13.12-9.

The tensile force f_i and moment m_i for bolt i of moment arm x_i are:

$$f_i = \frac{x_i}{\max(x_i)} F_{\max} \quad \text{and} \quad m_i = \frac{x_i^2}{\max(x_i)} F_{\max}$$

We can equate this total moment with M_{tot} calculated above and solve for F_{\max} .

$$390.03 \times F_{\max} = M_{\text{tot}} = 7.56 \times 10^7 \text{ in.lb.}$$

$$\text{Therefore, } F_{\max} = 193,739 \text{ lb.}$$

B.2 Bolt Stress

The tensile stress in the bolts is equal to:

$$\sigma = \frac{193,739}{1.313} = 147.6 \text{ ksi}$$

B.3 Attachment Bolt Block Analysis

The maximum moment applied to the block weld is:

$$M_{\text{weld}} = 193,739 \times \frac{88.25 - 84.50}{2} = 363,261 \text{ in.lb}$$

The bending stress in the block weld is:

$$\sigma_b = \frac{M_{\text{weld}} \times c}{I_{\text{weld}}} = \frac{363,261 \times \frac{8}{2}}{124.5} = 11.7 \text{ ksi}$$

The shear stress in the block weld is:

$$\tau = \frac{F_{\max}}{A_{\text{weld}}} = \frac{193,739}{13.81} = 14.0 \text{ ksi}$$

The stress intensity in the block weld is:

$$S.I. = \sqrt{\sigma_b^2 + 4\tau^2} = \sqrt{11.7^2 + 4 \times 14.0^2} = 30.3 \text{ ksi}$$

A.2.13.12.11.2 Minimum Engagement Length for Attachment Bolt and Block

The minimum engagement length L_e for the bolt and block is ([8], p. 1490):

$$L_e = \frac{2A_t}{3.146 \times K_{n\max} \left[\frac{1}{2} + .57735n(E_{s\min} - K_{n\max}) \right]}$$

For a 1 1/2-6UNC 2A bolt:

A_t = tensile stress area = 1.405 in²;

n = number of threads per inch = 6;

$K_{n\max}$ = maximum minor diameter of internal threads = 1.350 in ([8], p. 1728);

$E_{s\min}$ = minimum pitch diameter of external threads = 1.3812 in ([8], p. 1728).

Substituting the values given above gives:

$$L_e = \frac{2 \times 1.405}{3.146 \times 1.350 \left[\frac{1}{2} + .57735 \times 6 \times (1.3812 - 1.350) \right]} = 1.088 \text{ in}$$

The required engagement length Q is ([8], p. 1491):

$$Q = J \times L_e$$

Where J is equal to ([8], p. 1490):

$$J = \frac{A_s \times S_{u(bolt)}}{A_n \times S_{u(block)}}$$

Where A_s and A_n are ([8], p. 1491):

$$\begin{cases} A_s = 3.1416nL_eK_{n\max} \left[\frac{1}{2n} + .57735(E_{s\min} - K_{n\max}) \right] \\ A_n = 3.1416nL_eD_{s\min} \left[\frac{1}{2n} + .57735(D_{s\min} - E_{n\max}) \right] \end{cases}$$

For a 1 1/2-6UNC 2A bolt:

$D_{s\min}$ = minimum major diameter of external threads = 1.4794 in ([8], p. 1728);

E_{nmax} = maximum pitch diameter of internal threads = 1.4022 in ([8], p. 1728).

Therefore:

$$\begin{cases} A_s = 3.1416 \times 6 \times 1.088 \times 1.35 \times \left[\frac{1}{2 \times 6} + .57735 \times (1.3812 - 1.350) \right] = 2.81 \text{ in}^2 \\ A_n = 3.1416 \times 6 \times 1.088 \times 1.4794 \times \left[\frac{1}{2 \times 6} + .57735 \times (1.4794 - 1.4022) \right] = 3.88 \text{ in}^2 \end{cases}$$

So:

$$J = \frac{2.81 \times 165}{3.88 \times 70} = 1.71$$

The required engagement length is therefore:

$$Q = 1.71 \times 1.088 = 1.86 \text{ in}$$

The threaded length is 3.50 in, which is greater than 1.86 in.

A.2.13.12.11.3 Bolt Torque

A bolt tensile stress σ_t of 15,000 psi is assumed.

$$F_a = \sigma_t \times A_t = 15,000 \times 1.405 = 21,075 \text{ lb}$$

Where A_t is the bolt tensile stress area.

$$Q = K \times D_b \times F_a = 0.135 \times 1.50 \times 21,075 = 4,268 \text{ in.lb} = 356 \text{ ft.lb}$$

Where F_a is the bolt force, Q is the applied torque, K is the nut factor, and D_b the nominal bolt diameter at the threads.

A bolt torque of 350 to 375 ft.lb is specified.

For a bolt torque of 350 ft.lb:

$$F_a = \frac{Q}{K \times D_b} = \frac{350 \times 12}{0.135 \times 1.50} = 20,741 \text{ lb}$$

For a bolt torque of 375 ft.lb:

$$F_a = \frac{Q}{K \times D_b} = \frac{375 \times 12}{0.135 \times 1.50} = 22,222 \text{ lb}$$

Therefore, the maximum tensile stress in the bolt is:

$$\sigma = \frac{22,222}{1.405} = 15.8 \text{ ksi}$$

This is less than the yield stress of the bolts, 144 ksi.

A.2.13.12.11.4 Conclusions

The stresses are summarized in Table A.2.13.12-10. All of the stresses calculated for the impact limiter bolts, attachment bolt blocks, and lifting lugs are less than the allowable stresses regardless of the method used. Therefore, the NUHOMS® – MP197HB impact limiter attachments are structurally adequate.

The required engagement length is 1.86 in, which is less than the threaded length of 3.50 in.

A.2.13.12.12 References

1. NOT USED.
2. LS-DYNA Keyword User's Manual, Volumes 1 & 2, Version 9.71s, Rev. 7600.398 August 17, 2006, Livermore Software Technology Corporation.
3. Wood Handbook: Wood as an Engineering Material, Forest Products Laboratory, General Technical Report, FPL-GTR-113, United States Department of Agriculture.
4. Karl Klein, Johannes Will, and Thomas Seider, "Numerical Simulation of Wood Filled Impact Limiter with LS-DYNA," November 10-12, 2004, International Congress Center Dresden, Germany.
5. Alexander A. Ryabov, Vladimir I. Romanov, Sergey S. Kukanov, and Sergey G. Skurikhin, "Numerical Simulation of Dynamic Deformation of Air Transport Package PAT-2 in Accident Impacts," 9th International LS-DYNA Users Conference.
6. Standard Handbook for Mechanical Engineers, Baumeister & Marks, 7th Edition, McGraw-Hill, 1967.
7. ASME Boiler and Pressure Vessel Code, Section II, Materials Specifications, Parts A, B, C, and D, 2004 with 2006 addenda.
8. Machinery Handbook, 26th Edition, Industrial Press, 2000.

Table A.2.13.12-1
Effective plastic strain vs. scale factor for concrete material

Effective Plastic Strain	Scale Factor, η
0	0
0.00094	0.289
0.00296	0.465
0.00837	0.629
0.01317	0.774
0.0234	0.893
0.04034	1.0
1.0	1.0

Table A.2.13.12-2
Tabulated pressures vs. volumetric strain for concrete material

Volumetric Strain, ϵ	Pressure (psi)
0	0
-0.006	4,600
-0.0075	5,400
-0.01	6,200
-0.012	6,600
-0.02	7,800
-0.038	10,000
-0.06	12,600
-0.0755	15,000
-0.097	18,700

Table A.2.13.12-3
Wood Segment Room Temperature Material Properties

	Redwood	Balsa
Density, ρ	$3.445 \times 10^{-5} \text{ lbm/in}^3$ (23 lb/ft ³)	$1.647 \times 10^{-5} \text{ lbm/in}^3$ (11 lb/ft ³)
Shear Modulus, G parallel to grain	9,801 psi	1,513 psi
Shear Modulus, G perpendicular to grain	68,599 psi	11,194 psi
Elastic Modulus parallel to grain	942,000 psi	303,000 psi
Elastic Modulus perpendicular to grain	75,135 psi	4,537 psi

Note: The properties listed in this table are originated from [3] and are adjusted to benchmark against the 1/3 scale impact limiter drop test results.

Table A.2.13.12-4
Wood Segment Material Properties - 20 °F

	Redwood	Balsa
Density, ρ	$3.445 \times 10^{-5} \text{ lbm/in}^3$ (23 lb/ft ³)	$1.647 \times 10^{-5} \text{ lbm/in}^3$ (11 lb/ft ³)
Shear Modulus, G parallel to grain	11,759 psi	1,816 psi
Shear Modulus, G perpendicular to grain	82,319 psi	13,433 psi
Elastic Modulus parallel to grain	1,132,000 psi	364,000 psi
Elastic Modulus perpendicular to grain	90,160 psi	5,444 psi

Table A.2.13.12-5
Pressure vs. Volumetric Strain for 100% Average Room Temperature Wood Properties

Redwood Parallel to Grain	
Volumetric Strain ($\Delta V/V$)	Pressure (psi)
-1	-381,788
-0.6	-5,094
-0.0043	-5,034
0.000	0
0.0043	5,034
0.6	5,094
0.601	1
1	1

Redwood Perpendicular to Grain	
Volumetric Strain ($\Delta V/V$)	Pressure (psi)
-1	-339,384
-0.6	-573
-0.0059	-552
0.000	0
0.0059	552
0.6	573
0.601	1
1	1

Balsa Parallel to Grain	
Volumetric Strain ($\Delta V/V$)	Pressure (psi)
-1	-62,072
-0.8	-1,499
-0.0036	-1,381
0.000	0
0.0036	1,381
0.8	1,499
0.801	1
1	1

Balsa Perpendicular to Grain	
Volumetric Strain ($\Delta V/V$)	Pressure (psi)
-1	-60,836
-0.8	-292
-0.049	-278
0.000	0
0.049	278
0.8	292
0.801	1
1	1

Note: The properties listed in this table are originated from [3] and are adjusted to benchmark against the 1/3 scale impact limiter drop test results.

Table A.2.13.12-6
Pressure vs. Volumetric Strain for Wood Properties -20 °F

Redwood Parallel to Grain	
Volumetric Strain ($\Delta V/V$)	Pressure (psi)
-1	-458,145
-0.6	-6,114
-0.0043	-6,042
0.000	0
0.0043	6,042
0.6	6,114
0.601	1
1	1

Redwood Perpendicular to Grain	
Volumetric Strain ($\Delta V/V$)	Pressure (psi)
-1	-407,260
-0.6	-686
-0.0059	-662
0.000	0
0.0059	662
0.6	686
0.601	1
1	1

Balsa Parallel to Grain	
Volumetric Strain ($\Delta V/V$)	Pressure (psi)
-1	-74,449
-0.8	-1,760
-0.0036	-1,658
0.000	0
0.0036	1658
0.8	1760
0.801	1
1	1

Balsa Perpendicular to Grain	
Volumetric Strain ($\Delta V/V$)	Pressure (psi)
-1	-73,004
-0.8	-350
-0.049	-334
0.000	0
0.049	334
0.8	350
0.801	1
1	1

Table A.2.13.12-7
Peak Nodal Accelerations, Wood Crush Depths, and Impact Duration Comparisons
(1/3 Scale Test Results vs. 1/3 Scale LS-DYNA Analysis)

		Test Results	LS-DYNA Model
End Drop (-20°F)	Acceleration	65g	65.8g
	Impact Duration	0.010 sec.	0.012 sec.
	Wood Crush Depth	2.5"	2.5"
Side Drop	Acceleration	61g	61.5g
	Impact Duration	0.012 sec.	0.014 sec.
	Wood Crush Depth	2.69"-2.75"	2.75"
20° Slap Down 1 st Impact	Acceleration at Center of Cask	17g	18.2g
	Acceleration at Bottom of Cask	36g	34.9g
	Impact Duration	0.016 sec.	0.023 sec.
	Wood Crush Depth Bottom Limiter	4.92"	5.5"
20° Slap Down 2 nd Impact	Acceleration at Center of Cask	32g	41.1g
	Acceleration at Top of Cask	73g	78.4g
	Impact Duration	0.009 sec.	0.012 sec.
	Wood Crush Depth Upper Limiter	2.42" ⁽¹⁾	3.0"

NOTE:

⁽¹⁾ Re-examination of the MP197 test results: It shows that the crush depth is 2.42" instead of 4.72" as specified in Appendix 2.10.9 of the MP197 main SAR.

Table A.2.13.12-8
Summary of the Full Scale Impact Limiter Analysis Results

Drop Scenario		Peak Acceleration (g)	Impact Duration (sec)	Impact Limiter Crush Depth (in)	Time History Figure Number
30' End Drop (Room Temp)		44.9	0.05	10.2"	A.2.13.12-27
30' End Drop (-20°F)		49.7	0.045	9.3"	A.2.13.12-28(a)
30' End Drop (-40°F)		52.0	0.045	9.0"	A.2.13.12-28(b)
30' CG Over Corner Drop		33.4	0.090	27.2"	A.2.13.12-30
30' Side Drop		47.3	0.055	11.5"	A.2.13.12-29
30' Slap Down 20°	1 st Impact	28.1	0.075	15"	A.2.13.12-31
	2 nd Impact	52.2	0.045	11.3"	A.2.13.12-32
30' Slap Down 10°	1 st Impact	39.0	0.060	13.4"	A.2.13.12-33
	2 nd Impact	55.2	0.050	13.9"	A.2.13.12-34
1' Normal Condition End Drop		15.4	0.035	1.1"	A.2.13.12-35
1' Normal Condition Side Drop		11.0	0.045	1"	A.2.13.12-36

Table A.2.13.12-9
Calculation of Total Moment

	Angular location	Vertical distance (in)	Moment arm (in)	Moment (/F_{max})
Bolt #1	15°	84.87	84.87	84.87
Bolt #2	45°	73.45	73.45	63.57
Bolt #3	75°	53.67	53.67	33.94
Bolt #4	105°	30.83	30.83	11.20
Bolt #5	135°	11.05	11.05	1.44
Bolt #6	165°	-0.37	0.00	0.00
Bolt #7	195°	-0.37	0.00	0.00
Bolt #8	225°	11.05	11.05	1.44
Bolt #9	255°	30.83	30.83	11.20
Bolt #10	285°	53.67	53.67	33.94
Bolt #11	315°	73.45	73.45	63.57
Bolt #12	345°	84.87	84.87	84.87
Total				390.03

Table A.2.13.12-10
Summary of Stresses (ksi)

Component		Calculated (Base on Tensile Force)	Calculated (Base on Moments)	Allowable
Impact Limiter Attachment Bolts		159.9	147.6	165.0
Attachment Block Welds	Shear	15.2	14.0	29.4
	Stress Intensity	32.9	30.3	80.0

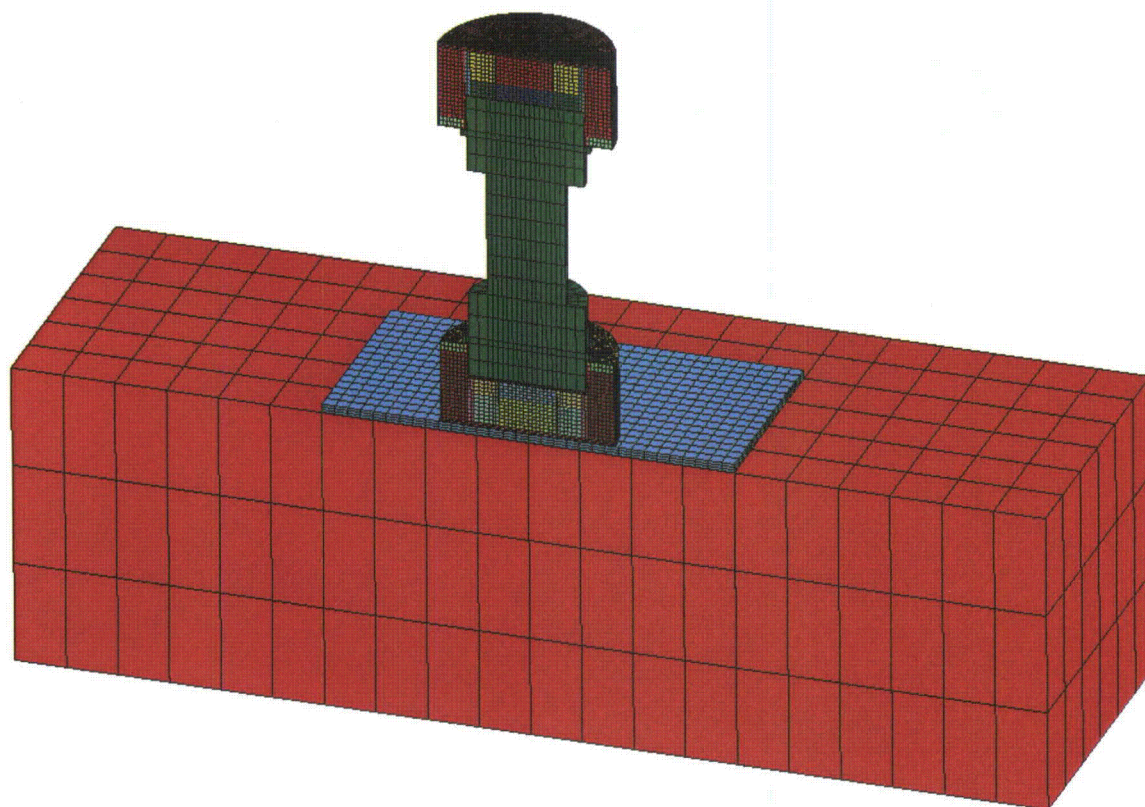


Figure A.2.13.12-1
1/3 Scale Impact Limiter Finite Element Model Overview

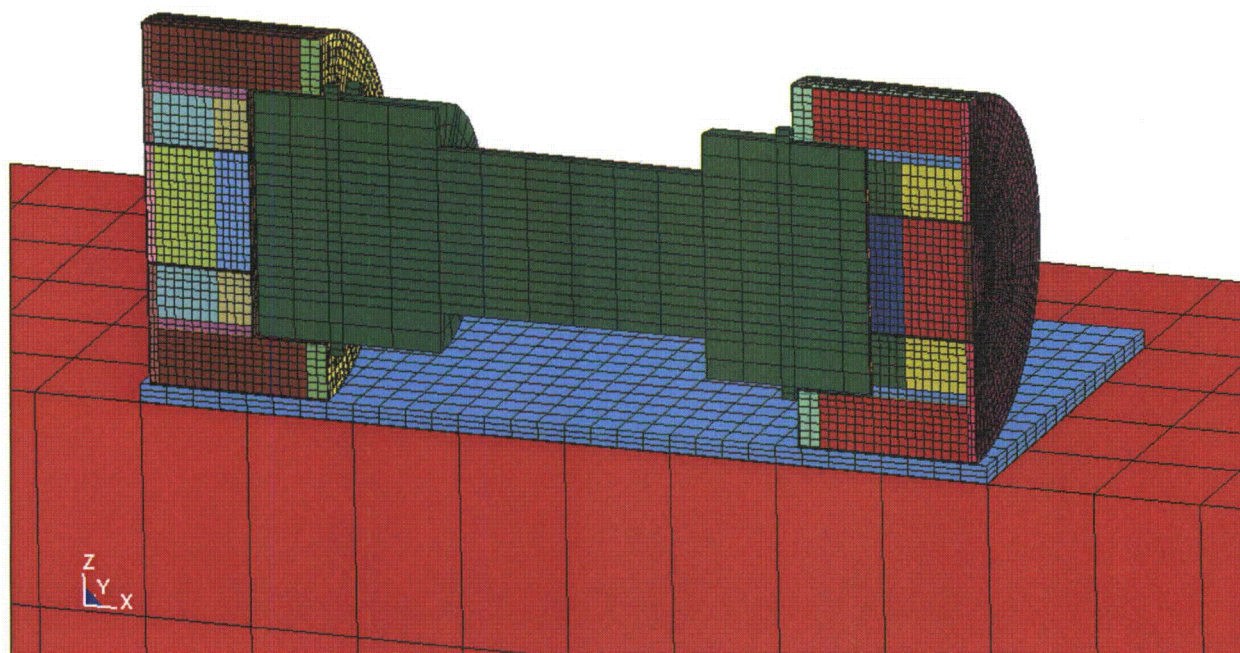


Figure A.2.13.12-2
1/3 Scale Impact Limiter Finite Element Model for Side Drop

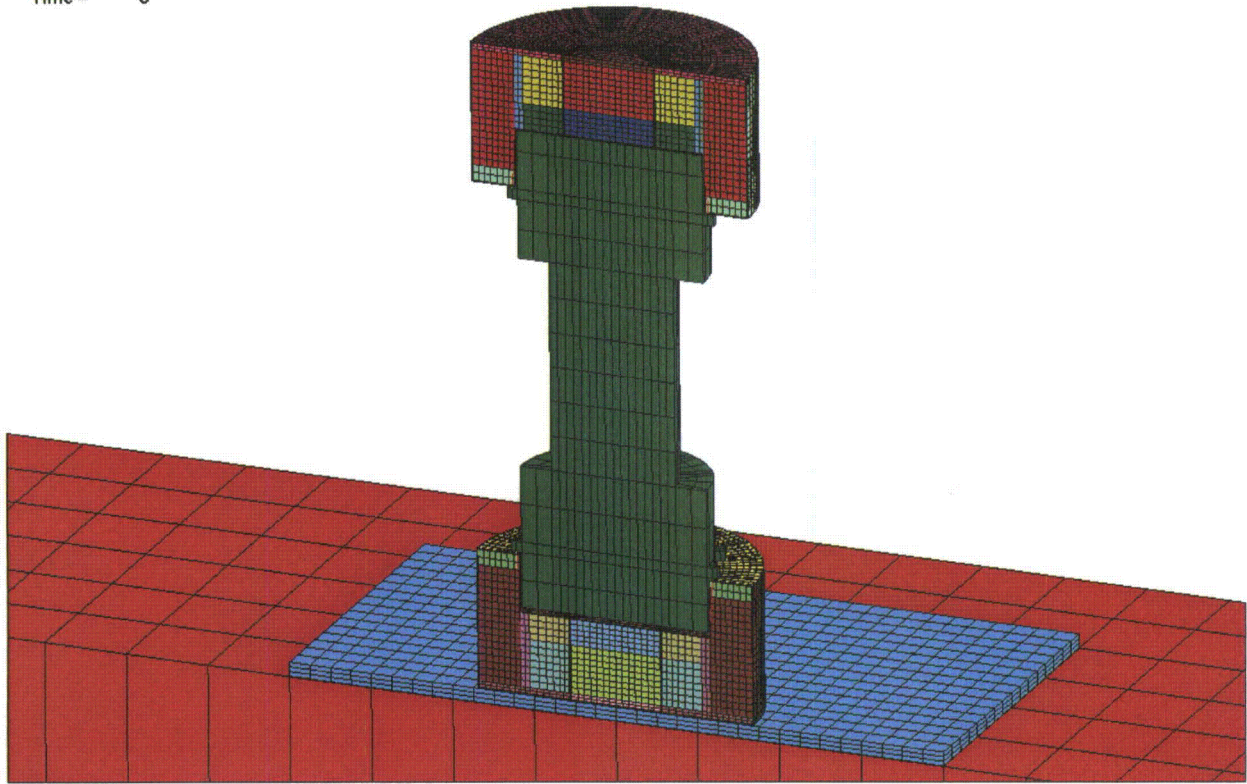
MP197 1/3 SCALE IMPACT LIMITER ANALYSIS
Time = 0

Figure A.2.13.12-3
1/3 Scale Impact Limiter Finite Element Model for End Drop

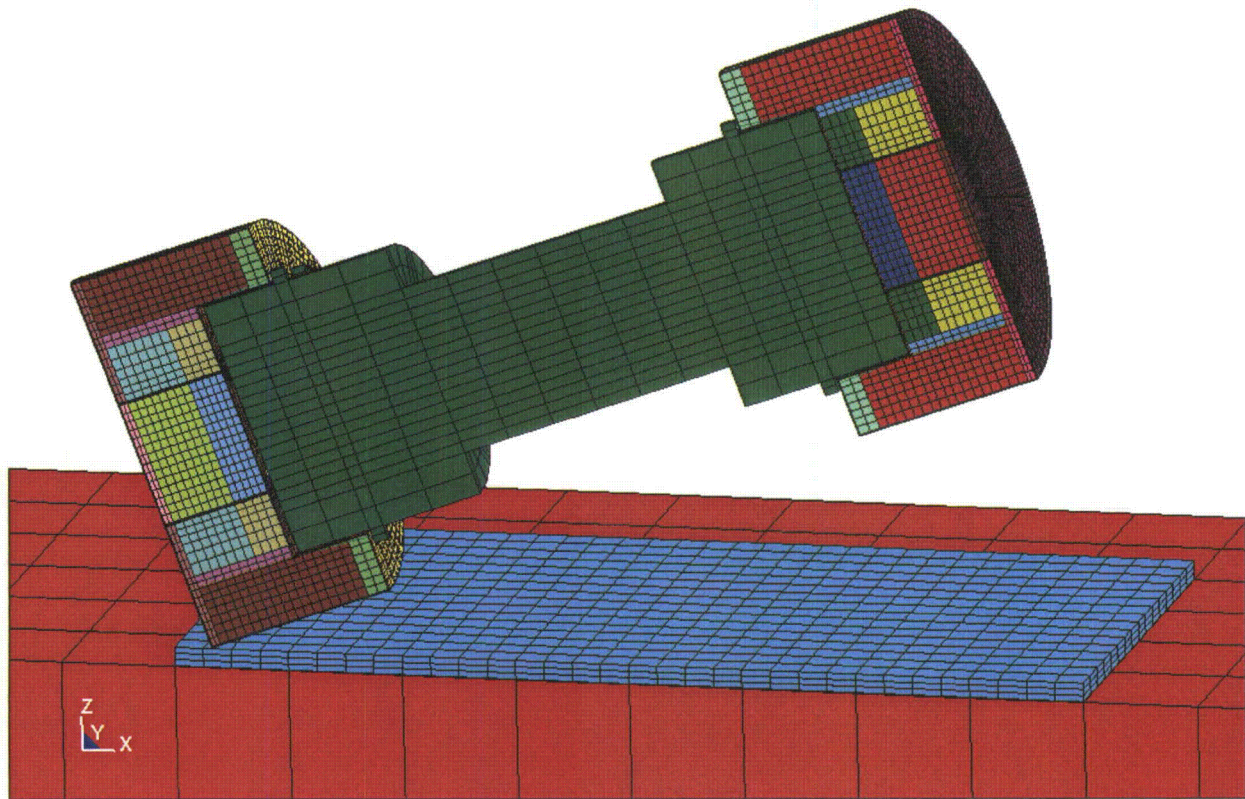


Figure A.2.13.12-4
1/3 Scale Impact Limiter Finite Element Model for 20° Slap Down Drop

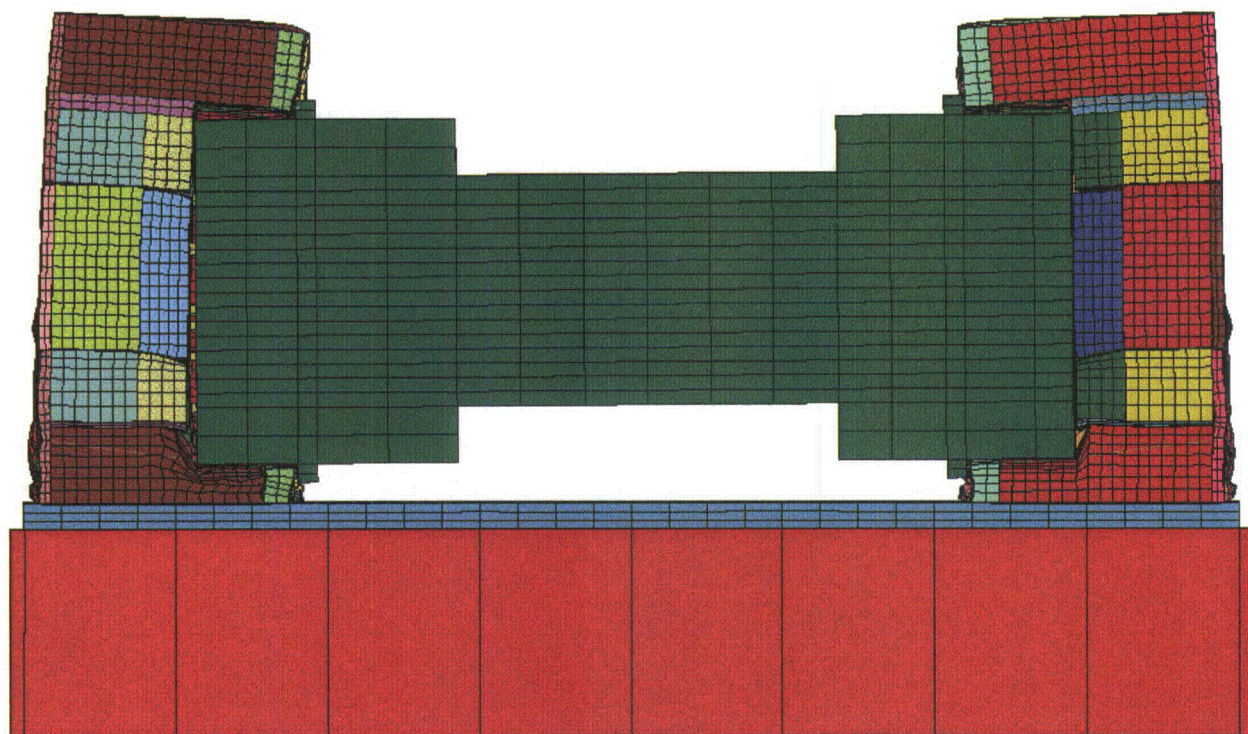


Figure A.2.13.12-5
Plot of Maximum Deformation for 1/3 Scale Side Drop

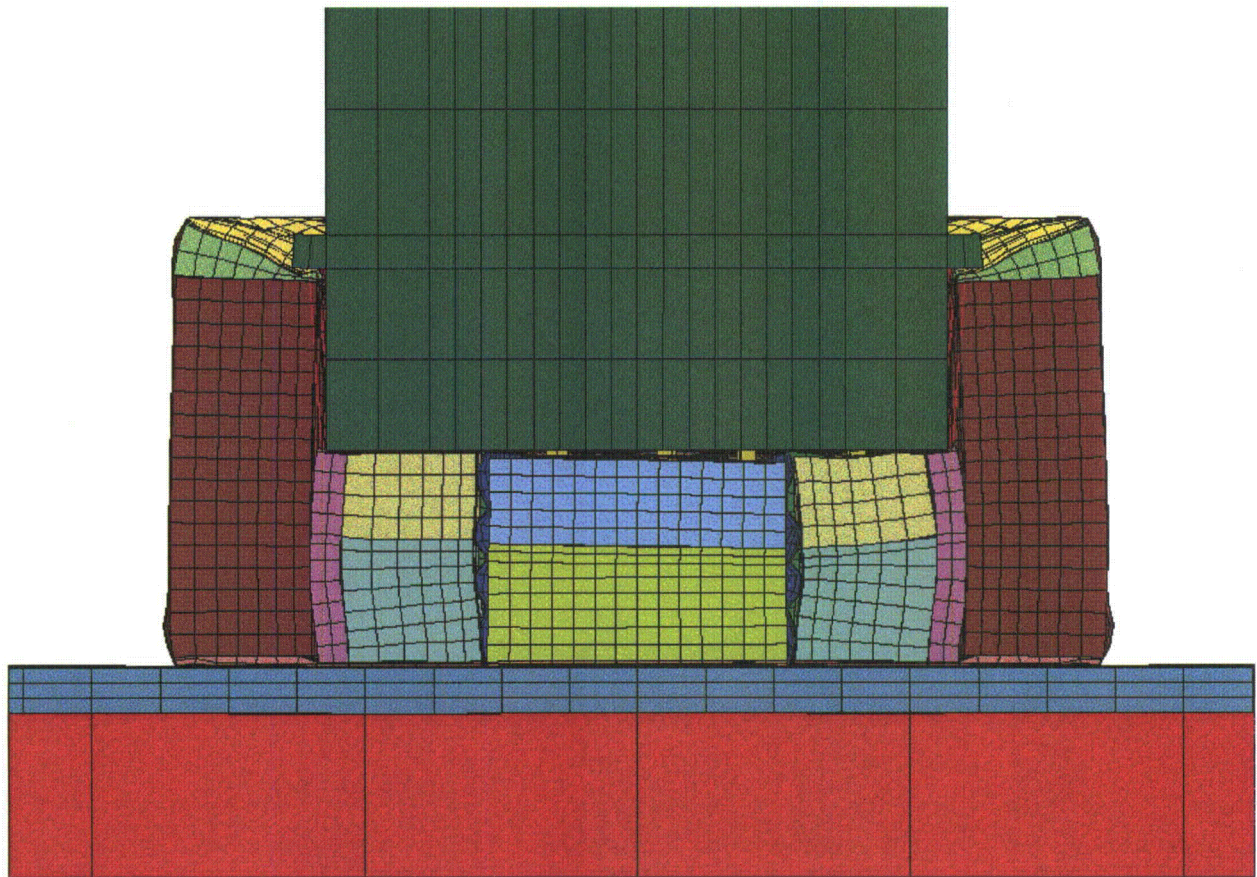


Figure A.2.13.12-6
Plot of Maximum Deformation for 1/3 Scale End Drop (-20°F)

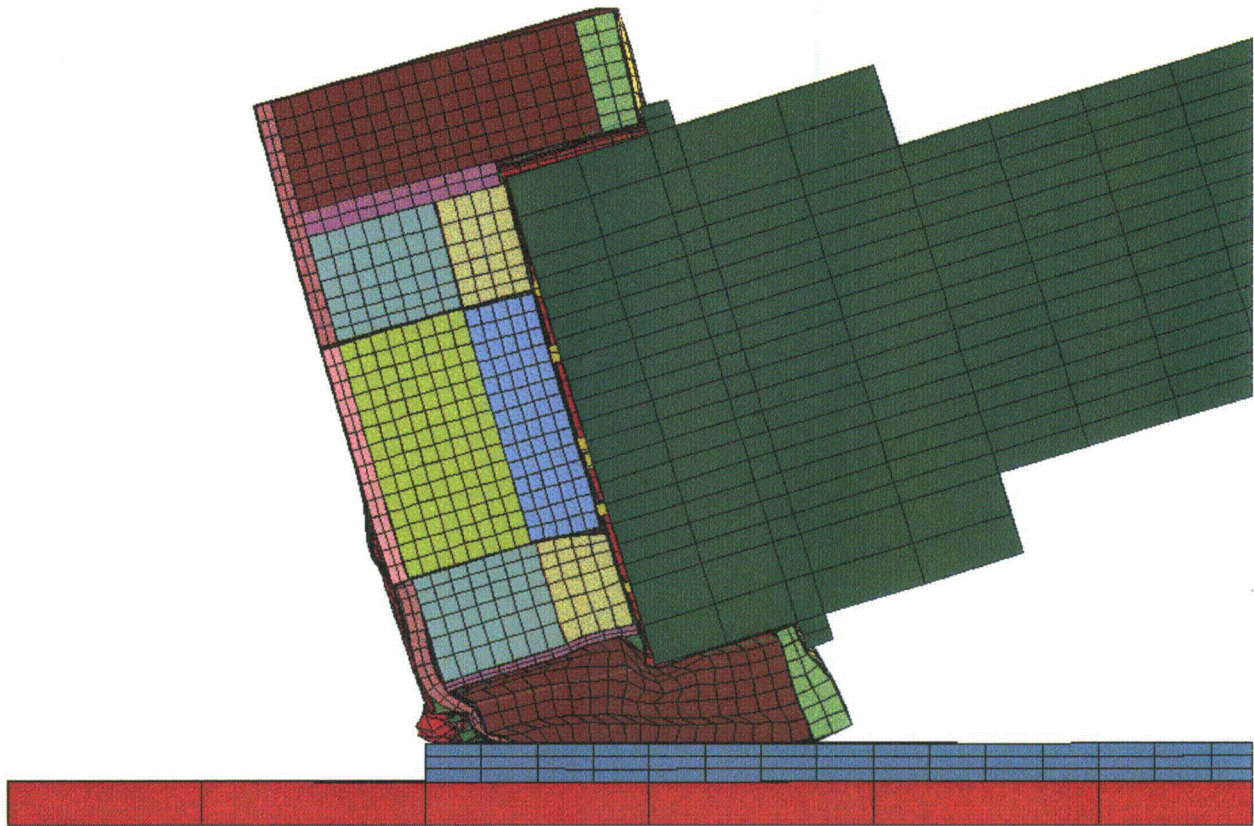


Figure A.2.13.12-7
Plot of Maximum Deformation for 1/3 Scale 20° Slap Down Drop
(First Impact)

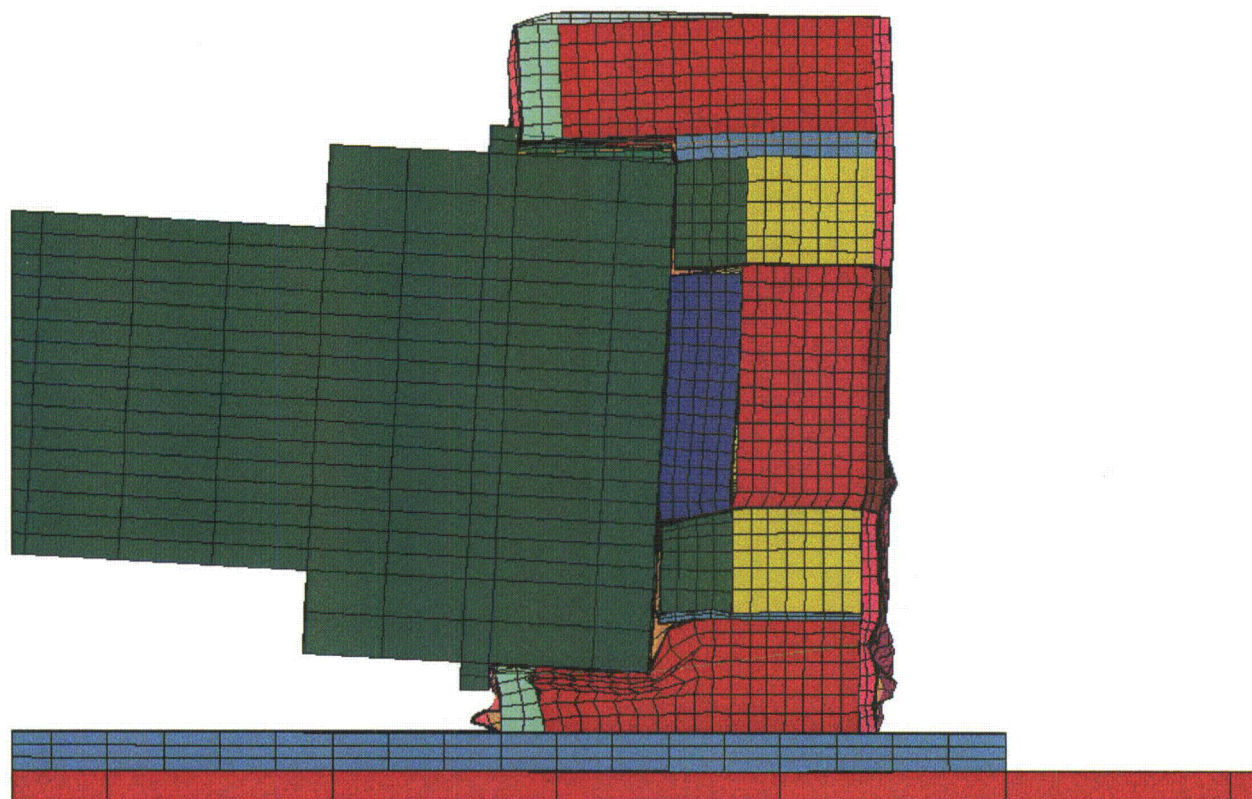
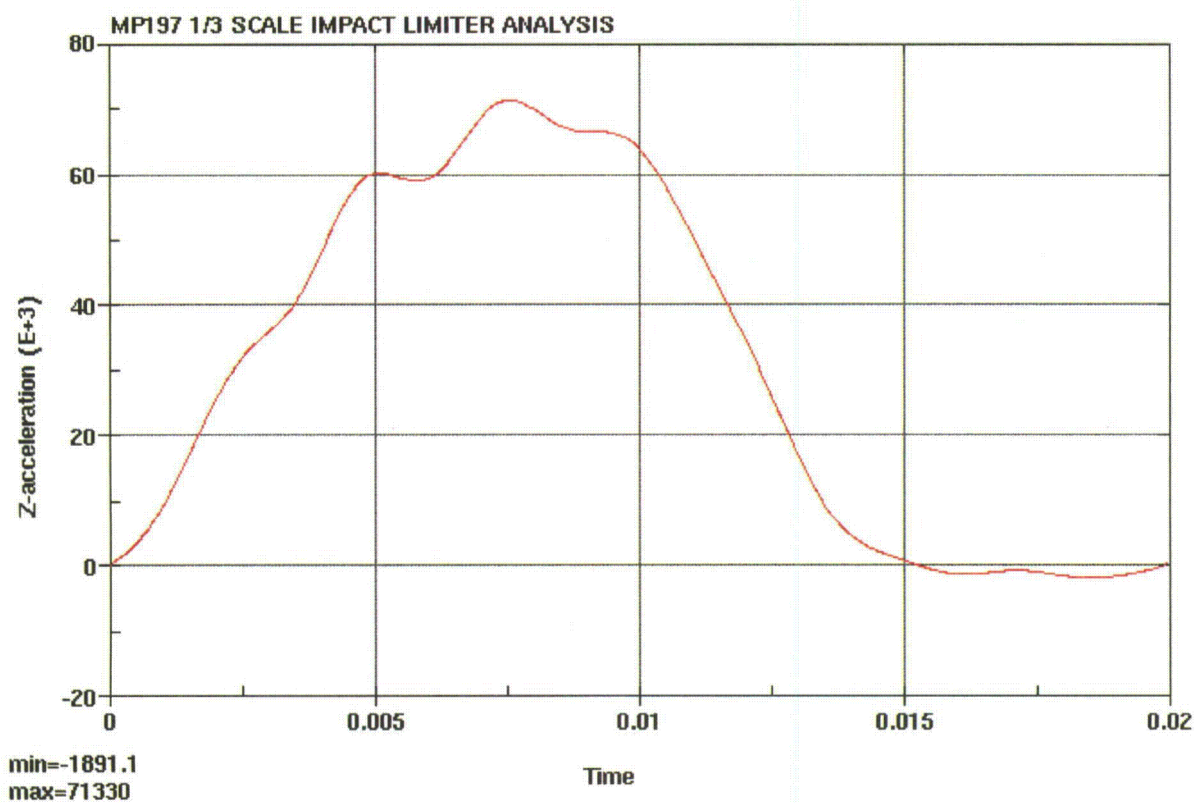


Figure A.2.13.12-8
Plot of Maximum Deformation for 1/3 Scale 20° Slap Down Drop
(Second Impact)



Note: The acceleration unit is in/sec^2 and unit for time is sec.

Figure A.2.13.12-9
1/3 Scale Side Drop Acceleration Time History
(From LS-DYNA)

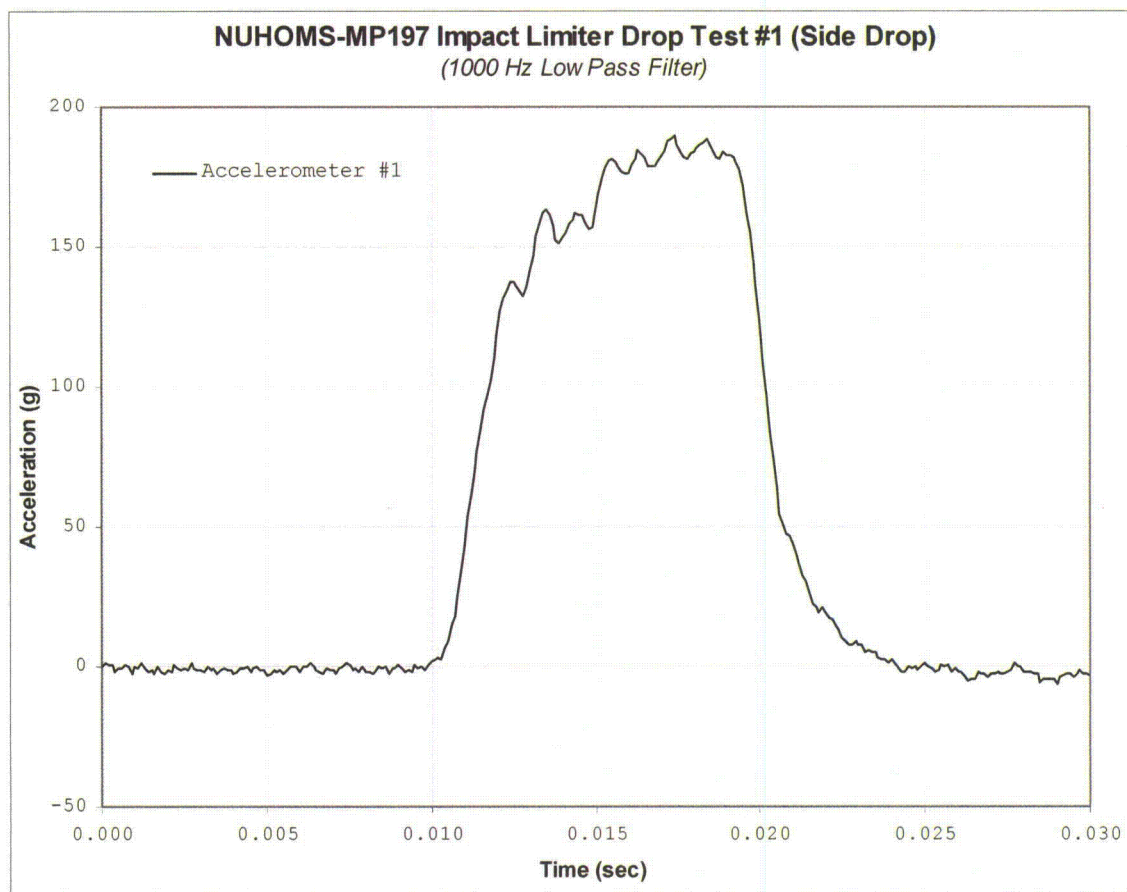


Figure A.2.13.12-10
1/3 Scale Side Drop Acceleration Time History, Accelerometer 1
(From Testing)

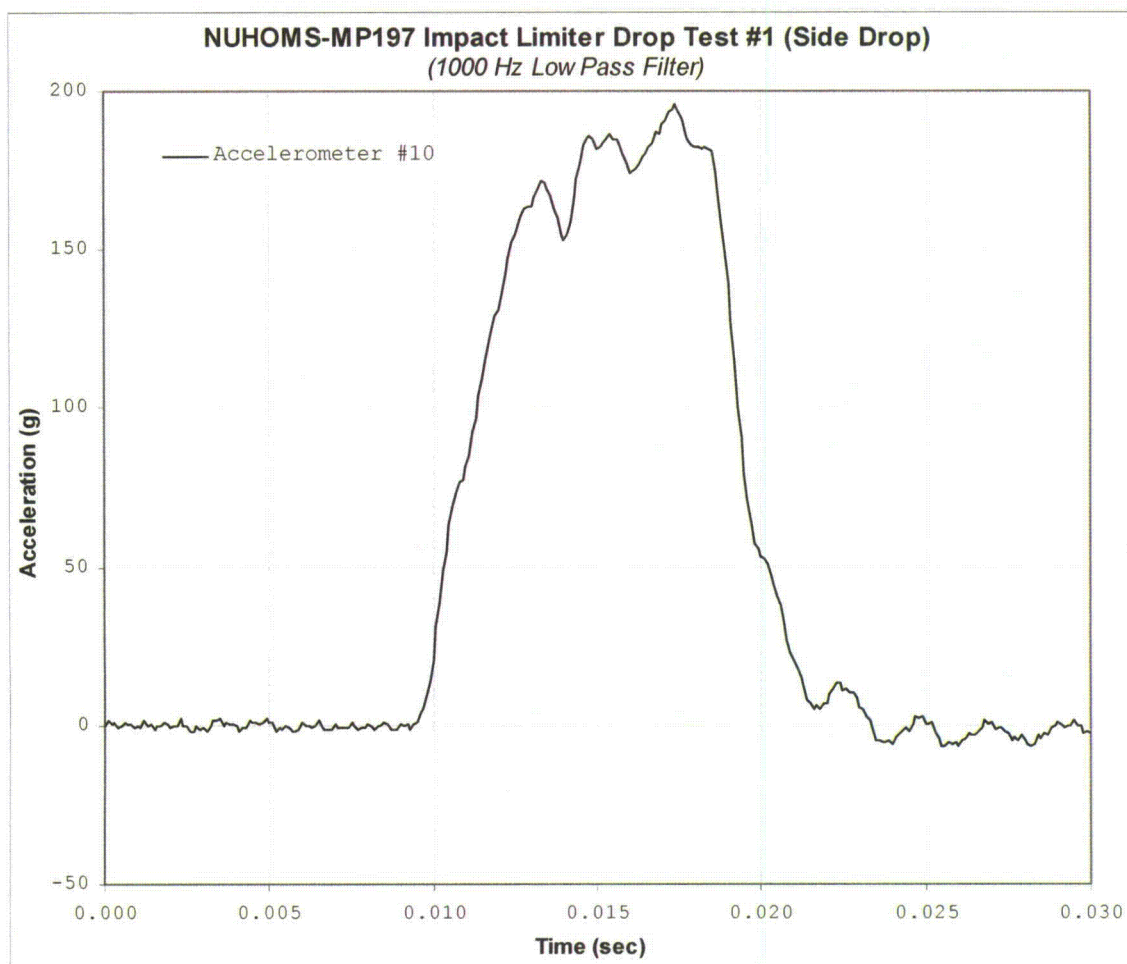
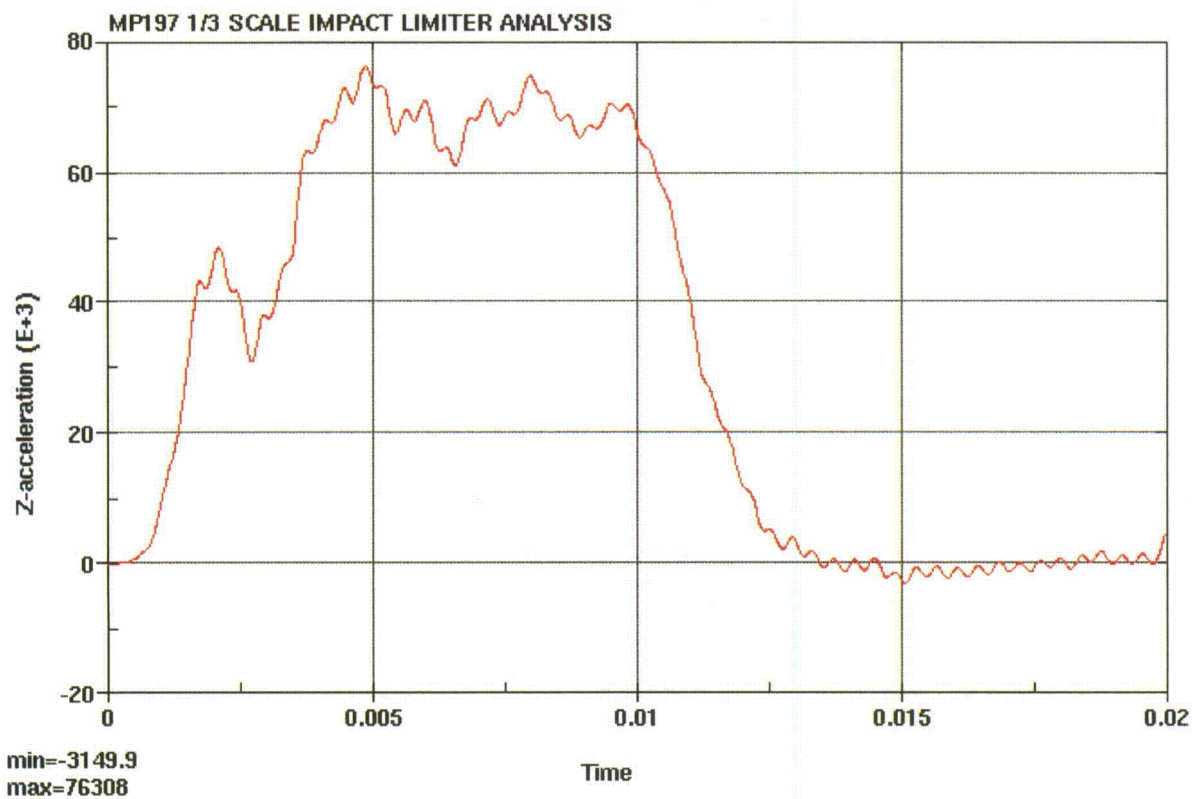


Figure A.2.13.12-11
1/3 Scale Side Drop Acceleration Time History, Accelerometer 10
(From Testing)



Note: The acceleration unit is in/sec^2 and unit for time is sec.

Figure A.2.13.12-12
1/3 Scale End Drop (-20°F) Acceleration Time History
(From LS-DYNA)

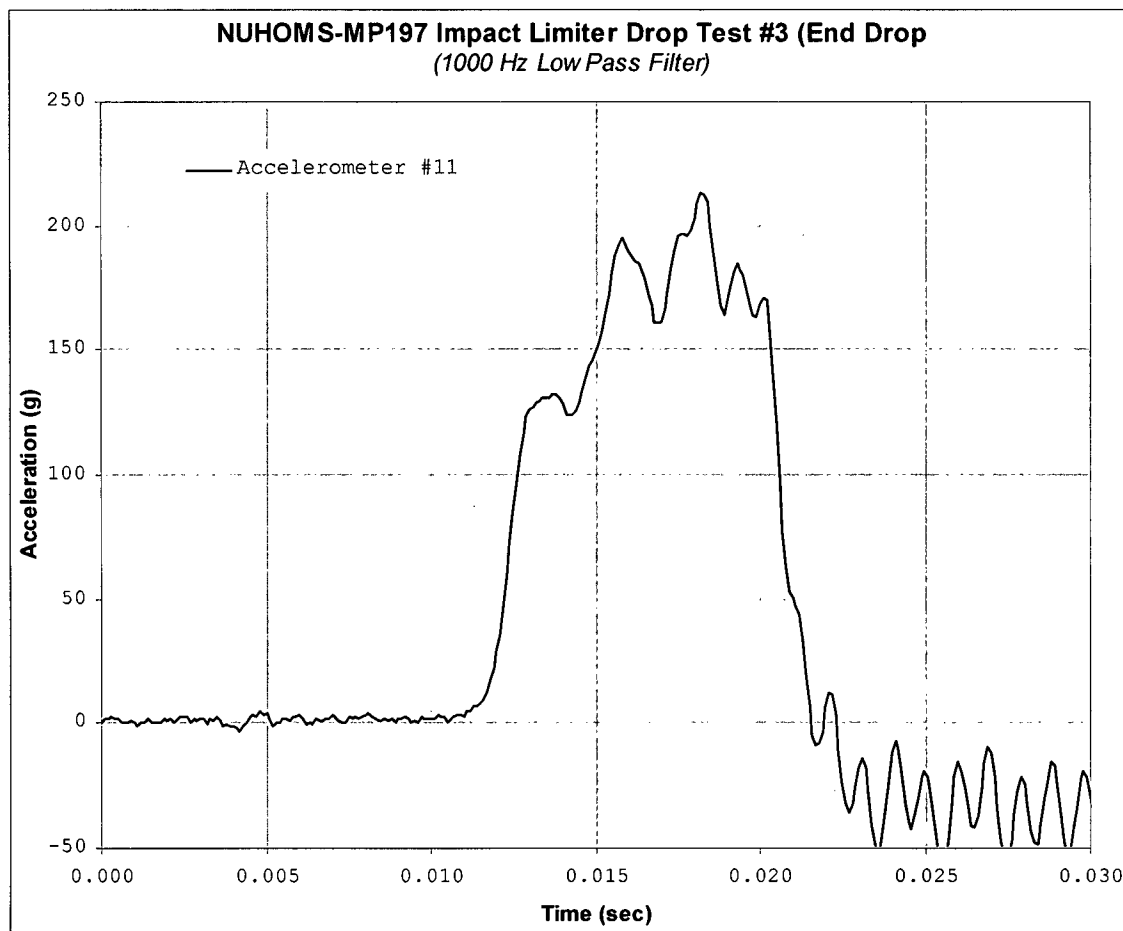


Figure A.2.13.12-13
1/3 Scale End Drop (-20°F) Acceleration Time History, Accelerometer 11
(Accelerometer Located At Bottom End-From Testing)

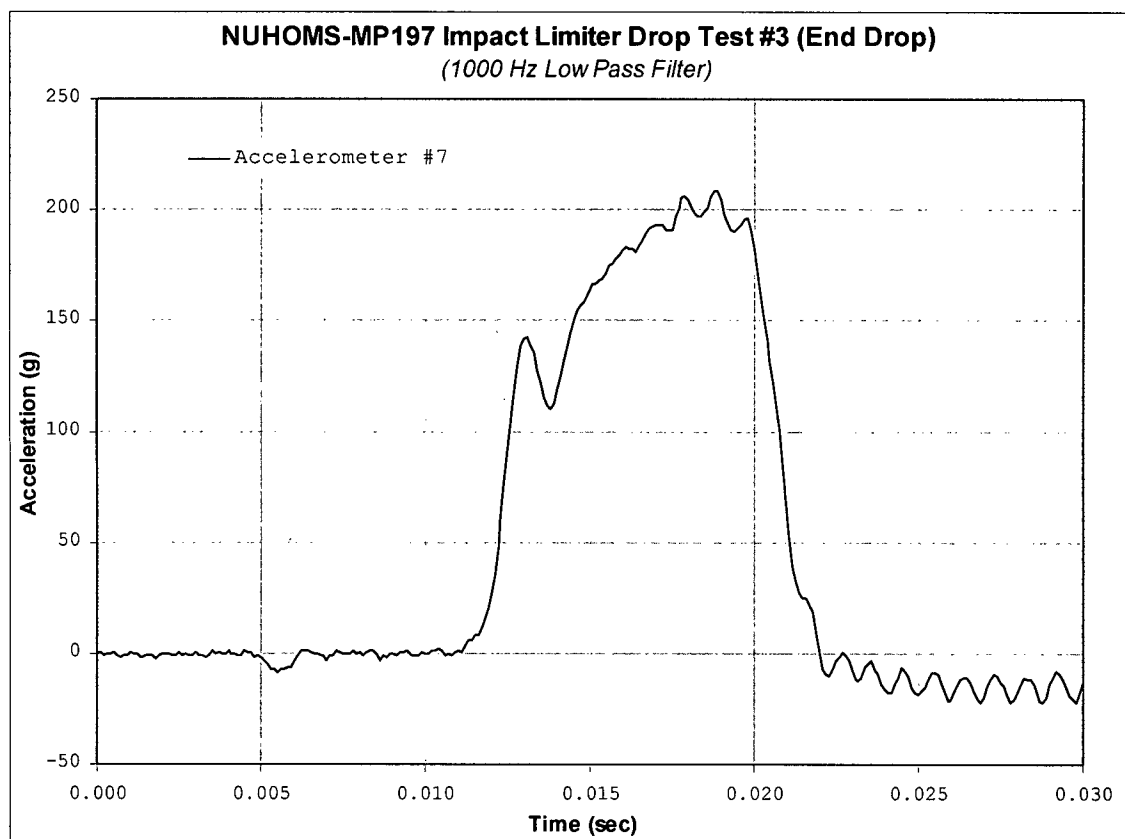
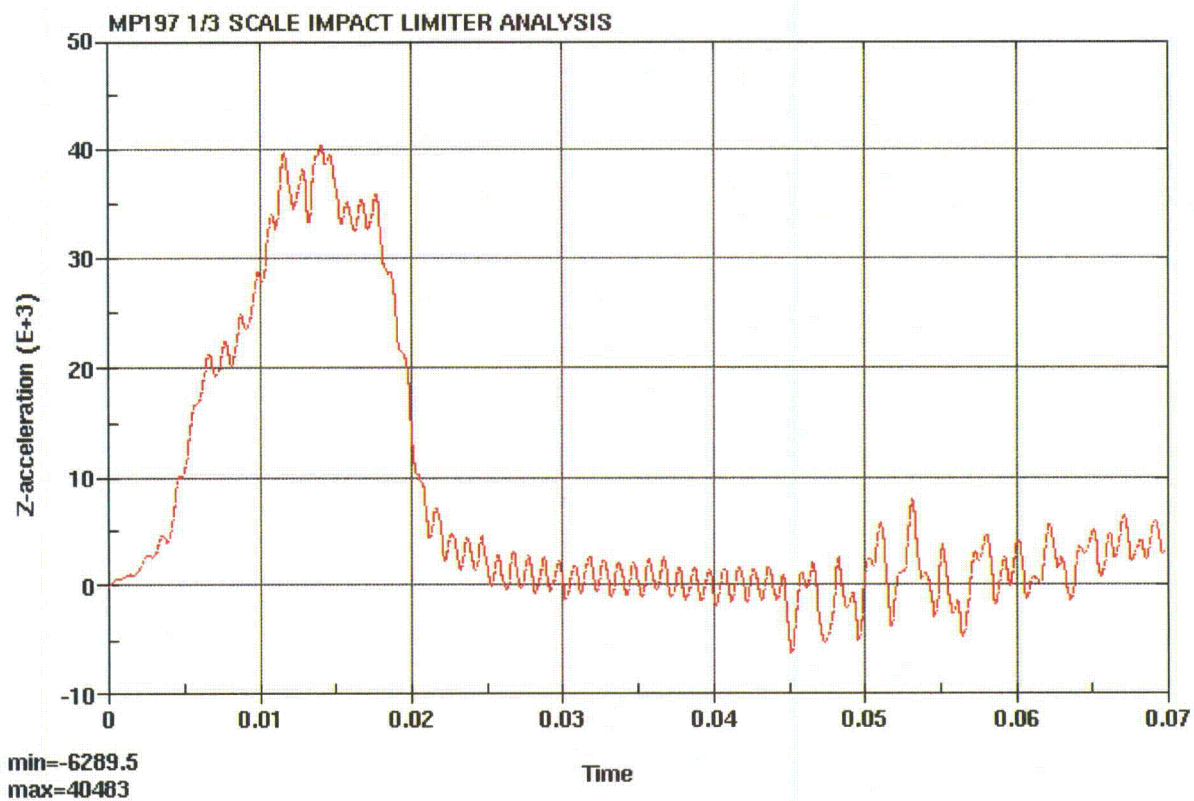
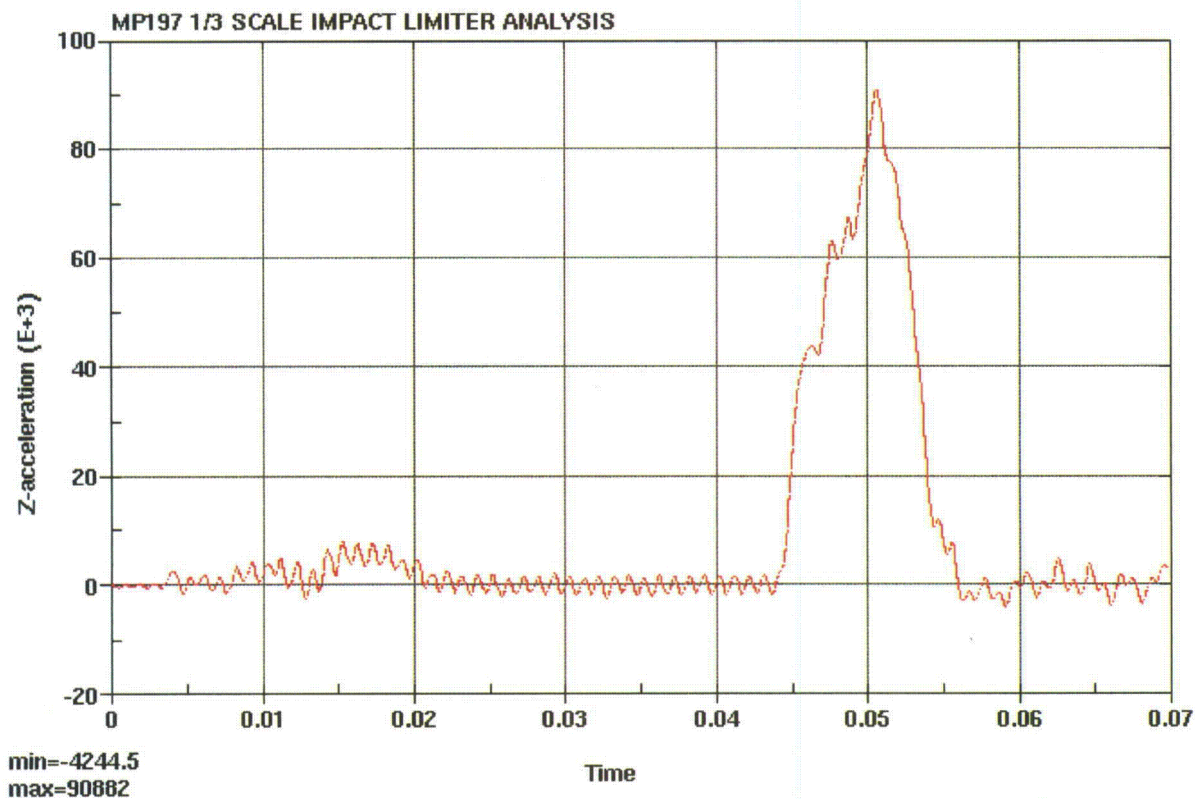


Figure A.2.13.12-14
1/3 Scale End Drop (-20°F) Acceleration Time History, Accelerometer 7
(Accelerometer Located At Center of Gravity-From Testing)



Note: The acceleration unit is in/sec² and unit for time is sec.

Figure A.2.13.12-15
1/3 Scale 20° Slap Down Drop Acceleration Time History
(First Impact-From LS-DYNA)



Note: The acceleration unit is in/sec^2 and unit for time is sec.

Figure A.2.13.12-16
1/3 Scale 20° Slap Down Drop Acceleration Time History
(Second Impact-From LS-DYNA)

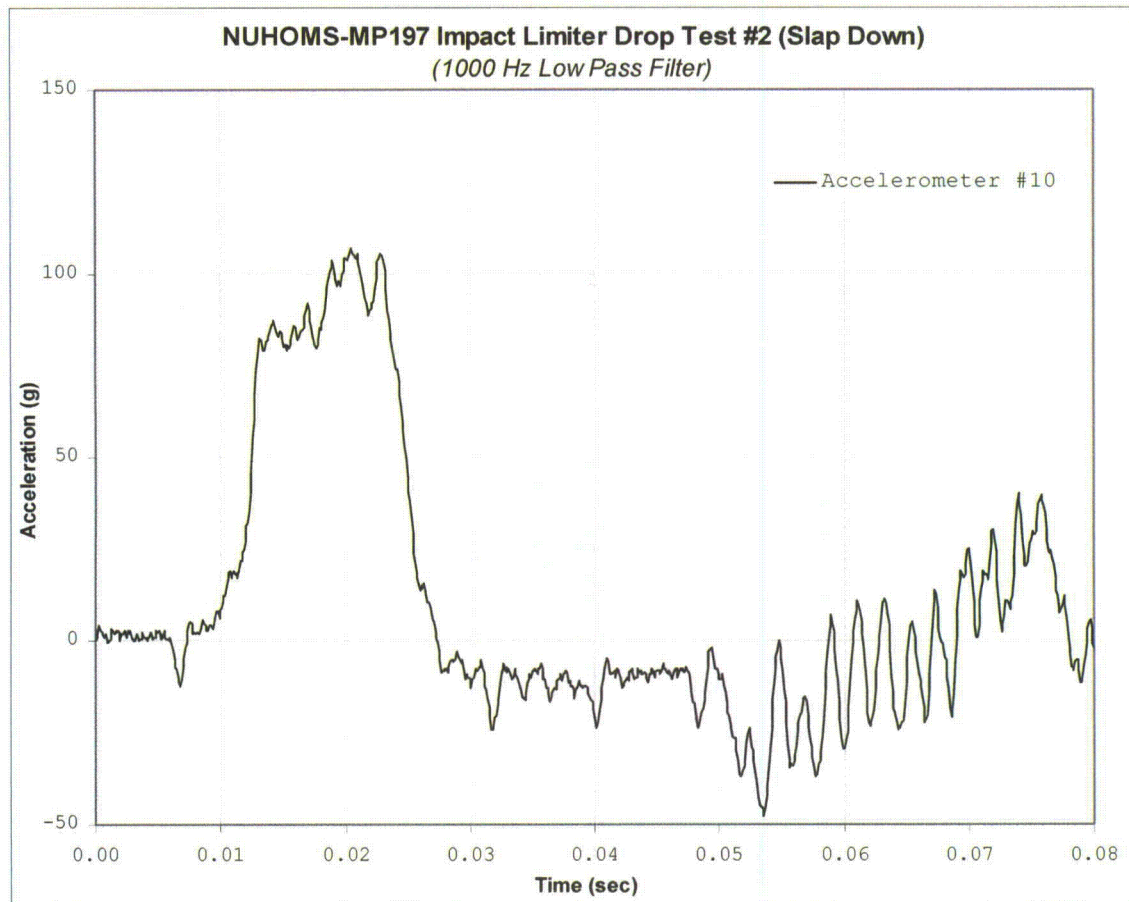


Figure A.2.13.12-17
1/3 Scale 20° Slap Down Drop Acceleration Time History, Accelerometer 10
(First Impact-From Testing)

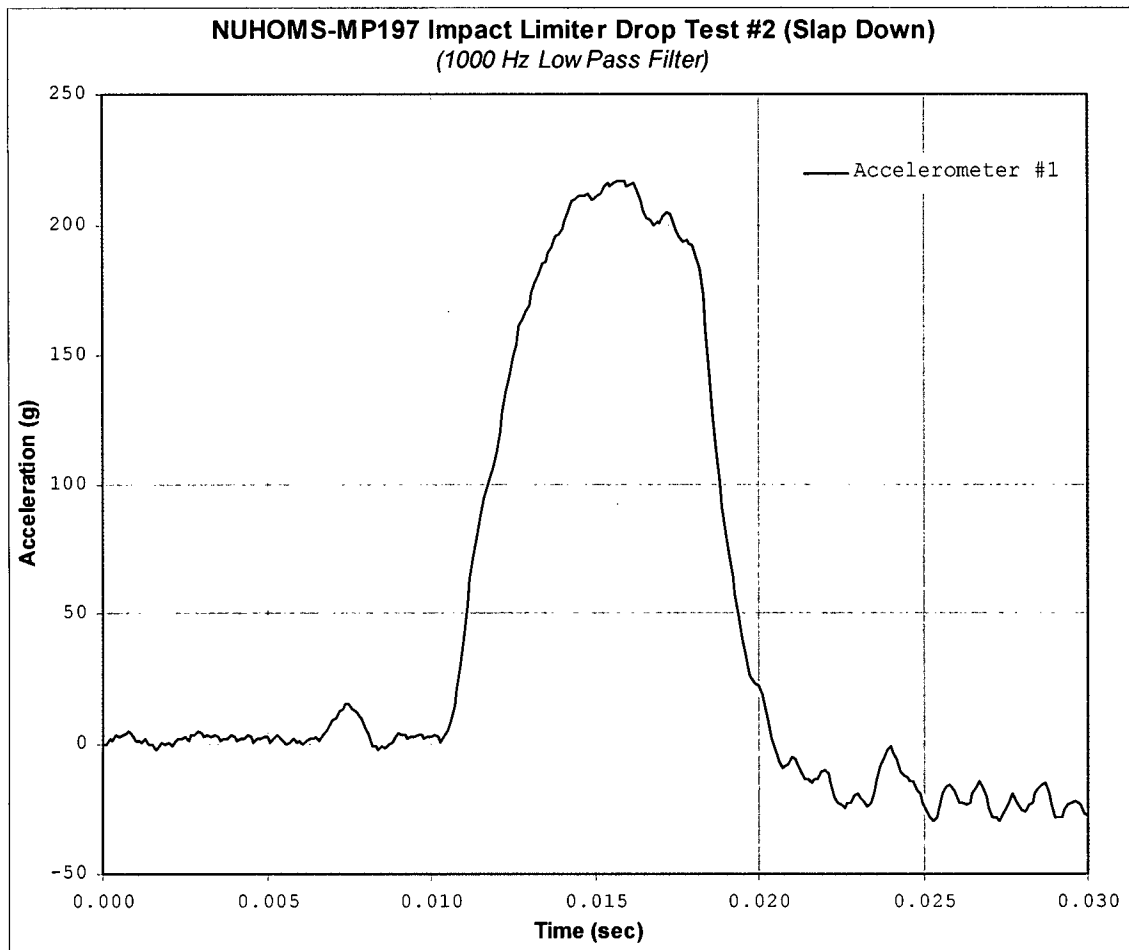


Figure A.2.13.12-18
1/3 Scale 20° Slap Down Drop Acceleration Time History, Accelerometer 1
(Second Impact-From Testing)

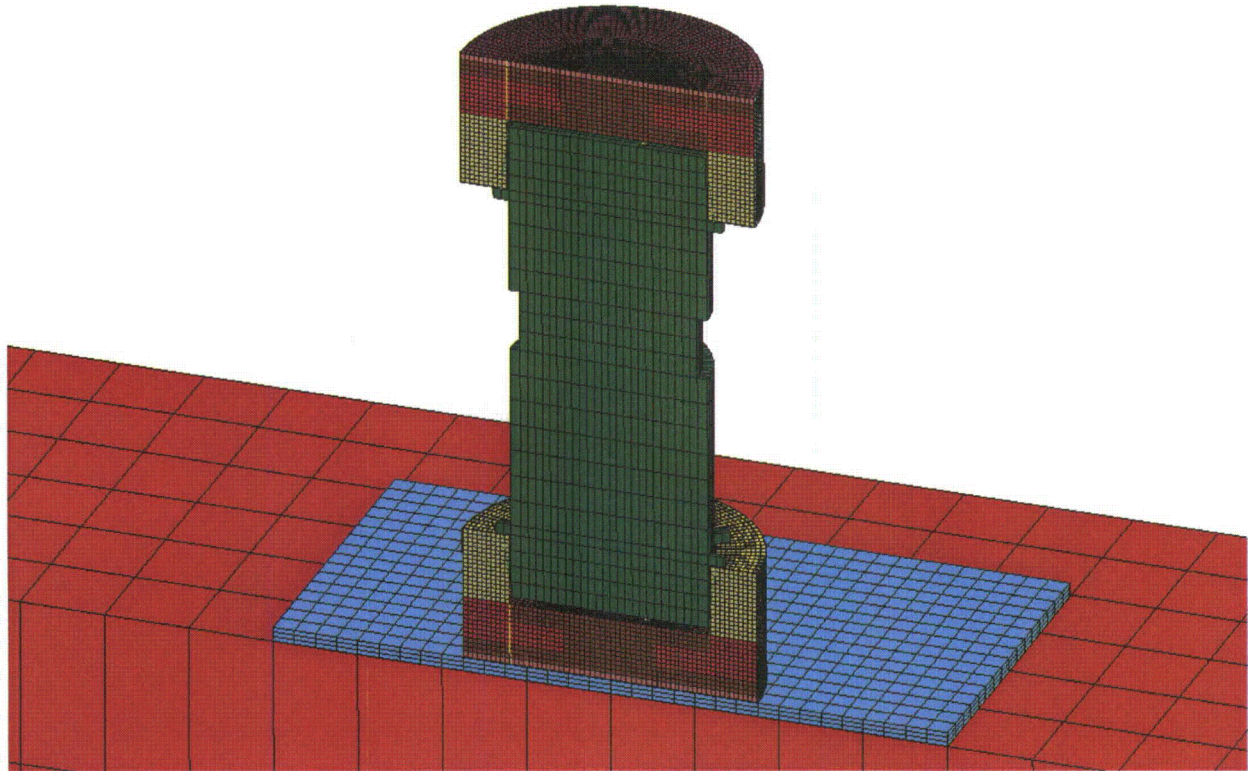


Figure A.2.13.12-19
Full Scale MP-197HB Impact Limiter Finite Element Model Overview

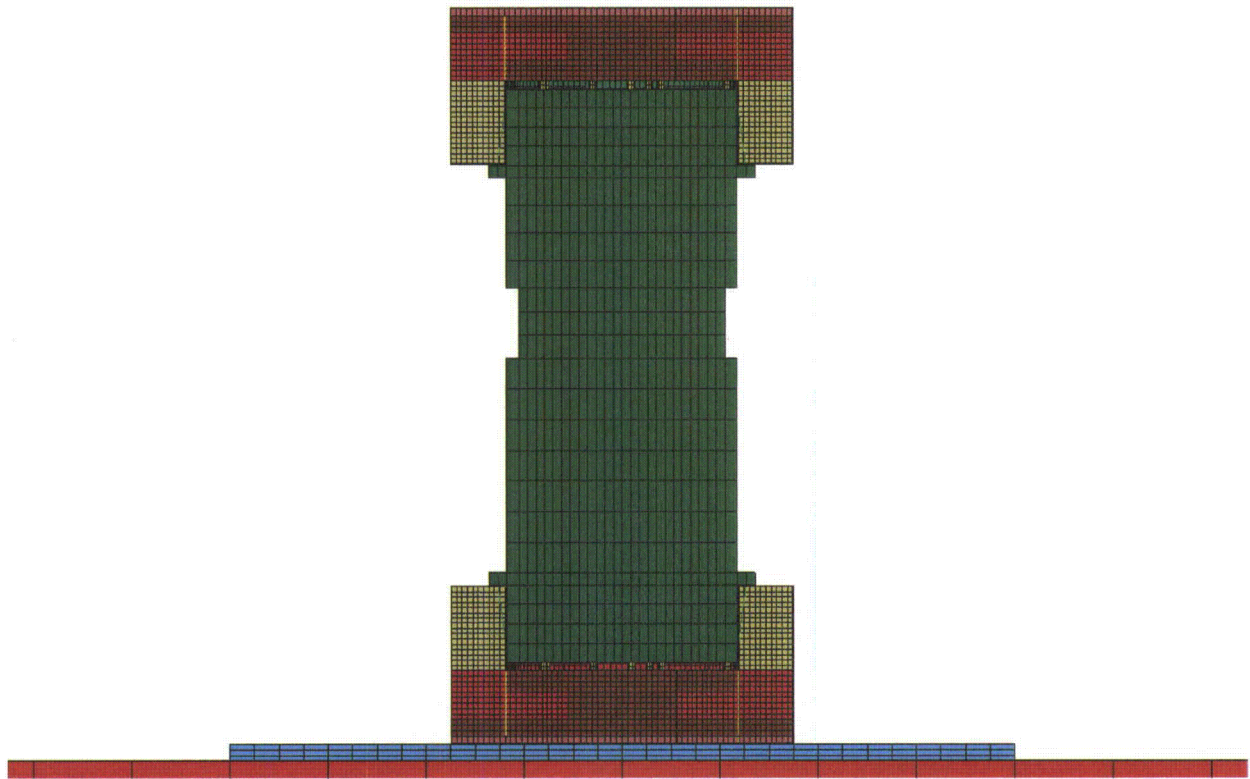


Figure A.2.13.12.-20
Full Scale MP-197HB Impact Limiter Finite Element Model for End Drop Orientation

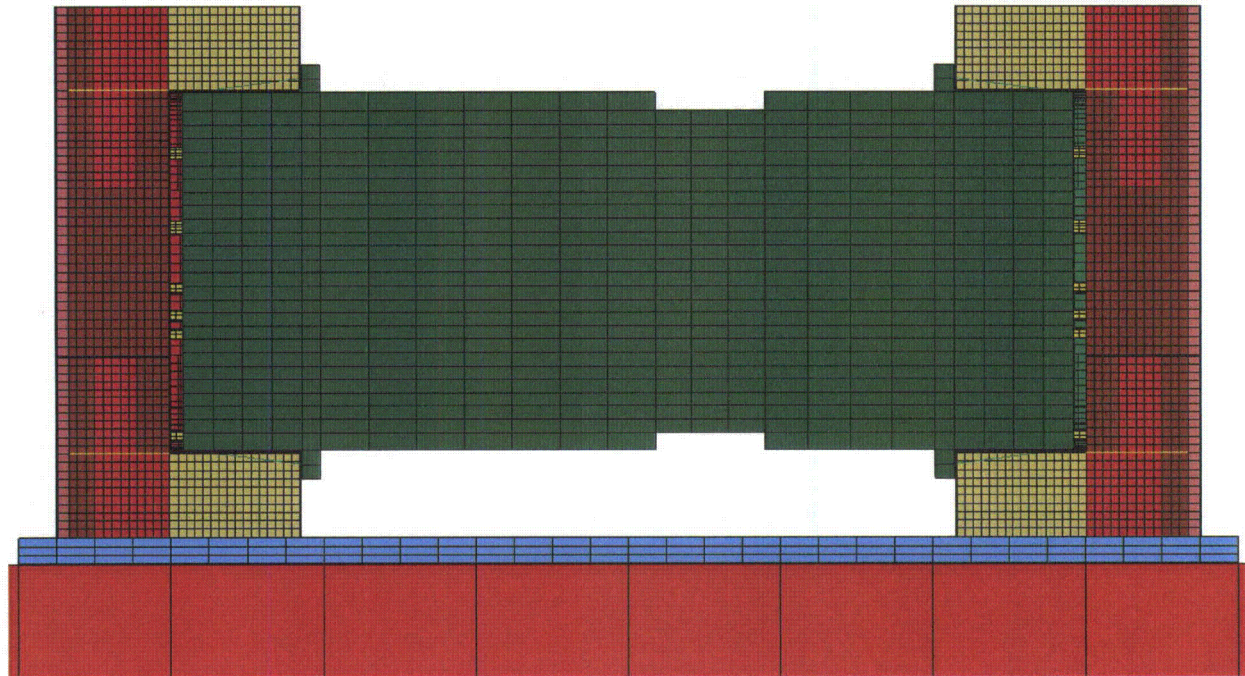


Figure A.2.13.12-21
Full Scale MP-197HB Impact Limiter Finite Element Model for Side Drop Orientation

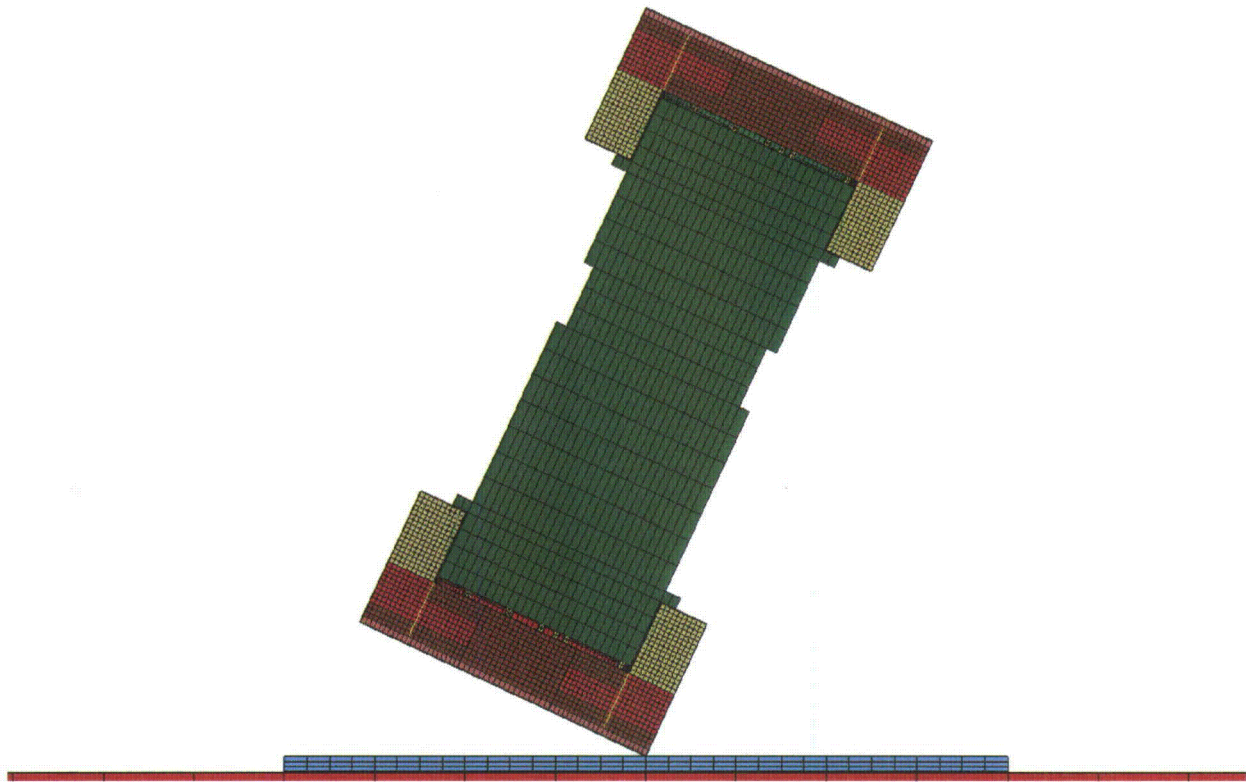


Figure A.2.13.12-22
Full Scale MP-197HB Impact Limiter Finite Element Model for CG Over Corner Orientation

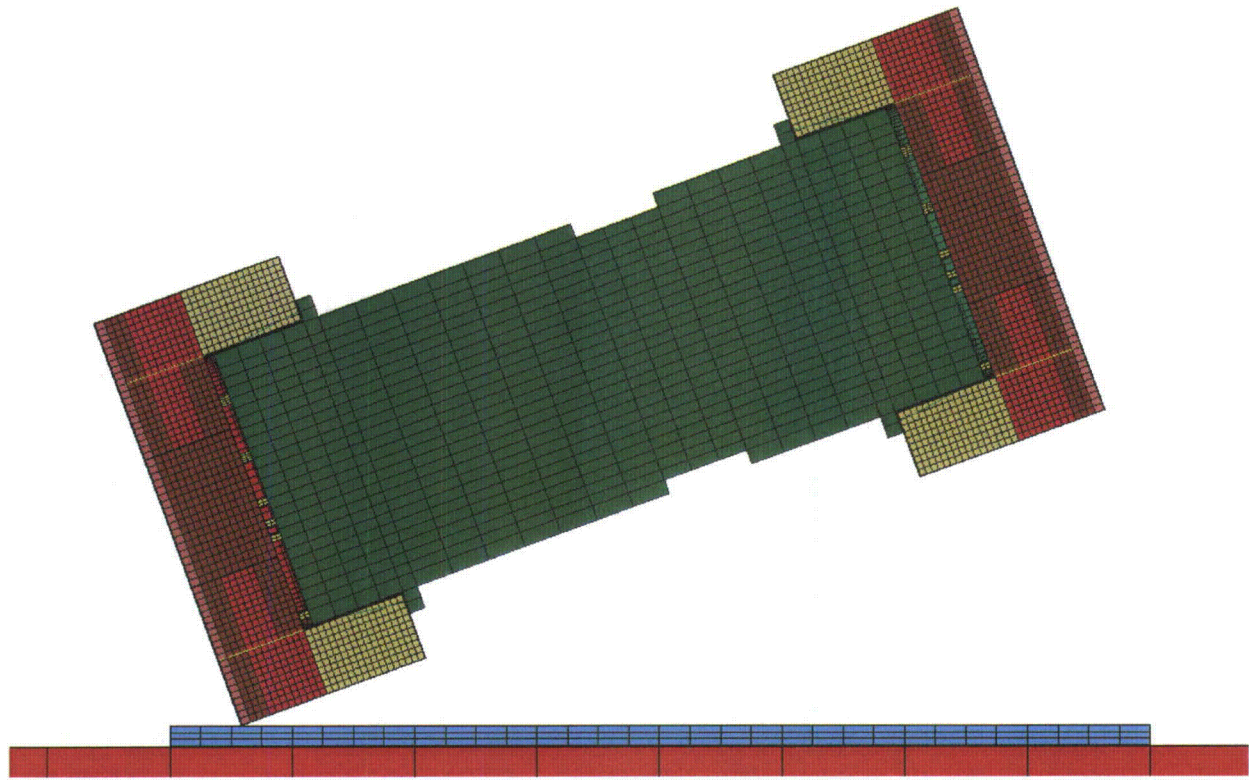


Figure A.2.13.12-23
Full Scale MP-197HB Impact Limiter Finite Element Model for 20° Slap Down Orientation

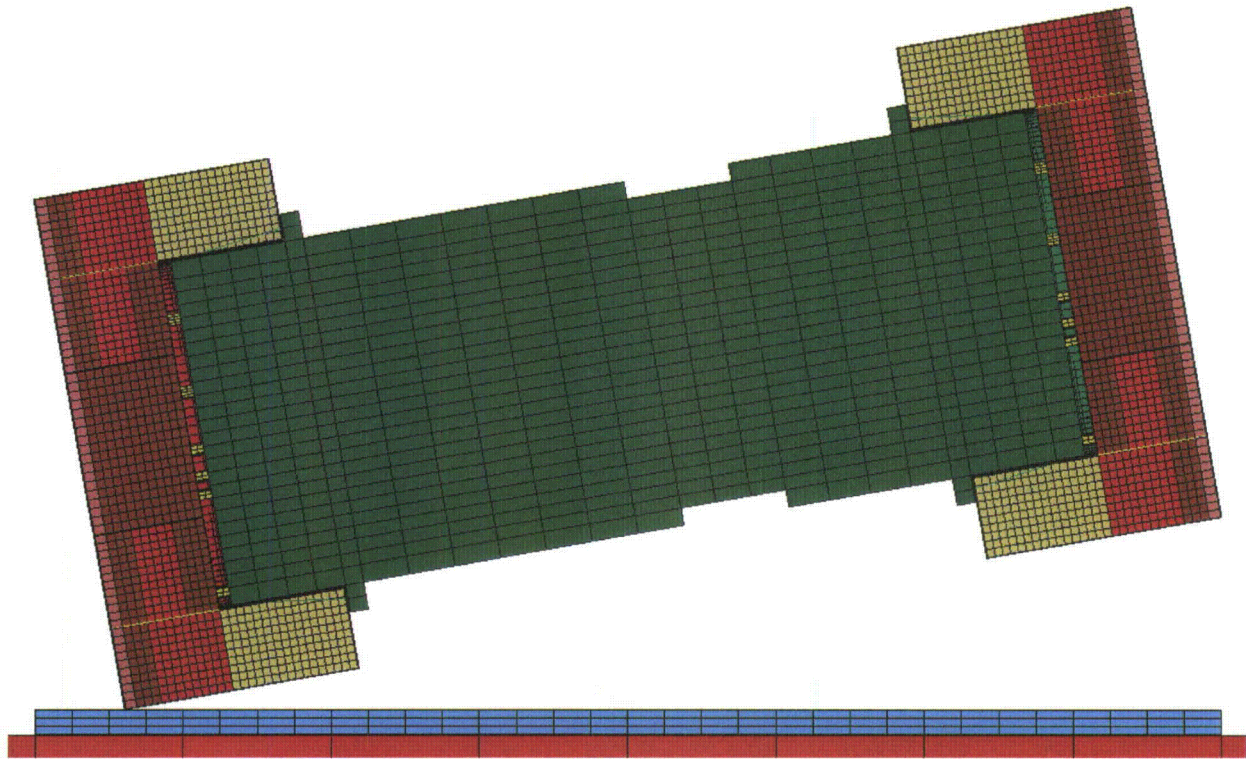


Figure A.2.13.12-24
Full Scale MP-197HB Impact Limiter Finite Element Model for 10° Slap Down Orientation

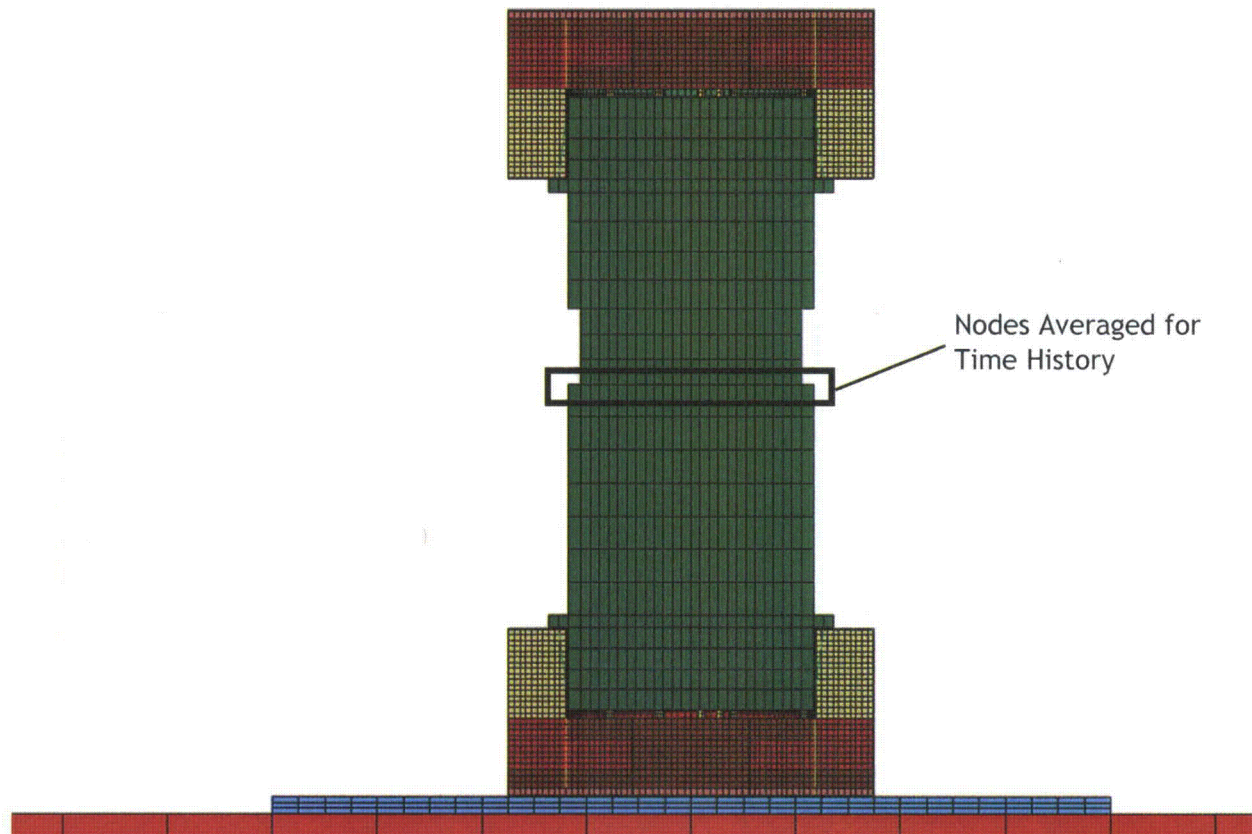


Figure A.2.13.12-25
Region of Nodes Averaged for Time History (All cases other than Slap Down)

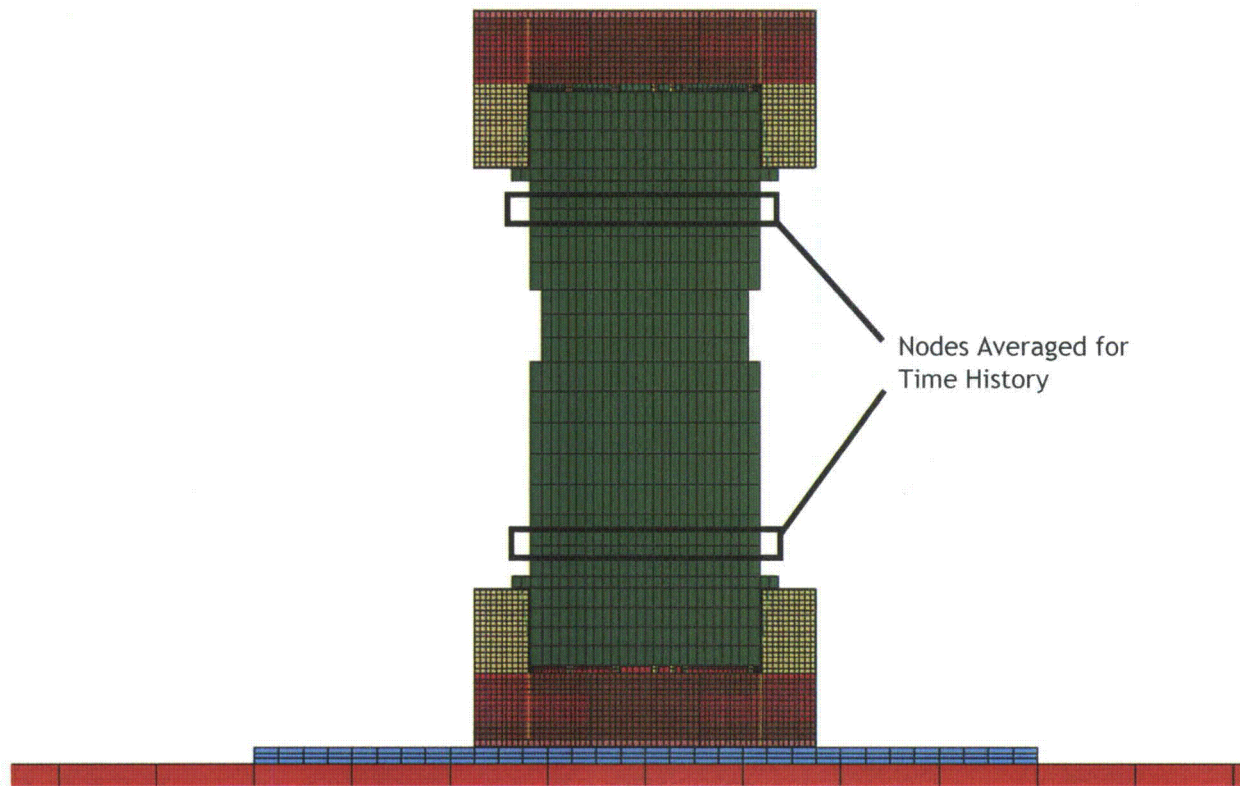


Figure A.2.13.12-26
Region of Nodes Averaged for Time History (Slap Down Cases)

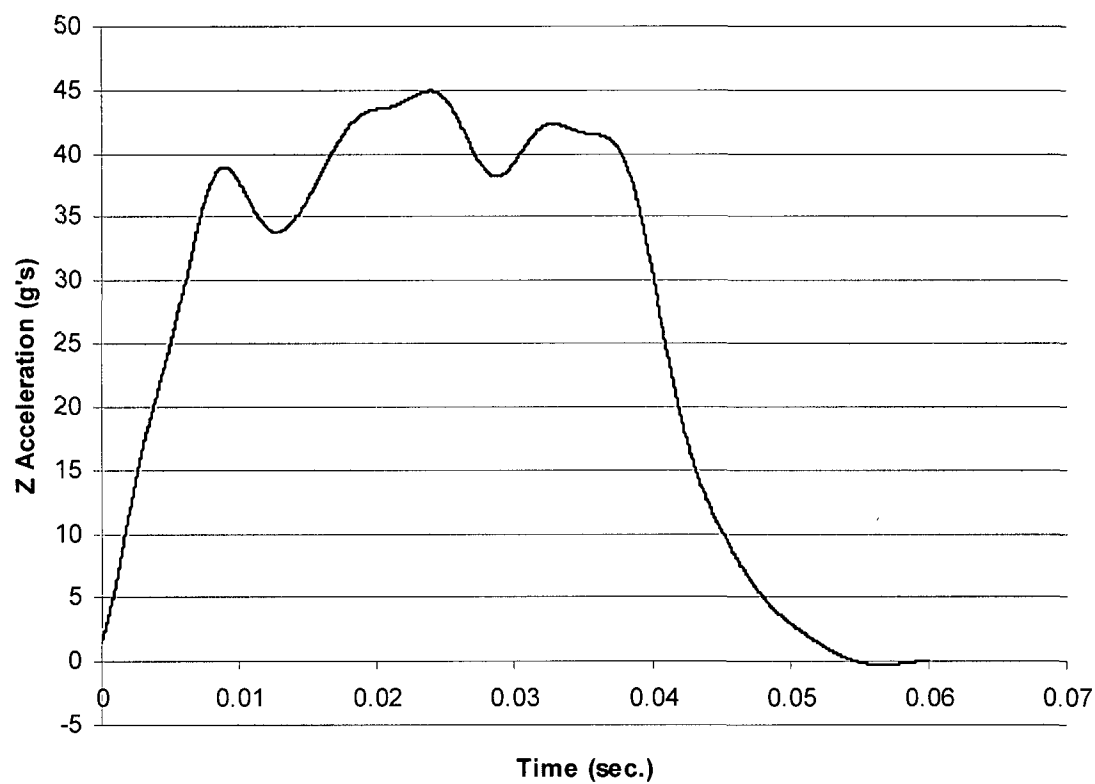
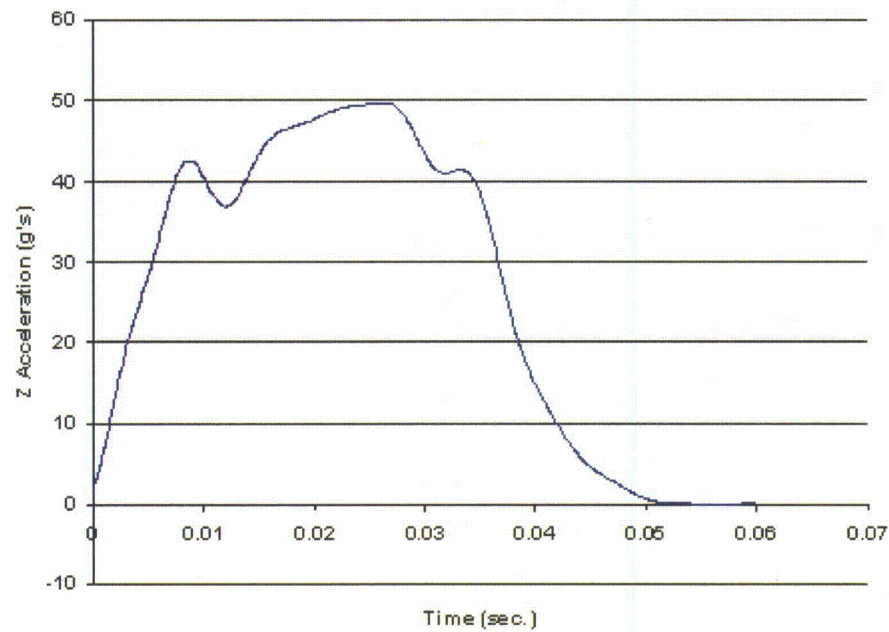
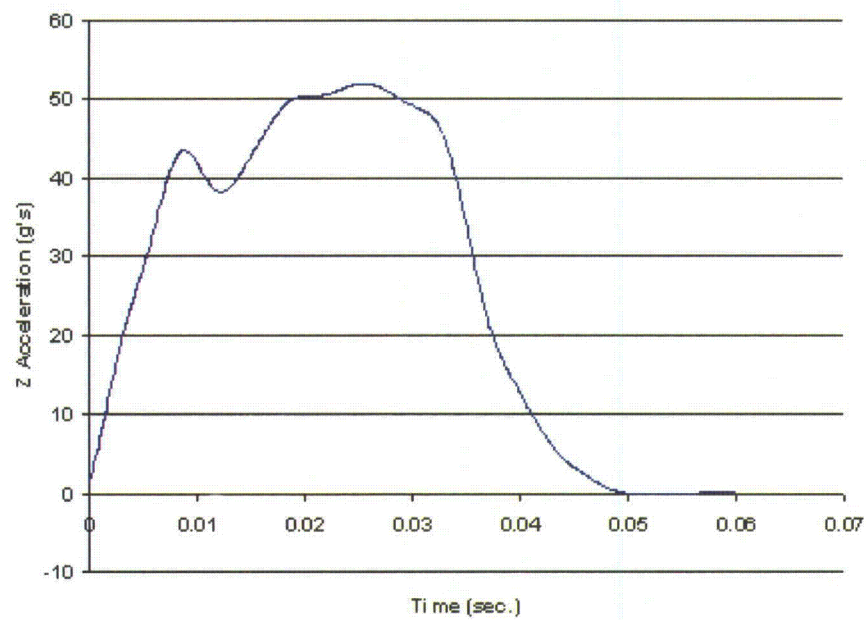


Figure A.2.13.12-27
Full Scale 30' End Drop Acceleration Time History (Room Temperature)



(a) -20 °F



(b) -40 °F

Figure A.2.13.12-28
Full Scale 30' End Drop Acceleration Time History (-20 °F and -40 °F)

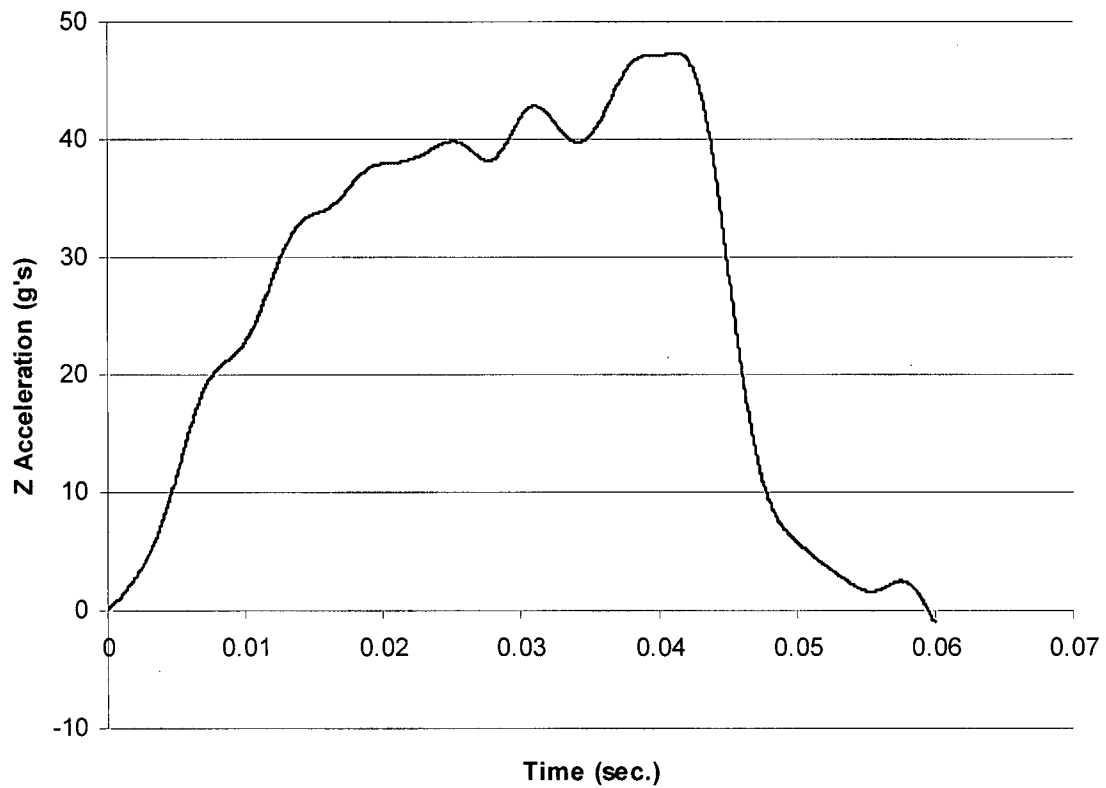


Figure A.2.13.12-29
Full Scale 30' Side Drop Acceleration Time History

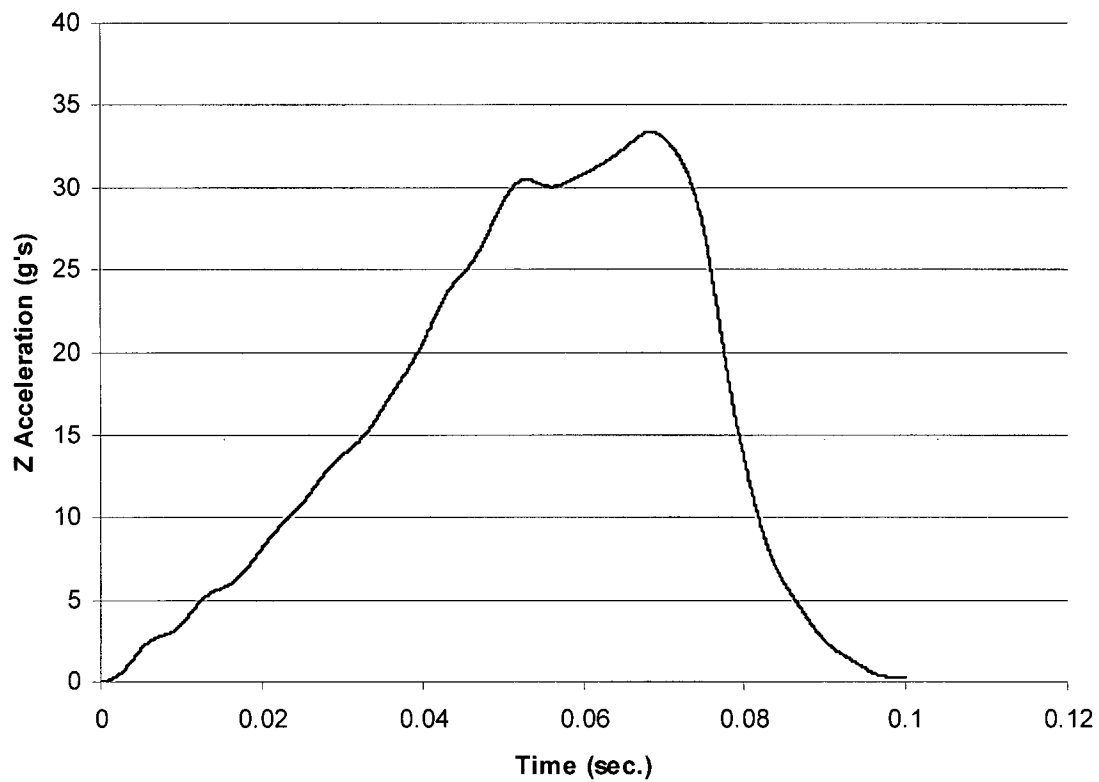


Figure A.2.13.12-30
Full Scale 30' CG Over Corner Drop Acceleration Time History

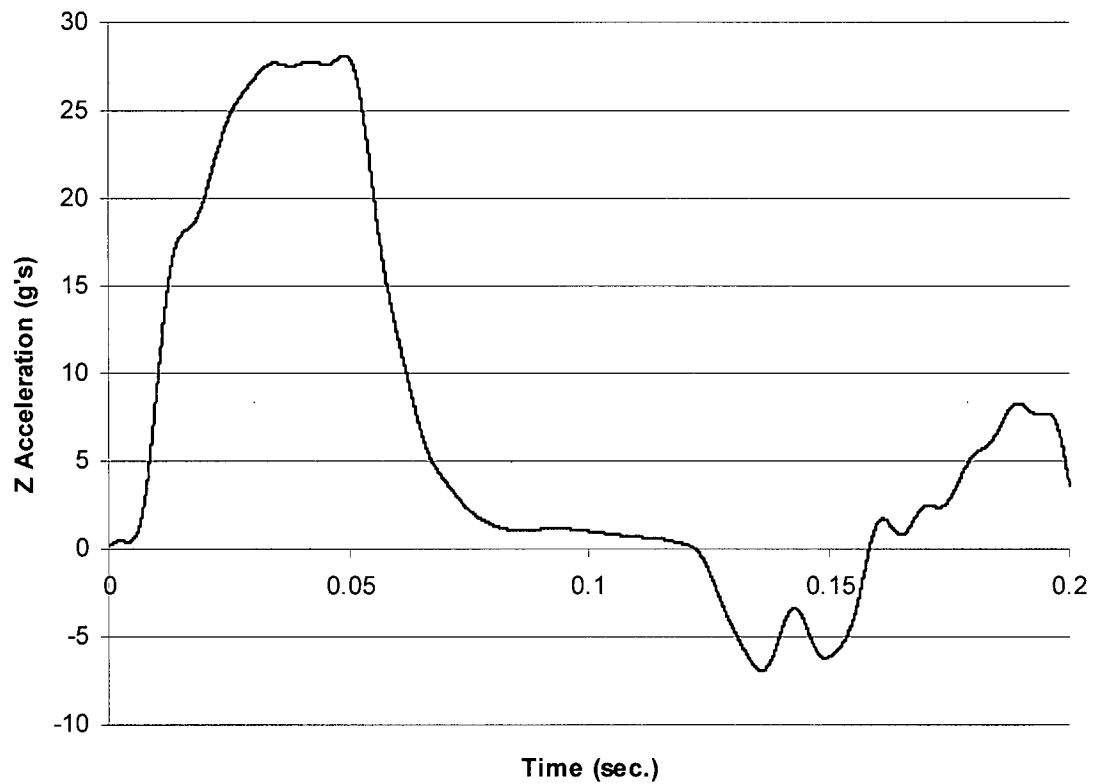


Figure A.2.13.12-31
Full Scale 30' 20° Slap Down Drop Acceleration Time History (First Impact)

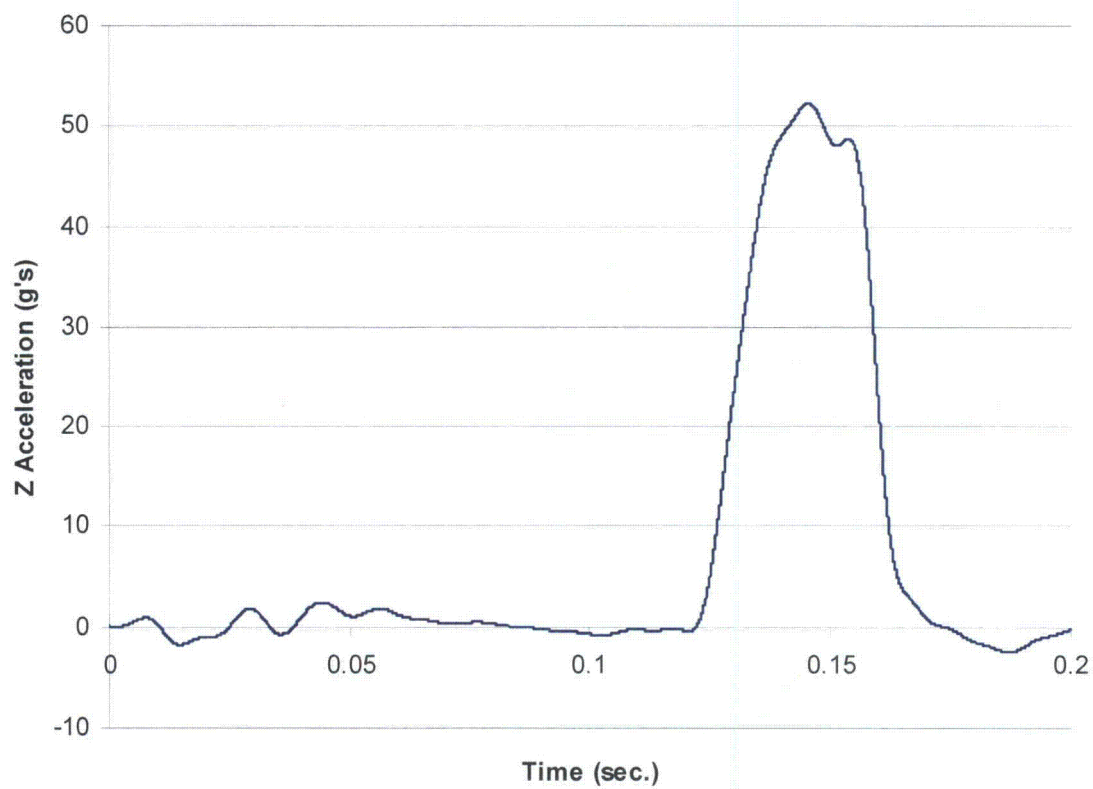


Figure A.2.13.12-32
Full Scale 30' 20° Slap Down Drop Acceleration Time History (Second Impact)

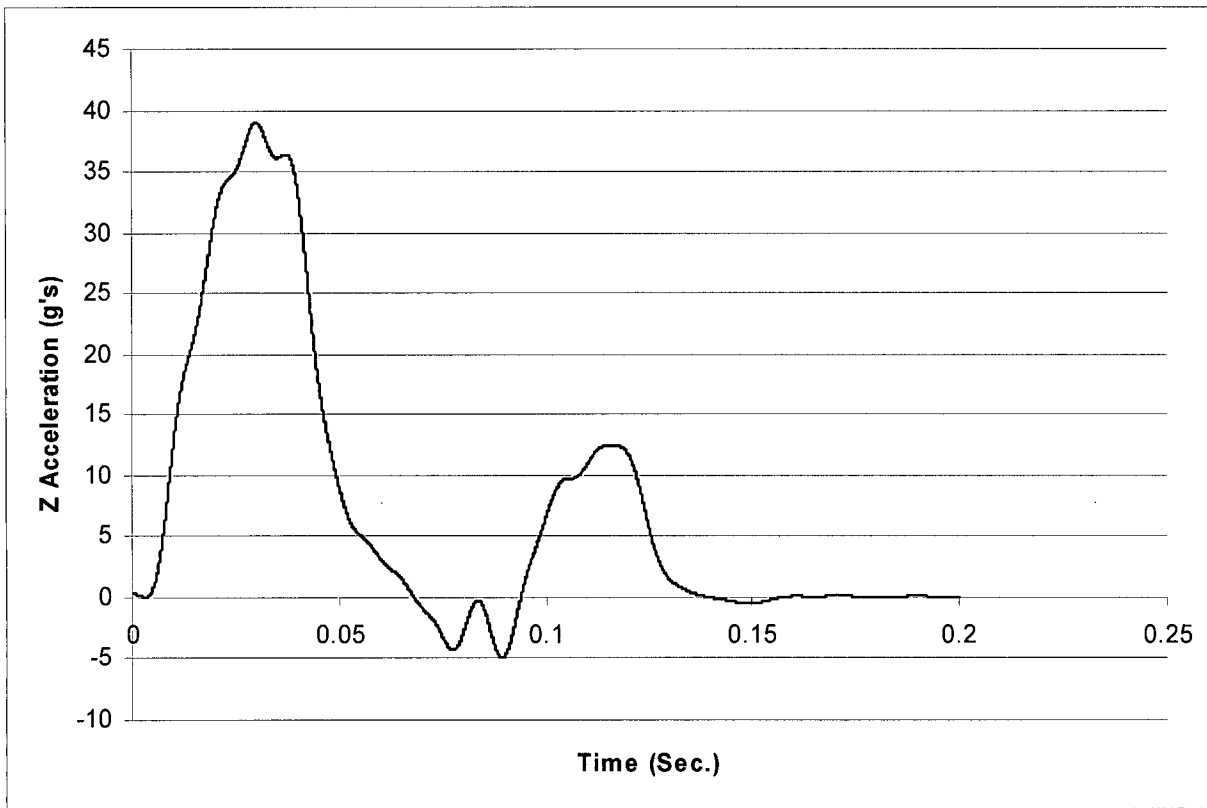


Figure A.2.13.12-33
Full Scale 30' 10° Slap Down Drop Acceleration Time History (First Impact)

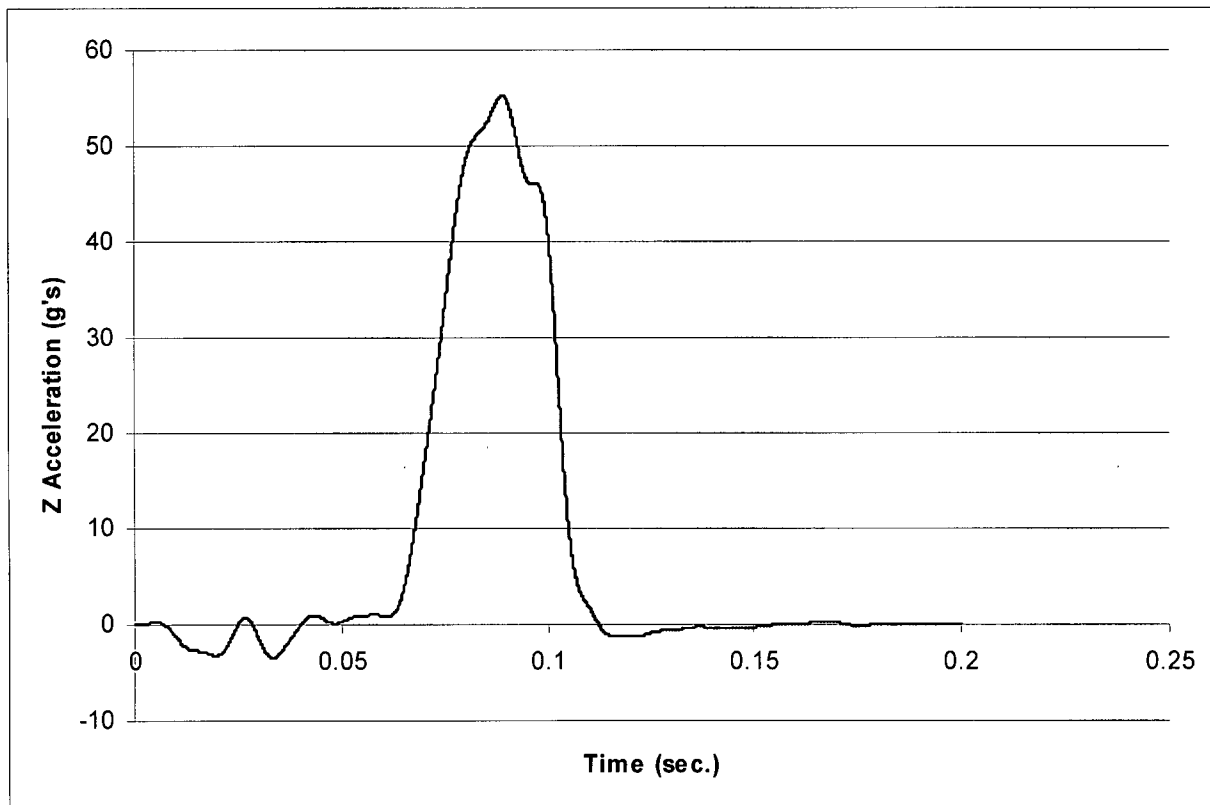


Figure A.2.13.12-34
Full Scale 30' 10° Slap Down Drop Acceleration Time History (*Second Impact*)

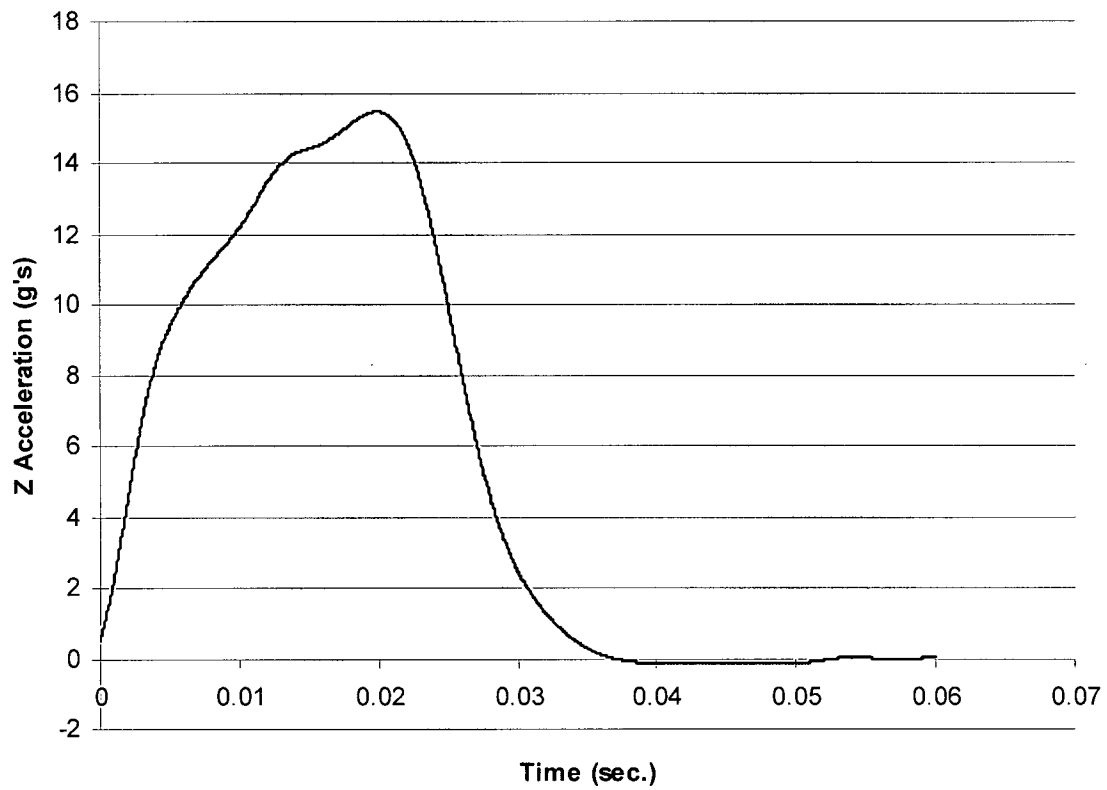


Figure A.2.13.12-35
Full Scale 1 Foot Normal Condition End Drop Acceleration Time History

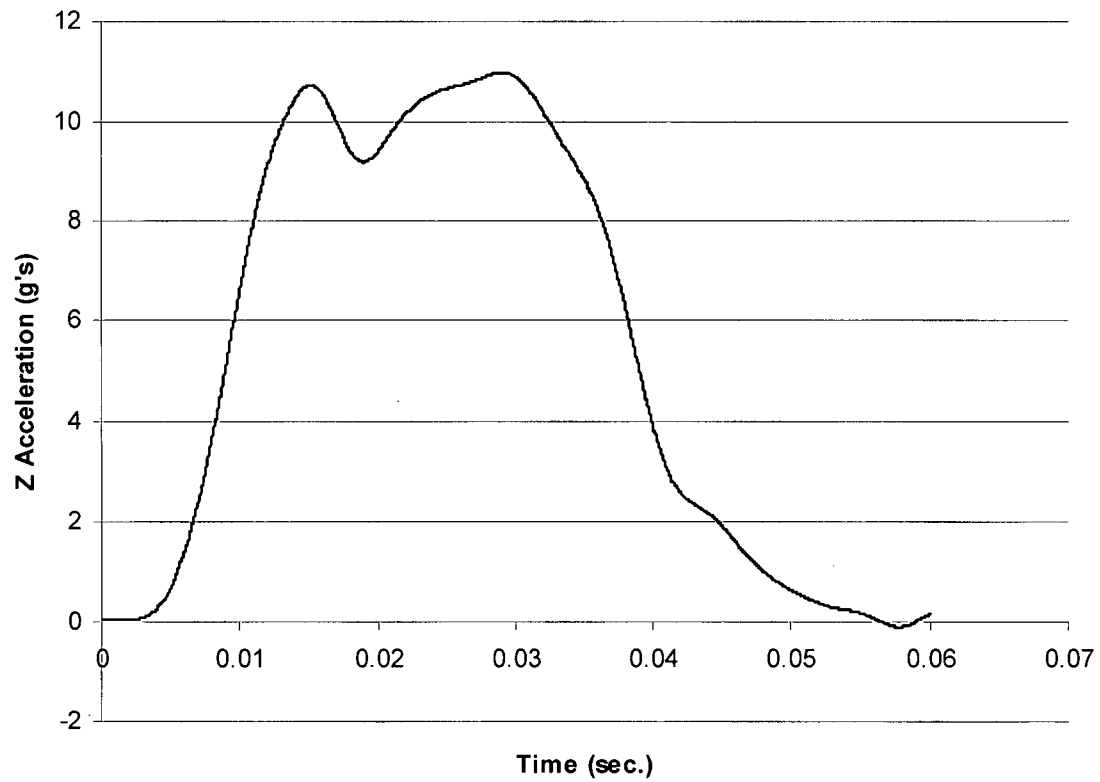


Figure A.2.13.12-36
Full Scale 1 Foot Normal Condition Side Drop Acceleration Time History

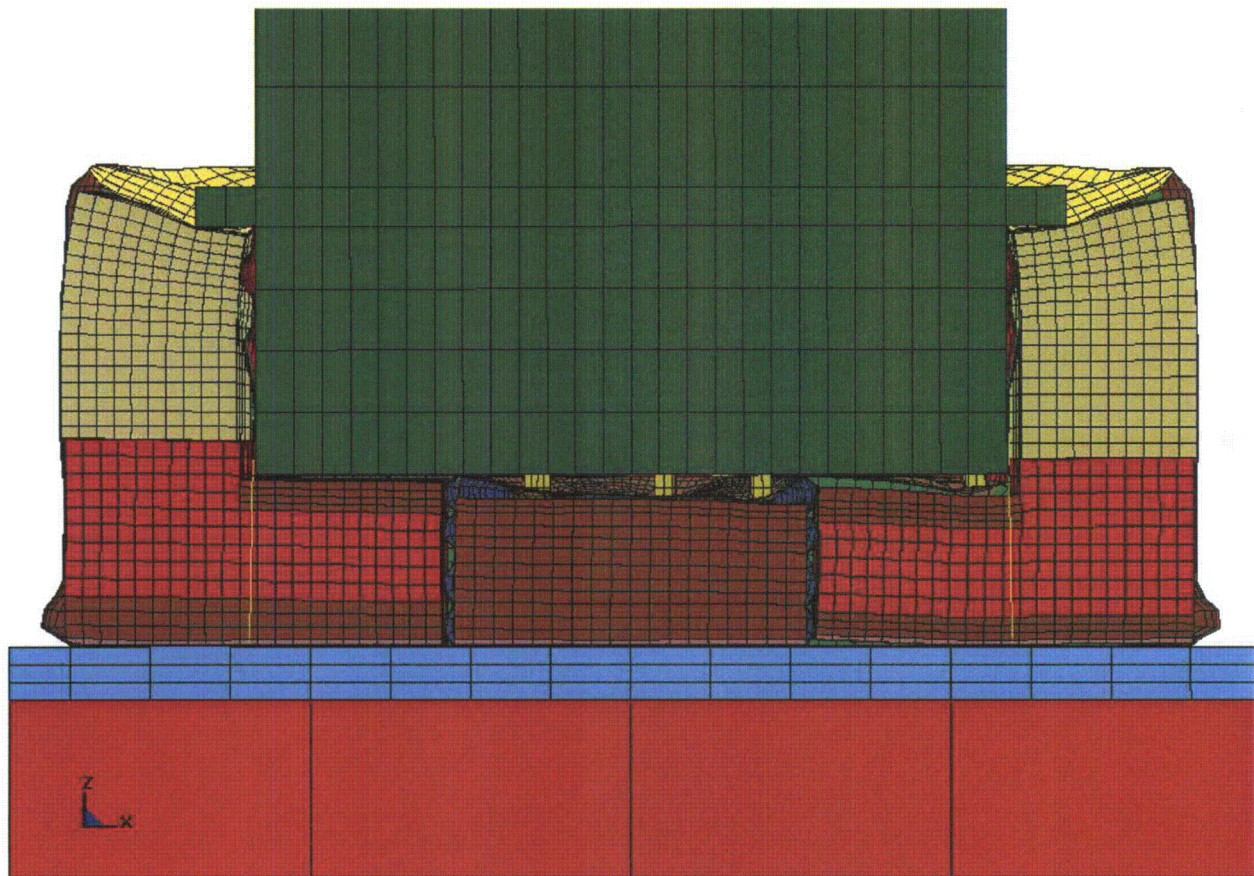


Figure A.2.13.12-37
Plot of Maximum Deformation for 30' End Drop- Full Scale

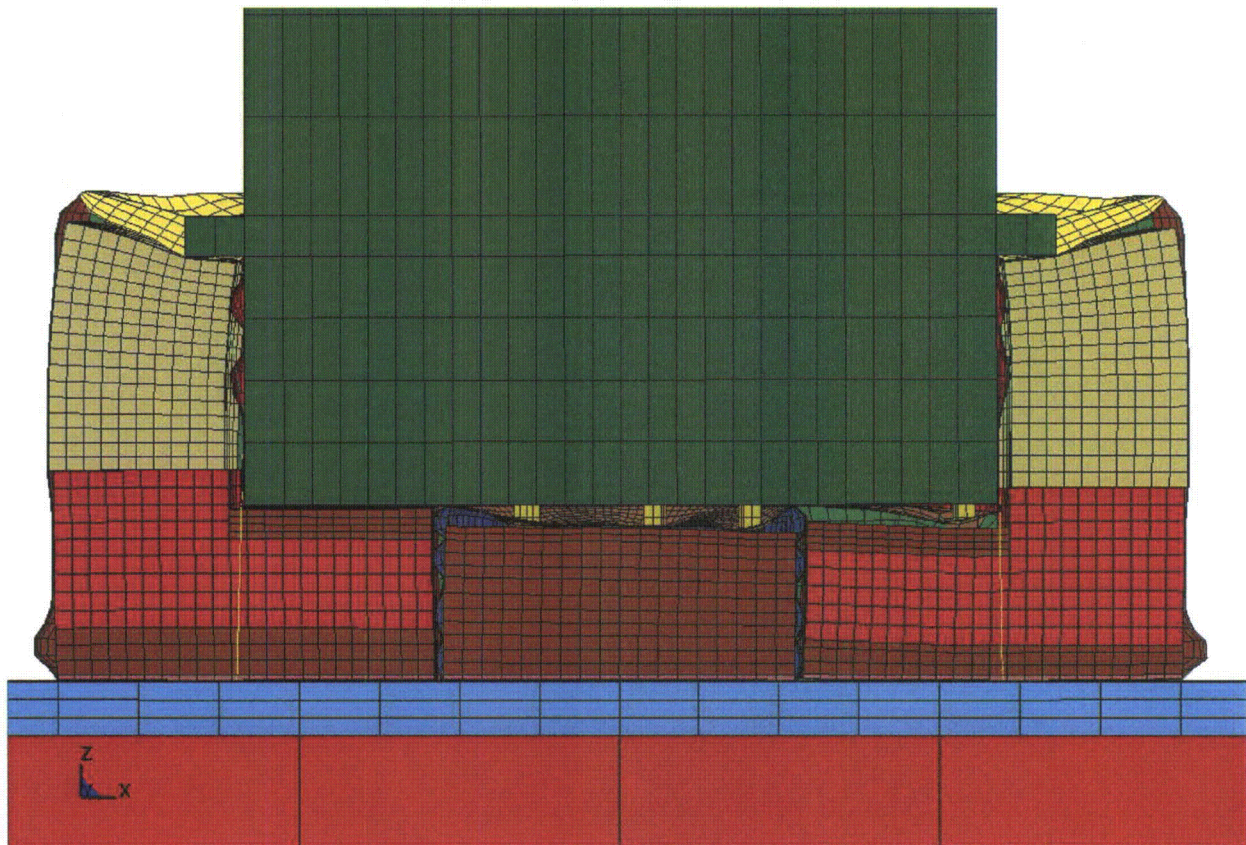


Figure A.2.13.12-38
Plot of Maximum Deformation for 30° End Drop (-20°F) – Full Scale

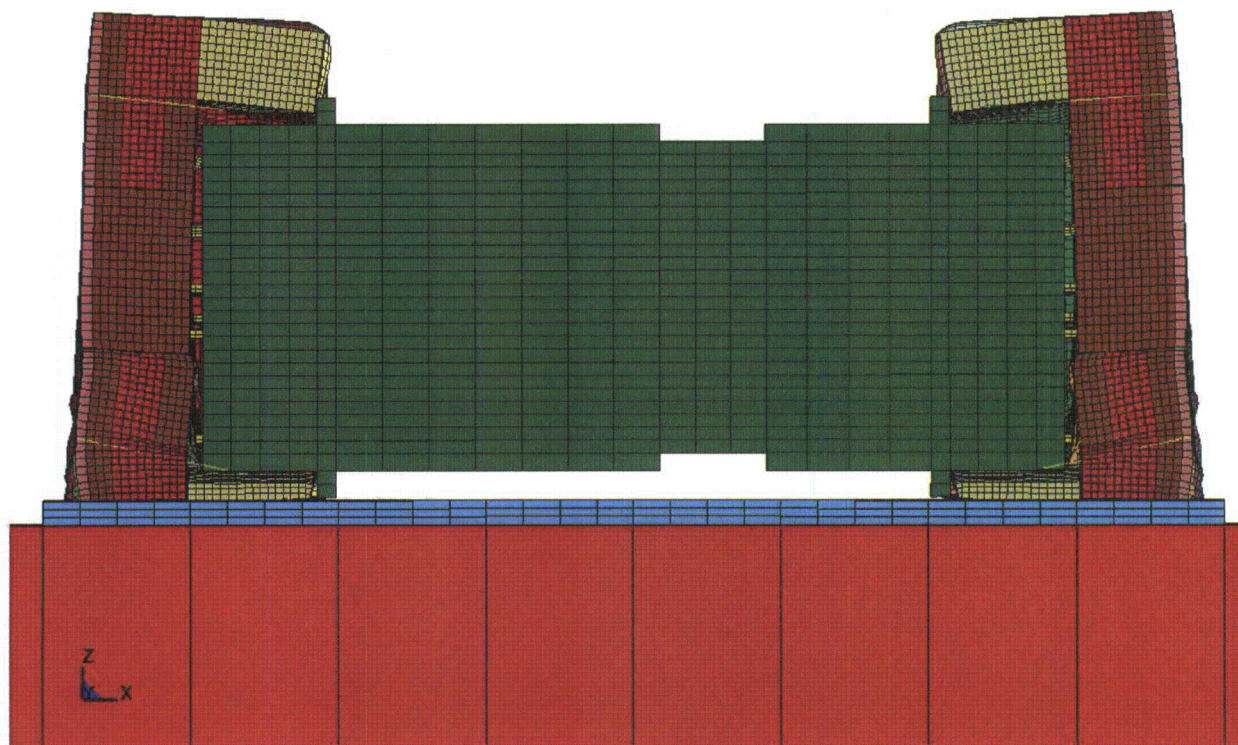


Figure A.2.13.12-39
Plot of Maximum Deformation for 30' Side Drop – Full Scale

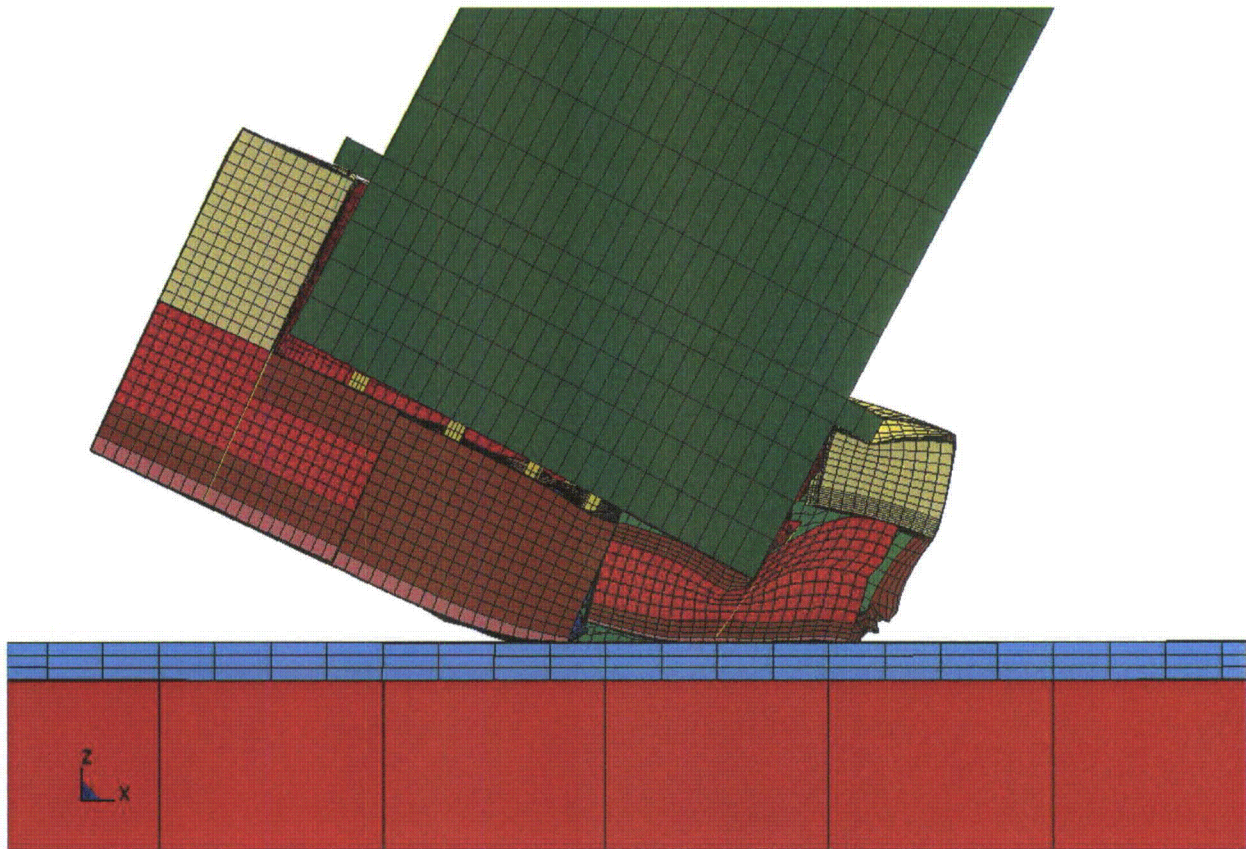


Figure A.2.13.12-40
Plot of Maximum Deformation for 30' CG Over Corner Drop – Full Scale

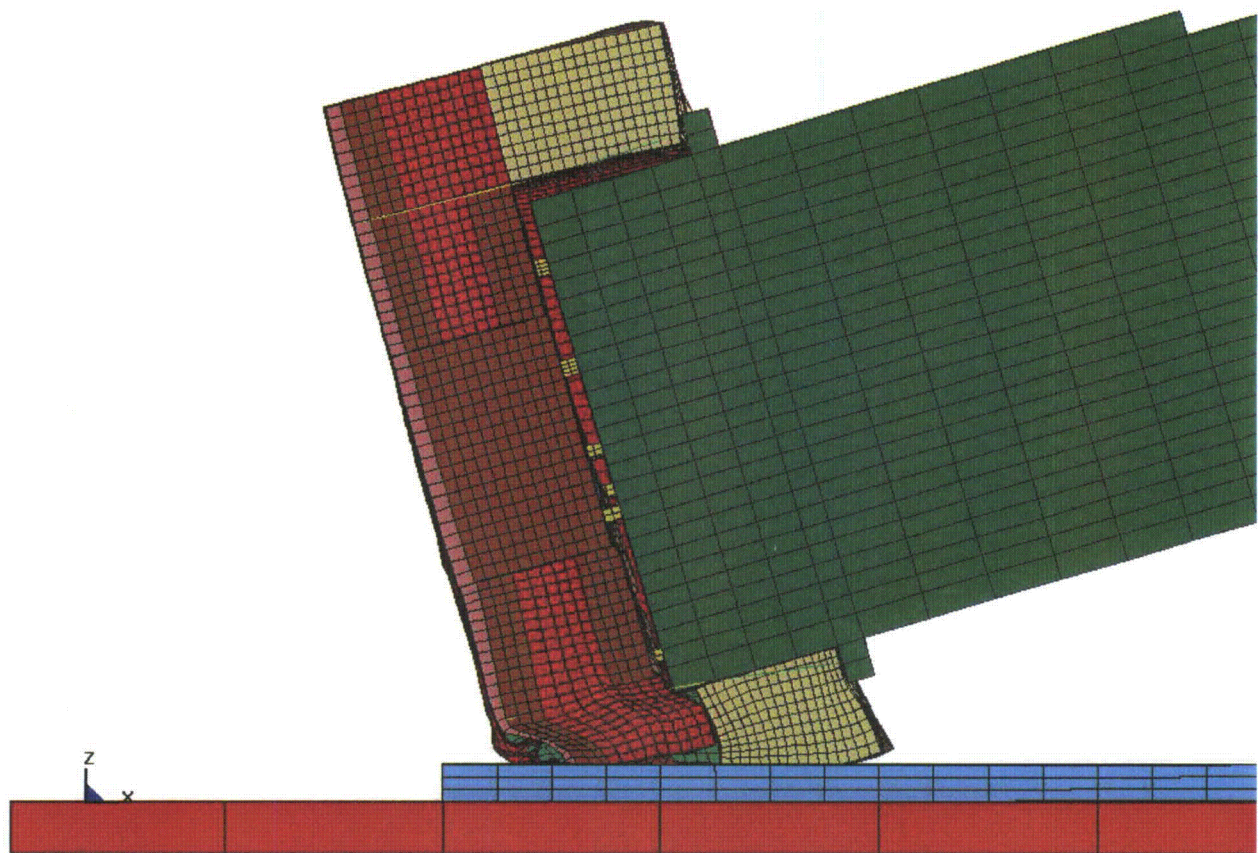


Figure A.2.13.12-41
Plot of Maximum Deformation for 30' 20° Slap Down Drop – Full Scale (First Impact)

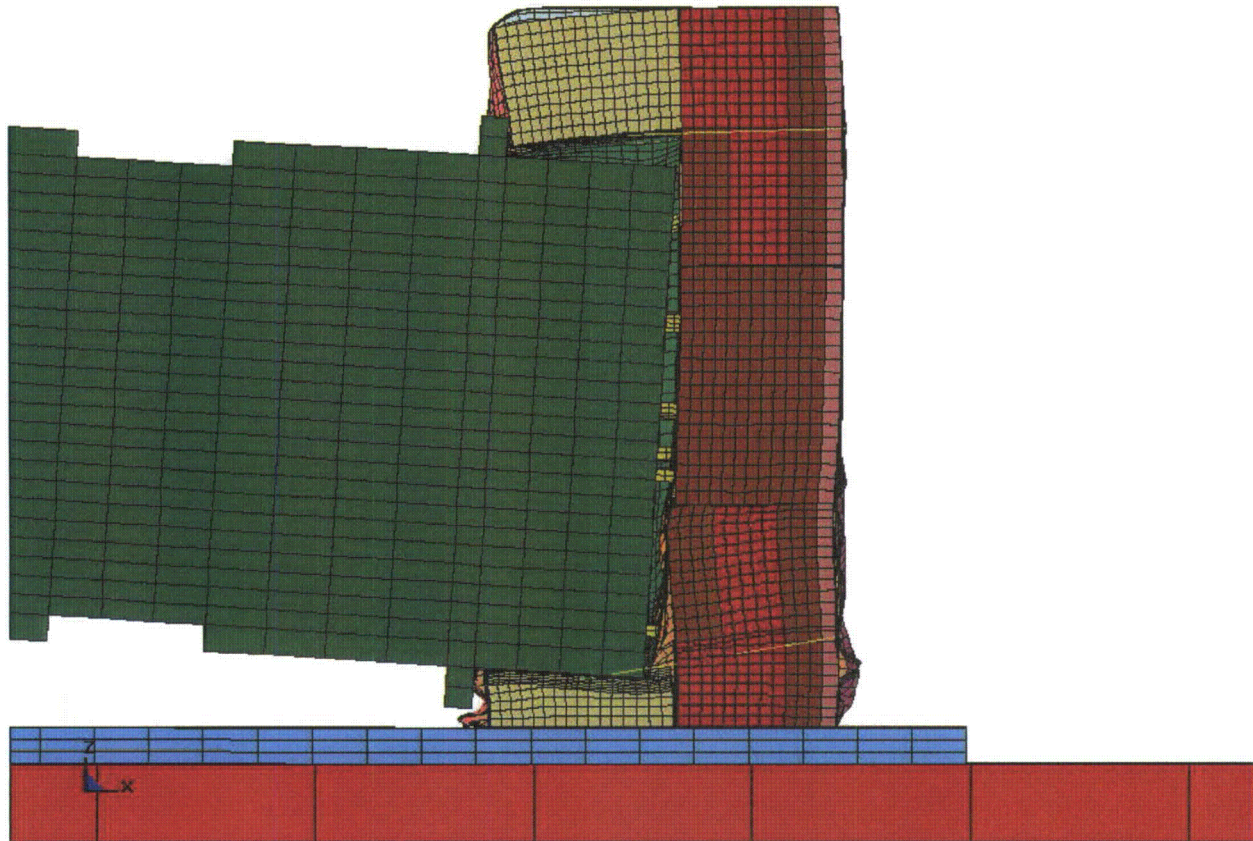


Figure A.2.13.12-42
Plot of Maximum Deformation for 30' 20° Slap Down Drop – Full Scale (Second Impact)

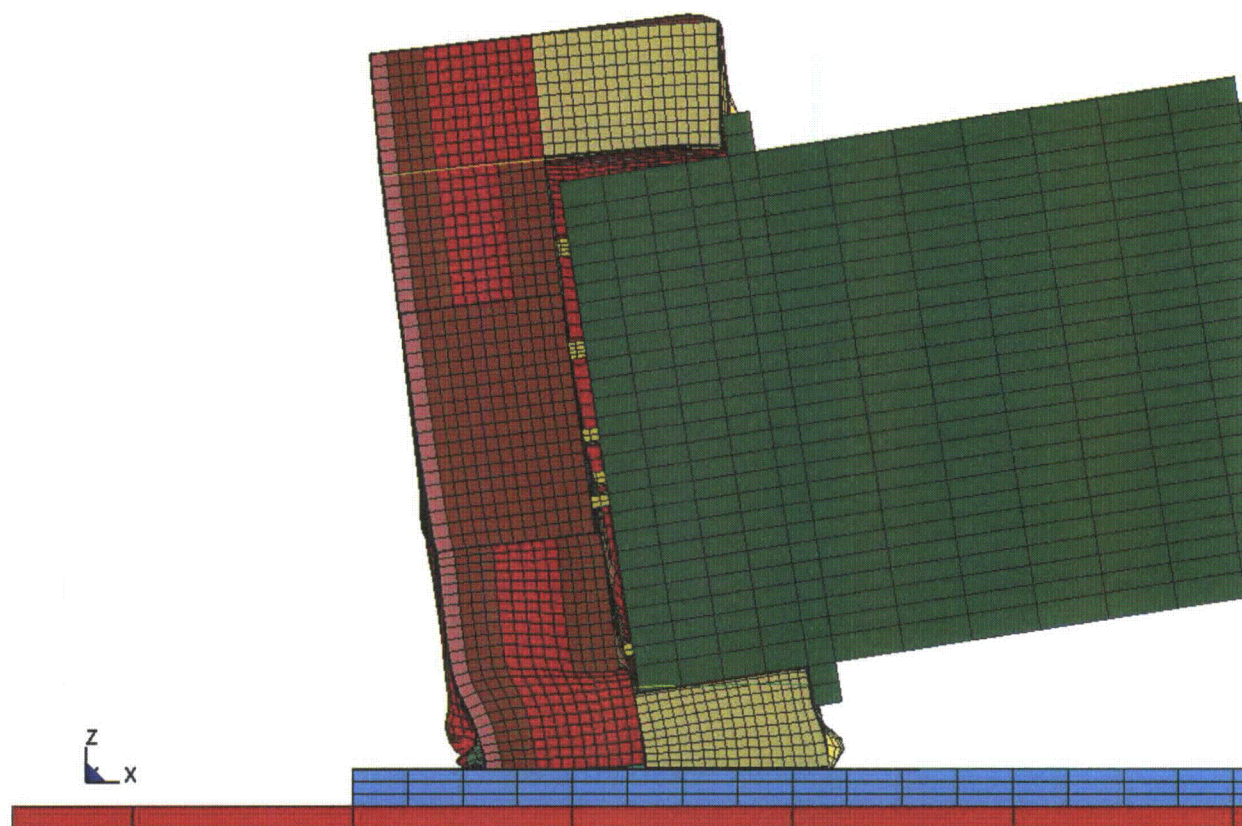


Figure A.2.13.12-43
Plot of Maximum Deformation for 30' 10° Slap Down Drop-Full Scale (First Impact)

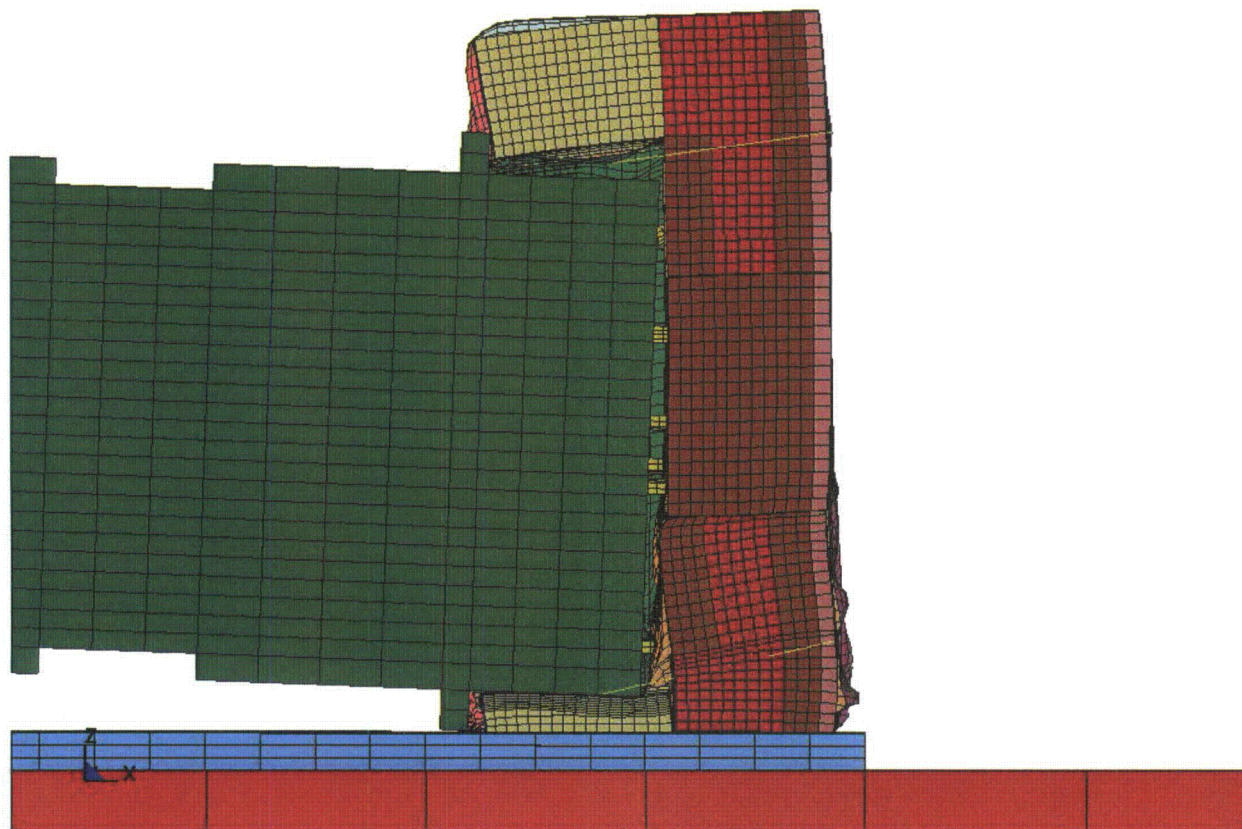


Figure A.2.13.12-44
Plot of Maximum Deformation for 30' 10° Slap Down Drop—Full Scale (Second Impact)

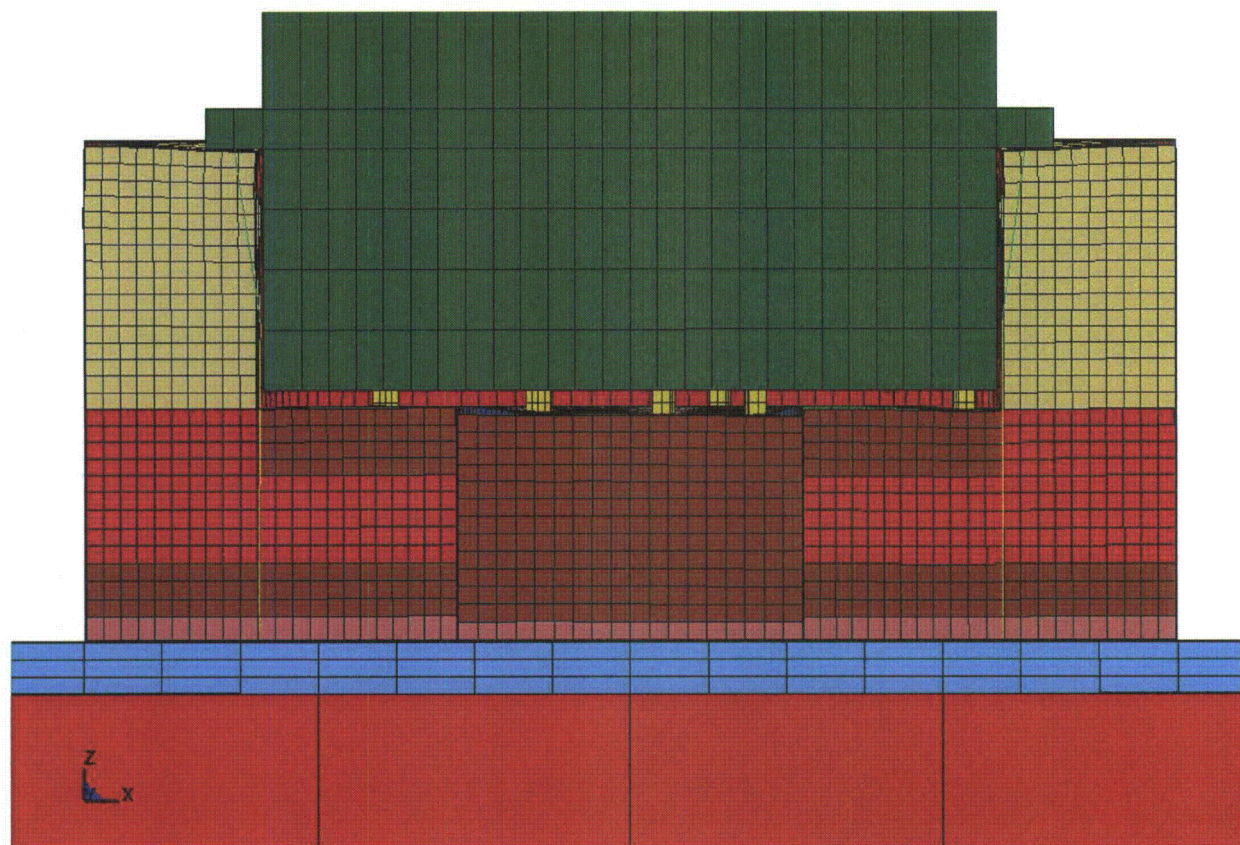


Figure A.2.13.12-45
Plot of Maximum Deformation for 1 Foot Normal Condition End Drop – Full Scale

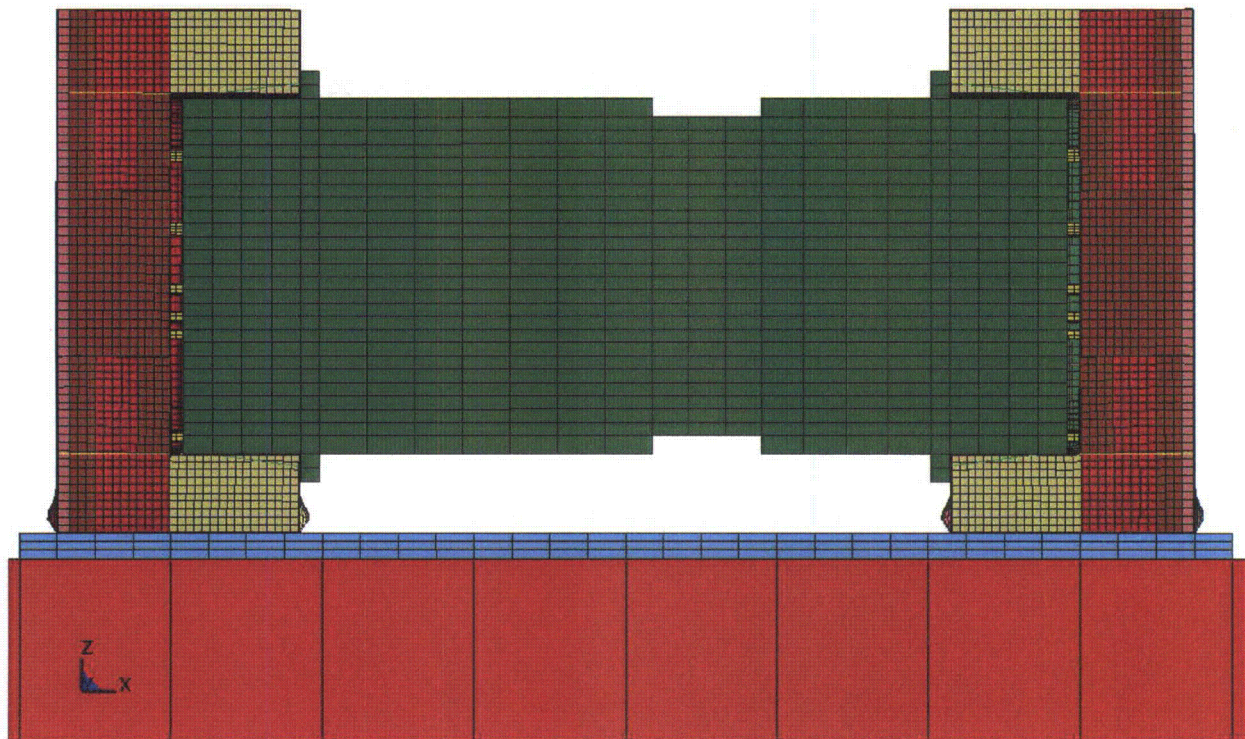


Figure A.2.13.12-46
Plot of Maximum Deformation for 1 Foot Normal Condition Side Drop – Full Scale

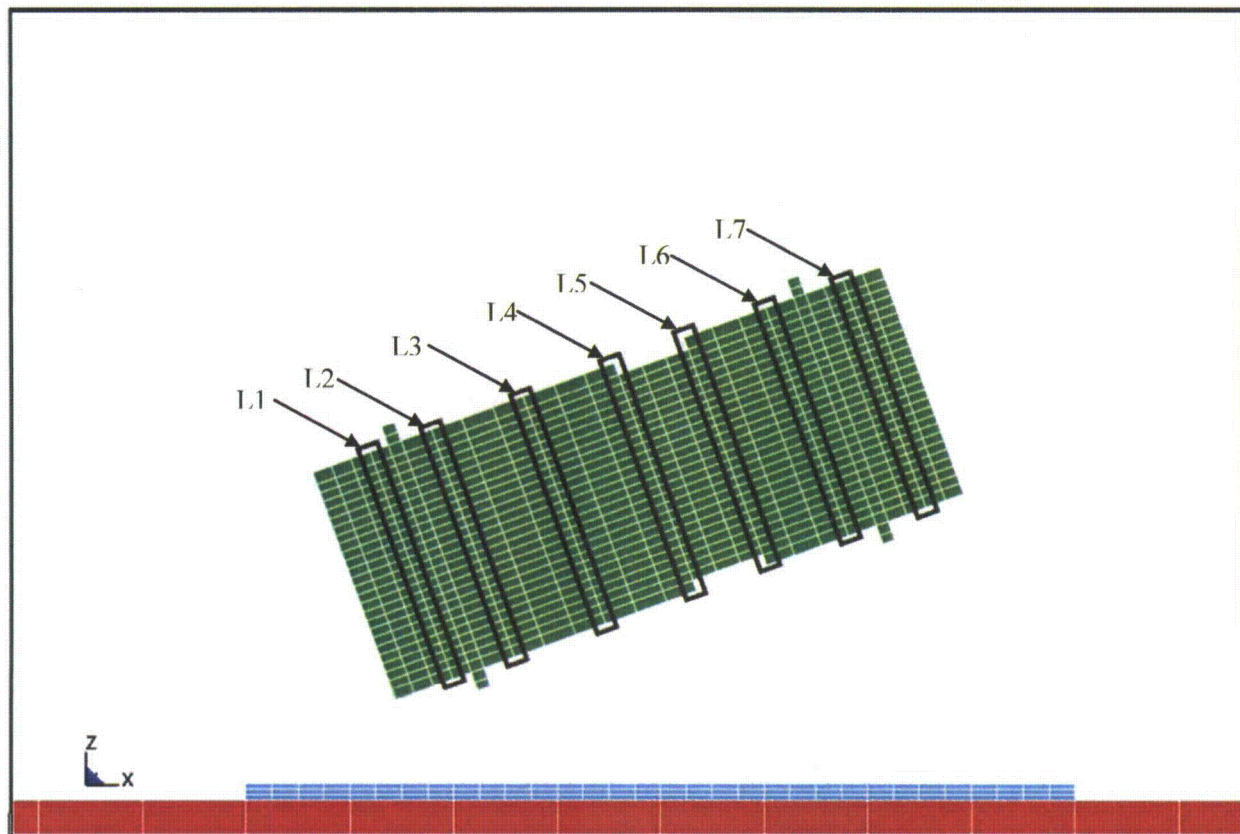


Figure A.2.13.12-47
Locations of Nodes Used to Compute Rotational Acceleration – Full Scale

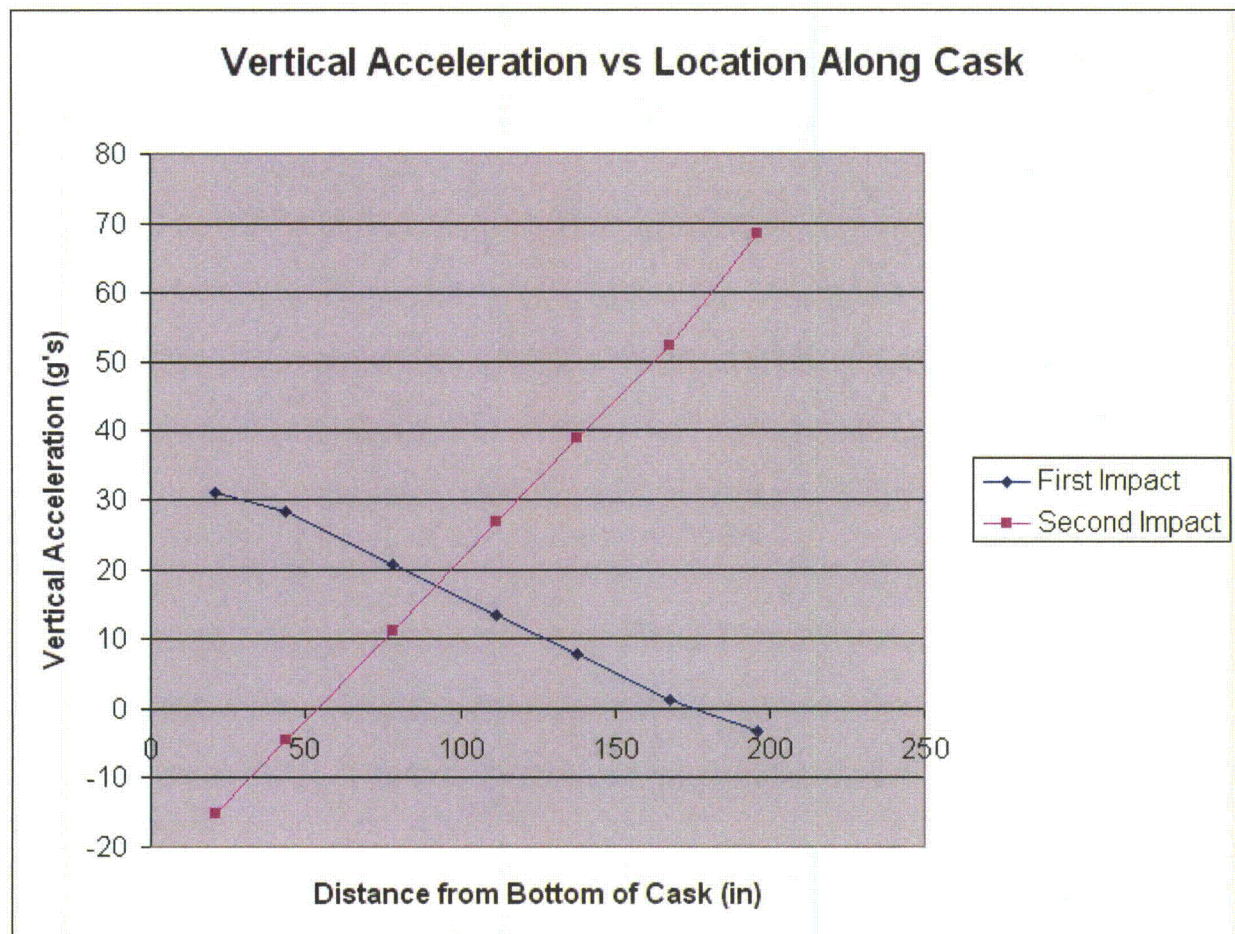


Figure A.2.13.12-48
Vertical Acceleration Along Cask During First And Second Impact to Compute Rotational Acceleration
for 20° Slap Down Drop

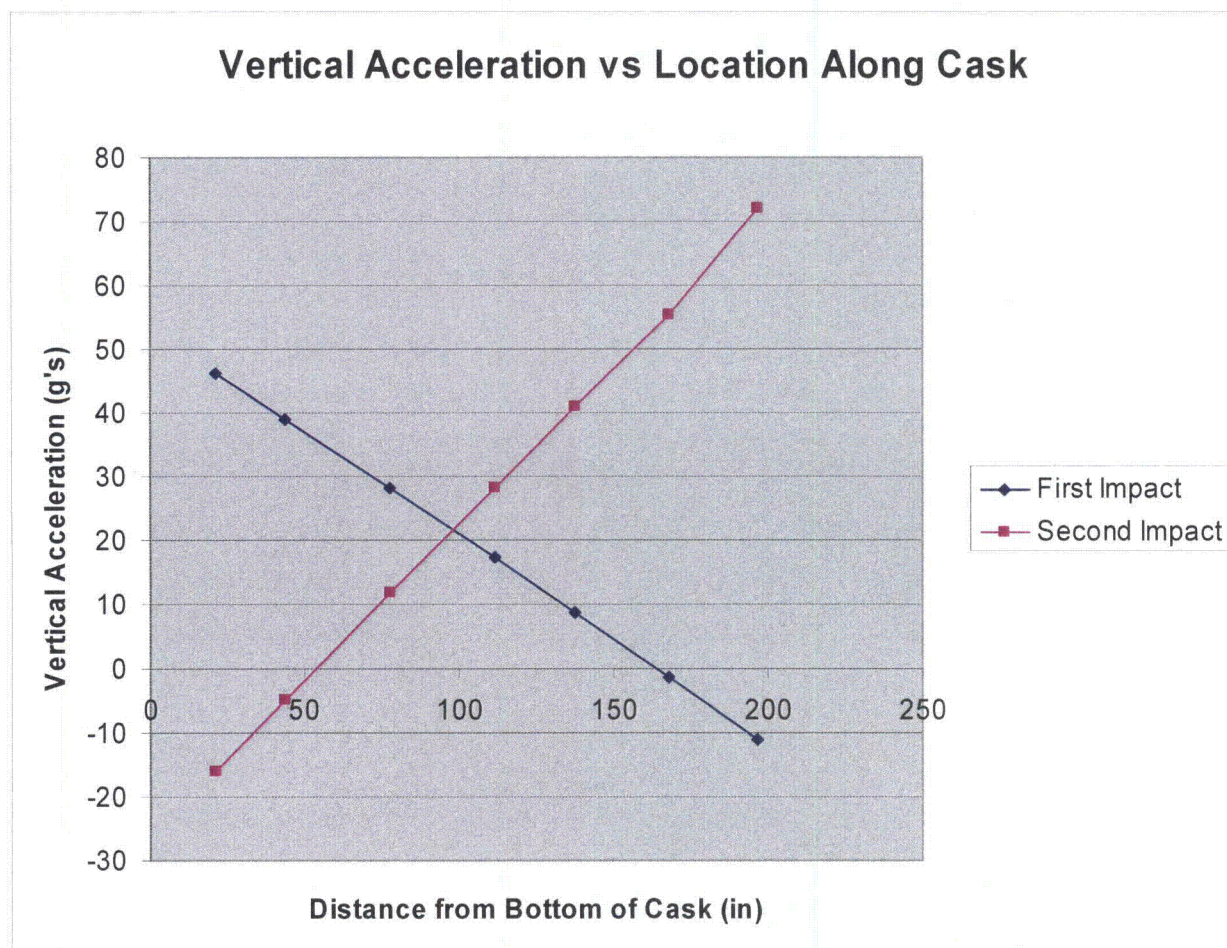


Figure A.2.13.12-49
Vertical Acceleration Along Cask During First And Second Impact to Compute Rotational Acceleration
for 10° Slap Down

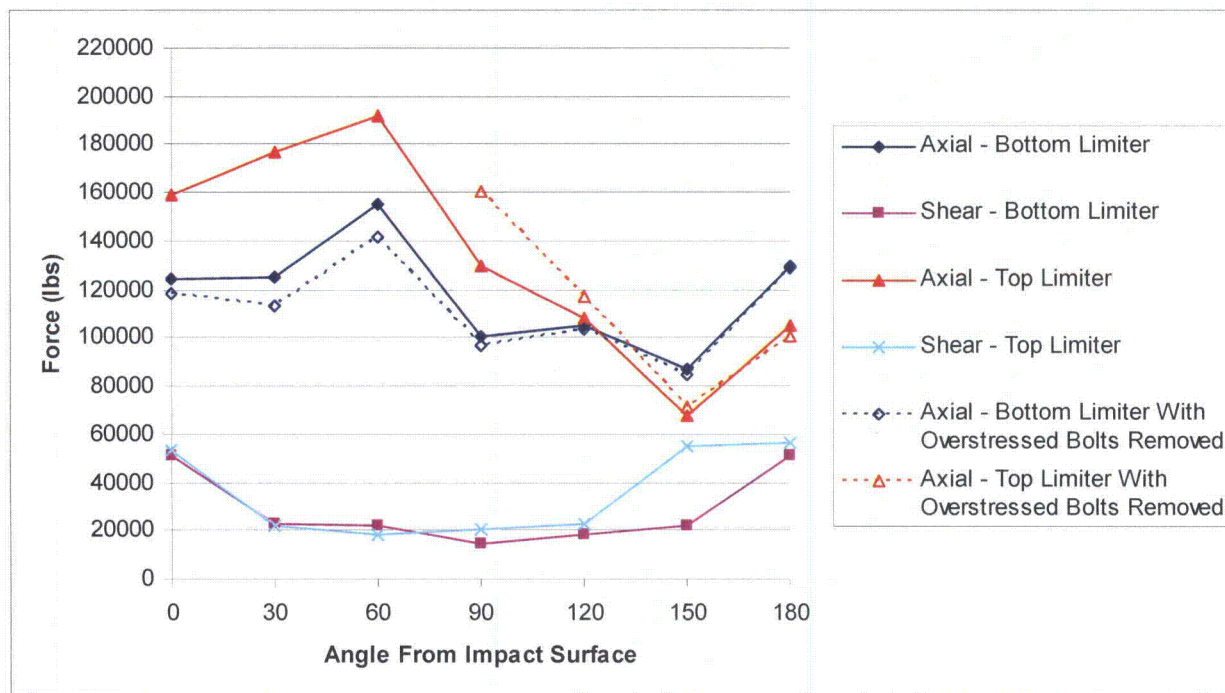


Figure A.2.13.12-50
Bolt Forces Around Top and Bottom Impact Limiters for 20° Slap Down Drop

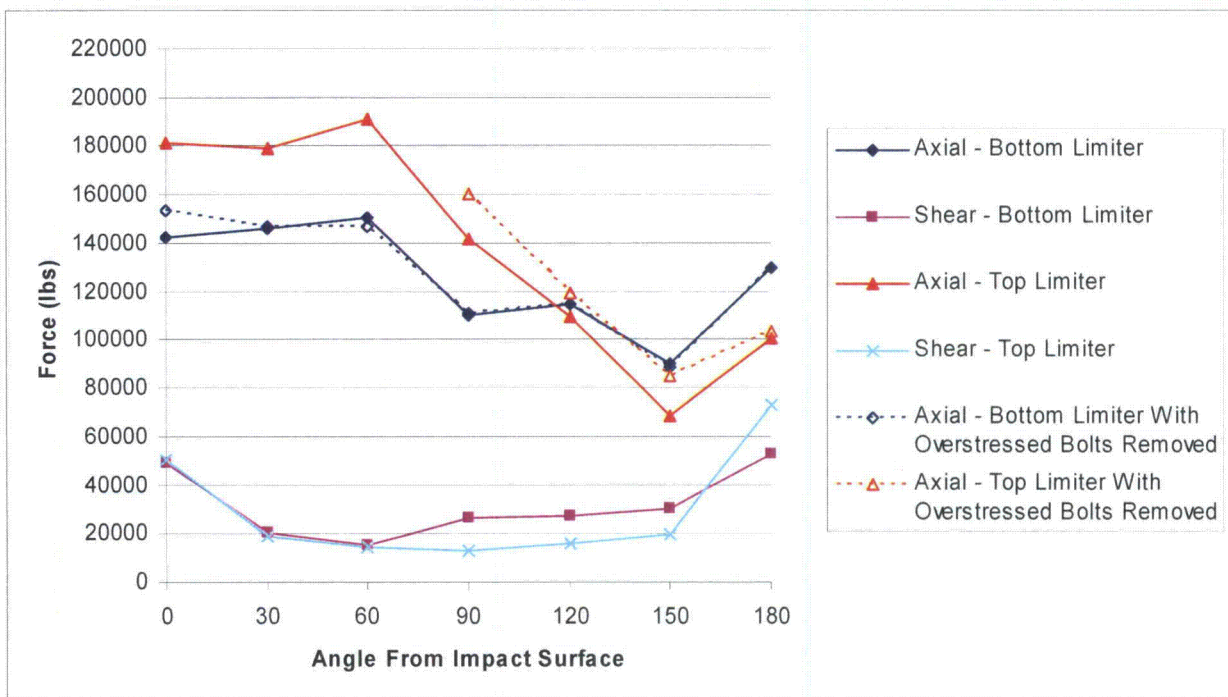


Figure A.2.13.12-51
Bolt Forces Around Top and Bottom Impact Limiters for 10° Slap Down Drop

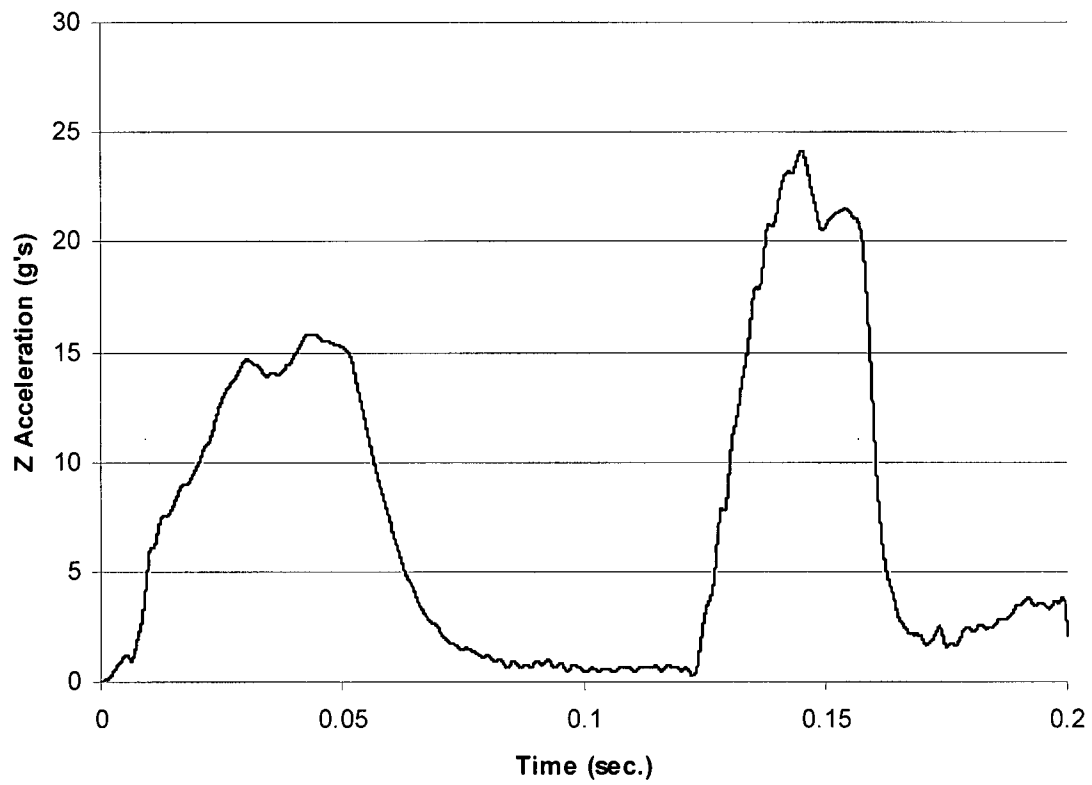


Figure A.2.13.12-52
Cask Rigid Body Resultant Acceleration for 20° Slap Down Drop – Full Scale

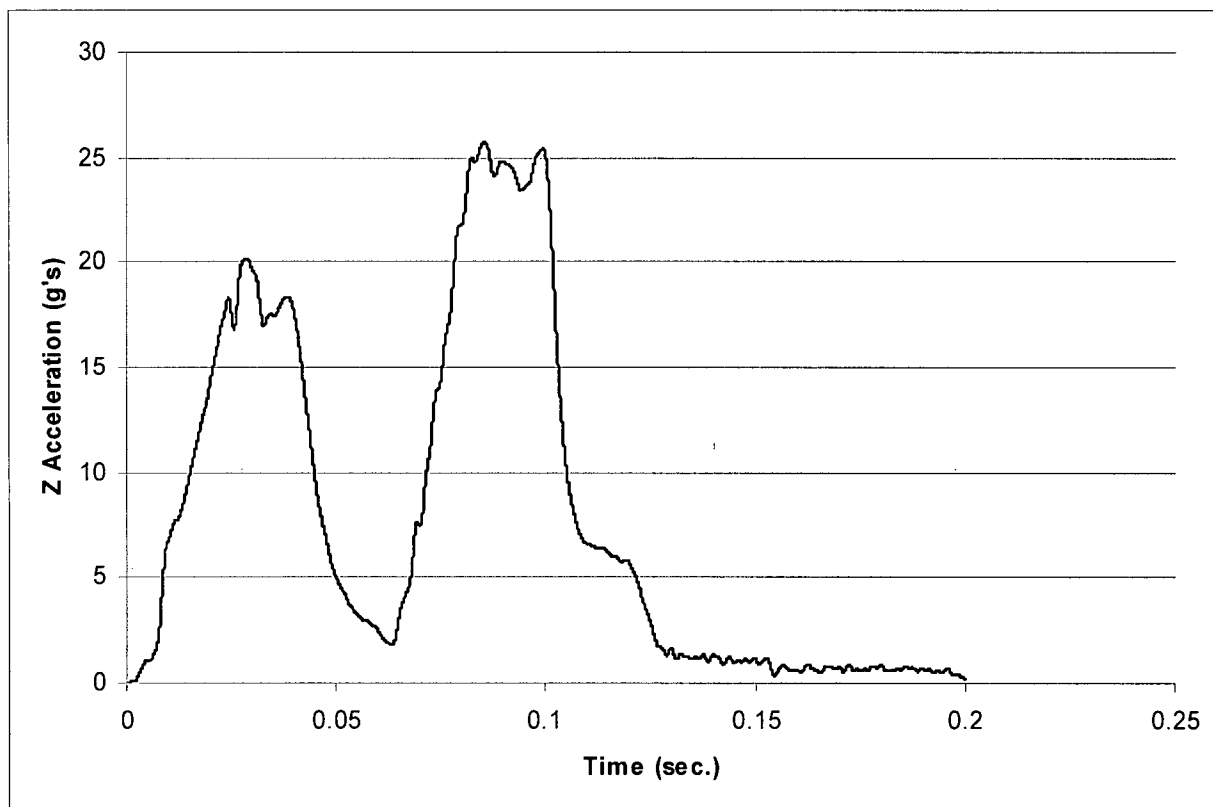


Figure A.2.13.12-53
Cask Rigid Body Resultant Acceleration for 10° Slap Down Drop—Full Scale

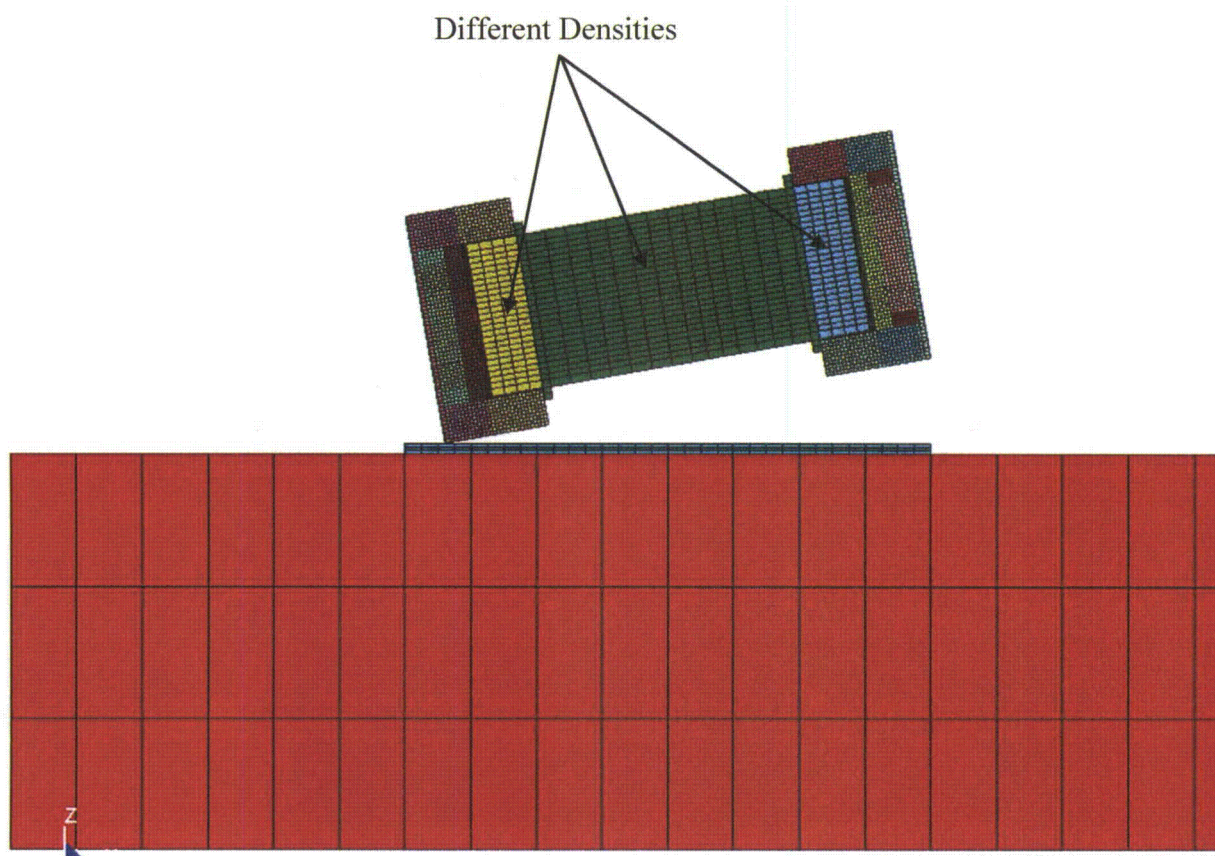


Figure A.2.13.12-54
Overview of New Cask Model with Three Density Sections – Full Scale

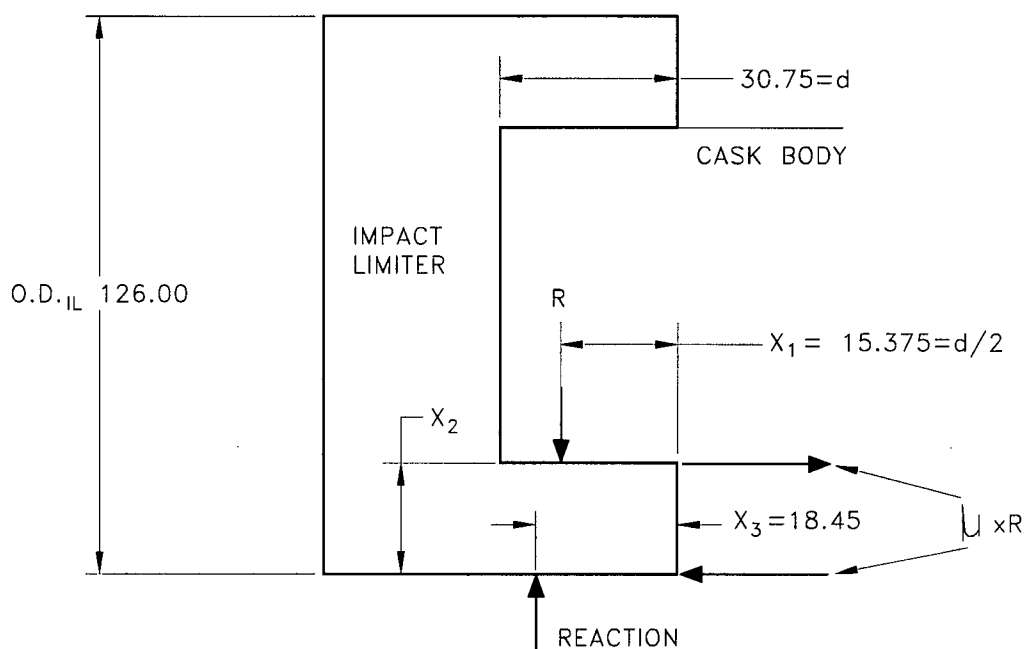


Figure A.2.13.12-55
Free Body Diagram of Top Impact Limiter during Shallow Angle Slap Down Drop

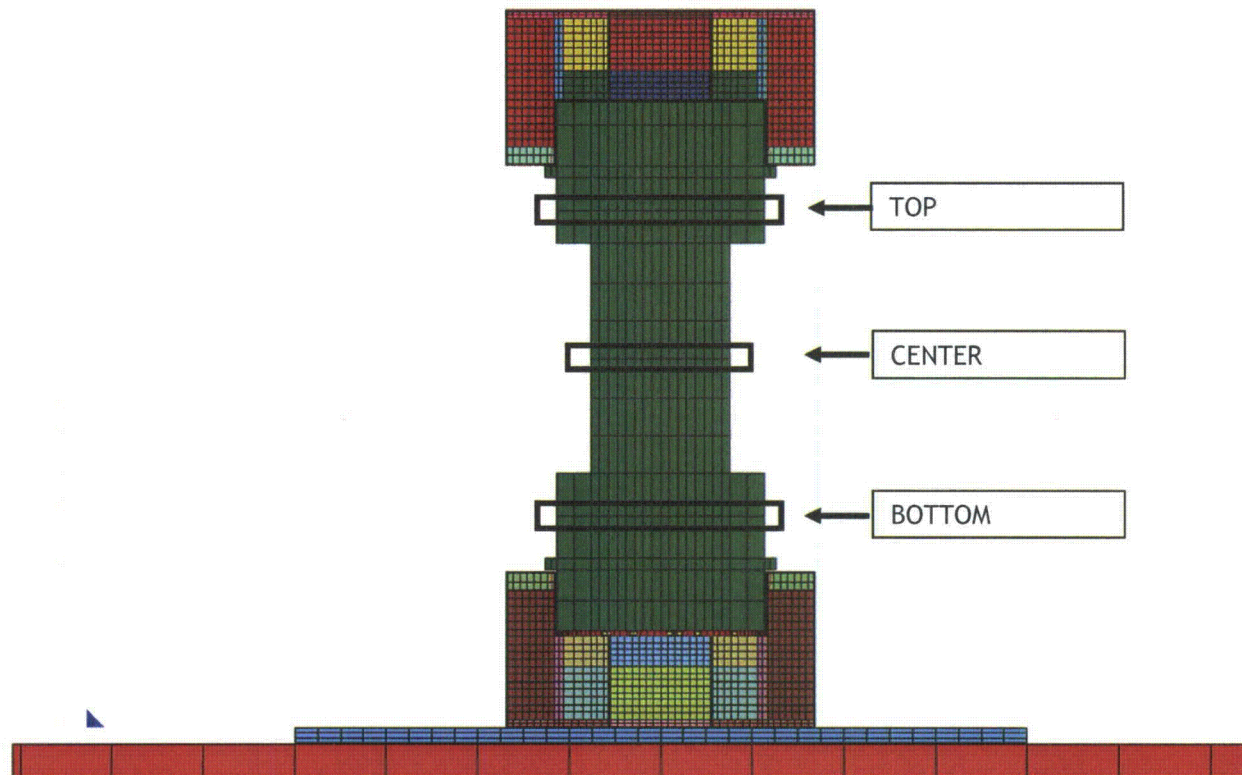


Figure A.2.13.12-56
Location of Nodes Selected to Average Accelerations

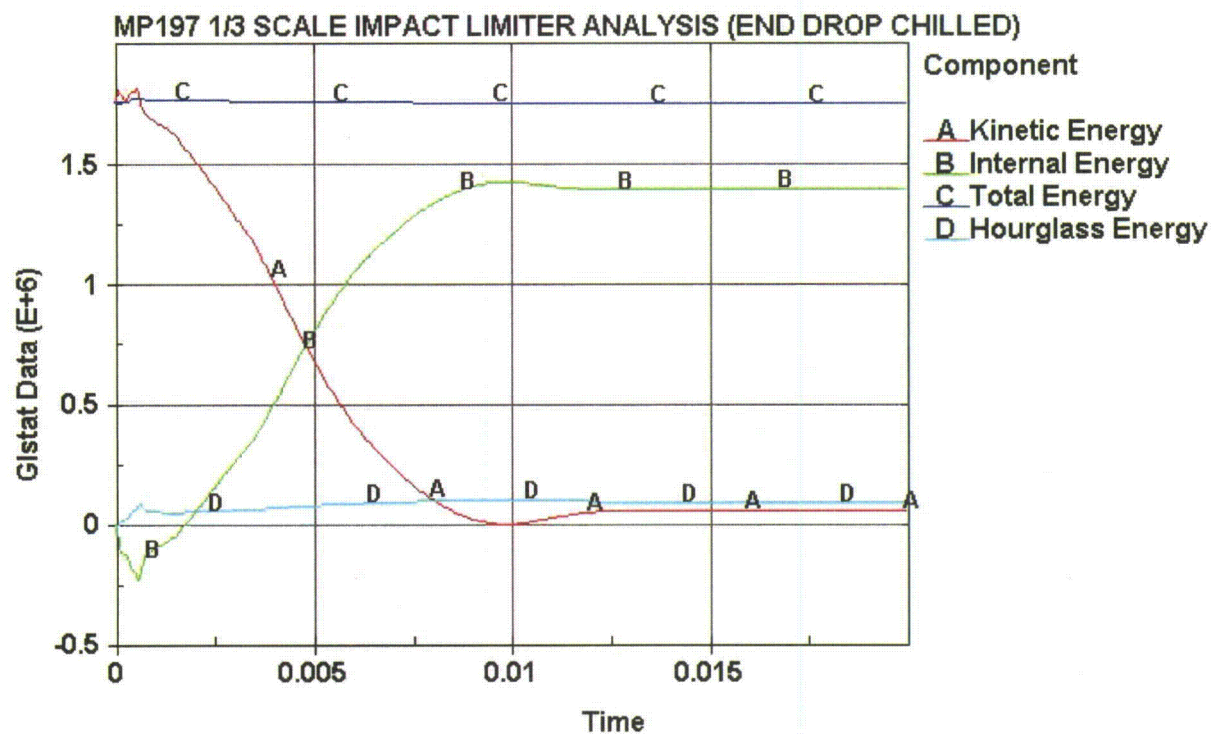


Figure A.2.13.12-57
LS-DYNA Energy Plots (in-lbf) 30' End Drop-1/3 Scale Benchmark Model

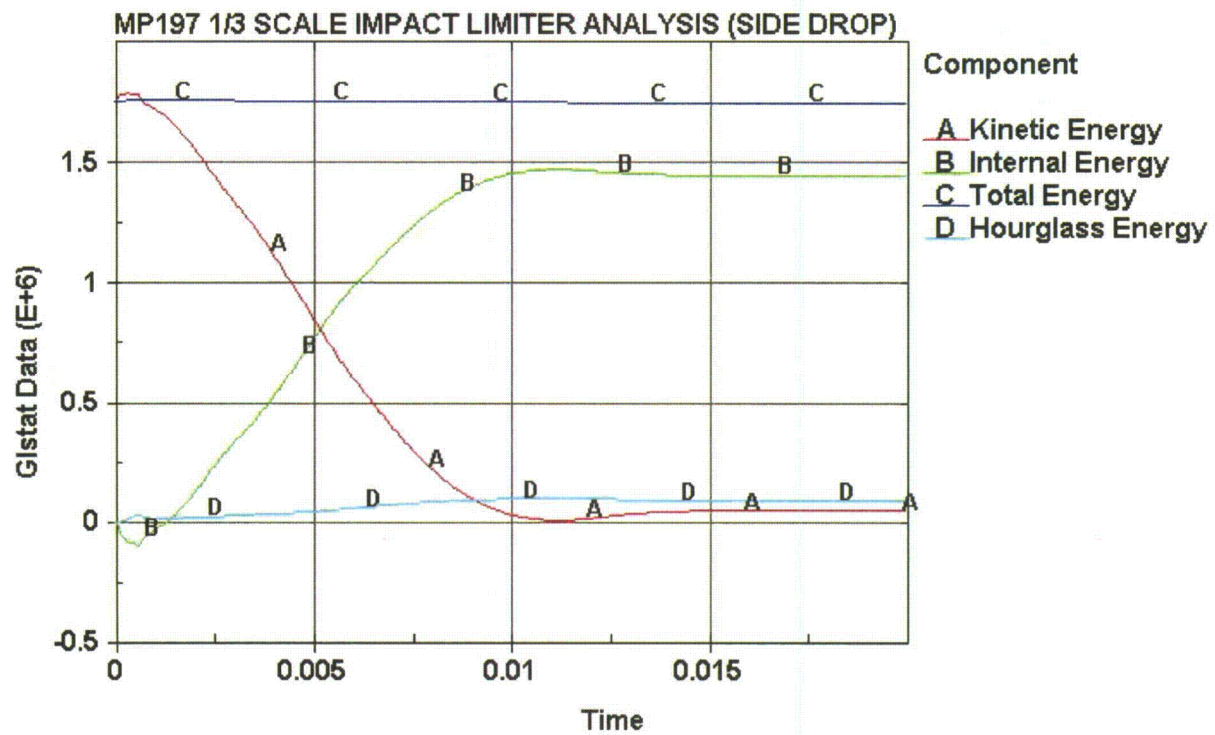


Figure A.2.13.12-58
LS-DYNA Energy Plots (in-lbf) 30' Side Drop—1/3 Scale Benchmark Model

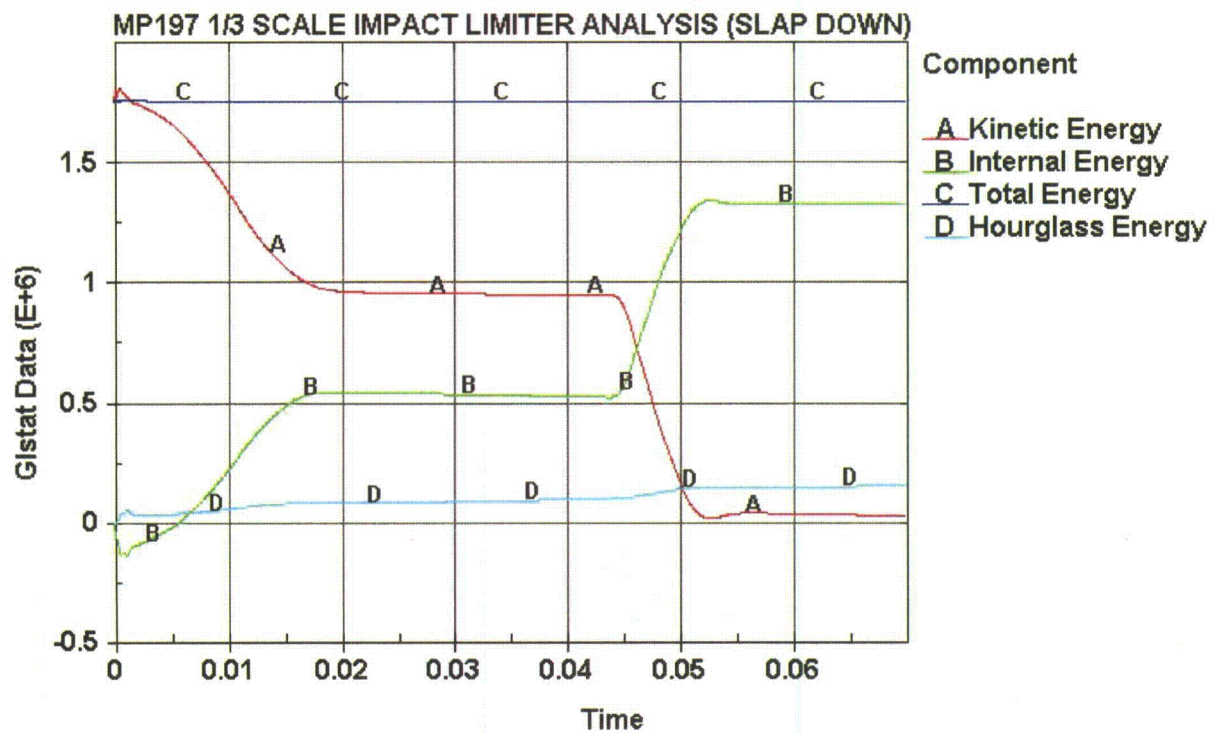


Figure A.2.13.12-59
LS-DYNA Energy Plots (in-lbf) 30' Slap Down-1/3 Scale Benchmark Model

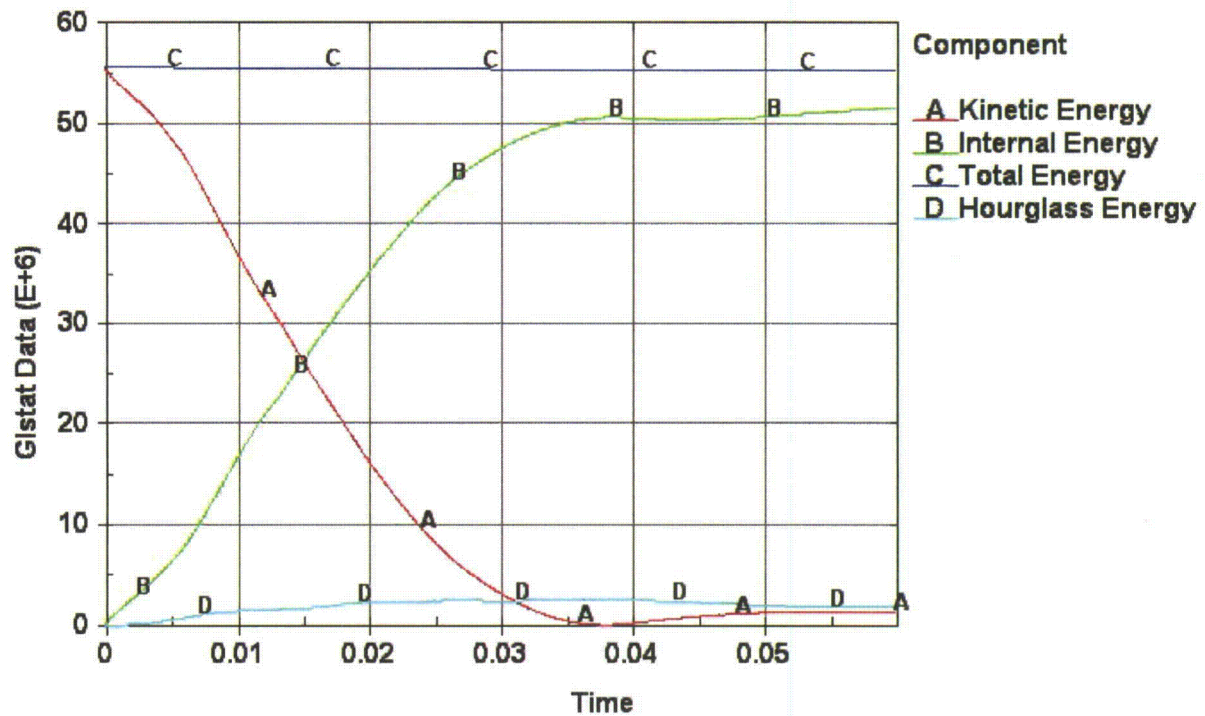


Figure A.2.13.12-60
LS-DYNA Energy (in-lbf) Plots 30' End Drop (Room Temperature)–Full Scale Model

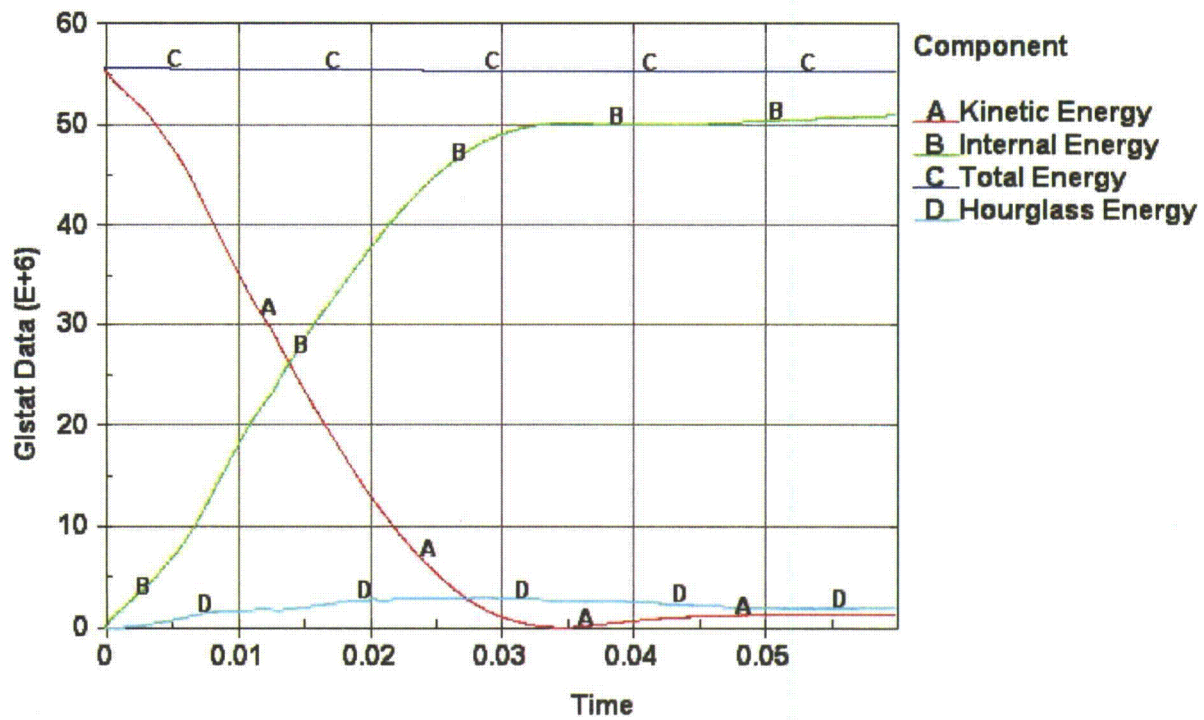


Figure A.2.13.12-61
LS-DYNA Energy (in-lbf) Plots 30' End Drop (-20 °F) -Full Scale Model

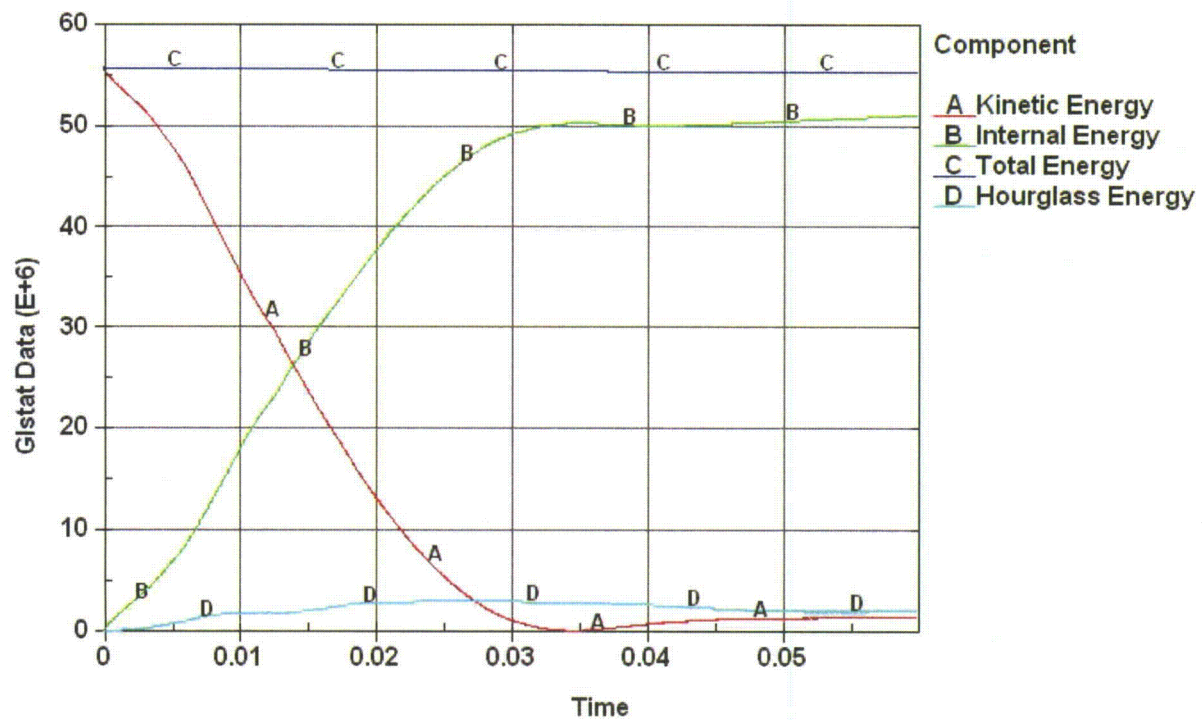


Figure A.2.13.12-62
LS-DYNA Energy (in-lbf) Plots 30' End Drop (-40 °F)–Full Scale Model

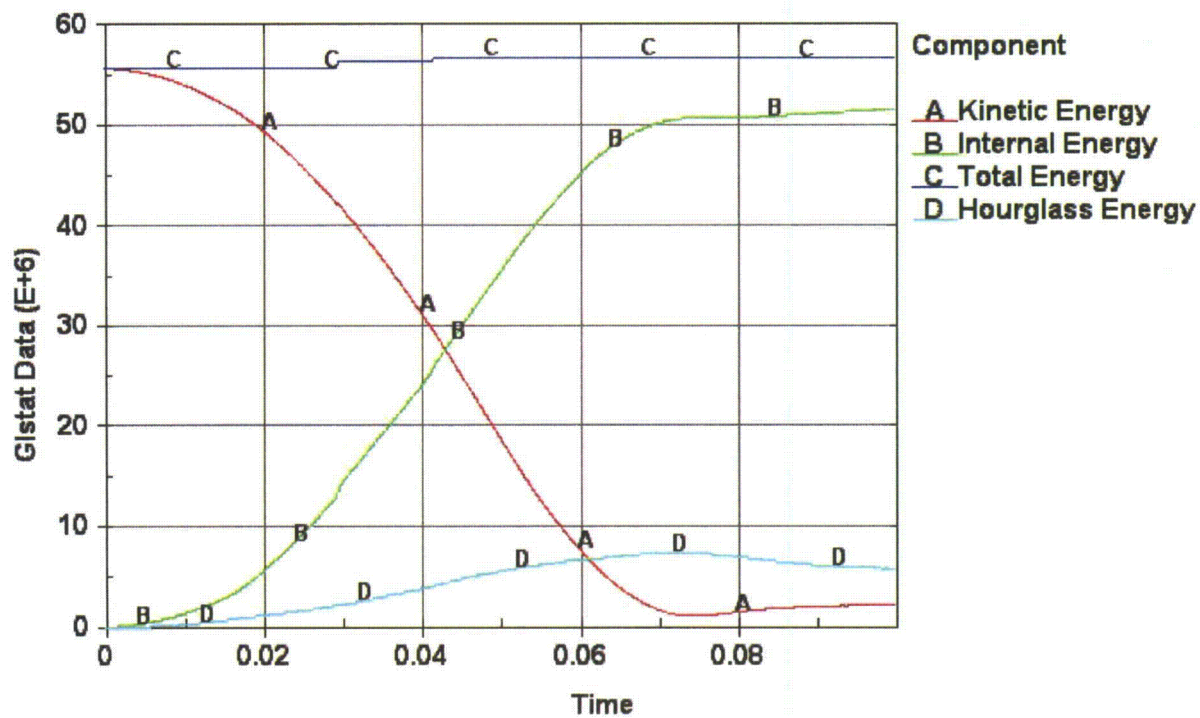


Figure A.2.13.12-63
LS-DYNA Energy (in-lbf) Plots 30' CG Over Corner-Full Scale Model

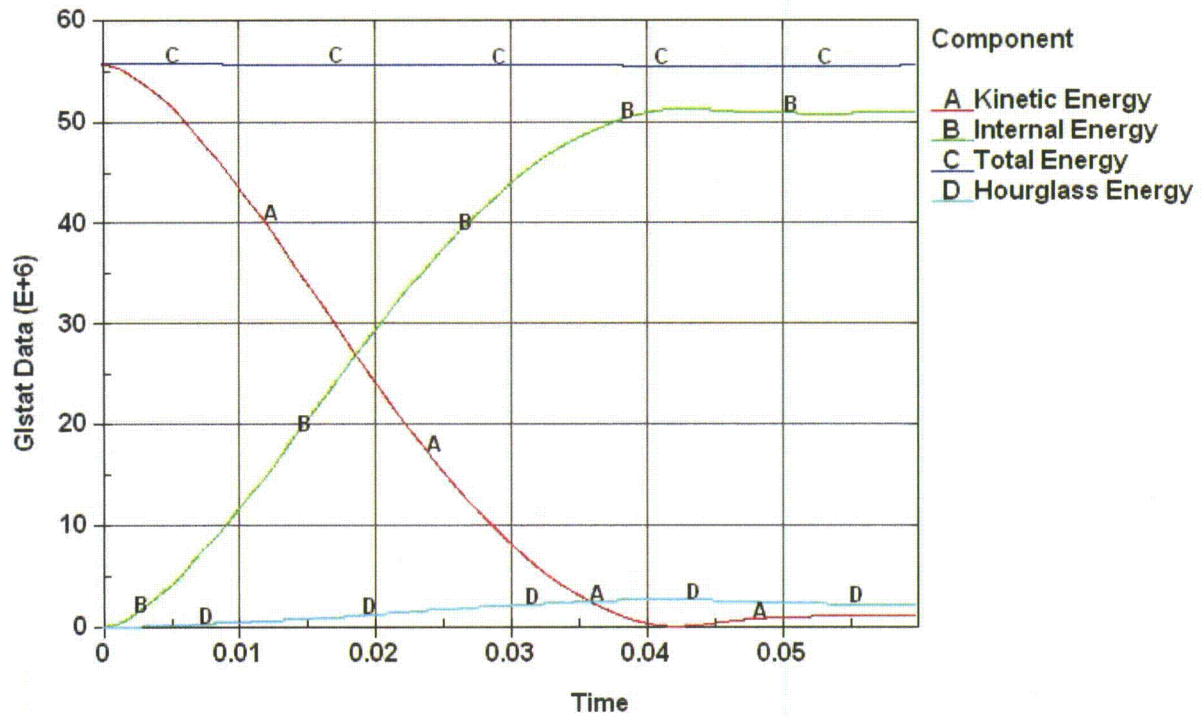


Figure A.2.13.12-64
LS-DYNA Energy (in-lbf) Plots 30' Side Drop-Full Scale Model

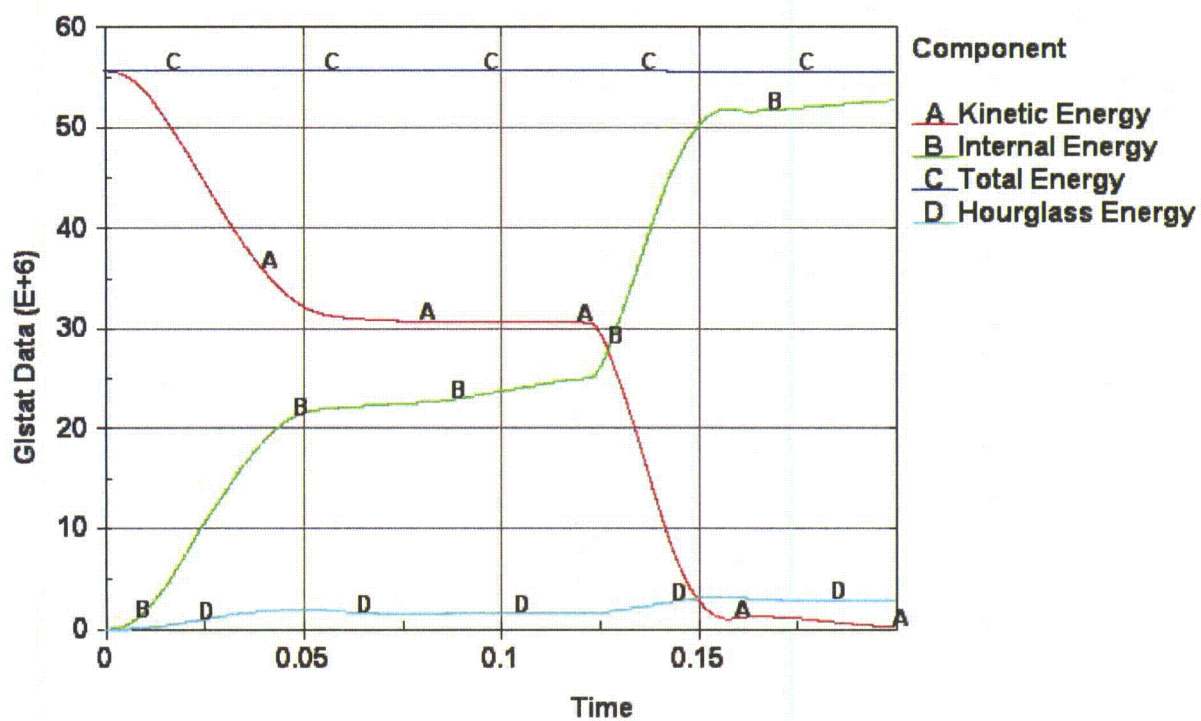


Figure A.2.13.12-65
LS-DYNA Energy (in-lbf) Plots 30' Side Drop Slap Down 20°-Full Scale Model

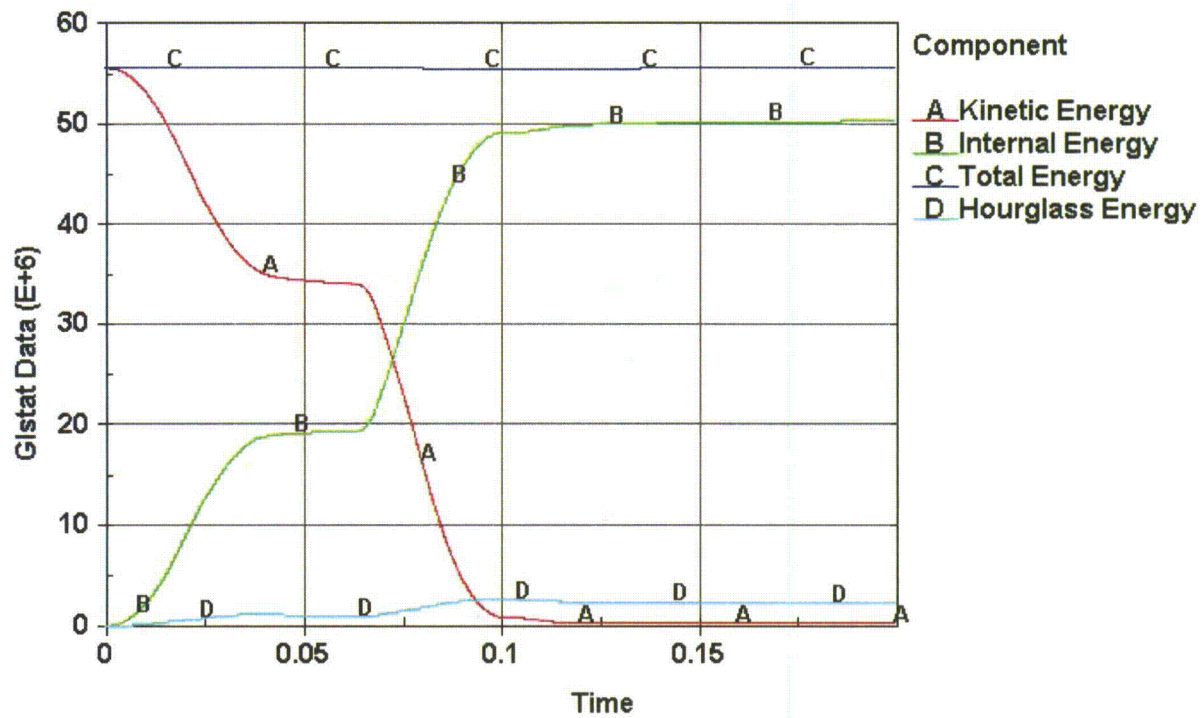


Figure A.2.13.12-66
LS-DYNA Energy (in-lbf) Plots 30' Side Drop Slap Down 10° -Full Scale Model

Appendix A.2.13.13 MP197HB ASME Code Alternatives

CONTENTS

A.2.13.13.1 Introduction.....	A.2.13.13-1
A.2.13.13.2 References.....	A.2.13.13-2

LIST OF TABLES

Table A.2.13.13-1	ASME Code Alternatives for the NUHOMS [®] - MP197HB Cask Containment Boundary	A.2.13.13-3
Table A.2.13.13-2	Alternatives to the ASME Code for the NUHOMS [®] - 24PT4 DSC Confinement Boundary	A.2.13.13-4
Table A.2.13.13-3	Alternatives to the ASME Code for the NUHOMS [®] - 24PT4 DSC Basket Assembly	A.2.13.13-5
Table A.2.13.13-4	Alternatives to the ASME Code for the NUHOMS [®] - 32PT DSC Confinement Boundary	A.2.13.13-6
Table A.2.13.13-5	Alternatives to the ASME Code Exceptions for the NUHOMS [®] -32PT DSC Basket Assembly	A.2.13.13-8
Table A.2.13.13-6	Alternatives to the ASME Code for the NUHOMS [®] - 24PTH DSC Confinement Boundary	A.2.13.13-9
Table A.2.13.13-7	Alternatives to the ASME Code for the NUHOMS [®] - 24PTH DSC Basket Assembly	A.2.13.13-11
Table A.2.13.13-8	Alternatives to the ASME Code for the NUHOMS [®] - 32PTH DSC Confinement Boundary	A.2.13.13-13
Table A.2.13.13-9	Alternatives to the ASME Code for the NUHOMS [®] - 32PTH DSC Basket Assembly	A.2.13.13-15
Table A.2.13.13-10	Alternatives to the ASME Code for the NUHOMS [®] - 32PTH Type 1 DSC Confinement Boundary	A.2.13.13-16
Table A.2.13.13-11	Alternatives to the ASME Code for the NUHOMS [®] - 32PTH Type 1 DSC Basket Assembly	A.2.13.13-18
Table A.2.13.13-12	Alternatives to the ASME Code for the NUHOMS [®] - 32PTH1 DSC Confinement Boundary	A.2.13.13-20
Table A.2.13.13-13	Alternatives to the ASME Code for the NUHOMS [®] - 32PTH1 DSC Basket Assembly	A.2.13.13-22
Table A.2.13.13-14	Alternatives to the ASME Code for the NUHOMS [®] - 37PTH DSC Confinement Boundary	A.2.13.13-24
Table A.2.13.13-15	Alternatives to the ASME Code for the NUHOMS [®] - 37PTH DSC Basket Assembly	A.2.13.13-26
Table A.2.13.13-16	ASME Code Alternatives for the NUHOMS [®] -61BT DSC Confinement Boundary	A.2.13.13-27
Table A.2.13.13-17	ASME Code Alternatives for the NUHOMS [®] -61BT DSC Basket	A.2.13.13-28
Table A.2.13.13-18	ASME Code Alternatives for the NUHOMS [®] -61BTH DSC Confinement Boundary	A.2.13.13-29

Table A.2.13.13-19	ASME Code Alternatives for the NUHOMS [®] -61BTH DSC Basket.....	A.2.13.13-31
Table A.2.13.13-20	ASME Code Alternatives for the NUHOMS [®] -69BTH DSC Confinement Boundary	A.2.13.13-32
Table A.2.13.13-21	ASME Code Alternatives for the NUHOMS [®] -69BTH DSC Basket.....	A.2.13.13-34

Appendix A.2.13.13

MP197HB ASME Code Alternatives

NOTE: References in this Appendix are shown as [1], [2], etc. and refer to the reference list in Section A.2.13.13.2.

A.2.13.13.1 Introduction

This appendix provides tables which describe the ASME Code alternatives proposed for the NUHOMS® MP197HB transport cask and the DSCs allowed as payloads.

A.2.13.13.2 References

1. American Society of Mechanical Engineers, ASME Boiler and Pressure Vessel Code, Section II, Section III, and Appendices, see Chapter A.2, Section A.2.1.2.1 for applicable editions.
2. 10 CFR PART 71, Packaging and Transportation of Radioactive Material.
3. Cases of ASME Boiler and Pressure Vessel Code, N-595-1 and N-595-2.
4. 10 CFR Part 72, "Licensing Requirements for the Independent Storage of Spent Nuclear Fuel, High-Level Radioactive Waste, and Reactor-Related Greater Than Class C Waste."
5. AWS D1.3-98, "Structural Welding Code Steel."
6. ANSI N14.5-1997, "Leakage Tests on Packages for Shipment."
7. Interim Staff Guidance - 15, Rev. 0, "Materials Evaluation."
8. 49 CFR Part 173, Shippers — General Requirements for Shipments and Packaging
9. SNT-TC-1A, "American Society for Nondestructive Testing, Personnel Qualification and Certification in Nondestructive Testing."
10. *Regulatory Guide 7.11, "Fracture Toughness Criteria of Base Material for Ferritic Steel Shipping Cask Containment Vessels with a Maximum Wall Thickness of 4 Inches (0.1m)," June 1991.*
11. *Regulatory Guide 7.12, "Fracture Toughness Criteria of Base Material for Ferritic Steel Shipping Cask Containment Vessels with a Maximum Wall Thickness Greater than 4 Inches (0.1m) But not Exceeding 12 Inches (0.3m)," June 1991.*

Table A.2.13.13-1
ASME Code Alternatives for the NUHOMS®-MP197HB Cask Containment Boundary

Reference ASME Code Section/Article	Code Requirement	Exception, Justification & Compensatory Measures
NCA	All	Not compliant with NCA [1].
NB-1100	Requirements for Code Stamping of Components.	The NUHOMS®-MP197HB cask containment boundary is designed & fabricated in accordance with the ASME Code, Section III, Subsection NB [1] to the maximum extent practical. However, Code Stamping is not required. As Code Stamping is not required, the fabricator is not required to hold an ASME "N" or "NPT" stamp, or to be ASME Certified.
NB-1131	The design specification shall define the boundary of a component to which other components are attached.	A code design specification is not prepared for the NUHOMS®-MP197HB cask. A TN design criteria is prepared in accordance with TN's QA program.
NB-2130 NB-4121	Material must be supplied by ASME approved material suppliers. Material Certification by Certificate Holder.	All materials designated as ASME on the SAR drawings are certified to meet all ASME Code criteria but is not eligible for certification or Code Stamping if a non-ASME fabricator is used. As the fabricator is not required to be ASME certified, material certification to NB-2130 is not possible. Material traceability & certification are maintained in accordance with TN's NRC approved QA program.
NB-7000	Overpressure Protection.	No overpressure protection is provided for the NUHOMS®-MP197HB cask. The function of the NUHOMS®-MP197HB cask is to contain radioactive materials under normal, off-normal, and hypothetical accident conditions postulated to occur during transportation. The NUHOMS®-MP197HB cask is designed to withstand the maximum internal pressure considering 100% fuel rod failure at maximum accident temperature. The NUHOMS®-MP197HB cask is pressure tested in accordance with the requirements of 10CFR71 [2] and TN's approved QA program.
NB-8000	Requirements for nameplates, stamping & reports per NCA-8000.	The NUHOMS®-MP197HB cask nameplates provide the information required by 10CFR71 and 49CFR173 [8] as appropriate. Code stamping is not required for the NUHOMS®-MP197HB cask. QA Data packages are prepared in accordance with the requirements of 10CFR71 and TN's approved QA program.
NB-3122.1	No structural strength shall be attributed to cladding	<i>The thickness of the weld overlay/cladding is included in the analytical models described in Chapter A.2 to calculate the behavior of the MP197HB cask for NCT and HAC loading conditions. Weld overlay/cladding will meet the normal ASME Code weld qualification requirements. In addition, a testing program to demonstrate that the weld overlay/cladding bond strength is adequate to transmit all loads, and that the HAZ meets the nil ductility requirements of RGs 7.11 [10] and 7.12 [11] will be performed prior to cask fabrication. An annual UT inspection of the weld overlay/cladding surface will also be performed to ensure that the interface bond remains intact.</i>

Table A.2.13.13-1
ASME Code Alternatives for the NUHOMS®-MP197HB Cask Containment Boundary
(Concluded)

<i>Reference ASME Code Section/Article</i>	<i>Code Requirement</i>	<i>Exception, Justification & Compensatory Measures</i>
<i>NB-5221</i>	<i>Volumetric (RT) inspection of CAT. B weld required</i>	<i>Fabrication sequence for inner and outer shells makes RT of 2 closure welds very difficult. May need to use UT or multilayer MT/PT to provide volumetric examination.</i>

Table A.2.13.13-2
Alternatives to the ASME Code for the NUHOMS®-24PT4 DSC Confinement Boundary

Reference ASME Code Section/Article	Code Requirement	Alternative, Justification & Compensatory Measures
NCA	All	Not compliant with NCA [1].
NB-1100	Requirements for Code Stamping of Components.	The DSC shell is designed & fabricated in accordance with the ASME Code, Section III, Subsection NB [1] to the maximum extent practical. However, Code Stamping is not required. As Code Stamping is not required, the fabricator is not required to hold an ASME "N" or "NPT" stamp, or to be ASME Certified.
NB-2130 NB-4121	Material must be supplied by ASME approved material suppliers. Material Certification by Certificate Holder.	All materials designated as ASME on the FSAR drawings are obtained from ASME approved MM or MS supplier(s) with ASME CMTR's. Material is certified to meet all ASME Code criteria but is not eligible for certification or Code Stamping if a non-ASME fabricator is used. As the fabricator is not required to be ASME certified, material certification to NB-2130 is not possible. Material traceability & certification are maintained in accordance with TN's NRC approved QA program.
NB-6111	All completed pressure retaining systems shall be pressure tested.	The shield plug support ring and vent and siphon block are not pressure tested due to the manufacturing sequence. The support ring is not a pressure-retaining item and the siphon block weld is helium leak tested after fuel is loaded and the inner top closure plate installed in accordance with Code Case N-595-1 [3].
NB-7000	Overpressure Protection.	No overpressure protection is provided for the DSC. The function of the DSC is to contain radioactive materials under normal, off-normal and hypothetical accident conditions postulated to occur during transportation and storage. The DSC is designed to withstand the maximum internal pressure considering 100% fuel rod failure at maximum accident temperature. The DSC is pressure tested to 120% of normal operating design pressure. An overpressure protection report is not prepared for the DSC.
NB-8000	Requirements for nameplates, stamping & reports per NCA-8000.	The DSC nameplate provides the information required by 10CFR71 [2], 49CFR173 [8] and 10CFR72 [4] as appropriate. Code stamping is not required for the DSC. In lieu of code stamping, QA Data packages are prepared in accordance with the requirements of 10CFR71, 10CFR72 and TN's approved QA program.

Table A.2.13.13-3
Alternatives to the ASME Code for the NUHOMS®-24PT4 DSC Basket Assembly

Reference ASME Code Section/Article	Code Requirement	Alternative, Justification & Compensatory Measures
NCA	All	Not compliant with NCA [1]. Quality Assurance is provided according to 10 CFR 71 Subpart H in lieu of NCA-4000.
NG/NF-1100	Requirements for Code Stamping of Components.	The DSC baskets are designed & fabricated in accordance with the ASME Code, Section III, Subsection NG/NF [1] to the maximum extent practical as described in the FSAR, but Code Stamping is not required. As Code Stamping is not required, the fabricator is not required to hold an ASME N or NPT stamp or be ASME Certified.
NG/NF-2130 NG/NF-4121	Material must be supplied by ASME approved material suppliers. Material Certification by Certificate Holder.	All materials designated as ASME on the FSAR drawings are obtained from ASME approved MM or MS supplier with ASME CMTR's. Material is certified to meet all ASME Code criteria but is not eligible for certification or Code Stamping if a non-ASME fabricator is used. As the fabricator is not required to be ASME certified, material certification to NG/NF-2130 is not possible. Material traceability & certification are maintained in accordance with TN's NRC approved QA program.
Table NG-3352-1	Permissible Joint Efficiency Factors.	Joint efficiency (quality) factor of 1 is assumed for the guidesleeve longitudinal weld. Table NG-3352-1 permits a quality factor of 0.5 for full penetration weld with visual inspection. Inspection of both faces provides $n = (2 \times 0.5) = 1$. This is justified by thin gauge of material (0.12 inch) with visual examination of both surfaces which ensures that any significant deficiencies would be observed and corrected.
NG/NF-8000	Requirements for nameplates, stamping & reports per NCA-8000.	The DSC nameplate provides the information required by 10CFR71 [2], 49CFR173 [8] and 10CFR72 [4] as appropriate. Code stamping is not required for the DSC. In lieu of code stamping, QA Data packages are prepared in accordance with the requirements of 10CFR71, 10CFR72 and TN's approved QA program.
N/A	N/A.	Oversleeve to guidesleeve welds are non-code welds which meet the requirements of AWS D1.3-98 [5], the Structural Welding Code-Sheet Steel.
NG-3000 / Section II, Part D, Table 2A	Maximum temperature limit for Type 304 plate material is 800°F.	The DSC guidesleeves, oversleeves and failed fuel cans do not comply with ASME Code limit of 800°F for Type 304 steel for the postulated blocked vent accident for approximately 25 hours. The maximum predicted temperature of those components for this event is less than 900°F. In accordance with Table I-14.5 of Article NH, the expected reduction in material strength is small (less than 1 ksi) and the calculated stress ratio is very small.

Table A.2.13.13-4
Alternatives to the ASME Code for the NUHOMS®-32PT DSC Confinement Boundary

Reference ASME Code Section/Article	Code Requirement	Alternatives, Justification & Compensatory Measures
NCA	All.	Not compliant with NCA [1]. Quality Assurance is provided according to 10 CFR 71 Subpart H in lieu of NCA-4000.
NCA-1140	Use of Code editions and addenda.	Code edition and addenda other than those specified in Section A.2.1.2.1 may be used for construction, but in no case earlier than 3 years before that specified in the Table. Materials produced and certified in accordance with ASME Section II [1] material specifications from Code Editions and Addenda other than those specified in Section A.2.1.2.1 may be used as long as the materials meet all the requirements of Article 2000 of the applicable Subsection of the Section III Edition and Addenda used for construction.
NB-1100	Requirements for Code Stamping of Components, Code reports and certificates, etc.	Code Stamping is not required. As Code Stamping is not required, the fabricator is not required to hold an ASME "N" or "NPT" stamp, or to be ASME Certified.
NB-1132	Attachments with a pressure retaining function, including stiffeners, shall be considered part of the component.	Bottom shield plug and outer bottom cover plate are outside code jurisdiction; these components together are much larger than required to provide stiffening for the inner bottom cover plate; the weld that retains the outer bottom cover plate and with it the bottom shield plug is subject to root and final PT examination.
NB-2130	Material must be supplied by ASME approved material suppliers.	Material is certified to meet all ASME Code criteria but is not eligible for certification or Code Stamping if a non-ASME fabricator is used. As the fabricator is not required to be ASME certified, material certification to NB-2130 is not possible. Material traceability and certification are maintained in accordance with TN's NRC approved QA program.
NB-4121	Material Certification by Certificate Holder.	
NB-4243 and NB-5230	Category C weld joints in vessels and similar weld joints in other components shall be full penetration joints. These welds shall be examined by UT or RT and either PT or MT.	The joints between the top outer and inner cover plates and containment shell are designed and fabricated per ASME Code Case N-595-2 [3], which provides alternative requirements for the design and examination of spent fuel canister closures. This includes the inner top cover plate weld around the vent & siphon block and the vent and siphon block welds to the shell. The closure welds are partial penetration welds and the root and final layer are subject to PT examination (in lieu of volumetric examination) in accordance with the provisions of ASME Code Case N-595-2. The 32PT closure system employs austenitic stainless steel shell, lid materials, and welds. Because austenitic stainless steels are not subject to brittle failure at the operating temperatures of the DSC, crack propagation is not a concern. Thus, multi-level PT examination provides reasonable assurance that flaws of interest will be identified. The PT examination is done by qualified personnel, in accordance with Section V and the acceptance standards of Section III, Subsection NB-5000. This alternative does not apply to other shell confinement welds, i.e., the longitudinal and circumferential welds applied to the DSC shell, and the inner bottom cover plate-to-shell weld which comply with NB-4243 and NB-5230.

Table A.2.13.13-4
 Alternatives to the ASME Code for the NUHOMS®-32PT DSC Confinement Boundary
 (Concluded)

Reference ASME Code Section/Article	Code Requirement	Alternatives, Justification & Compensatory Measures
NB-6100 and 6200	All pressure retaining components and completed systems shall be pressure tested. The preferred method shall be hydrostatic test.	The NUHOMS®-32PT DSC is pressure tested in accordance with ASME Code Case N-595-2 [3]. The shield plug support ring and the vent and siphon block are not pressure tested due to the manufacturing sequence. The support ring is not a pressure-retaining item and the vent and siphon block weld is helium leak tested after fuel is loaded to the same criteria as the inner top closure plate-to-shell weld (ANSI N14.5-1997 leaktight criteria) [6].
NB-7000	Overpressure Protection.	No overpressure protection is provided for the NUHOMS® DSCs. The function of the DSC is to contain radioactive materials under normal, off-normal and hypothetical accident conditions postulated to occur during transportation and storage. The DSC is designed to withstand the maximum possible internal pressure considering 100% fuel rod failure at maximum accident temperature.
NB -8000	Requirements for nameplates, stamping & reports per NCA-8000.	The NUHOMS® DSC nameplate provides the information required by 10CFR71 [2], 49CFR173 [8] and 10CFR72 [4] as appropriate. Code stamping is not required for the DSC. QA data packages are prepared in accordance with the requirements of TN's approved QA program.
NB-5000	NDE Personnel must be qualified to a specific edition of SNT-TC-1A.	Permit use of more recent edition of SNT-TC-1A [9].

Table A.2.13.13-5
Alternatives to the ASME Code Exceptions for the NUHOMS®-32PT DSC Basket Assembly

Reference ASME Code Section/Article	Code Requirement	Alternatives, Justification & Compensatory Measures
NCA	All.	Not compliant with NCA [1]. Quality Assurance is provided according to 10 CFR 71 Subpart H in lieu of NCA-4000.
NCA-1140	Use of Code editions and addenda.	Code edition and addenda other than those specified in Section A.2.1.2.1 may be used for construction, but in no case earlier than 3 years before that specified in the Table. Materials produced and certified in accordance with ASME Section II [1] material specification from Code Editions and Addenda other than those specified in Section A.2.1.2.1 may be used, as long as the materials meet all the requirements of Article 2000 of the applicable Subsection of the Section III Edition and Addenda used for construction.
NG-1100	Requirements for Code Stamping of Components, Code reports and certificates, etc.	Code Stamping is not required. As Code Stamping is not required, the fabricator is not required to hold an ASME "N" or "NPT" [1] stamp, or to be ASME Certified.
NG-2000	Use of ASME Material.	Some baskets include neutron absorber and aluminum plates that are not ASME Code Class 1 material. They are used for criticality safety and heat transfer, and are only credited in the structural analysis with supporting their own weight and transmitting bearing loads through their thickness. Material properties in the ASME Code for Type 6061 aluminum are limited to 400°F to preclude the potential for annealing out the hardening properties. Annealed properties (as published by the Aluminum Association and the American Society of Metals) are conservatively assumed for the solid aluminum rails for use above the Code temperature limits.
NG-2130	Material must be supplied by ASME approved material suppliers.	Material is certified to meet all ASME Code criteria but is not eligible for certification or Code Stamping if a non-ASME fabricator is used. As the fabricator is not required to be ASME certified, material certification to NG-2130 is not possible. Material traceability and certification are maintained in accordance with TN's NRC approved QA program.
NG-4121	Material Certification by Certificate Holder.	
NG -8000	Requirements for nameplates, stamping & reports per NCA-8000.	The NUHOMS® DSC nameplate provides the information required by 10CFR71 [2], 49CFR173 [8] and 10CFR72 [4] as appropriate. Code stamping is not required for the DSC. QA data packages are prepared in accordance with the requirements of TN's approved QA program.
NG-3000/ Section II, Part D, Table 2A	Maximum temperature limit for XM-19 plate material is 800°F.	Not compliant with ASME Section II Part D Table 2A material temperature limit for XM-19 steel for the postulated accident cases. Maximum plate material temperatures are less than 900°F, the expected reduction in material strength is small (less than 1 ksi by extrapolation), and the only primary stresses in the basket grid are deadweight stresses.

Table A.2.13.13-6
Alternatives to the ASME Code for the NUHOMS®-24PTH DSC Confinement Boundary

Reference ASME Code Section/Article	Code Requirement	Alternatives, Justification & Compensatory Measures
NCA	All.	Not compliant with NCA [1]. Quality Assurance is provided according to 10 CFR 71 Subpart H in lieu of NCA-4000.
NCA-1140	Use of Code editions and addenda.	Code edition and addenda other than those specified in Section A.2.1.2.1 may be used for construction, but in no case earlier than 3 years before that specified in the Table. Materials produced and certified in accordance with ASME Section II [1] material specification from Code Editions and Addenda other than those specified in Section A.2.1.2.1 may be used, as long as the materials meet all the requirements of Article 2000 of the applicable Subsection of the Section III Edition and Addenda used for construction.
NB-1100	Requirements for Code Stamping of Components, Code reports and certificates, etc.	Code Stamping is not required. As Code Stamping is not required, the fabricator is not required to hold an ASME "N" or "NPT" [1] stamp, or to be ASME Certified.
NB-1132	Attachments with a pressure retaining function, including stiffeners, shall be considered part of the component.	Bottom shield plug assembly, outer bottom cover plate, lifting posts, grapple ring, grapple ring support are outside code jurisdiction; these components together are much larger than required to provide stiffening for the inner bottom cover plate; the weld that retains the outer bottom cover plate and with it the bottom shield plug is subject to root and final PT examination.
NB-2130	Material must be supplied by ASME approved material suppliers.	Material is certified to meet all ASME Code criteria but is not eligible for certification or Code Stamping if a non-ASME fabricator is used. As the fabricator is not required to be ASME certified, material certification to NB-2130 is not possible. Material traceability and certification are maintained in accordance with TN's NRC approved QA program.
NB-4121	Material Certification by Certificate Holder.	
NB-4243 and NB-5230	Category C weld joints in vessels and similar weld joints in other components shall be full penetration joints. These welds shall be examined by UT or RT and either PT or MT.	The joints between the top outer and inner cover plates (or top forging assembly for the 24PTH-S-LC) and confinement shell are designed and fabricated per ASME Code Case N-595-2 [3], which provides alternative requirements for the design and examination of spent fuel canister closures. This includes the inner top cover plate weld around the vent & siphon block and the vent and siphon block welds to the shell. The closure welds are partial penetration welds and the root and final layer are subject to PT examination (in lieu of volumetric examination) in accordance with the provisions of ASME Code Case N-595-2. The 24PTH closure system employs austenitic stainless steel shell, lid materials, and welds. Because austenitic stainless steels are not subject to brittle failure at the operating temperatures of the DSC, crack propagation is not a concern. Thus, multi-level PT examination provides reasonable assurance that flaws of interest will be identified. The PT examination is done by qualified personnel, in accordance with Section V and the acceptance standards of Section III, Subsection NB-5000. This alternative does not apply to other shell confinement welds, i.e., the longitudinal and circumferential welds of the DSC shell, and the inner bottom cover plate-to-shell weld (or bottom forging to shell weld, as applicable) which comply with NB-4243 and NB-5230.

Table A.2.13.13-6
 Alternatives to the ASME Code for the NUHOMS®-24PTH DSC Confinement Boundary
 (Concluded)

Reference ASME Code Section/Article	Code Requirement	Alternatives, Justification & Compensatory Measures
NB-6100 and 6200	All pressure retaining components and completed systems shall be pressure tested. The preferred method shall be hydrostatic test.	The NUHOMS®-24PTH DSC is pressure tested in accordance with ASME Code Case N-595-2. The shield plug support ring and the vent and siphon block are not pressure tested due to the manufacturing sequence. The support ring is not a pressure-retaining item and the vent and siphon block weld is helium leak tested after fuel is loaded to the same criteria as the inner top closure plate-to-shell weld (ANSI N14.5-1997 leaktight criteria).
NB-7000	Overpressure Protection.	No overpressure protection is provided for the NUHOMS® DSCs. The function of the DSC is to contain radioactive materials under normal, off-normal and hypothetical accident conditions postulated to occur during transportation and storage. The DSC is designed to withstand the maximum possible internal pressure considering 100% fuel rod failure at maximum accident temperature.
NB -8000	Requirements for nameplates, stamping & reports per NCA-8000.	The NUHOMS® DSC nameplate provides the information required by 10CFR71 [2], 49CFR173 [8] and 10CFR72 [4] as appropriate. Code stamping is not required for the DSC. QA data packages are prepared in accordance with the requirements of TN's approved QA program.
NB-5000	NDE Personnel must be qualified to a specific edition of SNT-TC-1A.	Permit use of more recent edition of SNT-TC-1A [9].

Table A.2.13.13-7
Alternatives to the ASME Code for the NUHOMS®-24PTH DSC Basket Assembly

Reference ASME Code Section/Article	Code Requirement	Alternatives, Justification & Compensatory Measures
NCA	All.	Not compliant with NCA [1]. Quality Assurance is provided according to 10 CFR 71 Subpart H in lieu of NCA-4000.
NCA-1140	Use of Code editions and addenda.	Code edition and addenda other than those specified in Section A.2.1.2.1 may be used for construction, but in no case earlier than 3 years before that specified in the Table. Materials produced and certified in accordance with ASME Section II [1] material specification from Code Editions and Addenda other than those specified in Section A.2.1.2.1 may be used, as long as the materials meet all the requirements of Article 2000 of the applicable Subsection of the Section III Edition and Addenda used for construction.
NG-1100	Requirements for Code Stamping of Components, Code reports and certificates, etc.	Code Stamping is not required. As Code Stamping is not required, the fabricator is not required to hold an ASME "N" or "NPT" [1] stamp, or to be ASME Certified.
NG-2000	Use of ASME Material.	Some baskets include neutron absorber and aluminum plates that are not ASME Code Class 1 material. They are used for criticality safety and heat transfer, and are only credited in the structural analysis with supporting their own weight and transmitting bearing loads through their thickness. Material properties in the ASME Code for Type 6061 aluminum are limited to 400°F to preclude the potential for annealing out the hardening properties. Annealed properties (as published by the Aluminum Association and the American Society of Metals) are conservatively assumed for the aluminum transition rails for use above the Code temperature limits.
NG-2130	Material must be supplied by ASME approved material suppliers.	Material is certified to meet all ASME Code criteria but is not eligible for certification or Code Stamping if a non-ASME fabricator is used. As the fabricator is not required to be ASME certified, material certification to NG-2130 is not possible. Material traceability and certification are maintained in accordance with TN's NRC approved QA program.
NG-4121	Material Certification by Certificate Holder.	
NG -8000	Requirements for nameplates, stamping & reports per NCA-8000.	The NUHOMS® DSC nameplate provides the information required by 10CFR71 [2], 49CFR173 [8] and 10CFR72 [4] as appropriate. Code stamping is not required for the DSC. QA data packages are prepared in accordance with the requirements of TN's approved QA program.
NG-3000/ Section II, Part D, Table 2A	Maximum temperature limit for Type 304 plate material is 800°F.	Not compliant with ASME Section II Part D Table 2A material temperature limit for Type 304 steel for the postulated accident cases. Maximum plate material temperature is less than 900°F, the expected reduction in material strength is small (less than 1 ksi by extrapolation), and the only primary stresses in the basket grid are deadweight stresses.

Table A.2.13.13-7

Alternatives to the ASME Code for the NUHOMS®-24PTH DSC Basket Assembly
(Concluded)

Reference ASME Code Section/Article	Code Requirement	Alternatives, Justification & Compensatory Measures
NG-3352	Table NG 3352-1 lists the permissible welded joints.	<p>The fusion (spot) type welds between the stainless steel insert plates (straps) and the stainless steel fuel compartment tube are not permissible welds per Table NG-3352-1. These welds are qualified by testing. The required minimum tested capacity of the welded connection (at each side of the tube) shall be 36 Kips (at room temperature). This value is based on a margin of safety (test-to-design) of 1.6, which is larger than the Code-implied margin of safety for Level D loads. The minimum capacity shall be determined by shear tests of individual specimens made from production material. The tests shall be corrected for temperature differences (test-to-design) and for material properties (actual-to-ASME Code minimum values) to demonstrate that the capacity of the welded connection with ASME minimum properties, tested at design temperatures, will meet the 36 Kips test requirement. The capacity of the welded connection is determined from the test of the weld pattern of a typical insert plate to the tube connection.</p> <p>A joint efficiency (quality) factor of 1.0 is utilized for the fuel compartment longitudinal seam welds. Table NG-3352-1 permits a joint efficiency (quality) factor of 0.5 to be used for full penetration weld examined by ASME Section V visual examination (VT). For the 24PTH DSC, the compartment seam weld is thin and the weld will be made in one pass. Both surfaces of weld (inside and outside) will be fully examined by VT and therefore a factor of $2 \times 0.5 = 1.0$, will be used in the analysis. This is justified as both surfaces of the single weld pass/layer will be fully examined, and the stainless steel material that comprises the fuel compartment tubes is very ductile.</p>

Table A.2.13.13-8
 Alternatives to the ASME Code for the NUHOMS® 32PTH DSC Confinement Boundary

Reference ASME Code Section/Article	Code Requirement	Alternatives, Justification & Compensatory Measures
NCA	All	Not compliant with NCA [1]. Quality Assurance is provided according to 10 CFR 71 Subpart H [2] in lieu of NCA-4000.
NB-1100	Requirements for Code Stamping of Components.	The canister shell, the inner top cover/shield plug, the inner bottom cover, and the siphon/vent port cover are designed & fabricated in accordance with the ASME Code, Section III, Subsection NB [1] to the maximum extent practical. However, Code Stamping is not required. As Code Stamping is not required, the fabricator is not required to hold an ASME "N" or "NPT" stamp, or to be ASME Certified.
NB-2130 NB-4121	Material must be supplied by ASME approved material suppliers. Material Certification by Certificate Holder.	Material is certified to meet all ASME Code criteria but is not eligible for certification or Code Stamping if a non-ASME fabricator is used. As the fabricator is not required to be ASME certified, material certification to NB-2130 is not possible. Material traceability & certification are maintained in accordance with TN's NRC approved QA program.
NB-4243 and NB-5230	Category C weld joints in vessels and similar weld joints in other components shall be full penetration joints. These welds shall be examined by UT or RT and either PT or MT.	The shell to the outer top cover weld, the shell to the inner top cover/shield plug weld (including option 2 or option 3 inner top cover as described in the SAR), and the siphon/vent cover welds, are all partial penetration welds. As an alternative to the NDE requirements of NB-5230, for Category C welds, all of these closure welds will be multi-layer welds and receive a root and final PT examination, except for the shell to the outer top cover weld. The shell to the outer top cover weld will be a multi-layer weld and receive multi-level PT examination in accordance with the guidance provided in ISG-15 [7] for NDE. The multi-level PT examination provides reasonable assurance that flaws of interest will be identified. The PT examination is done by qualified personnel, in accordance with Section V and the acceptance standards of Section III, Subsection NB-5000. All of these welds will be designed to meet the guidance provided in ISG-15 for stress reduction factor.
NB-2531	Vent & siphon Port Cover; straight beam UT per SA-578 for all plates for vessel.	SA-578 applies to 3/8" and thicker plate only; allow alternate UT techniques to achieve meaningful UT results.
NB- 6000	All completed pressure retaining systems shall be pressure tested.	The 32PTH is not a complete or "installed" pressure vessel until the top closure is welded following placement of Fuel Assemblies within the DSC. Due to the inaccessibility of the shell and lower end closure welds following fuel loading and top closure welding, as an alternative, the pressure testing of the DSC is performed in two parts. The DSC shell, shell bottom, including all longitudinal and circumferential welds, is pneumatically tested and examined at the fabrication facility. The shell to the inner top cover/shield plug closure weld (including option 2 or option 3 inner top cover as described in the SAR) are pressure tested and examined for leakage in accordance with NB-6300 in the field. The siphon/vent cover welds will not be pressure tested; these welds and the shell to the inner top cover/shield plug closure weld (including option 2 or option 3 inner top cover as described in the SAR) are helium leak tested after the pressure test. Per NB-6324 the examination for leakage shall be done at a pressure equal to the greater of the Design pressure or three-fourths of the test pressure. As an alternative, if the examination for leakage of these field welds, following the pressure test, is performed using helium leak detection techniques, the examination pressure may be reduced to 1.5 psig. This is acceptable given the significantly greater sensitivity of the helium leak detection method.

Table A.2.13.13-8
 Alternatives to the ASME Code for the NUHOMS® 32PTH DSC Confinement Boundary
 (Concluded)

Reference ASME Code Section/Article	Code Requirement	Alternatives, Justification & Compensatory Measures
NB-7000	Overpressure Protection.	No overpressure protection is provided for the 32PTH DSC. The function of the 32PTH DSC is to contain radioactive materials under normal, off-normal, and hypothetical accident conditions postulated to occur during transportation. The 32PTH DSC is designed to withstand the maximum internal pressure considering 100% fuel rod failure at maximum accident temperature. The 32PTH DSC is pressure tested in accordance with the requirements of 10CFR71 and TN's approved QA program.
NB-8000	Requirements for nameplates, stamping & reports per NCA-8000.	The 32PTH DSC nameplates provide the information required by 10CFR71 [2], 49CFR173 [8], and 10CFR72 [4] as appropriate. Code stamping is not required for the 32PTH DSC. QA Data packages are prepared in accordance with the requirements of 10CFR71, 10CFR72, and TN's approved QA program.
NB-1132	Attachments with a pressure retaining function, including stiffeners, shall be considered part of the component.	Outer bottom cover, bottom plate, bottom casing plate, side casing plate, top shield plug casing plate, lifting posts, grapple ring and grapple ring support are outside code jurisdiction; these components together are much larger than required to provide stiffening for the confinement boundary cover. These component welds are subject to root and final PT examinations.
NB-5000	NDE Personnel must be qualified to a specific edition of SNT-TC-1A.	Permit use of more recent edition of SNT-TC-1A [9].
NCA-1140	Use of Code editions and addenda.	Code edition and addenda other than those specified in Section A.2.1.2.1 may be used for construction, but in no case earlier than 3 years before that specified in the Table. Materials produced and certified in accordance with ASME Section II [1] material specification from Code Editions and Addenda other than those specified in Section A.2.1.2.1 may be used, as long as the materials meet all the requirements of Article 2000 of the applicable Subsection of the Section III Edition and Addenda used for construction.

Table A.2.13.13-9
Alternatives to the ASME Code for the NUHOMS® 32PTH DSC Basket Assembly

Reference ASME Code Section/Article	Code Requirement	Alternatives, Justification & Compensatory Measures
NG/NF-1100	Requirement for Code Stamping of Components.	The 32PTH DSC baskets are designed & fabricated in accordance with the ASME Code, Section III, Subsection NG to the maximum extent practical as described in the SAR, but Code Stamping is not required. As Code Stamping is not required, the fabricator is not required to hold an ASME N or NPT stamp or be ASME Certified.
NG/NF-2130 NG/NF-4121	Material must be supplied by ASME approved material suppliers. Material Certification by Certificate Holder.	Material is certified to meet all ASME Code criteria but is not eligible for certification or Code Stamping if a non-ASME fabricator is used. As the fabricator is not required to be ASME certified, material certification to NG/NF-2130 is not possible. Material traceability & certification are maintained in accordance with TN's NRC approved QA program. The poison material and aluminum plates are not used for structural analysis, but to provide criticality control and heat transfer. They are not ASME Code Class I materials. See note 1.
NG-3352	Table NG 3352-1 lists the permissible welded joints.	The fusion welds between the stainless steel insert plates and the stainless fuel compartment tube are not included in Table NG-3352-1. These welds are qualified by testing. The required minimum tested capacity of the welded connection shall be 17.1 kips per weld or 34.2 kips at each face of the tube (at room temperature). The capacity shall be demonstrated by qualification and production testing. Testing shall be performed using, or corrected to, the lowest tensile strength of material used in the basket assembly or to minimum specified tensile strength. Testing may be performed on individual welds, or on weld patterns representative of one wall of the tube. ASME Code Section IX does not provide tests for qualification of these type of welds. Therefore, these welds are qualified using Section IX to the degree applicable together with the testing described here. The welds will be visually inspected to confirm that they are located over the insert plates, in lieu of the visual acceptance criteria of NG-5260 which are not appropriate for this type of weld.
NG-3000/ Section II, Part D, Table 2A	Maximum temperature limit for Type 304 plate material is 800°F.	Not compliant with ASME Section II Part D Table 2A material temperature limit for Type 304 steel for the postulated accident cases. Maximum plate material temperature is less than 1050°F, the expected reduction in material strength is small, and the only primary stresses in the basket grid are deadweight stresses.
NCA	All.	Not compliant with NCA.
NCA-1140	Use of Code editions and addenda.	Code edition and addenda other than those specified in Section A.2.1.2.1 may be used for construction, but in no case earlier than 3 years before that specified in the Table. Materials produced and certified in accordance with ASME Section II [1] material specification from Code Editions and Addenda other than those specified in Section A.2.1.2.1 may be used, as long as the materials meet all the requirements of Article 2000 of the applicable Subsection of the Section III Edition and Addenda used for construction.

Note:1. Because Subsection NCA does not apply, the NCA-3820 requirements for accreditation or qualification of material organizations do not apply. CMTR's shall be provided using NCA-3862 for guidance.

Table A.2.13.13-10
Alternatives to the ASME Code for the NUHOMS® 32PTH Type 1 DSC Confinement Boundary

Reference ASME Code Section/Article	Code Requirement	Alternatives, Justification & Compensatory Measures
NCA	All	Not compliant with NCA [1]. Quality Assurance is provided according to 10 CFR 71 Subpart H [2] in lieu of NCA-4000.
NB-1100	Requirements for Code Stamping of Components.	The canister shell, the inner top cover/shield plug, the inner bottom cover, and the siphon/vent port cover are designed & fabricated in accordance with the ASME Code, Section III, Subsection NB [1] to the maximum extent practical. However, Code Stamping is not required. As Code Stamping is not required, the fabricator is not required to hold an ASME "N" or "NPT" stamp, or to be ASME Certified.
NB-2130 NB-4121	Material must be supplied by ASME approved material suppliers. Material Certification by Certificate Holder.	Material is certified to meet all ASME Code criteria but is not eligible for certification or Code Stamping if a non-ASME fabricator is used. As the fabricator is not required to be ASME certified, material certification to NB-2130 is not possible. Material traceability & certification are maintained in accordance with TN's NRC approved QA program.
NB-4243 and NB-5230	Category C weld joints in vessels and similar weld joints in other components shall be full penetration joints. These welds shall be examined by UT or RT and either PT or MT.	The shell to the outer top cover weld, the shell to the inner top cover/shield plug weld (including option 2 or option 3 inner top cover as described in the SAR), and the siphon/vent cover welds, are all partial penetration welds. As an alternative to the NDE requirements of NB-5230, for Category C welds, all of these closure welds will be multi-layer welds and receive a root and final PT examination, except for the shell to the outer top cover weld. The shell to the outer top cover weld will be a multi-layer weld and receive multi-level PT examination in accordance with the guidance provided in ISG-15 [7] for NDE. The multi-level PT examination provides reasonable assurance that flaws of interest will be identified. The PT examination is done by qualified personnel, in accordance with Section V and the acceptance standards of Section III, Subsection NB-5000. All of these welds will be designed to meet the guidance provided in ISG-15 for stress reduction factor.
NB-2531	Vent & siphon Port Cover; straight beam UT per SA-578 for all plates for vessel.	SA-578 applies to 3/8" and thicker plate only; allow alternate UT techniques to achieve meaningful UT results.
NB- 6000	All completed pressure retaining systems shall be pressure tested.	The 32PTH Type 1 is not a complete or "installed" pressure vessel until the top closure is welded following placement of Fuel Assemblies within the DSC. Due to the inaccessibility of the shell and lower end closure welds following fuel loading and top closure welding, as an alternative, the pressure testing of the DSC is performed in two parts. The DSC shell, shell bottom, including all longitudinal and circumferential welds, is pneumatically tested and examined at the fabrication facility. The shell to the inner top cover/shield plug closure weld (including option 2 or option 3 inner top cover as described in the SAR) are pressure tested and examined for leakage in accordance with NB-6300 in the field. The siphon/vent cover welds will not be pressure tested; these welds and the shell to the inner top cover/shield plug closure weld (including option 2 or option 3 inner top cover as described in the SAR) are helium leak tested after the pressure test. Per NB-6324 the examination for leakage shall be done at a pressure equal to the greater of the Design pressure or three-fourths of the test pressure. As an alternative, if the examination for leakage of these field welds, following the pressure test, is performed using helium leak detection techniques, the examination pressure may be reduced to 1.5 psig. This is acceptable given the significantly greater sensitivity of the helium leak detection method.

Table A.2.13.13-10
 Alternatives to the ASME Code for the NUHOMS® 32PTH Type 1 DSC Confinement Boundary
 (Concluded)

Reference ASME Code Section/Article	Code Requirement	Alternatives, Justification & Compensatory Measures
NB-7000	Overpressure Protection.	No overpressure protection is provided for the 32PTH Type 1 DSC. The function of the 32PTH Type 1 DSC is to contain radioactive materials under normal, off-normal, and hypothetical accident conditions postulated to occur during transportation. The 32PTH DSC is designed to withstand the maximum internal pressure considering 100% fuel rod failure at maximum accident temperature. The 32PTH DSC is pressure tested in accordance with the requirements of 10CFR71 and TN's approved QA program.
NB-8000	Requirements for nameplates, stamping & reports per NCA-8000.	The 32PTH Type 1 DSC nameplates provide the information required by 10CFR71 [2], 49CFR173 [8], and 10CFR72 [4] as appropriate. Code stamping is not required for the 32PTH Type 1 DSC. QA Data packages are prepared in accordance with the requirements of 10CFR71, 10CFR72, and TN's approved QA program.
NB-1132	Attachments with a pressure retaining function, including stiffeners, shall be considered part of the component.	Outer bottom cover, bottom plate, bottom casing plate, side casing plate, top shield plug casing plate, lifting posts, grapple ring and grapple ring support are outside code jurisdiction; these components together are much larger than required to provide stiffening for the confinement boundary cover. These component welds are subject to root and final PT examinations.
NB-5000	NDE Personnel must be qualified to a specific edition of SNT-TC-1A.	Permit use of more recent edition of SNT-TC-1A [9].
NCA-1140	Use of Code editions and addenda.	Code edition and addenda other than those specified in Section A.2.1.2.1 may be used for construction, but in no case earlier than 3 years before that specified in the Table. Materials produced and certified in accordance with ASME Section II [1] material specification from Code Editions and Addenda other than those specified in Section A.2.1.2.1 may be used, as long as the materials meet all the requirements of Article 2000 of the applicable Subsection of the Section III Edition and Addenda used for construction.

Table A.2.13.13-11
Alternatives to the ASME Code for the NUHOMS® 32PTH Type 1 DSC Basket Assembly

Reference ASME Code Section/Article	Code Requirement	Alternatives, Justification & Compensatory Measures
NG/NF-1100	Requirement for Code Stamping of Components.	The 32PTH Type 1 DSC baskets are designed & fabricated in accordance with the ASME Code, Section III, Subsection NG to the maximum extent practical as described in the SAR, but Code Stamping is not required. As Code Stamping is not required, the fabricator is not required to hold an ASME N or NPT stamp or be ASME Certified.
NG/NF-2130 NG/NF-4121	Material must be supplied by ASME approved material suppliers. Material Certification by Certificate Holder.	Material is certified to meet all ASME Code criteria but is not eligible for certification or Code Stamping if a non-ASME fabricator is used. As the fabricator is not required to be ASME certified, material certification to NG/NF-2130 is not possible. Material traceability & certification are maintained in accordance with TN's NRC approved QA program. The poison material and aluminum plates are not used for structural analysis, but to provide criticality control and heat transfer. They are not ASME Code Class I materials. See note 1.
NG-3352	Table NG 3352-1 lists the permissible welded joints.	<p>The fusion welds between the stainless steel insert plates and the stainless fuel compartment tube are not included in Table NG-3352-1. These welds are qualified by testing. The required minimum tested capacity of the welded connection shall be 17.1 kips per weld or 34.2 kips at each face of the tube (at room temperature). The capacity shall be demonstrated by qualification and production testing. Testing shall be performed using, or corrected to, the lowest tensile strength of material used in the basket assembly or to minimum specified tensile strength. Testing may be performed on individual welds, or on weld patterns representative of one wall of the tube.</p> <p>ASME Code Section IX does not provide tests for qualification of these type of welds. Therefore, these welds are qualified using Section IX to the degree applicable together with the testing described here.</p> <p>The welds will be visually inspected to confirm that they are located over the insert plates, in lieu of the visual acceptance criteria of NG-5260 which are not appropriate for this type of weld.</p> <p>A joint efficiency (quality) factor of 1.0 is utilized for the fuel compartment longitudinal seam welds. Table NG-3352-1 permits a joint efficiency (quality) factor of 0.5 to be used for full penetration weld examined by ASME Section V visual examination (VT). For the 32PTH Type 1 DSC, the compartment seam weld is thin and both surfaces of weld (inside and outside) will be fully examined by VT and therefore a factor of $2 \times 0.5 = 1.0$, will be used in the analysis. This is justified as both surfaces of the single weld pass/layer will be fully examined, and the stainless steel material that comprises the fuel compartment tubes is very ductile.</p>
NG-3000/ Section II, Part D, Table 2A	Maximum temperature limit for Type 304 plate material is 800°F.	Not compliant with ASME Section II Part D Table 2A material temperature limit for Type 304 steel for the postulated accident cases is less than 1050°F, the expected reduction in material strength is small (less than 1 ksi by extrapolation), and the only primary stresses in the basket grid are deadweight stresses.
NCA	All.	Not compliant with NCA.

Note:1. Because Subsection NCA does not apply, the NCA-3820 requirements for accreditation or qualification of material organizations do not apply. CMTR's shall be provided using NCA-3862 for guidance.

Table A.2.13.11
Alternatives to the ASME Code for the NUHOMS[®] 32PTH Type 1 DSC Basket Assembly
(Concluded)

Reference ASME Code Section/Article	Code Requirement	Alternatives, Justification & Compensatory Measures
NCA-1140	Use of Code editions and addenda.	<p>Code edition and addenda other than those specified in Section A.2.1.2.1 may be used for construction, but in no case earlier than 3 years before that specified in the Table.</p> <p>Materials produced and certified in accordance with ASME Section II [1] material specification from Code Editions and Addenda other than those specified in Section A.2.1.2.1 may be used, as long as the materials meet all the requirements of Article 2000 of the applicable Subsection of the Section III Edition and Addenda used for construction.</p>

Table A.2.13.13-12
Alternatives to the ASME Code for the NUHOMS® 32PTH1 DSC Confinement Boundary

Reference ASME Code Section/Article	Code Requirement	Alternatives, Justification & Compensatory Measures
NCA	All.	Not compliant with NCA [1]. Quality Assurance is provided according to 10 CFR 71 Subpart H [2] in lieu of NCA-4000.
NCA-1140	Use of Code editions and addenda.	Code edition and addenda other than those specified in Section A.2.1.2.1 may be used for construction, but in no case earlier than 3 years before that specified in the Table. Materials produced and certified in accordance with ASME Section II [1] material specification from Code Editions and Addenda other than those specified in Section A.2.1.2.1 may be used, as long as the materials meet all the requirements of Article 2000 of the applicable Subsection of the Section III Edition and Addenda used for construction.
NB-1100	Requirements for Code Stamping of Components, Code reports and certificates, etc.	Code Stamping is not required. As Code Stamping is not required, the fabricator is not required to hold an ASME "N" or "NPT" [1] stamp, or to be ASME Certified.
NB-2130	Material must be supplied by ASME approved material suppliers.	Material is certified to meet all ASME Code criteria but is not eligible for certification or Code Stamping if a non-ASME fabricator is used. As the fabricator is not required to be ASME certified, material certification to NB-2130 is not possible. Material traceability and certification are maintained in accordance with TN's NRC approved QA program.
NB-4121	Material Certification by Certificate Holder.	
NB-4243 and NB-5230	Category C weld joints in vessels and similar weld joints in other components shall be full penetration joints. These welds shall be examined by UT or RT and either PT or MT.	The shell to the outer top cover weld, the shell to the inner top cover/shield plug weld (including optional design configurations for the inner top cover as described in the 32PTH1 DSC drawings), the siphon/vent cover welds, and the vent and siphon block welds to the shell are all partial penetration welds. As an alternative to the NDE requirements of NB-5230, for Category C welds, all of these closure welds are multi-layer welds and receive a root and final PT examination, except for the shell to the outer top cover weld. The shell to the outer top cover weld will be a multi-layer weld and receive multi-level PT examination in accordance with the guidance provided in ISG-15 [7] for NDE. The multi-level PT examination provides reasonable assurance that flaws of interest will be identified. The PT examination is done by qualified personnel, in accordance with Section V and the acceptance standards of Section III, Subsection NB-5000. All of these welds are designed to meet the guidance provided in ISG-15 for stress reduction factor.
NB-1132	Attachments with a pressure retaining function, including stiffeners, shall be considered part of the component.	Bottom shield plug and outer bottom cover plate are outside code jurisdiction; these components together are much larger than required to provide stiffening for the inner bottom cover plate; the weld that retains the outer bottom cover plate and with it the bottom shield plug is subject to root and final PT examination.

Table A.2.13.13-12
 Alternatives to the ASME Code for the NUHOMS® 32PTH1 DSC Confinement Boundary
 (Concluded)

Reference ASME Code Section/Article	Code Requirement	Alternatives, Justification & Compensatory Measures
NB-6100 and 6200	All pressure retaining components and completed systems shall be pressure tested. The preferred method shall be hydrostatic test.	<p>The NUHOMS® 32PTH1 DSC is not a complete vessel until the top closure is welded following placement of fuel assemblies within the DSC. Due to the inaccessibility of the shell and lower end closure welds following fuel loading and top closure welding, as an alternative, the pressure testing of the DSC is performed in two parts. The DSC shell and inner bottom plate/forging (including all longitudinal and circumferential welds), are pressure tested and examined at the fabrication facility.</p> <p>The shell to the inner top cover/shield plug closure weld (including optional design configurations for the inner top cover as described in the 32PTH1 DSC drawings) is pressure tested and examined for leakage in accordance with NB-6300 in the field.</p> <p>The siphon/vent cover welds are not pressure tested; these welds and the shell to the inner top cover/shield plug closure weld (including Optional design configurations for the inner top cover as described in the 32PTH1 DSC drawings) are helium leak tested after the pressure test.</p> <p>Per NB-6324 the examination for leakage shall be done at a pressure equal to the greater of the design pressure or three-fourths of the test pressure. As an alternative, if the examination for leakage of these field welds, following the pressure test, is performed using helium leak detection techniques, the examination pressure may be reduced to ≥ 1.5 psig. This is acceptable given the significantly greater sensitivity of the helium leak detection method.</p>
NB-7000	Overpressure Protection.	No overpressure protection is provided for the NUHOMS® DSCs. The function of the DSC is to contain radioactive materials under normal, off-normal and hypothetical accident conditions postulated to occur during transportation and storage. The DSC is designed to withstand the maximum possible internal pressure considering 100% fuel rod failure at maximum accident temperature.
NB-8000	Requirements for nameplates, stamping & reports per NCA-8000.	The NUHOMS® DSC nameplate provides the information required by 10CFR71 [2], 49CFR173 [8] and 10CFR72 [4] as appropriate. Code stamping is not required for the DSC. QA data packages are prepared in accordance with the requirements of TN's approved QA program.
NB-5000	NDE Personnel must be qualified to a specific edition of SNT-TC-1A.	Permit use of more recent edition of SNT-TC-1A [9].

Table A.2.13.13-13
Alternatives to the ASME Code for the NUHOMS® 32PTH1 DSC Basket Assembly

Reference ASME Code Section/Article	Code Requirement	Alternatives, Justification & Compensatory Measures
NCA	All.	Not compliant with NCA [1]. Quality Assurance is provided according to 10 CFR 71 Subpart H [2] in lieu of NCA-4000.
NCA-1140	Use of Code editions and addenda.	Code edition and addenda other than those specified in Section A.2.1.2.1 may be used for construction, but in no case earlier than 3 years before that specified in the Table. Materials produced and certified in accordance with ASME Section II [1] material specification from Code Editions and Addenda other than those specified in Section A.2.1.2.1 may be used, so long the materials meet all the requirements of Article 2000 of the applicable Subsection of the Section III Edition and Addenda used for construction.
NG/NF-1100	Requirements for Code Stamping of Components, Code reports and certificates, etc.	Code Stamping is not required. As Code Stamping is not required, the fabricator is not required to hold an ASME "N" or "NPT" [1] stamp, or to be ASME Certified.
NG-2000	Use of ASME Material.	Some baskets include neutron absorber and aluminum plates that are not ASME Code Class 1 material. They are used for criticality safety and heat transfer, and are only credited in the structural analysis with supporting their own weight and transmitting bearing loads through their thickness. Material properties in the ASME Code for Type 6061 aluminum are limited to 400°F to preclude the potential for annealing out the hardening properties. Annealed properties (as published by the Aluminum Association and the American Society of Metals) are conservatively assumed for the aluminum transition rails for use above the Code temperature limits.
NG/NF-2130	Material must be supplied by ASME approved material suppliers.	Material is certified to meet all ASME Code criteria but is not eligible for certification or Code Stamping if a non-ASME fabricator is used. As the fabricator is not required to be ASME certified, material certification to NG/NF-2130 is not possible. Material traceability and certification are maintained in accordance with TN's NRC approved QA program.
NG/NF-4121	Material Certification by Certificate Holder.	
NG-8000	Requirements for nameplates, stamping & reports per NCA-8000.	The NUHOMS® DSC nameplate provides the information required by 10CFR71 [2], 49CFR173 [8] and 10CFR72 [4] as appropriate. Code stamping is not required for the DSC. QA data packages are prepared in accordance with the requirements of TN's approved QA program.
NG-3000/ Section II, Part D, Table 2A	Maximum temperature limit for Type 304 plate material is 800°F.	Not compliant with ASME Section II Part D Table 2A material temperature limit for Type 304 steel for the postulated accident cases. The calculated maximum steady state temperatures for accident cases are less than 1000°F. The only primary stresses in the basket grid are deadweight stresses. The ASME Code allows use of SA240 Type 304 stainless steel to temperatures up to 1000°F, as shown in ASME Code, Section II, Part D, Table 1A. In the temperature range of interest (near 800°F), the S_m values for SA240 Type 304 shown in ASME Code, Section II Part D, Table 2A are identical to the allowable S values for the same material shown in Section B, Part D, Table 1A.

Table A.2.13.13-13
 Alternatives to the ASME Code for the NUHOMS® 32PTH1 DSC Basket Assembly
 (Concluded)

Reference ASME Code Section/Article	Code Requirement	Alternatives, Justification & Compensatory Measures
NG-3352	Table NG 3352-1 lists the permissible welded joints.	<p>The fusion welds between the stainless steel insert plates and the stainless fuel compartment tube are not included in Table NG-3352-1. These welds are qualified by testing. The required minimum tested capacity of the welded connection (at each side of the tube) shall be 45 kips (at room temperature). The capacity shall be demonstrated by qualification and production testing. Testing shall be performed using, or corrected to, the lowest tensile strength of material used in the basket assembly or to minimum specified tensile strength. Testing may be performed on individual welds, or on weld patterns representative of one wall of the tube.</p> <p>ASME Code Section IX does not provide tests for qualification of these type of welds. Therefore, these welds are qualified using Section IX to the degree applicable together with the testing described here.</p> <p>The welds will be visually inspected to confirm that they are located over the insert plates, in lieu of the visual acceptance criteria of NG-5260 which are not appropriate for this type of weld.</p>
		<p>A joint efficiency (quality) factor of 1.0 is utilized for the fuel compartment longitudinal seam welds. Table NG-3352-1 permits a joint efficiency (quality) factor of 0.5 to be used for full penetration weld examined by ASME Section V visual examination (VT). For the 32PTH1 DSC, the compartment seam weld is thin and the weld will be made in one pass. Both surfaces of weld (inside and outside) will be fully examined by VT and therefore a factor of $2 \times 0.5 = 1.0$, will be used in the analysis. This is justified as both surfaces of the single weld pass/layer will be fully examined, and the stainless steel material that comprises the fuel compartment tubes is very ductile.</p>

Table A.2.13.13-14
Alternatives to the ASME Code for the NUHOMS® 37PTH DSC Confinement Boundary

Reference ASME Code Section/Article	Code Requirement	Alternatives, Justification & Compensatory Measures
NCA	All.	Not compliant with NCA [1]. Quality Assurance is provided according to 10 CFR 71 Subpart H [2] in lieu of NCA-4000.
NCA-1140	Use of Code editions and addenda.	Code edition and addenda other than those specified in Section A.2.1.2.1 may be used for construction, but in no case earlier than 3 years before that specified in the Table. Materials produced and certified in accordance with ASME Section II [1] material specification from Code Editions and Addenda other than those specified in Section A.2.1.2.1 may be used, so long the materials meet all the requirements of Article 2000 of the applicable Subsection of the Section III Edition and Addenda used for construction.
NB-1100	Requirements for Code Stamping of Components, Code reports and certificates, etc.	Code Stamping is not required. As Code Stamping is not required, the fabricator is not required to hold an ASME "N" or "NPT" [1] stamp, or to be ASME Certified.
NB-2130	Material must be supplied by ASME approved material suppliers.	Material is certified to meet all ASME Code criteria but is not eligible for certification or Code Stamping if a non-ASME fabricator is used. As the fabricator is not required to be ASME certified, material certification to NB-2130 is not possible. Material traceability and certification are maintained in accordance with TN's NRC approved QA program.
NB-4121	Material Certification by Certificate Holder.	
NB-4243 and NB-5230	Category C weld joints in vessels and similar weld joints in other components shall be full penetration joints. These welds shall be examined by UT or RT and either PT or MT.	The shell to the outer top cover weld, the shell to the inner top cover/shield plug weld (including optional design configurations for the inner top cover as described in the 37PTH DSC drawings), the siphon/vent cover welds, and the vent and siphon block welds to the shell are all partial penetration welds. As an alternative to the NDE requirements of NB-5230, for Category C welds, all of these closure welds are multi-layer welds and receive a root and final PT examination, except for the shell to the outer top cover weld. The shell to the outer top cover weld will be a multi-layer weld and receive multi-level PT examination in accordance with the guidance provided in ISG-15 [7] for NDE. The multi-level PT examination provides reasonable assurance that flaws of interest will be identified. The PT examination is done by qualified personnel, in accordance with Section V and the acceptance standards of Section III, Subsection NB-5000. All of these welds are designed to meet the guidance provided in ISG-15 for stress reduction factor.
NB-1132	Attachments with a pressure retaining function, including stiffeners, shall be considered part of the component.	Bottom shield plug and outer bottom cover plate are outside code jurisdiction; these components together are much larger than required to provide stiffening for the inner bottom cover plate; the weld that retains the outer bottom cover plate and with it the bottom shield plug is subject to root and final PT examination.

Table A.2.13.13-14
 Alternatives to the ASME Code for the NUHOMS® 37PTH DSC Confinement Boundary
 (Concluded)

Reference ASME Code Section/Article	Code Requirement	Alternatives, Justification & Compensatory Measures
NB-6100 and 6200	All pressure retaining components and completed systems shall be pressure tested. The preferred method shall be hydrostatic test.	<p>The NUHOMS® 37PTH DSC is not a complete vessel until the top closure is welded following placement of fuel assemblies within the DSC. Due to the inaccessibility of the shell and lower end closure welds following fuel loading and top closure welding, as an alternative, the pressure testing of the DSC is performed in two parts. The DSC shell and inner bottom plate/forging (including all longitudinal and circumferential welds), are pressure tested and examined at the fabrication facility.</p> <p>The shell to the inner top cover/shield plug closure weld (including optional design configurations for the inner top cover as described in the 37PTH DSC drawings) is pressure tested and examined for leakage in accordance with NB-6300 in the field.</p> <p>The siphon/vent cover welds are not pressure tested; these welds and the shell to the inner top cover/shield plug closure weld (including Optional design configurations for the inner top cover as described in the 37PTH DSC drawings) are helium leak tested after the pressure test.</p> <p>Per NB-6324 the examination for leakage shall be done at a pressure equal to the greater of the design pressure or three-fourths of the test pressure. As an alternative, if the examination for leakage of these field welds, following the pressure test, is performed using helium leak detection techniques, the examination pressure may be reduced to ≥ 1.5 psig. This is acceptable given the significantly greater sensitivity of the helium leak detection method.</p>
NB-7000	Overpressure Protection.	No overpressure protection is provided for the NUHOMS® DSCs. The function of the DSC is to contain radioactive materials under normal, off-normal and hypothetical accident conditions postulated to occur during transportation and storage. The DSC is designed to withstand the maximum possible internal pressure considering 100% fuel rod failure at maximum accident temperature.
NB-8000	Requirements for nameplates, stamping & reports per NCA-8000.	The NUHOMS® DSC nameplate provides the information required by 10CFR71 [2], 49CFR173 [8] and 10CFR72 [4] as appropriate. Code stamping is not required for the DSC. QA data packages are prepared in accordance with the requirements of TN's approved QA program.
NB-5000	NDE Personnel must be qualified to a specific edition of SNT-TC-1A.	Permit use of more recent edition of SNT-TC-1A [9].

Table A.2.13.13-15
 Alternatives to the ASME Code for the NUHOMS® 37PTH DSC Basket Assembly

Reference ASME Code Section/Article	Code Requirement	Alternatives, Justification & Compensatory Measures
NCA	All.	Not compliant with NCA [1]. Quality Assurance is provided according to 10 CFR 71 Subpart H [2] in lieu of NCA-4000.
NCA-1140	Use of Code editions and addenda.	Code edition and addenda other than those specified in Section A.2.1.2.1 may be used for construction, but in no case earlier than 3 years before that specified in the Table. Materials produced and certified in accordance with ASME Section II [1] material specification from Code Editions and Addenda other than those specified in Section A.2.1.2.1 may be used, so long the materials meet all the requirements of Article 2000 of the applicable Subsection of the Section III Edition and Addenda used for construction.
NG/NF-1100	Requirements for Code Stamping of Components, Code reports and certificates, etc.	Code Stamping is not required. As Code Stamping is not required, the fabricator is not required to hold an ASME "N" or "NPT" [1] stamp, or to be ASME Certified.
NG-2000	Use of ASME Material.	Baskets include neutron absorber and aluminum plates that are not ASME Code Class 1 material. They are used for criticality safety and heat transfer, and are only credited in the structural analysis with supporting their own weight and transmitting bearing loads through their thickness. Material properties in the ASME Code for Type 6061 aluminum are limited to 400°F to preclude the potential for annealing out the hardening properties. Annealed properties (as published by the Aluminum Association and the American Society of Metals) are conservatively assumed for the aluminum transition rails for use above the Code temperature limits.
NG/NF-2130	Material must be supplied by ASME approved material suppliers.	Material is certified to meet all ASME Code criteria but is not eligible for certification or Code Stamping if a non-ASME fabricator is used. As the fabricator is not required to be ASME certified, material certification to NG/NF-2130 is not possible. Material traceability and certification are maintained in accordance with TN's NRC approved QA program.
NG/NF-4121	Material Certification by Certificate Holder.	
NG-8000	Requirements for nameplates, stamping & reports per NCA-8000.	The NUHOMS® DSC nameplate provides the information required by 10CFR71 [2], 49CFR173 [8] and 10CFR72 [4] as appropriate. Code stamping is not required for the DSC. QA data packages are prepared in accordance with the requirements of TN's approved QA program.

Table A.2.13.13-16
ASME Code Alternatives for the NUHOMS®-61BT DSC Confinement Boundary

Reference ASME Code Section/Article	Code Requirement	Alternatives, Justification & Compensatory Measures
NCA	All.	Not compliant with NCA [1]. Quality Assurance is provided according to 10 CFR 71 Subpart H [2] in lieu of NCA-4000.
NCA-1140	Use of Code editions and addenda.	Code edition and addenda other than those specified in Section A.2.1.2.1 may be used for construction, but in no case earlier than 3 years before that specified in the Table. Materials produced and certified in accordance with ASME Section II [1] material specification from Code Editions and Addenda other than those specified in Section A.2.1.2.1 may be used, as long as the materials meet all the requirements of Article 2000 of the applicable Subsection of the Section III Edition and Addenda used for construction.
NB-1100	Requirements for Code Stamping of Components, Code reports and certificates, etc.	Code Stamping is not required. As Code Stamping is not required, the fabricator is not required to hold an ASME "N" or "NPT" [1] stamp, or to be ASME Certified.
NB-1132	Attachments with a pressure retaining function, including stiffeners, shall be considered part of the component.	Bottom shield plug and outer bottom cover plate are outside code jurisdiction; these components together are much larger than required to provide stiffening for the inner bottom cover plate; the weld that retains the outer bottom cover plate and with it the bottom shield plug is subject to root and final PT examination.
NB-2130	Material must be supplied by ASME approved material suppliers.	Material is certified to meet all ASME Code criteria but is not eligible for certification or Code Stamping if a non-ASME fabricator is used. As the fabricator is not required to be ASME certified, material certification to NB-2130 is not possible. Material traceability and certification are maintained in accordance with TN's NRC approved QA program.
NB-4121	Material Certification by Certificate Holder.	
NB-4243 and NB-5230	Category C weld joints in vessels and similar weld joints in other components shall be full penetration joints. These welds shall be examined by UT or RT and either PT or MT.	The joints between the top outer and inner cover plates and containment shell are designed and fabricated per ASME Code Case N-595-1 [3]. This includes the inner top cover plate weld around the vent and siphon block. The welds are partial penetration welds and the root and final layer are PT examined. The weld between the vent and siphon block and the shell is made at the fabricator's shop and receives a final PT examination.
NB-6100 and 6200	All completed pressure retaining systems shall be pressure tested.	The vent and siphon block is not pressure tested due to the manufacturing sequence. The siphon block weld is helium leak tested when fuel is loaded and then covered with the outer top closure plate.
NB-7000	Overpressure Protection.	No overpressure protection is provided for the NUHOMS® DSCs. The function of the DSC is to contain radioactive materials under normal, off-normal and hypothetical accident conditions postulated to occur during transportation and storage. The DSC is designed to withstand the maximum possible internal pressure considering 100% fuel rod failure at maximum accident temperature.
NB -8000	Requirements for nameplates, stamping & reports per NCA-8000.	The NUHOMS® DSC nameplate provides the information required by 10CFR71 [2], 49CFR173 [8] and 10CFR72 [4] as appropriate. Code stamping is not required for the DSC. QA data packages are prepared in accordance with the requirements of TN's approved QA program.
NB-5000	NDE Personnel must be qualified to a specific edition of SNT-TC-1A.	Permit use of more recent edition of SNT-TC-1A [9].

Table A.2.13.13-17
ASME Code Alternatives for the NUHOMS®-61BT DSC Basket

Reference ASME Code Section/Article	Code Requirement	Alternatives, Justification & Compensatory Measures
NCA	All.	Not compliant with NCA [1]. Quality Assurance is provided according to 10 CFR 71 Subpart H [2] in lieu of NCA-4000.
NCA-1140	Use of Code editions and addenda.	Code edition and addenda other than those specified in Section A.2.1.2.1 may be used for construction, but in no case earlier than 3 years before that specified in the Table. Materials produced and certified in accordance with ASME Section II [1] material specification from Code Editions and Addenda other than those specified in Section A.2.1.2.1 may be used, so long the materials meet all the requirements of Article 2000 of the applicable Subsection of the Section III Edition and Addenda used for construction.
NG/NF-1100	Requirements for Code Stamping of Components, Code reports and certificates, etc.	Code Stamping is not required. As Code Stamping is not required, the fabricator is not required to hold an ASME "N" or "NPT" [1] stamp, or to be ASME Certified.
NG/NF-2000	Use of ASME Code Material.	Some baskets include neutron absorber and aluminum plates that are not ASME Code Class I material. They are used for criticality safety and heat transfer, and are only credited in the structural analysis with supporting their own weight and transmitting bearing loads through their thickness.
NG/NF-5520	<i>NDE personnel must be qualified to a specific edition of SNT-TC-1A.</i>	<i>Permit use of more recent edition of SNT-TC-1A.</i>
NG/NF-2130	<i>Material must be supplied by ASME approved material suppliers.</i>	<i>Material is certified to meet all ASME Code criteria but is not eligible for certification or Code stamping if a non-ASME fabricator is used. As the fabricator is not required to be ASME certified, material certification to NG/NF-2130 is not possible. Material traceability and certification are maintained in accordance with TN's NRC approved QA program.</i>
NG/NF-4121	<i>Material Certification by Certificate Holder</i>	
NG/NF-8000	<i>Requirements for nameplates, stamping & reports per NCA-8000</i>	<i>The NUHOMS® DSC nameplate provides the information required by 10CFR71, 49CFR173 and 10CFR72, as appropriate. Code stamping is not required for the DSC. QA data packages are prepared in accordance with the requirements of TN's approved QA program.</i>

Table A.2.13.13-18
ASME Code Alternatives for the NUHOMS®-61BTH DSC Confinement Boundary

Reference ASME Code Section/Article	Code Requirement	Alternatives, Justification & Compensatory Measures
NCA	All.	Not compliant with NCA [1]. Quality Assurance is provided according to 10 CFR 71 Subpart H [2] in lieu of NCA-4000.
NCA-1140	Use of Code editions and addenda.	Code edition and addenda other than those specified in Section A.2.1.2.1 may be used for construction, but in no case earlier than 3 years before that specified in the Table. Materials produced and certified in accordance with ASME Section II [1] material specification from Code Editions and Addenda other than those specified in Section A.2.1.2.1 may be used, as long as the materials meet all the requirements of Article 2000 of the applicable Subsection of the Section III Edition and Addenda used for construction.
NB-1100	Requirements for Code Stamping of Components, Code reports and certificates, etc.	Code Stamping is not required. As Code Stamping is not required, the fabricator is not required to hold an ASME "N" or "NPT" [1] stamp, or to be ASME Certified.
NB-1132	Attachments with a pressure retaining function, including stiffeners, shall be considered part of the component.	Bottom shield plug and outer bottom cover plate are outside code jurisdiction; these components together are much larger than required to provide stiffening for the inner bottom cover plate; the weld that retains the outer bottom cover plate and with it the bottom shield plug is subject to root and final PT examination.
NB-2130	Material must be supplied by ASME approved material suppliers.	Material is certified to meet all ASME Code criteria but is not eligible for certification or Code Stamping if a non-ASME fabricator is used. As the fabricator is not required to be ASME certified, material certification to NB-2130 is not possible. Material traceability and certification are maintained in accordance with TN's NRC approved QA program.
NB-4121	Material Certification by Certificate Holder.	
NB-4243 and NB-5230	Category C weld joints in vessels and similar weld joints in other components shall be full penetration joints. These welds shall be examined by UT or RT and either PT or MT.	The shell to the outer top cover weld, the shell to the inner top cover/weld, the siphon/vent cover welds and the vent and siphon block welds to the shell are all partial penetration welds. As an alternative to the NDE requirements of NB-5230 for Category C welds, all of these closure welds will be multi-layer welds and receive a root and final PT examination, except for the shell to the outer top cover weld. The shell to the outer top cover weld will be a multi-layer weld and receive multi-level PT examination in accordance with the guidance provided in ISG-15 for NDE. The multi-level PT Examination provides reasonable assurance that flaws of interest will be identified. The PT examination is done by qualified personnel, in accordance with Section V and the acceptance standards of Section III, Subsection NB-5000. All of these welds will be designed to meet the guidance provided in ISG-15 for stress reduction factor.

Table A.2.13.13-18
ASME Code Alternatives for the NUHOMS®-61BTH DSC Confinement Boundary
(Concluded)

Reference ASME Code Section/Article	Code Requirement	Alternatives, Justification & Compensatory Measures
NB-6100 and 6200	All completed pressure retaining systems shall be pressure tested.	<p>The 61BTH is not a complete or "installed" pressure vessel until the top closure is welded following placement of Fuel Assemblies with the DSC. Due to the inaccessibility of the shell and lower end closure welds following fuel loading and top closure welding, as an alternative, the pressure testing of the DSC is performed in two parts. The DSC shell (including all longitudinal and circumferential welds) is pressure tested and examined at the fabrication facility.</p> <p>The shell to the inner top cover closure weld are pressure tested and examined for leakage in accordance with NB-6300 in the field.</p> <p>The siphon/vent cover welds are not pressure tested; these welds and the shell to the inner top cover closure weld are helium leak tested after the pressure test.</p> <p>Per NB-6324 the examination for leakage shall be done at a pressure equal to the greater of the design pressure or three-fourths of the test pressure. As an alternative, if the examination for leakage of these field welds, following the pressure test, is performed using helium leak detection techniques, the examination pressure may be reduced to ≥ 1.5 psig. This is acceptable given the significantly greater sensitivity of the helium leak detection method.</p>
NB-7000	Overpressure Protection.	No overpressure protection is provided for the NUHOMS® DSCs. The function of the DSC is to contain radioactive materials under normal, off-normal and hypothetical accident conditions postulated to occur during transportation and storage. The DSC is designed to withstand the maximum possible internal pressure considering 100% fuel rod failure at maximum accident temperature.
NB-8000	Requirements for nameplates, stamping & reports per NCA-8000.	The NUHOMS® DSC nameplate provides the information required by 10CFR71 [2], 49CFR173 [8] and 10CFR72 [4] as appropriate. Code stamping is not required for the DSC. QA data packages are prepared in accordance with the requirements of TN's approved QA program.
NB-5000	NDE Personnel must be qualified to a specific edition of SNT-TC-1A.	Permit use of more recent edition of SNT-TC-1A [9].

Table A.2.13.13-19
ASME Code Alternatives for the NUHOMS®-61BTH DSC Basket

Reference ASME Code Section/Article	Code Requirement	Alternatives, Justification & Compensatory Measures
NCA	All.	Not compliant with NCA [1]. Quality Assurance is provided according to 10 CFR 71 Subpart H [2] in lieu of NCA-4000.
NCA-1140	Use of Code editions and addenda.	Code edition and addenda other than those specified in Section A.2.1.2.1 may be used for construction, but in no case earlier than 3 years before that specified in the Table. Materials produced and certified in accordance with ASME Section II [1] material specification from Code Editions and Addenda other than those specified in Section A.2.1.2.1 may be used, so long the materials meet all the requirements of Article 2000 of the applicable Subsection of the Section III Edition and Addenda used for construction.
NG-1100	Requirements for Code Stamping of Components, Code reports and certificates, etc.	Code Stamping is not required. As Code Stamping is not required, the fabricator is not required to hold an ASME "N" or "NPT" [1] stamp, or to be ASME Certified.
NG-2000	Use of ASME Material.	Some baskets include neutron absorber and aluminum plates that are not ASME Code Class 1 material. They are used for criticality safety and heat transfer, and are only credited in the structural analysis with supporting their own weight and transmitting bearing loads through their thickness. Material properties in the ASME Code for Type 6061 aluminum are limited to 400°F to preclude the potential for annealing out the hardening properties. Annealed properties (as published by the Aluminum Association and the American Society of Metals) are conservatively assumed for the aluminum transition rails for use above the Code temperature limits.
NG/NF-2130	Material must be supplied by ASME approved material suppliers.	Material is certified to meet all ASME Code criteria but is not eligible for certification or Code Stamping if a non-ASME fabricator is used. As the fabricator is not required to be ASME certified, material certification to NG/NF-2130 is not possible. Material traceability and certification are maintained in accordance with TN's NRC approved QA program.
NG/NF-4121	Material Certification by Certificate Holder.	
NG-3352	Table NG 3352-1 lists the permissible welded joints and quality factors.	The fuel compartment tubes may be fabricated from sheet with full penetration seam weldments. Per Table NG-3352-1 a joint efficiency (quality) factor of 0.5 is to be used for full penetration weldments examined in accordance with ASME Section V visual examination (VT). A joint efficiency (quality) factor of 1.0 is utilized for the fuel compartment longitudinal seam welds (if present) with VT examination. This is justified because the compartment seam weld is thin and the weldment is made in one pass; and both surfaces of the weldment (inside and outside) receive 100% VT examination. The 0.5 quality factor, applicable to each surface of the weldment, results in a quality factor of 1.0 since both surfaces are 100% examined. In addition, the fuel compartments have no pressure retaining function and the stainless steel material that comprises the fuel compartment tubes is very ductile.
NG -8000	Requirements for nameplates, stamping & reports per NCA-8000.	The NUHOMS® DSC nameplate provides the information required by 10CFR71 [2], 49CFR173 [8] and 10CFR72 [4] as appropriate. Code stamping is not required for the DSC. QA data packages are prepared in accordance with the requirements of TN's approved QA program.

Table A.2.13.13-20
ASME Code Alternatives for the NUHOMS®-69BTH DSC Confinement Boundary

Reference ASME Code Section/Article	Code Requirement	Alternatives, Justification & Compensatory Measures
NCA	All.	Not compliant with NCA [1]. Quality Assurance is provided according to 10 CFR 71 Subpart H [2] in lieu of NCA-4000.
NCA-1140	Use of Code editions and addenda.	Code edition and addenda other than those specified in Section A.2.1.2.1 may be used for construction, but in no case earlier than 3 years before that specified in the Table. Materials produced and certified in accordance with ASME Section II [1] material specification from Code Editions and Addenda other than those specified in Section A.2.1.2.1 may be used, as long as the materials meet all the requirements of Article 2000 of the applicable Subsection of the Section III Edition and Addenda used for construction.
NB-1100	Requirements for Code Stamping of Components, Code reports and certificates, etc.	Code Stamping is not required. As Code Stamping is not required, the fabricator is not required to hold an ASME "N" or "NPT" [1] stamp, or to be ASME Certified.
NB-1132	Attachments with a pressure retaining function, including stiffeners, shall be considered part of the component.	Bottom shield plug and outer bottom cover plate are outside code jurisdiction; these components together are much larger than required to provide stiffening for the inner bottom cover plate; the weld that retains the outer bottom cover plate and with it the bottom shield plug is subject to root and final PT examination.
NB-2130	Material must be supplied by ASME approved material suppliers.	Material is certified to meet all ASME Code criteria but is not eligible for certification or Code Stamping if a non-ASME fabricator is used. As the fabricator is not required to be ASME certified, material certification to NB-2130 is not possible. Material traceability and certification are maintained in accordance with TN's NRC approved QA program.
NB-4121	Material Certification by Certificate Holder.	
NB-4243 and NB-5230	Category C weld joints in vessels and similar weld joints in other components shall be full penetration joints. These welds shall be examined by UT or RT and either PT or MT.	The shell to the outer top cover weld, the shell to the inner top cover/weld, the siphon/vent cover welds and the vent and siphon block welds to the shell are all partial penetration welds. As an alternative to the NDE requirements of NB-5230 for Category C welds, all of these closure welds will be multi-layer welds and receive a root and final PT examination, except for the shell to the outer top cover weld. The shell to the outer top cover weld will be a multi-layer weld and receive multi-level PT examination in accordance with the guidance provided in ISG-15 [7] for NDE. The multi-level PT Examination provides reasonable assurance that flaws of interest will be identified. The PT examination is done by qualified personnel, in accordance with Section V and the acceptance standards of Section III, Subsection NB-5000. All of these welds will be designed to meet the guidance provided in ISG-15 for stress reduction factor.

Table A.2.13.13-20
ASME Code Alternatives for the NUHOMS®-69BTH DSC Confinement Boundary
(Concluded)

Reference ASME Code Section/Article	Code Requirement	Alternatives, Justification & Compensatory Measures
NB-6100 and 6200	All completed pressure retaining systems shall be pressure tested.	<p>The 69BTH is not a complete or "installed" pressure vessel until the top closure is welded following placement of Fuel Assemblies with the DSC. Due to the inaccessibility of the shell and lower end closure welds following fuel loading and top closure welding, as an alternative, the pressure testing of the DSC is performed in two parts. The DSC shell (including all longitudinal and circumferential welds) is pressure tested and examined at the fabrication facility.</p> <p>The shell to the inner top cover closure weld are pressure tested and examined for leakage in accordance with NB-6300 in the field.</p> <p>The siphon/vent cover welds are not pressure tested; these welds and the shell to the inner top cover closure weld are helium leak tested after the pressure test.</p> <p>Per NB-6324 the examination for leakage shall be done at a pressure equal to the greater of the design pressure or three-fourths of the test pressure. As an alternative, if the examination for leakage of these field welds, following the pressure test, is performed using helium leak detection techniques, the examination pressure may be reduced to ≥ 1.5 psig. This is acceptable given the significantly greater sensitivity of the helium leak detection method.</p>
NB-7000	Overpressure Protection.	No overpressure protection is provided for the NUHOMS® DSCs. The function of the DSC is to contain radioactive materials under normal, off-normal and hypothetical accident conditions postulated to occur during transportation and storage. The DSC is designed to withstand the maximum possible internal pressure considering 100% fuel rod failure at maximum accident temperature.
NB-8000	Requirements for nameplates, stamping & reports per NCA-8000.	The NUHOMS® DSC nameplate provides the information required by 10CFR71 [2], 49CFR173 [8] and 10CFR72 [4] as appropriate. Code stamping is not required for the DSC. QA data packages are prepared in accordance with the requirements of TN's approved QA program.
NB-5000	NDE Personnel must be qualified to a specific edition of SNT-TC-1A.	Permit use of more recent edition of SNT-TC-1A [9].

Table A.2.13.13-21
ASME Code Alternatives for the NUHOMS®-69BTH DSC Basket

Reference ASME Code Section/Article	Code Requirement	Alternatives, Justification & Compensatory Measures
NCA	All.	Not compliant with NCA [1]. Quality Assurance is provided according to 10 CFR 71 Subpart H [2] in lieu of NCA-4000.
NCA-1140	Use of Code editions and addenda.	Code edition and addenda other than those specified in Section A.2.1.2.1 may be used for construction, but in no case earlier than 3 years before that specified in the Table. Materials produced and certified in accordance with ASME Section II [1] material specification from Code Editions and Addenda other than those specified in Section A.2.1.2.1 may be used, so long the materials meet all the requirements of Article 2000 of the applicable Subsection of the Section III Edition and Addenda used for construction.
NG-1100	Requirements for Code Stamping of Components, Code reports and certificates, etc.	Code Stamping is not required. As Code Stamping is not required, the fabricator is not required to hold an ASME "N" or "NPT" [1] stamp, or to be ASME Certified.
NG-2000	Use of ASME Material.	Some baskets include neutron absorber and aluminum plates that are not ASME Code Class 1 material. They are used for criticality safety and heat transfer, and are only credited in the structural analysis with supporting their own weight and transmitting bearing loads through their thickness. Material properties in the ASME Code for Type 6061 aluminum are limited to 400°F to preclude the potential for annealing out the hardening properties. Annealed properties (as published by the Aluminum Association and the American Society of Metals) are conservatively assumed for the aluminum transition rails for use above the Code temperature limits.
NG/NF-2130	Material must be supplied by ASME approved material suppliers.	Material is certified to meet all ASME Code criteria but is not eligible for certification or Code Stamping if a non-ASME fabricator is used. As the fabricator is not required to be ASME certified, material certification to NG/NF-2130 is not possible. Material traceability and certification are maintained in accordance with TN's NRC approved QA program.
NG/NF-4121	Material Certification by Certificate Holder.	
NG-3352	Table NG 3352-1 lists the permissible welded joints and quality factors.	The fuel compartment tubes may be fabricated from sheet with full penetration seam weldments. Per Table NG-3352-1 a joint efficiency (quality) factor of 0.5 is to be used for full penetration weldments examined in accordance with ASME Section V visual examination (VT). A joint efficiency (quality) factor of 1.0 is utilized for the fuel compartment longitudinal seam welds (if present) with VT examination. This is justified because the compartment seam weld is thin and the weldment is made in one pass; and both surfaces of the weldment (inside and outside) receive 100% VT examination. The 0.5 quality factor, applicable to each surface of the weldment, results in a quality factor of 1.0 since both surfaces are 100% examined. In addition, the fuel compartments have no pressure retaining function and the stainless steel material that comprises the fuel compartment tubes is very ductile.
NG -8000	Requirements for nameplates, stamping & reports per NCA-8000.	The NUHOMS® DSC nameplate provides the information required by 10CFR71 [2], 49CFR173 [8] and 10CFR72 [4] as appropriate. Code stamping is not required for the DSC. QA data packages are prepared in accordance with the requirements of TN's approved QA program.

Appendix A.2.13.14

**Proprietary information on pages A.2.13.14-i and A.2.13.14-1 through
A.2.13.14-25 withheld pursuant to 10 CFR 2.390**